Commagene Journal of Biology

JUNE 2025 Volume IX Number 1

ABADER

Commagene Journal of Biology (Kommagene Biyoloji Dergisi) *Comm. J. Biol.*

Volume (Cilt): 9 • Number (Sayı): 1 • 2025 • Adıyaman, Türkiye (Türkiye)

An open access, peer reviewed, international journal of biology.
Açık erişimli, hakemli, biyoloji alanında uluslararası bir dergi.

Cover (Kapak): Harran Kertenkelesi, Harran Lizard, *Acanthodactylus harranensis* Baran, Kumlutaş, Lanza, Sindaco, Avcı & Crucitti, 2005,

Photograph (Fotoğraf): Dr. Mehmet Zülfü YILDIZ

Graphics and Design (Grafik ve Tasarım): Dr. Serdar SÖNMEZ

Table of Contents (İçindekiler) Volume (Cilt): 9 Number (Sayı): 1 • June (Haziran) 2025

Research Articles (Araştırma Makaleleri)

Review (Derleme)

Commagene Journal of Biology

Yılmaz et al., (2025) *Comm. J. Biol.* 9(1), 1-6.
DOI: 10.31594/commagene.1567576

e-ISSN 2602-456X

Research Article/Araştırma Makalesi

The Three Reptile New Locality Records and Their Ecological Niche Models in Hakkari Province, Eastern Anatolia, Türkiye

Can YILMAZ[1,5*], Çetin ILGAZ[2], Emin BOZKURT[3], Nazan ÜZÜM[4], Aziz AVCI[4]

[1]*Vocational School of Health Services, Hakkâri University, Hakkâri, TÜRKIYE*
[2]*Dokuz Eylül University, Department of Biology, Faculty of Science. Buca-İzmir, TÜRKIYE*
[3]*Çankırı Karatekin University, Eldivan Vocational School of Health Services. 18700, Çankırı, TÜRKIYE*
[4]*Aydın Adnan Menderes University, Department of Biology, Faculty of Science. Aydın, TÜRKIYE*
[5]*Hakkari University, Biodiversity Application and Research Centre, 30000 Hakkari, TÜRKIYE*
ORCID ID: Can YILMAZ: https://orcid.org/0000-0002-5994-508X; Çetin ILGAZ: http://orcid.org/0000-0001-7862-9106;
Emin BOZKURT http://orcid.org/0000-0001-8963-631X; Nazan ÜZÜM: https://orcid.org/0000-0003-4421-4302;
Aziz AVCI: https://orcid.org/0000-0001-8017-9714

Received: 15.10.2024 **Accepted:** 04.12.2024 **Published online:** 01.01.2025 **Issue published:** 30.06.2025

Abstract: In this study, three reptile species, *Mauremys caspica*, *Mediodactylus orientalis,* and *Laudakia stellio,* were recorded for the first time from Hakkari province, east Anatolia. The ranges of *M. caspica*, *M. orientalis* and *L. stellio* were extended 100 km, 281 km, and 175 km, respectively. For *M. orientalis* and *L. stellio,* these new locality records constitute the eastern border of the species in Türkiye. *M. caspica*, *M. orientalis* and *L. stellio* average AUC (Area Under the Curve) values were calculated as 0.861, 0.867, and 0.821, respectively. Annual mean temperature (Bio1) was determined as the most important bioclimatic variable for *M. orientalis* (79.3%) and *L. stellio* (52.8%), while mean temperature of wettest quarter (Bio8) was the most effective bioclimatic variable for *M. caspica* (37.4%). There is a possibility of new species records due to the important location of Hakkari province geographically; thus, we suggest additional studies in the area.

Keywords: *Mauremys caspica*, *Mediodactylus orientalis*, *Laudakia stellio*, range extension, bioclimatic.

Hakkari Ili, Doğu Anadolu, Türkiye'de Üç Sürüngen Yeni Lokalite Kaydı ve Ekolojik Niş Modelleri

Öz: Bu çalışmada, üç sürüngen türü olan *Mauremys caspica*, *Mediodactylus orientalis* ve *Laudakia stellio*, Doğu Anadolu'daki Hakkari ilinden ilk kez kaydedilmiştir. *M. caspica*, *M. orientalis* ve *L. stellio'nun* yayılışları sırasıyla 100 km, 281 km ve 175 km uzatılmıştır. *M. orientalis* ve *L. stellio* için bu yeni lokalite kayıtları türlerin Türkiye'deki doğu sınırını oluşturmaktadır. *M. caspica*, *M. orientalis* ve *L. stellio* ortalama AUC (Area Under the Curve) değerleri sırasıyla 0.861, 0.867 ve 0.821 olarak hesaplanmıştır. Yıllık ortalama sıcaklık (Bio1) *M. orientalis* (%79.3) ve *L. stellio* (%52.8) için en önemli biyoklimatik değişken olarak belirlenirken, en yağışlı mevsimdeki ortalama sıcaklık (Bio8) *M. caspica* (%37.4) için en etkili biyoklimatik değişken olmuştur. Hakkari ilinin coğrafik olarak önemli konumu nedeniyle yeni tür kayıtları olasılığı vardır, bu nedenle bölgede ek çalışmalar yapılmasını öneriyoruz.

Anahtar kelimeler: *Mauremys caspica*, *Mediodactylus orientalis*, *Laudakia stellio*, yayılış genişletme, biyoklimatik.

1. Introduction

Türkiye is a very rich country in terms of amphibian and reptile fauna in its region. There are 152 reptile species including 10 chelonians, 3 amphisbaenians, 79 lizards, and 60 snakes and 34 amphibians, including 18 salamanders and 16 frogs (Bozkurt & Olgun, 2020; Baran et al., 2021; Karakasi et al., 2021, Kurnaz & Şahin, 2021; Yılmaz et al., 2021; Arribas et al., 2022a, 2022b; Kurnaz et al., 2022; Kafimola et al., 2023). This richness is due to the environmental heterogeneity as there are mountains, different climate types, and vegetation diversity. Additionally, Türkiye is a natural corridor between Asia, Europe, and Africa and the migration movements of European and Asian species that took place in the glacial and interglacial periods in geological times shaped the faunistic structure of Türkiye. Species that migrated to Anatolia during the glacial period of the Quaternary remained in suitable habitats during the interglacial period (Kornilios et al., 2011).

Hakkari (36 57' to 37 48' N, 42 10' to 44 50' E) is located at the southeast end of the Eastern Anatolia Region and covers an area of 7,228 km^2. There are Cilo-Sat Mountains, Black Mountain, and Zap River. There are glacial and crater lakes on Cilo-Sat Mountains and on the outskirts of Black Mountain. The top elevation in the province is the Reşko summit with an elevation approximately 4168 m. on Cilo-Sat Mountains. While in the high parts of the province dominates the harsh continental climate similar to that of Eastern Anatolia, on the valley floor of the province the Mediterranean climate is observed (Hakkari İl Kültür ve Turizm Müdürlüğü 2022).

Hakkari is one of the doorways to Anatolian peninsula animal species coming from different areas of Asia and Europe (Demirsoy, 1996). Since Hakkari is bordered by Iran and Iraq, it is possible that herpetofaunic species, which are found in the mentioned countries but not in Türkiye, will be recorded in Hakkari with future studies. Thus, *Platyceps rhodorachis* (Jan, 1863) was recently

Corresponding author: canyilmaz@hakkari.edu.tr

given as a new record in Hakkari for Türkiye (Yılmaz et al., 2021). The herpetofaunal biodiversity of Hakkari province, however, was never systematically studied. The data available result from species-oriented studies and notes on herpetofauna (Mertens, 1953; Başoğlu & Özeti, 1973; Başoğlu & Baran, 1977; 1980, Eiselt et al., 1992; Baran & Atatür, 1998; Mahlow et al., 2013; Sindaco et al., 2014; Afsar et al., 2015; Jablonski et al., 2019; Yılmaz et al., 2021).

Given the possibility of new species records and the important location of Hakkari and since the inventory studies are important for species conservation plans, we aimed to determine the reptile diversity of the Hakkari province. Modeling the potential distribution areas for a given species is important in understanding the relationship between the actual distribution and the most suitable habitat for a species. The aim of this study is to contribute to the herpetofauna of Hakkari province, which does not have sufficient data in the literature, and to determine the possible distribution of newly recorded species by indicating their ecological niches.

2. Material and Method

The specimens were collected between April and September of 2019 and 2020. The localities where the specimens were seen and captured are shown in Figure A2, A3, and A4. The specimens were actively captured by hand, or using a scoop, if needed. The specimens were collected and fixed (collecting permit no. 21264211-288.04-E.1048399 issued by the Turkish Ministry of Agriculture and Forestry) using traditional processes (Başoğlu & Özeti, 1973; Başoğlu & Baran, 1977, 1980). Voucher specimens are stored at the Hakkari University Zoology Laboratory, Türkiye. We used literature for specimen's determination (Başoğlu & Baran, 1977, 1980; Baran et al., 2021). The morphometric measurements were taken using dial calipers with an accuracy of 0.01 mm. The pholidotic characters were determined under a stereomicroscope.

We conducted ecological niche modelling for the three species configuring new locality records. All the occurrence data of *M. caspica*, *M. orientalis*, and *L. stellio* in Türkiye were obtained from literature (74 records for *M. caspica*; 63 records for *M. orientalis*; 650 records for *L. stellio*). After spatial sample corrections, 71 records for *M. caspica*, 59 records for *M. orientalis*, and 441 records for *L. stellio* remained for analysis. The literatures from which the localities are taken respectively are given in Figure A2, A3, and A4. In cases in which the locality information was not georeferenced in literature, an online geographic system application (i.e., Google Earth Pro) was used to ascertain the most precise location possible.

We used 19 bioclimatic variables downloaded from CHELSA version 2.1 for current conditions (1981-2010) (https://chelsa-climate.org) with a spatial resolution of 30 arc-second (1 km^2) (Karger et al., 2017). Correlation coefficients higher than 0.75 accepted as correlated variables and these variables are excluded from the analysis. Correlation matrix was calculated from R implemented Niche Toolbox web server (Osorio-Olvera et al., 2020). Seven bioclimatic variables for *M. caspica* [Bio1 = Annual Mean Temperature; Bio2 = Mean Diurnal Range (Mean of monthly (max temp - min temp)); Bio3 = Isothermality (Bio2/Bio7) (×100); Bio4 = Temperature Seasonality (standard deviation ×100); Bio8 = Mean Temperature of Wettest Quarter; Bio12 = Annual Precipitation; Bio14 = Precipitation of Driest Month] (Fig. 1), six bioclimatic variables for *M. orientalis* [Bio1 = Annual Mean Temperature; Bio2 = Mean Diurnal Range (Mean of monthly (max temp - min temp)); Bio3 = Isothermality (Bio2/Bio7) (×100); Bio5 = Maximum Temperature of Warmest Month; Bio12 = Annual Precipitation; Bio14 = Precipitation of Driest Month] (F. 2) and nine bioclimatic variables for *L. stellio* [Bio1 = Annual Mean Temperature; Bio2 = Mean Diurnal Range (Mean of monthly (max temp - min temp)); Bio3 = Isothermality (Bio2/Bio7) (×100); Bio4 = Temperature Seasonality (standard deviation ×100); Bio5 = Maximum Temperature of Warmest Month; Bio8 = Mean Temperature of Wettest Quarter; Bio12 = Annual Precipitation; Bio14 = Precipitation of Driest Month; Bio15 = Precipitation Seasonality] (Fig. 3) remained for analysis after the correlation analysis.

Bioclimatic variables and occurrence data were imported to Maxent vers. 3.4.4 (Phillips et al., 2006). Maxent was performed with 50 subsampled replicates, 5000 iterations, and cloglog outputs. Area Under the Curve (AUC) were calculated for estimation of model performance. Predicted distribution maps obtained from Maxent were imported to ArcGIS vers 10.3.1 for visualization.

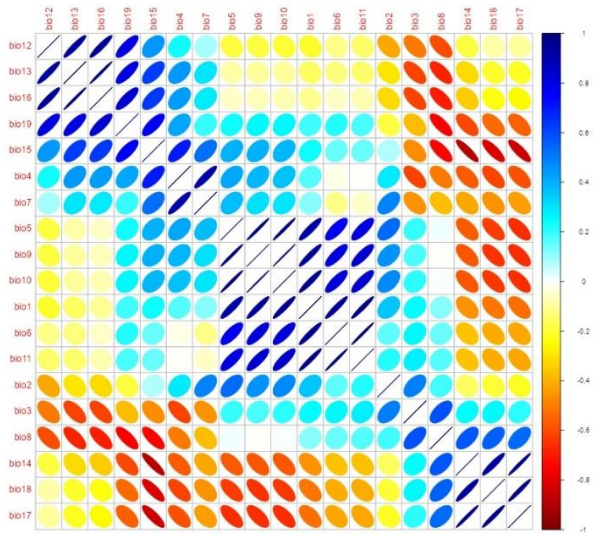

Figure 1. Corelation matrix of *Mauremys caspica*.

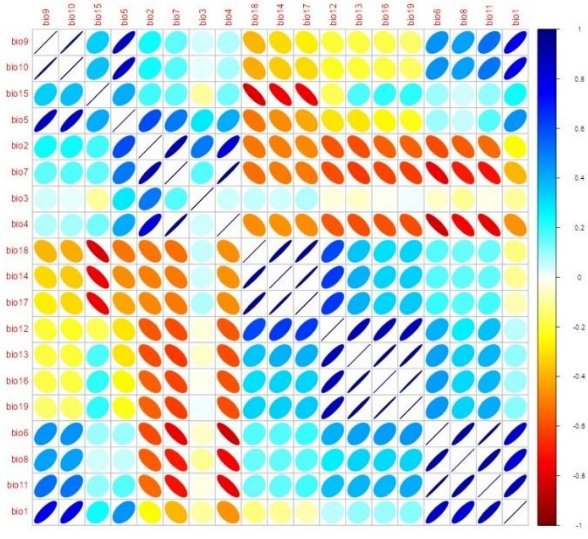

Figure 2. Correlation matrix of *Mediodactylus orientalis*.

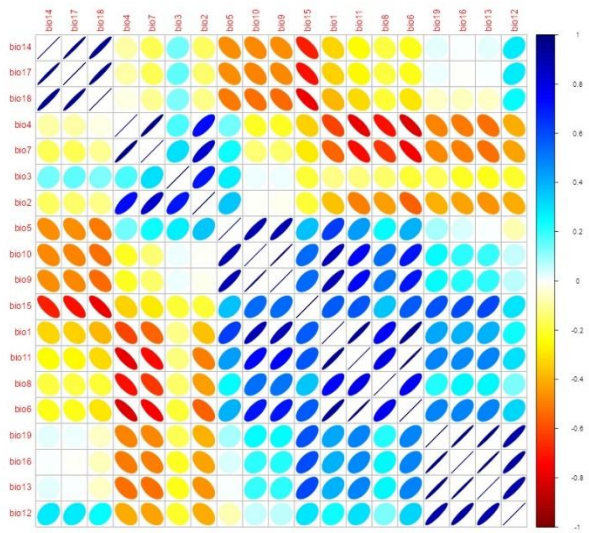

Figure 3. Correlation matrix of *Laudakia stellio*.

3. Results

The turtle *M. caspica* (Gmelin, 1774) and the lizards *M. orientalis* (Stepánek, 1937) and *L. stellio* (Linnaeus, 1758) were recorded for the first time in Hakkari (Additional Fig. A1).

Mauremys caspica (1♀, 11.06.2022, leg. C. Yılmaz, A. Avcı, Ç. Ilgaz, N. Üzüm, E., Bozkurt) was collected from Akçalı-Yeniyol Village of Hakkari. The specimen was released after measurements had been taken to assure determination (Additional Table A1). The distribution range of the species in Anatolia is extended by 100 km of air distance (from Çatak/Van) (Additional Fig. A2). The results of ecological niche modelling (Fig. 4) point to new suitable areas of occurrence for this species: central Anatolia, southeast Anatolia, Kars and Iğdır provinces, and inner parts of the east Black Sea Region (AUC value 0.861 ± 0.160). However, our new locality record for *M. caspica* seems like an unsuitable area. Mean temperature of wettest quarter (Bio8, 37.4%), temperature seasonality (Bio4, 26.0%), and annual precipitaton (Bio12, 16.2%) were the most important climatic variables determining suitable areas (Table 1).

Mediodactylus orientalis (1♀, 26.04.2019, leg. C. Yılmaz, A. Avcı, Ç. Ilgaz, N. Üzüm, E., Bozkurt; 1 juv., 18.05.2019, leg. C. Yılmaz, A. Avcı, Ç. Ilgaz, N. Üzüm, E., Bozkurt) was collected on old houses' walls in the center of Hakkari. The morphometric measurements and pholidolial features of the specimens are given in the Additional Table A2. The distribution range of the species in Anatolia is extended by 281 km of air distance (from Kızıltepe/Mardin to Center/Hakkari) (Additional Fig. A3). The results of the ecological niche modelling point new suitable areas to the species: Aegean Region, Antalya Basin, east Mediterranean Region, and southeast Anatolia (AUC value 0.867 ± 0.143, Fig. 5). Our new record seems like an unsuitable area for *M. orientalis* in terms of ecological niche model. The annual mean temperature (Bio1, 79.3%) and maximum temperature of warmest month (Bio5, 10.7%) were the most important climatic variables determining suitability of occurrence of *M. orientalis* in the area (Table 1).

Table 1. Biovariables. Percent contributions (P.C) and permutation importance (P.I) values of *M. caspica*, Me. orientalis and *L. stellio* under current bioclimatic conditions.

	M. caspica		*M. orientalis*		*L. stellio*	
	P.C	**P.I**	**P.C**	**P.I**	**P.C**	**P.I**
Bio1	7.5	19.3	79.3	82.7	52.8	57.5
Bio2	0.1	0.2	0.0	0.6	2.0	2.9
Bio3	4.6	5.0	3.0	1.8	1.0	1.6
Bio4	26.0	40.7	-	-	11.8	12.5
Bio5	-	-	10.7	1.5	4.6	1.4
Bio8	37.4	20.7	-	-	3.9	5.6
Bio12	16.2	1.2	5.9	5.9	3.8	4.7
Bio14	8.2	12.9	1.0	7.5	0.2	1.6
Bio15	-	-	-	-	20.0	12.3

Finally, *Laudakia. stellio* (1♂, Kırıkdağ, 14.07.2019, leg. C. Yılmaz, A. Avcı, Ç. Ilgaz, N. Üzüm, E., Bozkurt; 1♂ (subadult), 1 juv., Durankaya, 13.06.2021, leg. C. Yılmaz, A. Avcı, Ç. Ilgaz, N. Üzüm, E., Bozkurt) were collected on stony and rocky areas. The morphometric measurements and pholidolial features of the specimens are given in the Additional Table A3. The distribution range of the species in Anatolia is extended by 175 km of air distance (from between Hacımehmet, Hizan, Bitlis Province to Haruna Valley, Şemdinli, Hakkari, Province (Additional Fig. A4). The results of the ecological niche modelling (Fig. 6) point to new suitable areas in the region: Aegean Region, Mediterranean Region, and southwest of Thrace (AUC value 0.821 ± 0.054). The new locality of *L. stellio* turned out unsuitable as in Figure 4. The annual mean temperature (Bio1, 52.8%), precipitation seasonality (Bio15, 20.0%), and temperature seasonality (Bio4, 11.8%) were the most important climatic variables determining potential distribution in the area (Table 1).

4. Discussion

A total of 37 reptile species were recorded in Hakkari according to the results of the previous studies: including one tortoise, thirteen lizards, and twenty-three snakes (Başoğlu & Baran, 1977; Başoğlu & Baran, 1980; Eiselt et al.,

1992, Baran & Atatür, 1998; Mahlow et al., 2013; Sindaco et al., 2014; Jablonski et al., 2019, Baran et al., 2021; Yılmaz et al. 2021). We added new locality records to the list for three species, raising it to 40: one freshwater turtle (*M. caspica*) and two lizard species (*M. orientalis* and *L. stellio*).

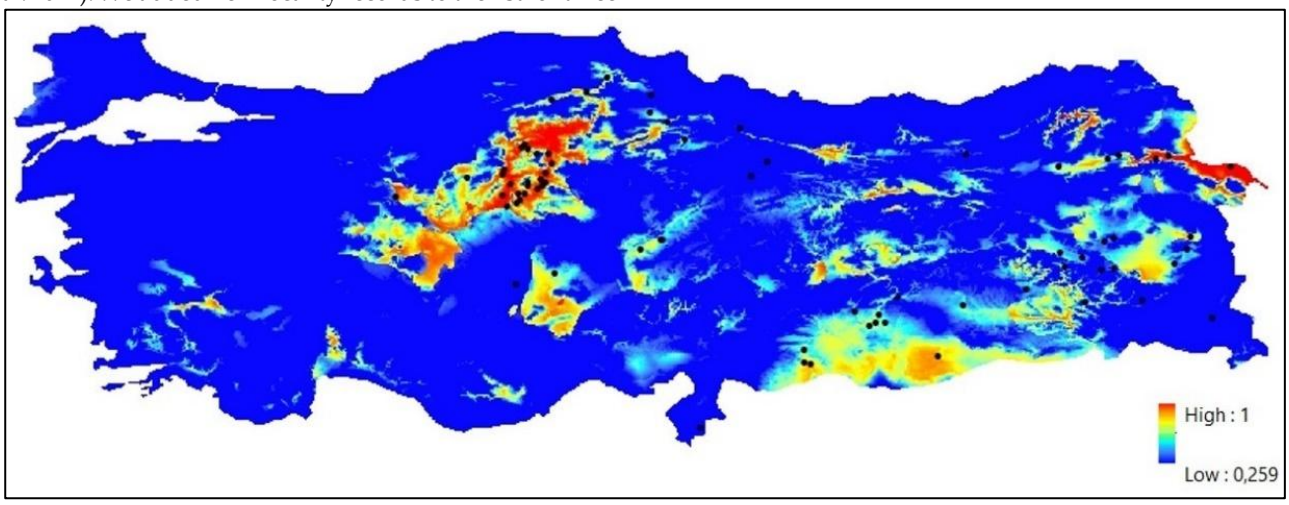

Figure 4. Predicted suitability under the current bioclimatic conditions of *Mauremys capsica,* dots show current locality records.

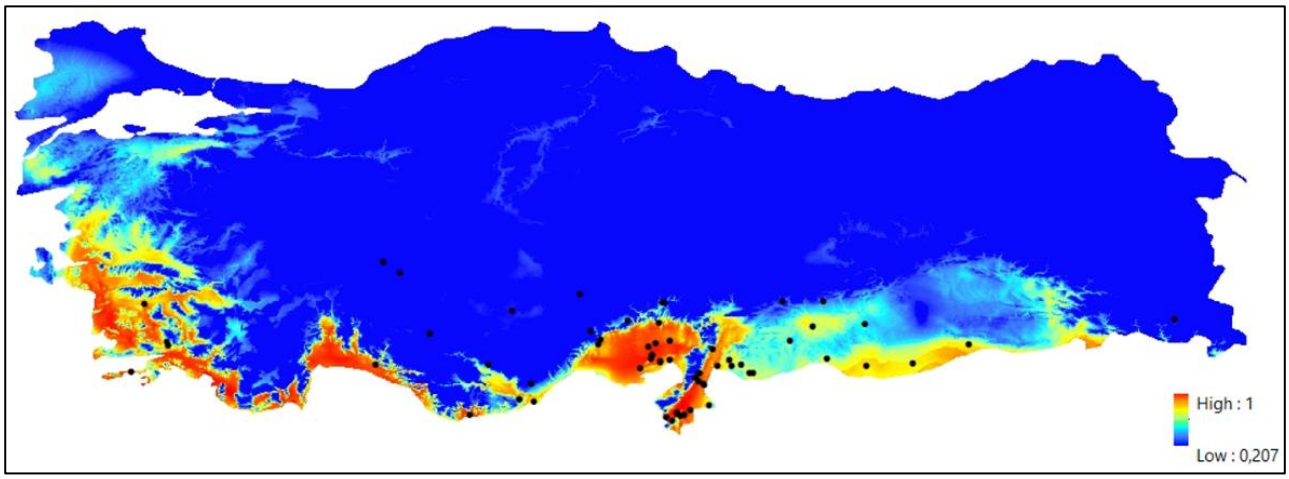

Figure 5. Predicted suitability under the current bioclimatic conditions of *Mediodactylus orientalis,* dots show current locality records.

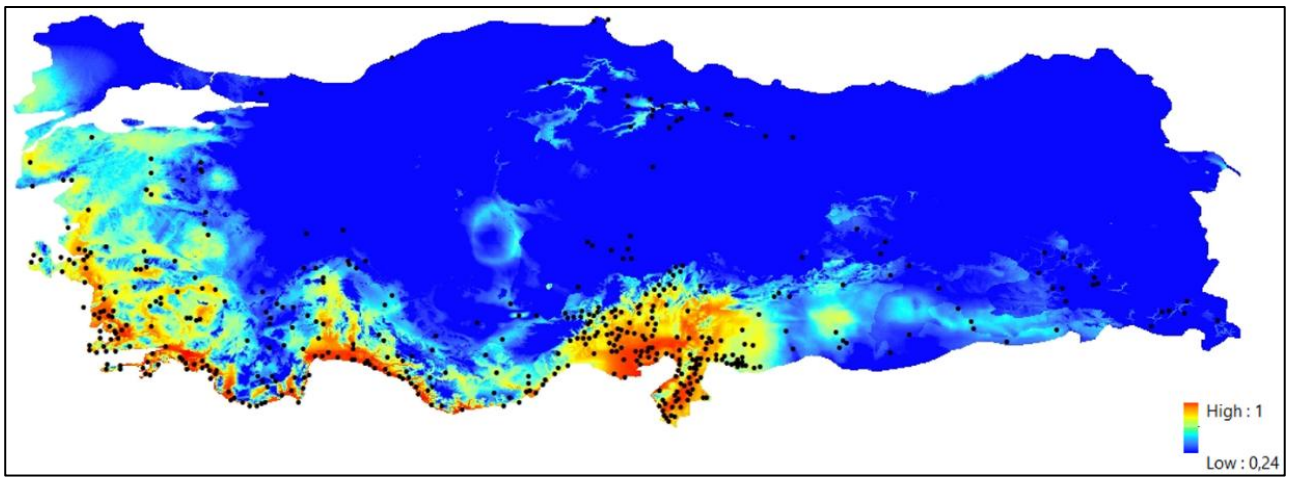

Figure 6. Predicted suitability under the current bioclimatic conditions of *Laudakia stellio,* dots show current locality records.

There are two species of the genus *Mauremys* in Türkiye, *M. caspica* and *M. rivulata* (Valenciennes, 1833) (Baran et al., 2021). These are the most abundant terrapins in the Near and Middle East and South-east Europe (Fritz et al., 2008). According to plastral pattern, these subspecies are different morphologically (Fritz et al., 2008). The ecological niche model and habitat preference of *M. caspica* was conducted by Kurnaz et al. for the first time. (2019). Also Kurnaz et al. (2019) reported that the environmental variables contributed to the highest gain for the distribution of *M. caspica* were Bio12 (annual precipitation), Bio10 (mean temperature of warmest

quarter), and Bio17 (precipitation of driest quarter). Their results also suggested that many regions were unsuitable areas, including Hakkari. The data obtained as a result of our study indicates that the distribution of the species may be wider in Anatolia as opposed to what has been suggested. Urbanization, excessive water withdrawal, and climate changes cause the loss of riverine habitat and these situations threaten aquatic organisms (Palmer et al., 2008). Habitat loss and fragmentation reduce the number of suitable areas and species have to inbreed and there is increased risk of extinction (Bardeh et al., 2021). Therefore, the potential distribution ranges of riverine depended species *M. caspica* were clearly determined by our study and this result can be useful for the conservation of this species.

Mediodactylus, which is one of the 26 genera of the Gekkonidae family, contains 17 species (Uetz et al., 2022).). Now, southern and south-eastern Aegean islands (Samos, Ikaria, and neighboring islets), southwestern Turkey, Cyprus, western Syria, northwestern Jordan, Lebanon, and northern Israel comprises the known distribution area of the species (Kotsakiozi et al., 2018). Our specimens are within the variation limits mentioned for the taxon in the literature (Baran & Gruber, 1982). According to the niche analysis conducted by Domeneghetti et al. (2014), it was stated that *M. kotschyi* has not yet spread in all climatically suitable areas in Italy and that factors other than climate may limit the distribution of the species. The authors also stated that this species may have come to Italy through human influence. In our study, *M. orientalis* was found 281 km away from its known distribution, suggesting that its distribution was similarly affected by human influence.

Regarding morphological data, the specimens of *L. stellio* from Hakkari examined in present study are within the variation limits mentioned for the taxon in the literature (Baran & Öz, 1985; Gül & Tosunoğlu, 2011). Şahin (2021) gave a new locality record for *L. stellio* from Devrek-Zonguldak and reported that Bio6 (minimum temperature of coldest month) and Bio12 (annual precipitation) were more contributing bioclimatic variables. There are differences between our study and Şahin (2021) in the most effective bioclimatic variables. This is due to the sites from which the climatic data were obtained, the programs used, and the localities used in the analysis.

Their ranges extended 175 and 281 km for *L. stellio* and *M. orientalis*, respectively. Result of ecological niche modeling, Hakkari is not seen as a suitable area for *L. stellio* and *M. orientalis*. The occurrence of the both species in such distant regions from their main distribution sites can be explained by various theories such as introduced by man as in *Phoenicolacerta laevis* in Georgia (Tarkhnishvili et al., 2017), habitat fragmentation as in *Podarcis siculus* (Senczuk et al., 2017), relict population as in *Lacerta agilis* in Sweden (Berglind, 2000) or lack of sufficient studies on the species. After the ecological niche model of our study, possible distribution areas can be studied and new population can be determined. Also, molecular approaches can be handled for *Me. orientalis* and *L. stellio* to understand the relationship between new locality and main distribution ranges.

Acknowledgements: The authors would like to thank M. Sait TAYLAN, Melek ERDEK, Serdar ÖZDINÇ, Haydar SEVEN, Necmettin YILMAZ and 14th Regional Directorate of Nature Conservation and National Parks of the Turkish Ministry of Agriculture and Forestry, Hakkari Branch Office for their helps during the field works. This work was financially supported by the Scientific Research Project by Hakkari University (Project No. FM19BAP2).

Ethics committee approval: This study was conducted in accordance with ethical standards for animal experiments. Legal research ethics committee approval was obtained from the Hakkari University Animal Experiments Ethics Committee (No: 20/03/2019-2459).

Conflict of interest: The authors declare that there is no conflict of interest.

Author Contributions: Conception – C.Y., Ç.I., E.B., N.Ü., A.A.; Design – C.Y., Ç.I., E.B., N.Ü., A.A.; Supervision – C.Y., Ç.I., E.B., N.Ü., A.A.; Fund – C.Y., Ç.I., E.B., N.Ü., A.A.; Materials – C.Y., Ç.I., E.B., N.Ü., A.A.; Data Collection and Processing – C.Y., Ç.I., E.B., N.Ü., A.A.; Analysis Interpretation – C.Y., Ç.I., E.B., N.Ü., A.A.; Literature Review – C.Y., Ç.I., E.B., N.Ü., A.A.; Writing – C.Y., Ç.I., E.B., N.Ü., A.A.; Critical Review – C.Y., Ç.I., E.B., N.Ü., A.A.

References

Afsar, M., Afsar, B., & Arıkan, H. (2015). Classification of the mountain frogs of the Bercelan Plateau (Hakkari), east Anatolia (Turkey). *Herpetozoa*, 28, 15-27.

Arribas, O., Candan, K., Kurnaz, M., Kumlutaş, Y., Caynak, E.Y., & Ilgaz, Ç. (2022a). A new cryptic species of the *Darevskia parvula* group from NE Anatolia (Squamata, Lacertidae). *Organisms Diversity & Evolution*, 22, 475-490. https://doi.org/10.1007/s13127-022-00540-4

Arribas, O., Candan, K., Kornilios, P., Ayaz, D., Kumlutaş, Y., Gül, S., … & Ilgaz, Ç. (2022b). Revising the taxonomy of *Darevskia valentini* (Boettger, 1892) and *Darevskia rudis* (Bedriaga, 1886) (Squamata, Lacertidae): a Morpho-Phylogenetic integrated study in a complex Anatolian scenario. *Zootaxa*, 5224, 001-068. https://doi.org/10.11646/zootaxa.5224.1.1

Baran, İ., & Gruber, U. (1982). Taxonomische unterschungen an Turkischen Gekkoniden. *Spixiana*, 5, 109-138.

Baran, İ., & Öz, M. (1985): Anadolu *Agama stellio* (Agamidae, Reptilia) Populasyonlarının Taksonomik Araştırılması. *Doğa Bilim Dergisi A2*, 9, 61-169.

Baran İ., & Atatür, M. K. (1998). Turkish Herpetofauna (Amphibians and Reptiles). Ankara, Republic of Turkey Ministry of Environment, 214 pp.

Baran, İ., Avcı, A., Kumlutaş, Y., Olgun, K., & Ilgaz, Ç. (2021). Türkiye Amfibi ve Sürüngenleri. Ankara, Türkiye, Palme Yayınları, 230 pp.

Başoğlu, M., & Özeti, N. (1973). Türkiye Amfibileri. İzmir. Ege Üniversitesi Fen Fakültesi Kitaplar Serisi, 155 pp.

Başoğlu, M., & Baran, İ. (1977). Türkiye Sürüngenleri, Kısım I. Kaplumbağa ve Kertenkeleler. İzmir, Türkiye, Ege Üniversitesi Basımevi, 272 pp.

Başoğlu, M., & Baran, İ. (1980). Türkiye Sürüngenleri, Kısım II. Yılanlar. İzmir, Türkiye, Ege Üniversitesi Basımevi, 218 pp.

Bardeh, F.G., Ashrafzadeh, M.R., Segherloo, I.H., & Rahimi, R. (2021). Modelling habitat suitability and connectivity of the Caspian pond turtle (*Mauremys caspica*) in Central Zagros, Iran. *Journal of Wildlife and Biodiversity*, 5(2), 1-14. https://doi.org/10.22120/jwb.2020.131961.1170

Berglind, S.A. (2000). Demography and management of relict sand lizard *Lacerta agilis* populations on the edge of extinction. *Ecological Bulletin*, 48, 123-142. https://doi.org/10.2307/20113253

Bozkurt, E., & Olgun, K. (2020). Taxonomic investigation of the genus *Ablepharus* (Sauria; Scincidae) with molecular and morphological methods in Anatolian populations. *Turkish Journal of Zoology*, 44, 134-145. https://doi.org/10.3906/zoo-1911-14

Demirsoy, A. (1996). Genel ve Türkiye Zoocoğrafyası "Hayvan Cografyası". Ankara, Metaksan A.Ş., 630 pp.

Domeneghetti, D., Marta, S., & Sbordoni, V. (2014). A modeling approach for the distribution of two Reptiles species: *Mediodactylus kotschyi* and *Zamenis situla*. In Atti X Congresso Nazionale Societas Herpetologica Italica pp. 203-205.

Eiselt, J., Darevsky, I.S., & Schmidtler, J.F. (1992). Untersuchungen an Felseidechsen (*Lacerta saxicola* - Komplex; Reptilia: Lacertidae) in der

östlichen Türkei. 1. *Lacerta valentini* Boettger. *Annalen des Naturhistorischen Museums in Wien Serie*, 93, 1-18.

Fritz, U., Ayaz, D., Buschbom, J., Kami, H.G., Mazanaeva, L.F., Aloufi, A.A., …& Hundsdörfer, A. K. (2008). Go east: phylogeographies of *Mauremys caspica* and *M. rivulata* – discordance of morphology, mitochondrial and nuclear genomic markers and rare hybridization. *Journal of Evolutionary Biology*, 21, 527-540. https://doi.org/10.1111/j.1420-9101.2007.01485.x

Gül, Ç., & Tosunoğlu, M. (2011). External morphological and osteological features of Turkish populations of *Laudakia stellio* (Linnaeus, 1758). *Herpetozoa*, 24, 73-88.

Hakkari İl Kültür ve Turizm Müdürlüğü 2022. Hakkari'nin Coğrafik Özellikleri. Retrieved from: https://hakkari.ktb.gov.tr/TR-159078/hakkarinin-konumu.html (accessed 7 February 2023).

IUCN. (2021). The IUCN Red List of Threatened Species. Version 2021-3. URL:https://www.iucnredlist.org.

Jablonski, D., Kukushkin, O., Avcı, A., Bunyatova, S., Kumlutaş, Y., Ilgaz, Ç., … & Jandzik, D. (2019). Biogeography of *Elaphe sauromates* (Pallas, 1814), with a description of a new rat snake species. *PeerJ*, 7, e6944. https://doi.org/10.7717/peerj.6944

Kafimola, S., Azimi, M., Saberi-Pirooz, R., Ilgaz, Ç., Kashani, G. M., Kapli, P., & Ahmadzadeh, F. (2023). Diversification in the mountains: Evolutionary history and molecular phylogeny of Anatolian rock lizards. *Molecular Phylogenetics and Evolution*, 180, 107675. https://doi.org/10.1016/j.ympev.2022.107675

Karakasi, D., Ilgaz, Ç., Kumlutas, Y., Candan, K., Gu̇çlu̇, Ö., Kankılıc, T., … & Poulakakis, N. (2021). More evidence of cryptic diversity in Anatololacerta species complex Arnold, Arribas and Carranza, 2007 (Squamata: Lacertidae) and re-evaluation of its current taxonomy. *Amphibia-Reptilia*, 42, 201-216. https://doi.org/10.1163/15685381-bja10045

Karger, D.N., Conrad, O., Böhner, J., Kawohl, T., Kreft, H., Soria-Auza, R. W., … & Kessler, M. (2017). Climatologies at high resolution for the earth's land surface areas. *Scientific Data*, 4(1), 1–20. https://doi.org/10.1038/sdata.2017.122

Kornilios, P., Ilgaz, Ç., Kumlutaş, Y., Giokas, S., Fraguedakis-Tsolis, S., & Chondropoulos, B. (2011). The role of Anatolian refugia in herpetofaunal diversity: An mtDNA analysis of *Typhlops vermicularis* Merrem, 1820 (Squamata, Typhlopidae). *Amphibia-Reptilia*, 32, 351-363. https://doi.org/10.1163/017353711X579858

Kotsakiozi, P., Jablonski, D., Ilgaz, Ç., Kumlutaş, Y., Avcı, A., Meiri, S., … & Poulakakis, N. (2018). Multilocus phylogenyand coalescent species delimitation in Kotschy's gecko, *Mediodactylus kotschyi*: hidden diversity and cryptic species. *Molecular Phylogenetics and Evolution*, 125, 177-187. https://doi.org/10.1016/j.ympev.2018.03.022

Kurnaz, M., Eroğlu, A. İ., & Kutrup, B. (2019). Distribution and habitat preference of the *Mauremys capsica* Gmelin, 1774 in Turkey. *Latest Trends in Zoology and Entomology Sciences*, 7, 49-61.

Kurnaz, M., & Şahin, M.K. (2021). Contribution to the Taxonomic Knowledge of *Acanthodactylus* (Squamata, Lacertidae): Description of a New Lacertid Lizard Species from Eastern Anatolia, Turkey. *Journal of Wildlife and Biodiversity*, 5, 100-119. https://doi.org/10.22120/jwb.2021.523523.1214

Kurnaz, M., Şahin, M.K., & Eroğlu, A.İ. (2022). Hidden diversity in a narrow valley: Description of new endemic Palearctic rock lizard *Darevskia* (Squamata: Lacertidae) species from northeastern Turkey. *Zoological Studies*, 61, 44. https://doi.org/10.6620/ZS.2022.61-44

Leviton, A.E., Anderson, S.C., Adler, K., & Minton, S.A. (1992). Handbook to Middle East Amphibians and Reptiles. Ohio, USA, Oxford press, 252 pp.

Mahlow, K., Frank, T., Josef, F.S., & Johannes, M. (2013). An annotated checklist, description and key to the dwarf snakes of the genus *Eirenis* Jan, 1863 (Reptilia: Squamata: Colubridae), with special emphasis on the dentition. *Vertebrate Zoology*, 63, 41-85. https://doi.org/10.3897/vz.63.e31413

Mertens, R. (1953). Amphibien und Reptilien aus der Türkei. İstanbul Üniversitesi Fen Fakültesi Mecmuası Seri B 17, 41-75.

Osorio-Olvera, L., Lira-Noriega, A., Soberon, J., Peterson, A. T., Falconi, M., Contreras-Díaz, R. G., … & Barve, N. (2020). ntbox: An r packagewith graphical user interface for modelling and evaluating multidimensional ecological niches. *Methods in Ecology and Evolution*, 11, 1199-1206. https://doi.org/10.1111/2041-210X.13452

Palmer, M.A., Reidy Liermann, C.A., Nilsson, C., Flörke, M., Alcamo, J., Lake, P.S., & Bond, N. (2008). Climate change and the world's river basin: anticipating management options. *Frontiers in Ecology and Evolutions*, 6, 81-89. https://doi.org/10.1890/060148

Phillips, S.J., Anderson, R.P., & Schapire, R.E. (2006). Maximum entropy modeling of species geographic distributions. *Ecological Modelling*, 190, 231–259. https://doi.org/10.1016/j.ecolmodel.2005.03.026

Senczuk, G., Colangelo, P., De Simone, E., Aloise, G., & Castiglia, R. (2017). A combination of long term fragmentationand glacial persistence drove theevolutionary history of the Italian wall lizard *Podarcis siculus*. *BMC Evolutionary Biology*, 17, 6. https://doi.org/10.1186/s12862-016-0847-1

Sindaco, R., Riccardo, N., & Benedetto, L. (2014). Catalogue of Arabian reptiles in the collections of the "La Specola" Museum, Florence. Scripta Herpetologica. *Studies on Amphibians and Reptiles in honour of Benedetto Lanza*, 137-164.

Şahin, M.K. (2021). The potential distribution and a new locality record of Roughtail Rock Agama (*Stellagama stellio*) from northwestern Anatolıa. Scientific Reports in Life Sciences, 2(2), 39–48.

Tarkhnishvili, D., Gabelaia, M., Kandaurov, A., Bukhnikashvili, A., & Iankoshvili, G. (2017). Isolated population of the Middle Eastern Phoenicolacerta laevis from the Georgian Black Sea Coast, and its genetic closeness to populations from southern Turkey. *Zoology in the Middle East*, 63, 311-315. https://doi.org/10.1080/09397140.2017.1361191

Turtle Taxonomy Working Group [Rhodin, A. G. J., Iverson, J. B., Bour, R., Fritz, U., Georges, A., Shaffer, H. B., van Dijk, P.P.]. (2021). Turtles of the World: Annotated Checklist and Atlas of Taxonomy, Synonymy, Distribution, and Conservation Status (9th Ed.). In: Rhodin, A. G. J., Iverson, J. B., van Dijk, P. P., Stanford, C. B., Goode, E. V., Buhlmann, K. A., Mittermeier R. A. (Eds.). Conservation Biology of Freshwater Turtles and Tortoises: A Compilation Project of the IUCN/SSC Tortoise and Freshwater Turtle Specialist Group. *Chelonian Research Monographs*, 8, 1-472.

Uetz, P., Freed, P., & Hošek, J. (2022). Species numbers by higher taxa. The Reptile Database. Retrieved from: http://www.reptile-database.org/

Yılmaz, C., Ilgaz, Ç., Üzüm, N., & Avcı, A. (2021). First record of Jan's Cliff Racer, *Platyceps rhodorachis* (Jan, 1863) (Serpentes: Colubridae) in Turkey. *Zoology in the Middle East*, 67, 92-94. https://doi.org/10.1080/09397140.2020.1865666

Supplemental Tables

Table A1. The morphometric measurements (in mm) of *Mauremys caspica* specimens examined in this study.

	Female
Straight Carapace Length	180.34
Curved Carapace Length	196.44
Maximum Carapace Width	121.04
Maximum Carapace Height	66.84
Midline Plastron Length	167.19
Plastron Width from Humeral	83.34
Plastron Width from Abdominal	84.50
Gular Suture Length	19.64
Humeral Suture Length	17.61
Pectoral Suture Length	23.92
Abdominal Suture Length	43.33
Femoral Suture Length	38.97
Anal Suture Length	14.19
Nuchal Length	10.50
Nuchal Width	11.87

Table A2. The morphometric measurements (left/right, mm) and pholidosial features (left/right)of *Mediodactylus orientalis* specimens examined in this study.

	Female	**Juvenil**
Supralabials	9/9	9/9
Sublabialias	8/8	8/8
Number of rows of longitudinal dorsal tubercules	10	9
Ventrals	24	23
Number of scales under the 4th toe of the hind foot	18/18	17/17
Snout-vent Length	47.33	25.38
Tail Length	-	27.68
Total Body Length	-	53.06
Head Length	11.71	6.64
Head Width	9.16	4.79
Distance between Nostril and Eye	3.15/3.32	-/-
Head Height	5.45	2.98
Vertical Eye Diameter	1.91/1.95	-/-
Distance between Eye and Ear Opening	3.82/3.78	-/-
Vertical Ear Diameter	1.97/1.79	-/-

Table A3. Their indexes and the morphometric measurements (left/right, mm), pholidosial features (left/right) of *Laudakia stellio* specimens examined in this study.

	Male	Male (Subadult)	Juvenil
Supralabials	11/11	12/11	11/12
Sublabialias	12/12	12/11	11/11
Ventrals	41	39	42
Subdigital Lamellae Underneath the Fourth Toe of the Hindlimb	21/20	20/20	20/20
Subdigital Lamellae underneath the Third Finger of the Forelimb	18/17	17/18	18/17
Scales in the 5th Ring from the Beginning of the Tail	18	16	19
Ventral Glandular Scales	32	30	30
Preanal Glandular Scales	34	33	32
Total Body Length	278.97	210.50	97.36
Snout-vent Length	131.26	94.70	41.70
Tail Length	147.71	115.80	55.66
Head Length	35.52	24.85	11.85
Head Width	39.21	26.42	11.04
Dorsal Spot Length	15.33	10.60	3.50
Dorsal Spot Width	10.20	6.26	12.90
Forelimb Length	55.64	41.04	19.26
Hindlimb Length	82.10	60.58	28.52
Head Height	16.98	12.00	6.85
Tail Length / Snout-vent Length	1.12	1.22	1.33
Head Index	90.59	94.06	107.34
Head Flatness Index	209.19	207.08	172.99
Head Length Index	27.06	26.24	28.42
Snout-vent Length / Head Length	3.69	3.81	3.52
Head Length / Head Width	0.90	0.94	1.07
Hindlimb Length / Forelimb Length (Foot Ratio)	1.47	1.48	1.48

Supplemental Figures

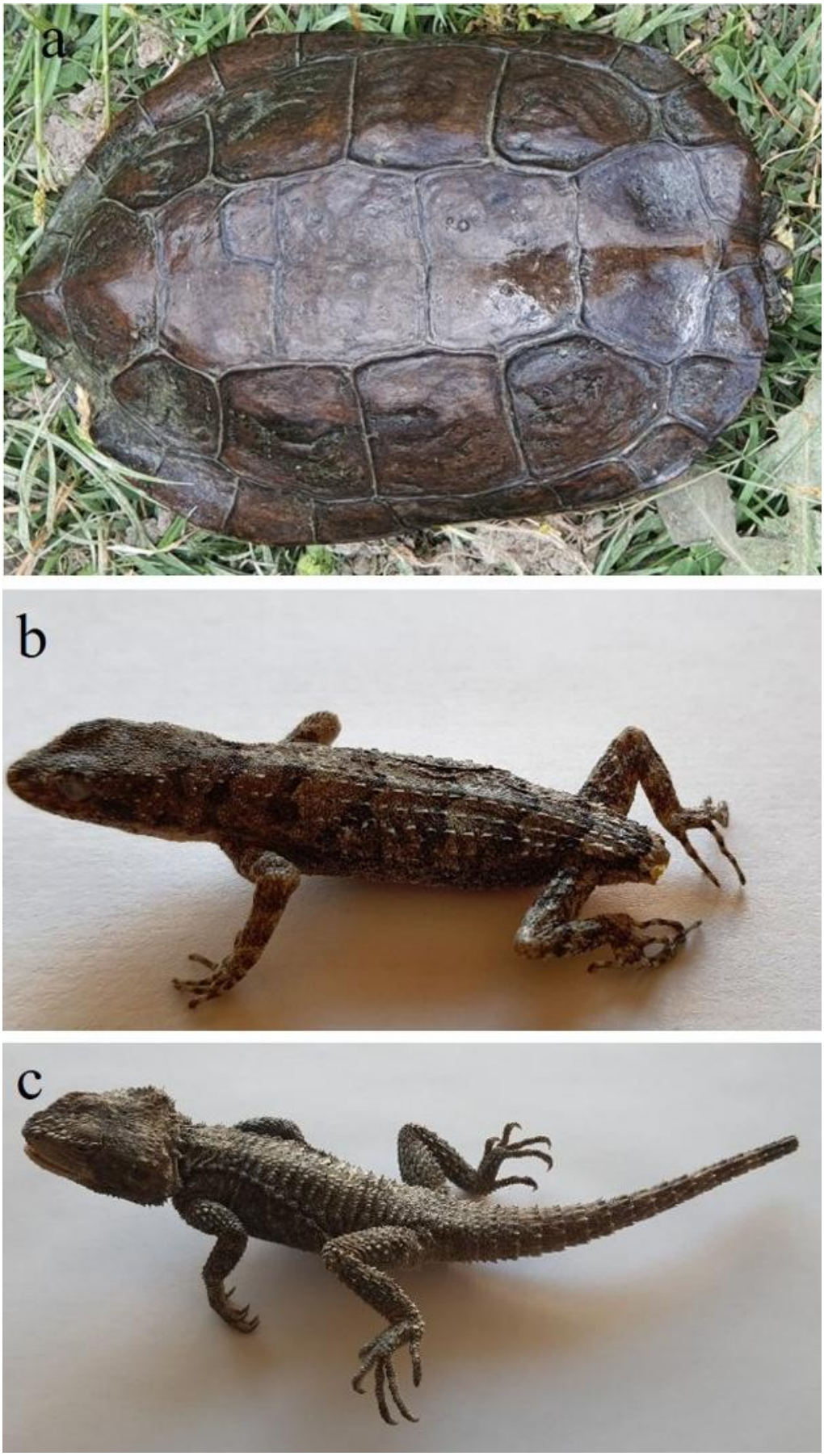

Figure A1. The reptiles recorded for the first time from Hakkari province. (a) *Mauremys caspica*, (a) *Mediodactylus orientalis*, (a) *Laudakia stellio*.

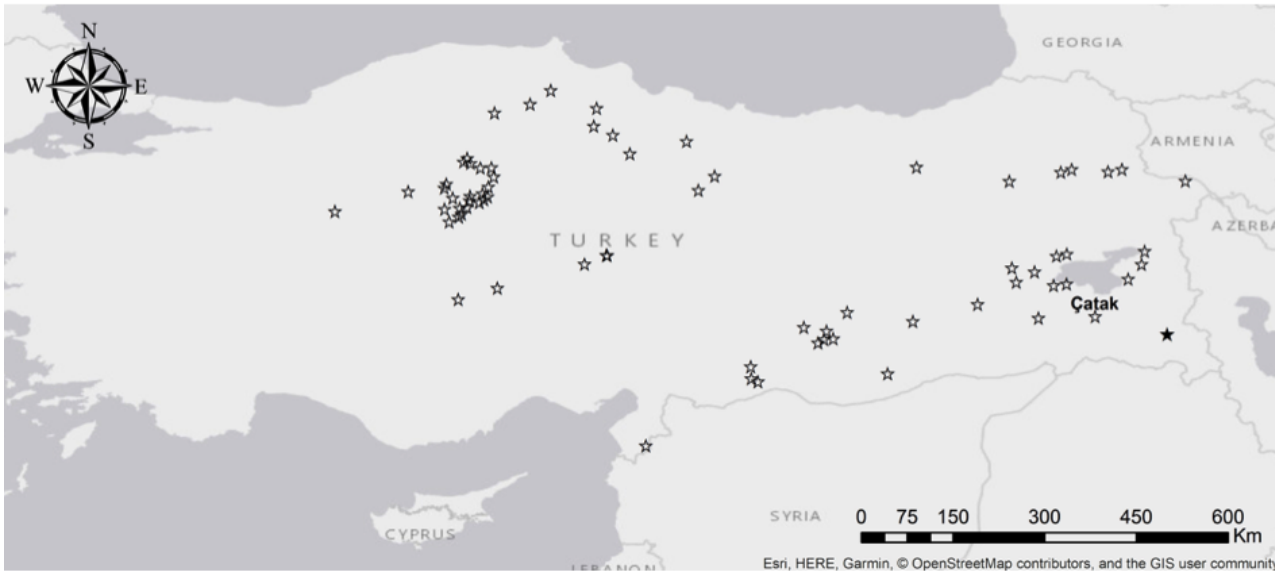

Figure A2. Distribution of *Maureymys caspica*, the known distribution according to the literature data, with a black star for the new locality. Data from Teynie (1981), Fritz and Freytag (1993), Schweiger (1994), Taşkavak et al. (1998), Fritz et al. (2008), Tosunoğlu et al. (2010), Akman et al. (2018), Kurnaz et al. (2019), Akman et al. (2020) and Yıldız et al. (2021).

Akman, B., Yıldız, M.Z., Özcan, A.F., Bozkurt, M.A., İğci, N., & Göçmen, B. (2018). On the Herpetofauna of the East Anatolian Province of Bitlis (Turkey). *Herpetozoa* 31, 69-82.

Akman, B., Çakmak, M., & Yıldız, M.Z. (2020). On the Herpetofauna of the Central Anatolian Province of Kırıkkale (Turkey) (Amphibia; Reptilia). *Acta Biologica Turcica*, 33, 70-78.

Fritz. U., & Freytag, O. (1993): The distribution of *Mauremys* in Asia Minor, and first record of *M. caspica caspica* (Gmelin, 1774) for the internally drained central basin of Anatolia (Testudines, Cryptodira, Bataguridae). *Herpetozoa*, 6(3/4), 97-103.

Fritz, U., Ayaz, D., Buschbom, J., Kami, H.G., Mazanaeva, L.F., Aloufi, A.A., …& Hundsdörfer, A.K. (2008). Go east, phylogeographies of *Mauremys caspica* and *M. rivulata* – discordance of morphology, mitochondrial and nuclear genomic markers and rare hybridization. *Journal of Evolutionary Biology*, 21, 527-540. https://doi.org/10.1111/j.1420-9101.2007.01485.x

Kurnaz, M., Eroğlu, A.İ., & Kutrup, B. (2019). Distribution and habitat preferences of the *Mauremys caspica* Gmelin, 1774 in Turkey. Chapter 3, 7, 49-61. In Latest Trends in Zoology and Entomology Sciences (eds. Ganguly). AkiNik Publications, New Delhi.

Schweiger, M. (1994). Ergänzende Bemerkungen zur Verbreitung von *Mauremys caspica* (Gmelin, 1774) in Kleinasien. *Herpetozoa*, 7(1/2), 67-70.

Taşkavak, E., Ceylan, T., Ülker, C., & Ergev, B. (1998). New records of *Mauremys caspica caspica* (Gmelin, 1774) from Kızılırmak Basin and the Ankara and Kayseri vicinities. *Emys*, 5(5), 19-28.

Teynie, A. (1981). Observation's herpétologiques en Turquie, 2ème Partie. *Bulletin de la Société. Herpétologique de France,* 58, 21-30.

Tosunoğlu, M., Gül, Ç., Dinçaslan, Y.E., & Uysal, İ. (2010). The herpetofauna of the east Turkish province of Iğdır. *Herpetozoa*, 23, 92-94.

Yıldız, M.Z., İğci, N., & Akman, B. (2021). Herpetofaunal inventory of Van Province, eastern Anatolia. *Journal of Threatened Taxa*, 13, 17670-17683.

Figure A3. Distribution of *Mediodactylus orientalis*, the known distribution according to the literature data, with a black star for the new locality. Data from Baran (1980), Uğurtaş et al. (2000), Baran et al. (2001), Uğurtaş et al. (2007), Hür et al. (2008), Afsar et al. (2011), Cihan and Tok (2014), Özcan and Üzüm (2014), Ege et al. (2015), Çiçek et al. (2015a), Afsar et al. (2017), Sarıkaya et al. (2017a, 2017b), Arslan et al. (2018), Çakmak (2018), Yıldız et al. (2019), Boran et al. (2020) and Candan et al. (2020).

Afsar, M., Ayaz, D., Afsar, B., Çiçek, K., & Tok, C.V. (2011): *Cyrtopodion* (*Mediodactylus*) *kotschyi* (Steindahner, 1870) from Çivril, Denizli (western Turkey). *Herpetozoa*, 24, 98-101.

Afsar, M., Çiçek, K., & Tok, C.V. (2017). More data on the distribution and morphology of *Mediodactylus kotschyi bolkarensis* (ROsLER, 1994), from Central Anatolia, Turkey. *Herpetozoa*, 30, 49-58.

Arslan, D., Olivier, A., Yaşar, Ç., Ismail, İ.B., Döndüren, Ö., Ernoul, L., …& Çiçek, K. (2018). Distribution and current status of herpetofauna in the Gediz Delta (Western Anatolia, Turkey). *Herpetology Notes*, 11, 1-15.

Baran, İ. (1980). Doğu ve Güneydoğu Anadolu'nun kaplumbağa ve kertenkele faunası. *Ege Üniversitesi Fen Fakültesi Dergisi*, 4, 203-219.

Baran, İ., Kumlutaş, Y., Olgun, K., Ilgaz, Ç., & Kaska, Y. (2001). The herpetofauna of the vicinity of Silifke. *Turkish Journal of Zoology*, 25. 245-249. https://journals.tubitak.gov.tr/zoology/vol25/iss3/11

Boran, B., Uysal, İ., & Tosunoğlu, M. (2020). Herpetofaunal diversity of Çanakkale southwest coastal zones. *Turkish Journal of Bioscience and Collections*, 4. 122-128. https://doi.org/10.26650/tjbc.20200055

Candan, K., Caynak Yildirim, E., Kumlutaş, Y., Özender, Ö., & Ilgaz, Ç. (2020) Meke Maarı (Konya) civarının herpetofaunası. *Balıkesir Üniversitesi Fen Bilimleri Enstitüsü Dergisi*, 22, 55-66.

Cihan, D., & Tok, C.V. (2014): Herpetofauna of the vicinity of Akşehir and Eber (Konya, Afyon), Turkey. *Turkish Journal of Zoology*, 38, 234-241. https://doi.org/10.3906/zoo-1309-33

Çakmak, Ş. (2018): Doğu ve Güneydoğu Anadolu Bölgesindeki bazı illerin Gekkonidae Faunası. (571960). Retrieved from https://tez.yok.gov.tr/UlusalTezMerkezi/tezSorguSonucYeni.jsp

Çiçek, K., Afşar, M., Kumaş, M., Ayaz, D., & Tok, C.V. (2015). Age growth and longevity of Kotschy s Gecko *Mediodactylus kotschyi* Steindachner 1870 Reptilia Gekkonidae from Central Anatolia Turkey. *Acta Zoologica Bulgarica*, 67, 399-404.

Ege, O., Yakin, B.Y., & Tok, C.V. (2015). Herpetofauna of the Lake District around Burdur. *Turkish Journal of Zoology*, 39, 1164-1168. https://doi.org/10.3906/zoo-1502-7

Hür, H., Uğurtaş, İ.H., & İşbilir, A. (2008): The amphibian and reptile species of Kazdağı National Park. *Turkish Journal of Zoology*, 32, 359-362. https://journals.tubitak.gov.tr/zoology/vol32/iss3/16

Özcan, S., & Üzüm, N. (2014). The herpetofauna of Madran Mountain (Aydın, Turkey). *Turkish Journal of Zoology*, 38, 108-113. https://doi.org/10.3906/zoo-1304-26

Sarıkaya, B., Karıs, M., Bozkurt, M.A., Yıldız, M.Z., & Göçmen, B. (2017a): The Herpetofauna of Niğde Province. 3rd International Congress on Zoology and Technology, Nevşehir Hacı Bektaş Veli Üniversity, 12-15 July 20 p.

Sarıkaya, B., Yıldız, M.Z., & Sezen, G. (2017b). The Herpetofauna of Adana Province (Turkey). *Commagene Journal of Biology*, 1, 1-11.

Uğurtaş, İ.H., Yıldırımhan, S.H., & Öz, M. (2000). Herpetofauna of the eastern region of the Amanos Mountain (Nur). *Turkish Journal of Zoology*, 24, 257-261.

Uğurtaş, İ.H., Kaya, R.S., & Akkaya, A. (2007). The herpetofauna of the islands in Uluabat Lake (Bursa). *Ekoloji*, 17, 7-10.

Yıldız, M.Z., Sarıkaya, B., & Bozkurt, M.A. (2019): The Herpetofauna of the province of Hatay (East Mediterranean Turkey). *Biological Diversity and Conservation*, 12. 197-205. https://doi.org/10.5505/biodicon.2019.93685

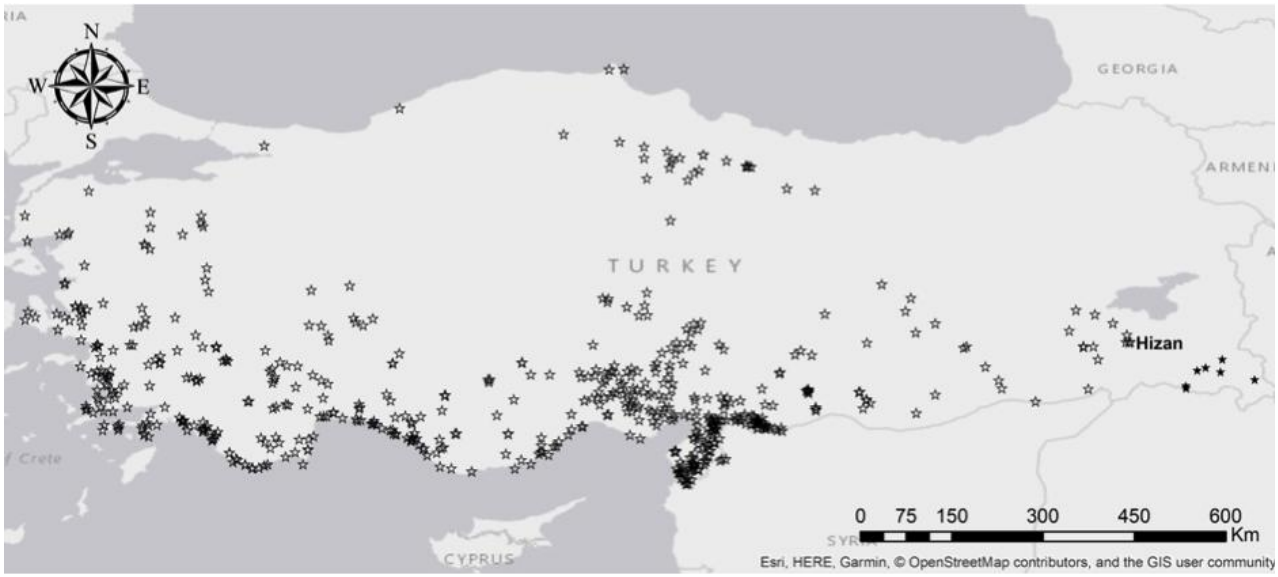

Figure A4. Distribution of *Laudakia stellio*, the known distribution according to the literature data, with a black star for the new localities. Data from Başoğlu and Hellmich (1970), Clark and Clark (1973), Baran (1980), Teynie (1987), Baran et al. (1989), Mulder (1995), Budak et al. (1998), Tok (1999), Uğurtaş et al. (2000), Düşen and Öz (2001), Kumlutaş et al. (2001), Uğurtaş et al. (2001), Erdoğan et al. (2002), Franzen and Wallach (2002), Tok et al. (2002), Göçmen et al. (2003), Geniez et al. (2004), Kumlutaş et al (2004), Lo Cascio and Masseti (2004), Almog et al. (2005), Kete et al. (2005), Kır (2005), Afsar (2006), Göçmen et al. (2007), Kumlutaş et al. (2007), Olgun et al. (2007), Akelma (2008), Hür et al. (2008), Eser (2009), Göçmen et al. (2009), Yıldız et al. (2009), Arıkan et al. (2010), Gül et al. (2010), Gül (2011), Gül and Tosunoğlu (2011), Tosunoğlu and Gül (2011), Özcan (2012), Ünal (2012), Cumhuriyet (2014), Göçmen et al. (2014), Karış and Göçmen (2014), Kumaş and Ayaz (2014), Tok and Çiçek (2014), Çiçek et al. (2015b), Ege et al. (2015), Kucharzewski (2015, 2016), Kumlutaş et al. (2015), Baycan and Tosunoğlu (2017), Göçmen et al. (2017), Sarıkaya et al. (2017b), Akman et al. (2018), Avcı et al. (2018), Bozkurt (2018), Günay et al. (2018) Mermer (2018), Şahin and Afsar (2018), Afsar et al. (2019), Yıldız et al. (2019), Gidiş and Başkale (2020), Yıldız (2020) and Bülbül et al. (2021).

Afsar, M. (2006). Sultandağları'nın Herpetofaunası (180023). Retrieved from https://tez.yok.gov.tr/UlusalTezMerkezi/tezSorguSonucYeni.jsp

Afsar, M., Yakın, B.Y., Çiçek, K., & Ayaz, D. (2019). A new subspecies of Ottoman viper, *Montivipera xanthina* (Gray, 1849), (Squamata, Viperidae) from Geyik Mountains, Mediterranean Turkey. *Ecologica Montenegrina*, 22, 214-225. https://doi.org/10.37828/em.2019.22.17

Akelma, R. (2008). Diyarbakır yöresi kurbağa ve sürüngen türlerinin araştırılması, Diyarbakır herpetofaunası (252769). Retrieved from https://tez.yok.gov.tr/UlusalTezMerkezi/tezSorguSonucYeni.jsp

Akman, B., Yıldız, M.Z., Özcan, A.F., Bozkurt, M.A., İğci, N., & Göçmen, B. (2018). On the Herpetofauna of the East Anatolian Province of Bitlis (Turkey). *Herpetozoa*, 31, 69-82.

Almog, A., Bonen, H., Herman, K., & Werner, Y.L. (2005). Subspeciation or none? The Hardun in the Aegean (Reptilia, Sauria, Agamidae, *Laudakia stellio*). *Journal of Natural History*, 39, 567-586. https://doi.org/10.1080/00222930400001293

Arıkan, H., & Çiçek, K. (2010). Morphology of peripheral blood cells from various species of Turkish herpetofauna. Acta Herpetologica 5, 179-198.

Avcı, A., Üzüm, N., Bozkurt, E., & Olgun, K. (2018). The herpetofauna of poorly known Tunceli province (Turkey). *Russian Journal of Herpetology*, 25, 17-24. https://doi.org/10.30906/1026-2296-2018-25-1-17-24

Baran, İ. (1980). Doğu ve Güneydoğu Anadolu'nun kaplumbağa ve kertenkele faunası. *Ege Üniversitesi Fen Fakültesi Dergisi*, 4, 203-219.

Baran, İ., Kasparek, M., & Öz, M. (1989). On the distribution of four species of *Agama* (Agamidae) in Turkey. *Zoology in the Middle East*, 3, 37-46. https://doi.org/10.1080/09397140.1989.10637572

Başoğlu, M., & Hellmich, W. (1970). Amphibien und reptilien aus dem östlichen Anatolien. *Ege Üniversitesi Fen Fakültesi İlmi Raporlar Serisi*, 93, 1-25.

Baycan, B., & Tosunoğlu, M. (2017). The catalog of Amphibia and Reptilia specimens in the Çanakkale Onsekiz Mart University Zoology Museum (COMU-ZM). *Turkish Journal of Bioscience and Collections*, 1, 38-55.

Bozkurt, M.A. (2018). Şanlıurfa Kızılkuyu Yaban Hayatı Koruma ve Geliştirme Sahasının herpetofaunası. Unpublished M.Sc. Dissertation. University of the Harran, Şanlıurfa.

Budak, A., Tok, C.V., & Mermer, A. (1998). A report on reptiles collected from Kumluca-Kalkan (Antalya), Turkey. *Turkish Journal of Zoology*, 22, 185-189.

Bülbül, U., Koç-Gür, H., Özkan, H., & Zaman, E. (2021). Morphological data and a locality record of *Stellagama stellio* (L. 1758) (Squamata, Agamidae) in Turkey. *Academic Research and Reviews in Science and Mathematics*, 1, 5-19.

Clark, R.J., & Clark, E.D. (1973). Report on a collection of Amphibians and Reptiles from Turkey. *Occasional Papers of the California Academy of Science,* 104, 1-62.

Cumhuriyet, O. (2014). Güllük Körfezi ve civarının herpetofaunası. Unpublished M.Sc. Dissertation. University of the Ege, İzmir.

Çiçek, K., Cumhuriyet, O., Bayrakçı, Y., & Ayaz, D. (2015). New locality records of *Eumeces schneideri* (Daudin, 1802) (Sauria, Scincidae) from western Anatolia, Turkey. *Turkish Journal of Zoology*, 39, 987-990. https://doi.org/10.3906/zoo-1410-5

Düşen, S., & Öz, M. (2001). A study on the feeding biology of *Laudakia* (=*Agama*) *stellio* (L. 1758) (Lacertilia, Agamidae) populations in the Antalya Region. *Turkish Journal of Zoology*, 25, 177-181.

Ege, O., Yakın, B.Y., & Tok, C.V. (2015). Herpetofauna of the Lake District around Burdur. *Turkish Journal of Zoology*, 39, 1164-1168. https://doi.org/10.3906/zoo-1502-7

Erdoğan, A., Öz, M., Sert, H., & Tunç, M.R. (2002). Antalya-Yamansaz Gölü ve yakın çevresinin avifaunası ve herpetofaunası. *Ekoloji Çevre Dergisi*, 11, 33-39.

Eser, Ö. (2009). Başkomutan Tarihi Milli Parkı'nın (Kocatepe Bölümü) herpetofaunası. Unpublished M.Sc. Dissertation. University of the Afyon Kocatepe, Afyon.

Franzen, M., & Wallach, V.A. (2002). New *Rhinotyphlops* from Southeastern Turkey (Serpentes, Typhlopidae). *Journal of Herpetology*, 36, 176-184. https://www.jstor.org/stable/1565989

Geniez, P., Geniez, M., & Viglione, J. (2004). New record suggests sympatry of *Lacerta pamphylica* Schmidtler, 1975 with L. trilineata Bedriaga, 1886. *Herpetozoa*, 17, 183-184.

Gidiş, M., & Başkale, E. (2020). The herpetofauna of Honaz Mountain National Park (Denizli province, Turkey) and threatening factors. *Amphibian & Reptile Conservation*, 14, 147-155.

Göçmen, B., Tosunoğlu, M., & Taşkavak, E. (2003). A taxonomic comparison of the Hardun, *Laudakia stellio* (Reptilia, Agamidae), population of southern Turkey (Hatay) and Cyprus. *Zoology in the Middle East*, 28, 25-32. https://doi.org/10.1080/09397140.2003.10637953

Göçmen, B., Nilson, G., Yıldız, M.Z., Arıkan, H., Yalçınkaya, D., & Akman, B. (2007). On the occurrence of the Black Cat Snake, *Telescopus nigriceps* (Ahl, 1924) (Serpentes, Colubridae) from the Southeastern Anatolia, Turkey with some taxonomical comments. *North-Western Journal of Zoology*, 3, 81-95.

Göçmen, B., Franzen, M., Yıldız, M.Z., Akman, B., & Yalçınkaya, D. (2009). New locality records of eremial snake species in southeastern Turkey (Ophidia, Colubridae, Elapidae, Typhlopidae, Leptotyphlopidae). *Salamandra*, 45, 110-114.

Göçmen, B., Geçit, M., & Karış, M. (2014). New locality records of the Striped Dwarf Snake, *Eirenis lineomaculatus* Schmidt, 1939 (Squamata, Ophidia, Colubridae) in Turkey. *Biherean Biologist*, 8, 126-128.

Göçmen, B., Mebert, K., Karış, M., Oğuz, M.A., & Ursenbacher, S. (2017). A new population and subspecies of the critically endangered Anatolian meadow viper *Vipera anatolica* Eiselt and Baran, 1970 in eastern Antalya province. *Amphibia-Reptilia*, 38, 289-305. https://doi.org/10.1163/15685381-00003111

Gül, Ç, Dinçaslan, Y.E., & Tosunoğlu, M. (2010). A new locality of the Starred Agama *Laudakia stellio* (Linnaeus, 1758), from Sinop, north Anatolia. *Herpetozoa*, 23, 98-100.

Gül, Ç. (2011). Türkiye *Laudakia stellio* (Linnaeus, 1758) (Sauria, Agamidae) Populasyonları Üzerinde Morfolojik, Osteolojik, Hematolojik ve Ekolojik Araştırmalar Retrieved from (274971). https://tez.yok.gov.tr/UlusalTezMerkezi/tezSorguSonucYeni.jsp

Günay, U.K., Yakın, B., Kaplan, Ç., & Tok, C.V. (2018). Herpetofauna and Avifauna of in the Vicinity of Araplar Gorge (Skamandros Valley, Çanakkale). *Doğanın Sesi*, 2, 3-17.

Hür, H., Uğurtaş, İ.H., & İşbilir, A. (2008). The amphibian and reptile species of Kazdağı National Park. *Turkish Journal of Zoology*, 32, 359-362.

Karış, M., & Göçmen, B. (2014). A new data on the distribution of the Hatay Lizard, *Phoenicolacerta laevis* (Gray, 1838) (Squamata, Lacertidae) from the western Anatolia. *Biharean Biologist*, 8, 56-59.

Kete, R., Yılmaz, İ., Karakulak, S., & Yıldırım, A. (2005). Bafa Gölü çevresi herpetofaunasının çeşitliliği. *Anadolu Üniversitesi Bilim ve Teknoloji Dergisi*, 6, 87-96.

Kır, İ. (2005). Karataş Gölü (Burdur) ve çevresinin balık, amfibi ve sürüngen faunası. *Çevkor*, 14, 23-25.

Kucharzewski, C. (2015). Herpetologische Reiseeindrücke aus der Südwest-Türkei. *Sauria*, 37, 3-15.

Kucharzewski, C. (2016). Weiterer Beitrag zur Herpetologie der Südwest-Türkei. *Sauria*, 38, 37-56.

Kumaş, M., & Ayaz, D. (2014). Age determination and long bone histology in *Stellagama stellio* (Linnaeus, 1758) (Squamata, Sauria, Agamidae) populations in Turkey. *Vertebrate Zoology*, 64, 113-126. https://doi.org/10.3897/vz.64.e31466

Kumlutaş, Y., Ilgaz, Ç., & Durmuş, S.H. (2001). Herpetofauna of Spil Mountain (Manisa) and its vicinity, Results of field surveys. *Anadolu Üniversitesi Bilim ve Teknoloji Dergisi*, 2, 63-66.

Kumlutaş, Y., Öz, M., Durmuş, H., Tunç, M.R., Özdemir, A., & Düşen, S. (2004). On some lizard species of the Western Taurus Range. *Turkish Journal of Zoology*, 28, 225-236.

Kumlutaş Y., Arıkan, H., Ilgaz, Ç., & Kaska, Y. (2007). A new subspecies, *Eumeces schneiderii* barani n. ssp (Reptilia, Sauria, Scincidae) from Turkey. *Zootaxa*, 1387, 27-38. https://doi.org/10.11646/zootaxa.1387.1.2

Kumlutaş, Y., Uğurtaş, İ.H., Koyun, M., & Ilgaz, Ç. (2015). A new locality records of *Stellagama stellio* (Linnaeus, 1758) (Sauria, Agamidae) in Anatolia. *Russian Journal of Herpetology*, 22, 149-153.

Lo Cascio, P., & Masseti, M. (2004). Distributional records for some herpetofaunal species in the islands of SW Turkey, with notes on the diet of *Laudakia stellio*. *Herpetological Bulletin*, 87, 25-28.

Mermer, A. (2018). Amphibians and Reptiles of Olympos-Beydağları (Antalya, Turkey) National Park and Its Vicinity. *Commagene Journal of Biology*, 2, 19-22.

Mulder, J. (1995). Herpetological observations in Turkey (1987-1995). *Deinsea*, 2, 51-66.

Olgun, K., Avcı, A., Ilgaz, Ç., Üzüm, N., & Yılmaz, C. (2007). A new species of *Rhynchocalamus* (Reptilia, Serpentes, Colubridae) from Turkey. *Zootaxa*, 1399, 57-68. https://doi.org/10.5281/zenodo.175393

Özcan, S. (2012). Madran Dağı (Aydın)'ın herpetofaunası (316487). Retrieved from https://tez.yok.gov.tr/UlusalTezMerkezi/tezSorguSonucYeni.jsp

Sarıkaya, B., Karıs, M., Bozkurt, M.A., Yıldız, M.Z., & Göçmen, B. (2017). The herpetofauna of Niğde Province. 3rd International Congress on Zoology and Technology, Nevşehir Hacı Bektaş Veli Üniversity, 12-15 July 20 p.

Şahin, M. K., & Afsar, M. (2018). Evaluation of the reptilian fauna in Amasya Province, Turkey with new locality records. *Gazi University Journal of Science*, 31, 1007-1020.

Teynie, A. (1981). Observation's herpétologiques en Turquie, 2ème Partie. Bulletin de la Société. *Herpétologique de France*, 58, 21-30.

Teynie, A. (1987). Observations Herpetologiques en Turquie Iere Partie. Bulletin de la Société *Herpétologique de France*, 43, 9-18.

Tok, C.V. (1999). Reşadiye (Datça) Yarımadası kertenkeleleri hakkında (Gekkonidae, Agamidae, Chamaeleonidae, Lacertidae, Scincidae, Amphisbaenidae). *Turkish Journal of Zoology*, 23, 157-175.

Tok, C.V., Cihan, D., & Ayaz, D. (2002). A new record of *Macrovipera lebetina obtusa* (Viperidae) from south-eastern Anatolia. *Zoology in the Middle East*, 25, 23-26. https://doi.org/10.1080/09397140.2002.10637901

Tok, C.V., & Çiçek, K. (2014). Amphibians and reptiles in the province of Çanakkale (Marmara Region, Turkey). *Herpetozoa*, 27, 65-76.

Tosunoğlu, M., Gül, Ç. (2011). Hematological reference intervals of four agamid lizard species from Turkey. *Herpetozoa*, 24, 51-59.

Uğurtaş, İ.H., Yıldırımhan, S.H., & Öz, M. (2000). Herpetofauna of the eastern region of the Amanos Mountain (Nur). *Turkish Journal of Zoology*, 24, 257-261.

Uğurtaş, İ.H., Papenfuss, T.J., & Orlov, N.L. (2001). New record of *Walterinnesia aegyptia* Lataste, 1887 (Ophidia; Elapidae; Bungarinae) in Turkey. *Russian Journal of Herpetology*, 8, 231-237.

Ünal, N. (2012). Kale İlçesi ve çevresinin herpetofaunası (326993). Retrieved from https://tez.yok.gov.tr/UlusalTezMerkezi/tezSorguSonucYeni.jsp

Yıldız, M.Z., Akman, B., Göçmen, B., & Yalçınkaya, D. (2009). New locality records for the Turkish worm lizard, *Blanus strauchi aporus* (Werner, 1898) (Sauria, Amphisbaenidae) in Southeast Anatolia, Turkey. *North-Western Journal of Zoology*, 5, 379-385.

Yıldız, M.Z., Sarıkaya, B., Bozkurt, M.A. (2019). The Herpetofauna of the province of Hatay (East Mediterranean Turkey). *Biological Diversity and Conservation*, 12, 197-205. https://doi.org/10.5505/biodicon.2019.93685

Yıldız, M.Z. (2020). Herpetofauna of Kilis province (Southeast Anatolia, Turkey). *Amphibian & Reptile Conservation*, 14, 145-156.

Commagene Journal of Biology

Gündüz et al., (2025) *Comm. J. Biol.* 9(1), 7-11.
DOI: 10.31594/commagene.1586888

e-ISSN 2602-456X

Research Article/Araştırma Makalesi

Confirmation of the Presence of *Dolomedes* Latreille, 1804 in Türkiye (Araneae, Pisauridae) with a New Record

Gökhan GÜNDÜZ*[1], Rahşen S. KAYA[2], Furkan EREN[3]

[1]*Bursa Uludağ University, Graduate School of Natural and Applied Sciences, Zoology Section, Bursa, TÜRKIYE*
[2]*Bursa Uludağ University, Faculty of Arts and Science, Department of Biology, Bursa, TÜRKIYE*
[3]*Sakarya University, Institute of Natural Sciences, Sakarya, TÜRKİYE*
ORCID ID: Gökhan GÜNDÜZ: https://orcid.org/0000-0001-8957-3267; Rahşen S. KAYA: https://orcid.org/0000-0002-3769-9105;
Furkan EREN: https://orcid.org/0009-0000-0184-0560

Received: 17.11.2024 **Accepted:** 19.12.2024 **Published online:** 01.01.2025 **Issue published:** 30.06.2025

Abstract: The presence of the spider genus *Dolomedes* Latreille, 1804 in Türkiye is confirmed and first record of *D. plantarius* (Clerck, 1757) is given. *Dolomedes* is known from an old but unverified record in Türkiye and it remains absent from the latest checklists. Here, we briefly summarize the information on this genus in Türkiye with newly collected materials. A morphological diagnosis and comparative photographs of male and female are provided for *D. plantarius*. Also, an updated map of its distribution in Türkiye is given.

Keywords: Spider, fauna, distribution, Anatolia.

Yeni Bir Tür Kaydı ile *Dolomedes* Latreille, 1804 Cinsinin (Araneae, Pisauridae) Türkiye'deki Varlığının Doğrulanması

Öz: Örümcek cinsi *Dolomedes* Latreille, 1804'in Türkiye'deki varlığı doğrulanmış ve *D. plantarius* (Clerck, 1757) türüne ait ilk kayıt verilmiştir. *Dolomedes* cinsi, Türkiye'de eski fakat doğrulanmamış bir kayıttan bilinmektedir ve güncel kontrol listelerinde yer almamaktadır. Bu çalışmada, Türkiye'de bu cinse ait bilgiler, yeni toplanan materyallerle birlikte özetlenmiştir. *Dolomedes plantarius* türü için morfolojik bir tanımlama ve erkek ile dişinin karşılaştırmalı fotoğrafları sunulmuştur. Ayrıca, türün Türkiye'deki dağılımını gösteren güncel bir harita verilmiştir.

Anahtar kelimeler: Örümcek, fauna, dağılım, Anadolu.

1. Introduction

Dolomedes Latreille, 1804 is the most speciose genus in Pisauridae Simon, 1890 with 105 described species and is distributed worldwide except for Antarctica (WSC, 2024). Members of the genus are generally known as "raft spiders" or "fishing spiders" (Roberts, 1995). They are semi-aquatic wandering spiders and form an important component of aquatic ecosystems. Being large and iconic, with semi-aquatic lifestyles and often predators of freshwater vertebrates in addition to invertebrates, *Dolomedes* species are model organisms in diverse fields such as behavioral ecology (Helsdingen, 1993).

There are two *Dolomedes* species in Europe: *D. fimbriatus* (Clerck, 1757) and *D. plantarius* (Clerck, 1757). *D. fimbriatus* exhibits a broad distribution extending from Europe to Japan, whereas *D. plantarius* is found in a narrower range from Europe to Russia and Kazakhstan (WSC, 2024). Since these two species are closely related and morphologically very similar to each other, the microscopic examination of the genital organs is essential so as to distinguish between the two species. Due to this morphological similarity and the habitat preferences of the genus, the borders of distribution of the two species in Europe and whether both species share the same habitats have not been clarified until recent studies (Helsdingen, 1993; Naumova, 2018).

Despite its wide distribution range, no recent study on *Dolomodes* in Türkiye has been conducted yet. The first record of the genus from Türkiye was published by Drensky (1915) who reported it from Tekirdağ province on the north-west coast of the Marmara Sea. This study is quite old and was based on only a few immature specimens and Naumova (2018) re-evaluated it stressing the need for a careful review of this record. Consequently, *Dolomedes* remains unlisted in the latest checklists from Türkiye (WSC, 2024).

In this paper, we document the first confirmed record of the genus *Dolomedes* and the first record of *D. plantarius* in Türkiye.

2. Material and Method

The samples examined in this study were collected from Sakarya Province in Marmara region of Türkiye (Figs. 1–2). Spiders were primarily collected using sweep nets on the surface of the Sakarya River. The Sakarya River, one of the major rivers in Türkiye, provides diverse habitats that support a wide range of species. The slow-flowing sections of the river are characterized by the presence of willow trees along the banks and low-growing vegetation. These features offer shade, structural diversity, and a suitable

Corresponding authors: biyogok@gmail.com

environment for *Dolomedes*. Additionally, sub-adult specimens were captured by pitfall traps near the bank of the Sakarya River. Some of the individuals from both sexes were photographed in the natural habitat. All photographs were taken by the first author. They are preserved in 70% ethanol and deposited in the Zoological Museum of Bursa Uludağ University, Türkiye (ZMUU, R.S. Kaya). The digital images were taken with a Leica DFC295 digital camera attached to a Leica S8APO stereo microscope. Measurements were taken from the dorsal side of the body and all measurements are in millimeters. The nomenclature follows World Spider Catalog (2024).

Figure 1. Habitat where the specimens were collected from the Sakarya River.

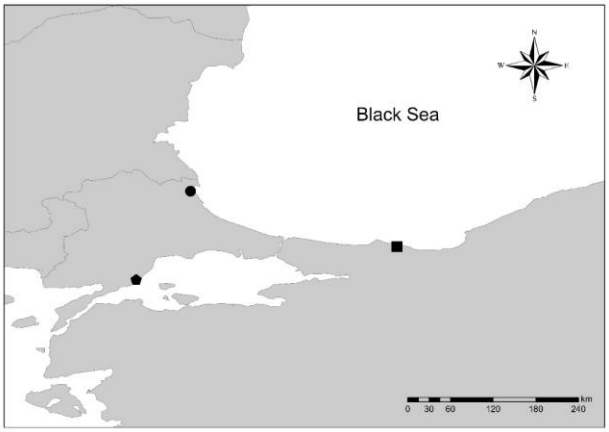

Figure 2. Map showing the distribution of the *Dolomedes* in Türkiye.

Square: *D. plantarius* collected in this study. Circle: Immature samples of *Dolomedes* collected in this study. Pentagon: Locality provided by Drensky (1915).

3. Results

Family Pisauridae Simon, 1890

Genus *Dolomedes* Latreille, 1804

Dolomedes plantarius (Clerck, 1757)

Material examined

1♂, 2♀♀, 4 sub adult ♀: Sakarya Province, Sakarya River, Karasu District, Tuzla Village, 18.08.2020, 41°04'42.6"N, 30°38'43.2"E, 35 m, leg. G. Gündüz; 2♂♂, 4♀♀, 3 sub adult ♂, 3 sub adult ♀: same locality, 07.06.2021, leg. G. Gündüz and F. Eren; 1 sub adult ♀: Sakarya Province, Sakarya River, Karasu District, Camidere Village, 01.04.2018–01.10.2018, 41°49'13"N, 27°56'40"E, 19 m, pitfall traps, leg. G. Gündüz.

Female

Measurements: Total length: 17.5- 22.7. Carapace: 7.5- 9.7 mm long and 6.5- 8.3 mm wide. Abdomen: 10.0-13.0 mm long and 6.2-6.8 mm wide. Femur I: 7.5- 9.7, femur II: 6.5- 8.3, femur III: 6.2- 8.1, femur IV: 7.7- 10.1; patella I: 3.0- 3.9, patella II: 2.5- 3.2, patella III: 2.9- 3.7, patella IV: 3.5- 4.5; tibia I: 7.2- 9.3, tibia II: 6.0- 7.8, tibia III: 5.9- 7.6, tibia IV: 7.1- 9,1; metatarsus I: 7.2- 9.2, metatarsus II: 5.7- 7.4, metatarsus III: 5.1- 6.6, metatarsus IV: 7.3- 9.3; tarsus I: 3.6- 4.6, tarsus II: 3.2- 4.1, tarsus III: 2.8- 3.6, tarsus IV: 3.6- 4.6.

Carapace brown to dark brown with distinct bands of relatively light hairs at margins. Chelicerae brown. Sternum light brown with dark margins. Palp and legs brown. Legs with robust spines and scopulae. Abdomen dark brown with bands of dark yellow hairs at the margins. Spinnerets pale yellow (Figs. 3–6).

Epigyne: Epigynal plate wider than long and clearly with a robust, sclerotized rectangular plate at posteriorly. Atrium tapering anteriorly (Figs. 11A–C).

Figure 3. Female general habitus of *D. plantarius* (Clerck, 1757).

Figure 4. A melanistic female of *D. plantarius* (Clerck, 1757) with its egg sac.

Figure 5. Subadult female of *D. plantarius* (Clerck, 1757).

Figure 6. Subadult female of *D. plantarius* (Clerck, 1757).

Male

Measurements: Total length: 12.9- 15.4. Carapace: 6.2- 7.4 mm long and 5.5- 6.5 mm wide. Abdomen: 6.7- 8.0 mm long and 5.3-5.6 mm wide. Femur I: 7.4- 8.7, femur II: 7.0- 8.3, femur III: 6.1- 7.3, femur IV: 7.6- 9.1; patella I: 2.5- 3.1, patella II: 2.0- 2.3, patella III: 2.4- 2.8, patella IV: 2.8- 3.4; tibia I: 6.0- 7.1, tibia II: 5.3- 6.3, tibia III: 4.3- 5.2, tibia IV: 7.0- 8.3; metatarsus I: 5.6- 6.8, metatarsus II: 5.2- 6.2, metatarsus III: 4.5- 5.4, metatarsus IV: 5.7- 6.8; tarsus I: 3.7- 4.4, tarsus II: 3.5- 4.2, tarsus III: 3.3- 3.9, tarsus IV: 4.0- 4.7.

Carapace brown to dark brown with distinct longitudinal stripes of relatively light hairs at margins. Chelicerae brown. Sternum light brown with dark margins. Palp and legs brown. Legs with robust spines and scopulae. Abdomen dark brown with bands of dark yellow hairs at margins. Spinnerets pale yellow (Figs. 7–9).

Palp: Tibia with a row of long bristles ventrally; tibial apophysis bifurcated. Median apophysis thin at the base and curved and thickened towards apex roughly beak-shaped. Conductor membranous. Embolus basally thick, long and curved (Figs 10A–B).

Distribution: Europe, Russia (Europe to South Siberia), Kazakhstan (WSC, 2024), new to Türkiye.

Habitat and Ecology: The sampling of *Dolomedes* was conducted in the slow-flowing sections of the Sakarya River, where the riverbanks are lined with willow trees and dense vegetation. It was observed that immature individuals spent most of their time beneath this dense cover, preying primarily on juvenile heteropterans

Figure 7. Immature male of *D. plantarius* (Clerck, 1757) while waiting for its prey.

Figure 8. Male general habitus of *D. plantarius* (Clerck, 1757).

Figure 9. Male general habitus of *D. plantarius* (Clerck, 1757).

4. Discussion

The only known record of the genus *Dolomedes* in Türkiye was provided by Drensky (1915) who identified several immature specimens collected from Tekirdağ Province in the Thracian part of Türkiye as *D. fimbriatus* (under the name *D. ornatus*). Drensky (1915) also noted: "young specimens at the stage of the last molting, found on the road between Merefle and Ganos which represents a new species for the Balkan Peninsula (Mürefte and Gaziköy, TR)". Recently, Naumova (2018) reviewed the genus in the Balkans and concluded that this record from Türkiye is unreliable as an identification of *D. fimbriatus* (Drensky, 1915; Naumova, 2018).

Figure 10. Male palp of *D. plantarius* (Clerck, 1757).

A. Male palp, ventral view. B. Male palpal tibia, retrolateral view.

Scale bars: A: 0.5, B: 0.1

In Europe, *D. plantarius* is considered rare and endangered. It is listed in the Red Book as vulnerable to extinction in countries such as England, Spain, Russia, Belarus, and Bulgaria (Deltshev, 2015) and is also categorized as vulnerable on the IUCN Red List (World Conservation Monitoring Centre, 1996). More extensive sampling and studies in recent years have provided a better understanding of the distribution, population trends, and habitat preferences of *D. plantarius* and *D. fimbriatus* (Naumova, 2018). Field observations from this study indicated that the *D. plantarius* population in Sakarya is substantial as numerous individuals were observed beyond those captured for sampling. Additionally, a large number of *Pirata piraticus* (Clerck, 1757) (Fig. 12) were also observed in the studied area. These two species share similar coloration and patterns, which may play a crucial role in their ability to camouflage in aquatic environments. Their appearances resemble submerged twigs; adaptations that likely help them avoid predators and improve hunting efficiency.

In addition to the material included in this study, fieldwork conducted in the İğneada Flooded Forests within Kırklareli Province in the Thrace region also yielded immature *Dolomedes* specimens (Fig. 2). Although these samples were not included in the study material due to their immature stage, we considered it valuable to report this information, as it provides significant data.

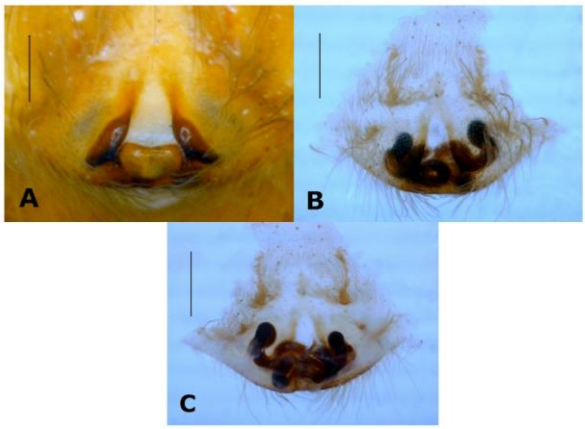

Figure 11. Epigyne of *D. plantarius* (Clerck, 1757).

A. Epigyne, ventral view. B. Macerated epigyne, ventral view. C. Vulva, dorsal view.

Scale bars: 0.1

Fig. 12: Female *Pirata piraticus* (Clerck, 1757) with its egg sac.

Ethics committee approval: Ethics committee approval is not required for this study.

Conflict of interest: The authors declare that there is no conflict of interest.

Author Contributions: Conception – G.G., R.S.K.; Design – G.G., R.S.K.; Supervision – G.G., R.S.K.; Materials – R.S.K., G.G., F.E.; Analysis Interpretation – R.S.K., G.G.; Literature Review R.S.K., G.G., F.E.; Writing – R.S.K., G.G., F.E.; Critical Review – R.S.K., G.G.

References

Deltshev, C. (2015). Fisher spider *Dolomedes plantarius* (Clerck, 1757). – In: Golemanski, V. et al. (eds.): Red Data Book of the Republic of Bulgaria. Vol. 2. Animals. Sofia: Bulgarian Academy of Sciences & Ministry of Environment and Waters, p. 61.

Drensky, P. (1915). Contribution à l'étude des Arachnides de la Trace du sud-est. – *La Revue de l'Académie Bulgare des Sciences*, 12 (5), 127-140.

Helsdingen, P.V. (1993). Ecology and distribution of *Dolomedes* in Europe (Araneida, Dolomedidae). *Bolletino dell'Accademia Gioenia di Scienze Naturali*, 26, 181-187.

Naumova, M. (2018). Review of the distribution of the genus *Dolomedes* Latreille, 1804 (Araneae: Pisauridae) on the Balkan Peninsula, with new records from Bulgaria. *Acta Zoologica Bulgarica*, 70(4), 479-486.

Roberts, M. J. (1995). Collins Field Guide: Spiders of Britain & Northern Europe. Harper Collins, London, 383 pp.

World Conservation Monitoring Centre. (1996). *Dolomedes plantarius*. The IUCN Red List of Threatened Species 1996: e.T6790A12806270.

https://doi.org/10.2305/IUCN.UK.1996.RLTS.T6790A12806270.en. Accessed on 15 November 2024.

World Spider Catalog (2024). World Spider Catalog. Version 25.0. Natural History Museum Bern, online at http://wsc.nmbe.ch, accessed on {27.05.2024}. https://doi.org/10.24436/2

Commagene Journal of Biology

Karış, (2025) *Comm. J. Biol.* 9(1), 12-16.
DOI: 10.31594/commagene.1605070

e-ISSN 2602-456X

Research Article/Araştırma Makalesi

In vitro Antiproliferative Activity of *Lissotriton schmidtleri* (Raxworthy, 1988) Skin Secretion on Human Breast Cancer (MCF7) Cell Line

Mert KARIŞ

Nevşehir Hacı Bektaş Veli University, Acıgöl Vocational School of Technical Sciences, Laboratory Technology Program, Nevşehir, TÜRKIYE
ORCID ID: Mert KARIŞ: https://orcid.org/0000-0003-0468-9290

Received: 21.12.2024 **Accepted:** 27.12.2024 **Published online:** 01.01.2025 **Issue published:** 30.06.2025

Abstract: In this study, the *in vitro* antiproliferative activity of *Lissotriton schmidtleri* skin secretion on estrogen-sensitive human breast cancer (MCF7) cells was reported for the first time. The effects of *L. schmidtleri* skin secretion at concentrations of 0.5, 5, and 50 µg/mL on the MCF7 cell line were evaluated using the MTT assay after 48 hours of incubation. According to the MTT assay results, *L. schmidtleri* skin secretion inhibited MCF7 cell viability by approximately 64% at a concentration of 50 µg/mL, with an IC_{50} value calculated as 20.81 ± 0.87 µg/mL. Based on these findings, it is suggested that *L. schmidtleri* skin secretion may serve as a potential anticancer agent against breast cancer.

Keywords: Amphibian skin secretion, MTT assay, *Lissotriton schmidtleri*, cytotoxicity, MCF7.

Lissotriton schmidtleri (Raxworthy, 1988) Deri Salgısının İnsan Meme Kanseri (MCF7) Hücre Hattı Üzerindeki *in vitro* Antiproliferatif Aktivitesi

Öz: Bu çalışmada, *Lissotriton schmidtleri* deri salgısının östrojen duyarlı insan meme kanseri (MCF7) hücreleri üzerindeki *in vitro* antiproliferatif aktivitesi ilk kez rapor edilmiştir. MCF7 hücre hattına, *L. schmidtleri* deri salgısının 0.5, 5 ve 50 µg/mL konsantrasyonları uygulanarak 48 saat inkübasyon sonundaki etkileri MTT testi ile belirlenmiştir. MTT testi sonucunda, *L. schmidtleri* deri salgısı, MCF7 hücre canlılığını 50 µg/mL konsantrasyonda yaklaşık %64 oranında inhibe etmiş ve IC_{50} değeri 20.81 ± 0.87 µg/mL olarak hesaplanmıştır. Elde edilen veriler ışığında, *L. schmidtleri* deri salgısının meme kanserine karşı potansiyel bir antikanser ajan olabileceği değerlendirilmiştir.

Anahtar kelimeler: Amfibi deri salgısı, MTT testi, *Lissotriton schmidtleri*, sitotoksisite, MCF7.

1. Introduction

Breast cancer is commonly seen among women and is one of the leading causes of cancer-related deaths. The World Health Organization (WHO) has reported that breast cancer is the most prevalent type of cancer among women. Moreover, the number of natural and synthetic substances that could exhibit therapeutic effects for the treatment of breast cancer is increasing (Wild, 2014).

In patients, it has been observed that the use of drugs developed in laboratory conditions also exposes healthy cells to various side effects (Smith et al., 2007). In chemotherapy, not only neoplastic cells but also proliferating healthy cells are affected, resulting in various side effects (such as nausea and vomiting) in patients (Hoskin & Ramamoorthy, 2007). Therefore, animal-derived substances have been a significant source of anticancer agents, with numerous compounds isolated from various animal sources demonstrating promising therapeutic potential (Wang et al., 2017). There are several of studies on the effects of animal-derived compounds and bioactive molecules obtained from such as bees (Kamran et al., 2020), spiders (Gao et al., 2007), snakes (Bradshaw et al., 2016), scorpions (Zargan et al., 2011), and amphibians (Sciani et al., 2013).

Lissotriton schmidtleri, also referred to as the Turkish smooth newt, inhabits regions ranging from northeastern Greece and southeastern Bulgaria through East Thrace, extending across the Bosphorus to western and northwestern Anatolia (Wielstra et al., 2015).

In newts, skin secretions play a crucial role in regulating water loss, acting as a barrier against pathogens, and serving as lubricants against predators (Wanninger et al., 2018). Additionally, newt skin secretions have been identified as promising candidates for treating cancer, HIV, and drug-resistant bacterial infections (Xu & Lai, 2015). The effects of newt skin secretions are not limited to these activities. The skin secretions of newts also possess antioxidant properties that help in neutralizing free radicals and protecting cells from oxidative damage. This antioxidant activity is crucial for maintaining cellular integrity and function (Indriani et al., 2023). Studies have shown that newt skin secretions can also promote wound healing and regulate immune reactions (Kröner et al., 2024). Karış et al. (2018) demonstrated that *Lissotriton vulgaris* (*L. schmidtleri* according to the current taxonomy) skin secretion has a remarkable anticancer effect on MDA-MB-231 (hormone-independent human mammary gland adenocarcinoma) cell line.

Holliday & Speirs (2011) indicated that MCF7 is the most widely used breast cancer cell line in research due to its high hormone sensitivity that is attributed to its

Corresponding author: mert.karis@hotmail.com

elevated expression of estrogen receptors (ER). The primary aim of this study was to evaluate the antiproliferative activity of *L. schmidtleri* skin secretion on the estrogen-dependent MCF7 cell line in order to assess its cytotoxic potential and extend the knowledge of its bioactivities.

2. Material and Method

2.1. Field studies and collection of skin secretions

Field studies were conducted in accordance with the activation periods of the *L. schmidtleri* (Fig. 1) and took place in February 2016 in İzmir province of Türkiye. A total of 7 individuals (3♂♂, 4♀♀) were found and captured by using a mesh dip net. The field study was carried out with the permission of the Republic of Türkiye Ministry of Agriculture and Forestry, General Directorate of Nature Conservation and National Parks, permit number: 2014-51946.

Figure 1. General aspect of a male (below) and a female (above) specimen of *Lissotriton schmidtleri*

Skin secretion was collected with a slightly modified method (Tyler et al., 1992) through mild electrical stimulation (5-8 V) using a stimulator (C.F. Palmer, London). For each individual, approximately 20 mL of ultra-pure water was used to rinse the secretions into falcon tubes. The skin secretion of all individuals was pooled, clarified by centrifugation (6000 × rpm for 10 minutes), and the supernatants were snap-frozen using liquid nitrogen. The samples were then lyophilized and stored at +4°C until further bioactivity assays were conducted. Secretion collection took place in the field and the newts were subsequently released unharmed back into their natural habitats. A total of 7 mg of lyophilized skin secretion was obtained.

2.2. Determination of the protein concentration

The protein content of the diluted skin secretion sample (2 mg/mL) in ultra-pure water was measured in triplicate using the BCA assay kit (Thermo Scientific, USA) with bovine serum albumin as the standard. Protein concentrations were determined using a UV/Vis spectrophotometer (Thermo Multiskan Spectrum, Bremen, Germany) at a wavelength of 562 nm.

2.3. Cell culture, MTT assay, and determination of IC_{50}

The MCF7 (human breast adenocarcinoma) cell line, purchased from ATCC (Manassas, VA, USA), was used to assess antiproliferative activity. All cells were cultured in Dulbecco's modified Eagle's medium F12 (DMEM/F12), supplemented with 10% fetal bovine serum (FBS), 2 mM/L glutamine, 100 U/mL penicillin, and 100 µg/mL streptomycin (Lonza, Visp, Switzerland). The cells were maintained at 37°C in a humidified atmosphere with 5% CO_2. Cytotoxicity of crude skin secretion was evaluated using a modified colorimetric MTT [3-(4,5-dimethyl-2-thiazolyl)-2,5-diphenyl-2H-tetrazolium bromide] assay (Mosmann, 1983) based on cell viability. Optical density (OD) was measured in triplicate at 570 nm with a reference wavelength of 620 nm, using a UV/Vis spectrophotometer (Thermo, Bremen, Germany). The cells were seeded at an initial concentration of $1x10^5$ cells/mL in 96-well plates and incubated for 24 hours. A non-cancerous cell line HEK-293 (human embrionic kidney) was screened with *L. vulgaris* skin secretion and all concentrations and incubation time were optimized by screening on cell lines repeatedly in a previously published study (Karış et al., 2018). Afterward, the cells were treated with varying concentrations (0.5, 5, and 50 µg/mL) of skin secretions and incubated for an additional 48 hours at 37 °C. Parthenolide, a plant-derived compound, was used as a positive cytotoxic control at concentrations of 0.125, 1.25, and 12.5 µg/mL. Parthenolide is known as a highly cytotoxic agent and frequently used as a positive control in anti-cancer research (Kreuger et al., 2012). Cell viability was determined by calculating the percentage of surviving cells in each culture following incubation with skin secretions. The viability (%) was calculated using the formula:

%Viable cells = [(absorbance of the treated cells) − (absorbance of blank)] / [(absorbance of control) − (absorbance of blank)] × 100

The IC_{50} values were determined by fitting the data to a sigmoidal curve using a four-parameter logistic model and the results were presented as the average of three independent measurements. The IC_{50} values were reported with a 95% confidence interval and calculations were performed using Prism 5 software (GraphPad5, San Diego, CA, USA). The absorbance values from the blank wells were subtracted from the treated and control cell wells and the half-maximal inhibition of growth (IC_{50}) was calculated relative to the untreated controls.

Morphological examinations of cells exposed to secretions at different concentrations were conducted using an inverted microscope (Olympus, Japan).

3. Results

The total protein and peptide concentration of *L. schmidtleri* skin secretion (2 mg/mL) was measured by using the BCA assay and determined as 1775 µg/mL.

The antiproliferative activity of the skin secretion sample was measured against the MCF7 cell line after 48 h incubation. The crude skin secretion of *L. schmidtleri* exhibited a concentration-dependent inhibitory effect on the viability of the MCF7 cells. The inhibition rates were calculated as 17% at a concentration of 0.5 µg/mL, 28% at 5 µg/mL, and 64% at 50 µg/mL (Fig. 2). Parthenolide (positive cytotoxic control agent), a plant-derived sesquiterpene lactone demonstrated inhibition rates of 20% at 0.125 µg/mL, 32% at 1.25 µg/mL, and 76% at 12.5 µg/mL on the MCF7 cell line.

Half maximal inhibitory concentration (IC_{50}) of *L. schmidtleri* skin secretion was calculated as 20.81 ± 0.87 µg/mL (Table 1). The IC_{50} value of positive control parthenolide was found as 2.74 ± 0.09 µg/mL.

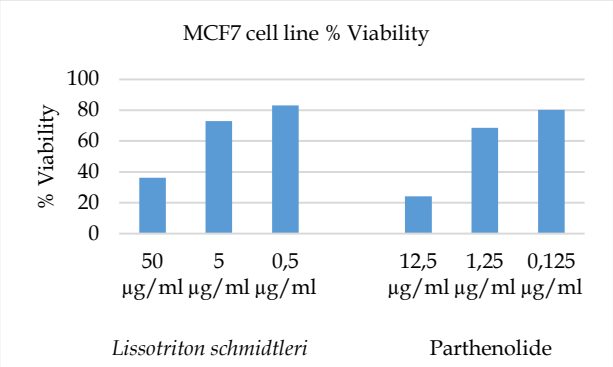

Figure 2. Viability of MCF7 cell line following skin secretion treatment for 48 h. Cell viability was determined by MTT assay, control was exposed to vehicle only which was taken as 100% viability.

Table 1. The IC_{50} values (µg/mL) for MCF7 cell line following 48 h skin secretion exposure by MTT assay. Parthenolide was used as positive control.

Sample	MCF7 (breast)
Parthenolide	2.74 ± 0.09
L. schmidtleri	20.81 ± 0.87

Increasing concentrations led to a greater number of rounded cells, growth inhibition, and a high occurrence of various morphological abnormalities along with larger cell-free areas compared to untreated control cells (Fig. 3).

4. Discussion and Conclusion

The skin secretions of urodele amphibians are complex mixtures consisting of peptides, proteins, and other bioactive compounds (Barros et al., 2022). These secretions serve multiple physiological purposes for the amphibians such as antimicrobial defense, predator deterrence, and environmental adaptation (Clarke, 1997).

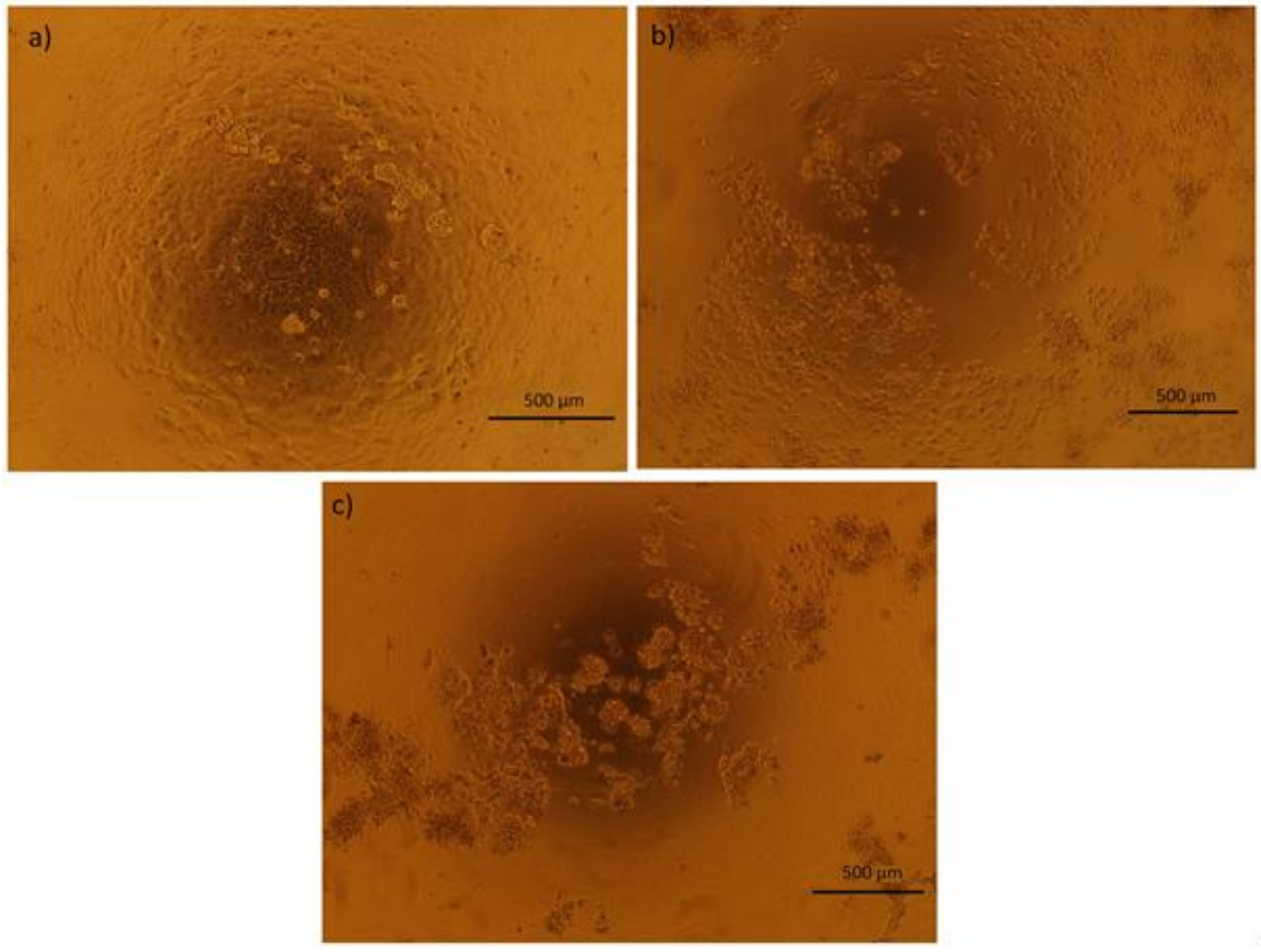

Figure 3. Morphological changes of MCF7 cells following 48 h exposure a) control, b) parthenolide (1.25 µg/mL), c) *L. schmidtleri* skin secretion (50 µg/mL)

As a potential anticancer agent, amphibian-derived dermaseptins are known to insert into the lipid bilayer of the membrane, causing leakage of intracellular contents and eventual cell death. This mechanism is particularly effective against cancer cells, which often have altered membrane characteristics compared to normal cells (Bartels et al., 2019). Molecules in the amphibian skin secretions may induce apoptosis in cancer cells through mitochondrial damage and activation of pro-apoptotic proteins (Oelkrug et al., 2015). For instance, bombinin (a peptide isolated from the skin secretion of *Bombina orientalis*) induces apoptosis in cancer cells by triggering mitochondrial depolarization and caspase activation. By promoting the intrinsic apoptotic pathway, these peptides can selectively target and kill cancer cells while sparing normal tissue (Wang et al., 2024). Temporins (an

antimicrobial peptide isolated from *Hylarana guentheri*) induce cell cycle arrest in cancer cells. This mechanism halts the proliferation of cancer cells by interfering with the progression of the cell cycle, particularly at the G1/S or G2/M checkpoints (Liu et al., 2024).

Karış et al. (2018) determined that *L. vulgaris* (now *L. schmidtleri*) has a high cytotoxic effect with an IC_{50} value of 1.58 µg/mL against MDA-MB-231, a hormone-independent human mammary gland adenocarcinoma cell line and inhibited 85% cell viability at 50 µg/mL concentration. In this study, *L. schmidtleri* showed a lower level of antiproliferative activity against an estrogen-dependent MCF7 (human breast adenocarcinoma) with an IC_{50} value of 20.81 ± 0.87 µg/mL and 65% growth inhibition rate at 50 µg/mL concentration. The altered cytotoxic effects on MCF7 and MDA-MB-231 may occur as the cause of having different subtypes. Breast cancer comprises several molecular subtypes, with the luminal subtype (i.e., MCF7) being the most common and characterized by estrogen receptor-positive (ER+) status. The luminal A subtype, in particular, is defined by ER+, progesterone receptor-negative (PR−), and HER2-negative (HER2−) markers (Perou & Borresen-Dale, 2011). On the other hand, triple negative MDA-MB-231 (ER−, PR− and, HER2−) cells are reported as basal B subtype (claudin-low) breast cancer, which is part of basal-like subtype (Neve et al., 2006).

Sciani et al. (2013) screened the cytotoxic effects of skin secretions of seven species of the genus *Rhinella* on MCF7 cell line resulting in the IC_{50} values ranging between 40-50 µg/mL. *L. schmidtleri* skin secretion showed much higher and more potent activity (20.81 ± 0.87 µg/mL) against MCF7 cells. Wang et al. (2012) performed a cytotoxicity analysis of temporin-1CEa peptide obtained from the skin secretion of *Rana chensinensis* and they found the IC_{50} value on MCF7 cell line as 34.50 µM at 48 h which is also supporting the potential *L. schmidtleri* skin secretion on MCF7 cells. Santana et al. (2020) studied the figainin-1 peptide from the skin secretion of *Boana raniceps* on MCF7 cells and detected IC_{50} value was 13.7 µM. Dermaseptin-PT9 peptide from *Phyllomedusa tarsius* skin secretion showed very similar antiproliferative effect (70%) on MCF7 at 50 µM peptide concentration (Li et al., 2019), which is found 64% in this study with 50 µg/mL *L. schmidtleri* skin secretion exposure. These results support the potential of *L. schmidtleri* skin secretion on MCF7 cell line.

In conclusion, *L. schmidtleri* skin secretion represents a promising and underexplored source of bioactive compounds with potential cytotoxic effects on breast cancer. With their unique biochemistry, selective cytotoxicity, and diverse mechanisms of action, amphibian-derived products could offer significant advantages over conventional therapies. Further research and clinical studies are essential to fully understand and harness the potential of these biological treasures in the fight against breast cancer and other diseases.

Acknowledgment: I would like to extend my thanks to AREL (Research and Education Laboratory, Ege University School of Medicine) for their laboratory facilities during the study. Also, many thanks to Ayşe NALBANTSOY (Ege University) for her vauable suggestions and providing the cell line.

Ethics committee approval: This study was performed in accordance with ethical standards of animal experiments. Legal research ethics committee approval permissions for the study were obtained from the Ege University, Animal Experiments Local Ethics Committee (No: 2014-002).

Conflict of interest: The author declares that there is no conflict of interest.

References

Barros, A.L., Hamed, A., Marani, M., Moreira, D.C., Eaton, P., Plácido, A., ... & Leite, J.R.S. (2022). The arsenal of bioactive molecules in the skin secretion of urodele amphibians. *Frontiers in Pharmacology*, 12, 810821. https://doi.org/10.3389/fphar.2021.810821

Bartels, E.J.H., Dekker, D., & Amiche, M. (2019). Dermaseptins, multifunctional antimicrobial peptides: A review of their pharmacology, effectivity, mechanism of action, and possible future directions. *Frontiers in Pharmacology*, 10, 1421. https://doi.org/10.3389/fphar.2019.01421

Bradshaw, M.J., Saviola, A.J., Fesler, E., & Mackessy, S.P. (2016). Evaluation of cytotoxic activities of snake venoms toward breast (MCF-7) and skin cancer (A-375) cell lines. *Cytotechnology*, 68, 687-700. https://doi.org/10.1007/s10616-014-9820-2

Clarke, B.T. (1997). The natural history of amphibian skin secretions, their normal functioning and potential medical applications. *Biological Reviews*, 72(3), 365-379. https://doi.org/10.1017/S0006323197005045

Gao, L., Yu, S., Wu, Y., & Shan, B. (2007). Effect of spider venom on cell apoptosis and necrosis rates in MCF-7 cells. *DNA and Cell Biology*, 26(7), 485-489. https://doi.org/10.1089/dna.2007.0579

Holliday, D.L., & Speirs, V. (2011). Choosing the right cell line for breast cancer research. *Breast Cancer Research*, 13, 1-7. https://doi.org/10.1186/bcr2889

Hoskin, D.W., & Ramamoorthy, A. (2008). Studies on anticancer activities of antimicrobial peptides. *Biochimica et Biophysica Acta (BBA)-Biomembranes*, 1778(2), 357-375. https://doi.org/10.1016/j.bbamem.2007.11.008

Indriani, S., Karnjanapratum, S., Nirmal, N.P., & Nalinanon, S. (2023). Amphibian skin and skin secretion: An exotic source of bioactive peptides and its application. *Foods*, 12(6), 1282. https://doi.org/10.3390/foods12061282

Kamran, M.R., Zargan, J., Alikhani, H.K., & Hajinoormohamadi, A. (2020). The Comparative cytotoxic effects of apis mellifera crude venom on MCF-7 Breast Cancer cell line in 2D and 3D cell cultures. *International Journal of Peptide Research and Therapeutics*, 26, 1819-1828. https://doi.org/10.1007/s10989-019-09979-0

Karış, M., Şener, D., Yalçın, H.T., Nalbantsoy, A., & Göçmen, B. (2018). Major biological activities and protein profiles of skin secretions of *Lissotriton vulgaris* and *Triturus ivanbureschi*. *Turkish Journal of Biochemistry*, 43(6), 605-612. https://doi.org/10.1515/tjb-2017-0306

Kröner, L., Lötters, S., & Hopp, M.T. (2024). Insights into caudate amphibian skin secretions with a focus on the chemistry and bioactivity of derived peptides. *Biological Chemistry*, 405(9-10), 641-660. https://doi.org/10.1515/hsz-2024-0035

Kreuger, M.R.O., Grootjans, S., Biavatti, M.W., Vandenabeele, P., & D'Herde, K. (2012). Sesquiterpene lactones as drugs with multiple targets in cancer treatment: focus on parthenolide. *Anti-cancer Drugs*, 23(9), 883-896. https://doi.org/10.1097/CAD.0b013e328356cad9

Li, M., Xi, X., Ma, C., Chen, X., Zhou, M., Burrows, J.F., ... & Wang, L. (2019). A novel dermaseptin isolated from the skin secretion of *Phyllomedusa tarsius* and its cationicity-enhanced analogue exhibiting effective antimicrobial and anti-proliferative activities. *Biomolecules*, 9(10), 628. https://doi.org/10.3390/biom9100628

Liu, Y., Liu, H., Zhang, J., & Zhang, Y. (2024). Temporin-GHaK Exhibits Antineoplastic Activity against Human Lung Adenocarcinoma by Inhibiting the Wnt Signaling Pathway through miRNA-4516. *Molecules*, 29(12), 2797. https://doi.org/10.3390/molecules29122797

Mosmann, T. (1983). Rapid colorimetric assay for cellular growth and survival: application to proliferation and cytotoxicity assays. *Journal of Immunological Methods*, 65(1-2), 55-63. https://doi.org/10.1016/0022-1759(83)90303-4

Neve, R.M., Chin, K., Fridlyand, J., Yeh, J., Baehner, F. L., Fevr, T., ... & Gray, J.W. (2006). A collection of breast cancer cell lines for the study of functionally distinct cancer subtypes. *Cancer Cell*, 10(6), 515-527. https://doi.org/10.1016/j.ccr.2006.10.008

Oelkrug, C., Hartke, M., & Schubert, A. (2015). Mode of action of anticancer peptides (ACPs) from amphibian origin. *Anticancer Research*, 35(2), 635-643.

Perou, C.M., & Børresen-Dale, A.L. (2011). Systems biology and genomics of breast cancer. *Cold Spring Harbor Perspectives in Biology*, 3(2), a003293. https://doi.org/10.1101/cshperspect.a003293

Santana, C.J.C., Magalhães, A.C.M., dos Santos Júnior, A.C., Ricart, C.A.O., Lima, B.D., Álvares, A.D.C.M., ... & Castro, M.S. (2020). Figainin 1, a novel amphibian skin peptide with antimicrobial and antiproliferative properties. *Antibiotics*, 9(9), 625. https://doi.org/10.3390/antibiotics9090625

Sciani, J.M., de-Sá-Júnior, P.L., Ferreira, A.K., Pereira, A., Antoniazzi, M.M., Jared, C., & Pimenta, D.C. (2013). Cytotoxic and antiproliferative effects of crude amphibian skin secretions on breast tumor cells. *Biomedicine & Preventive Nutrition*, 3(1), 10-18. https://doi.org/10.1016/j.bionut.2012.11.001

Smith, R.A., Cokkinides, V., & Eyre, H.J. (2007). Cancer screening in the United States, 2007: a review of current guidelines, practices, and prospects. *CA: A Cancer Journal for Clinicians*, 57(2), 90-104. https://doi.org/10.3322/canjclin.57.2.90

Tyler, M.J., Stone, D.J., & Bowie, J.H. (1992). A novel method for the release and collection of dermal, glandular secretions from the skin of frogs. *Journal of Pharmacological and Toxicological Methods*, 28(4), 199-200. https://doi.org/10.1016/1056-8719(92)90004-k

Wang, C., Li, H.B., Li, S., Tian, L.L., & Shang, D.J. (2012). Antitumor effects and cell selectivity of temporin-1CEa, an antimicrobial peptide from the skin secretions of the Chinese brown frog (*Rana chensinensis*). *Biochimie*, 94(2), 434-441. https://doi.org/10.1016/j.biochi.2011.08.011

Wang, L., Dong, C., Li, X., Han, W., & Su, X. (2017). Anticancer potential of bioactive peptides from animal sources. *Oncology Reports*, 38(2), 637-651. https://doi.org/10.3892/or.2017.5778

Wang, X., Tang, P., Gong, Y., Yao, H., Liang, M., Qu, H., ... & Jiang, Q. (2024). Bombinin-BO1 induces hepatocellular carcinoma cell-cycle arrest and apoptosis via the HSP90A-Cdc37-CDK1 axis. *iScience*, 27(8), 110382. https://doi.org/10.1016/j.isci.2024.110382

Wanninger, M., Schwaha, T., & Heiss, E. (2018). Form and Function of the skin glands in the Himalayan newt *Tylototriton verrucosus*. *Zoological Letters*, 4, 1-10. https://doi.org/10.1186/s40851-018-0095-x

Wielstra, B., Bozkurt, E., & Olgun, K. (2015). The distribution and taxonomy of *Lissotriton* newts in Turkey (Amphibia, Salamandridae). *ZooKeys*, 484, 11-23. https://doi.org/10.3897/zookeys.484.8869

Wild, C. (2014). *World cancer report 2014* (pp. 482-494). C. P. Wild, & B. W. Stewart (Eds.). Geneva, Switzerland: World Health Organization.

Xu, X., & Lai, R. (2015). The chemistry and biological activities of peptides from amphibian skin secretions. *Chemical Reviews*, 115(4), 1760-1846. https://doi.org/10.1021/cr4006704

Zargan, J., Umar, S., Sajad, M., Naime, M., Ali, S., & Khan, H.A. (2011). Scorpion venom (*Odontobuthus doriae*) induces apoptosis by depolarization of mitochondria and reduces S-phase population in human breast cancer cells (MCF-7). *Toxicology in vitro*, 25(8), 1748-1756. https://doi.org/10.1016/j.tiv.2011.09.002

Commagene Journal of Biology

Uysal et al., (2025) *Comm. J. Biol.* 9(1), 17-27.
DOI: 10.31594/commagene.1553393

e-ISSN 2602-456X

Research Article/Araştırma Makalesi

Analysis of Bird Populations in the Wetland Areas Surrounding the Çanakkale/Dardanelles Strait

İbrahim UYSAL[1,*], Didem KURTUL[2], Ceren Nur ÖZGÜL[2], Murat TOSUNOĞLU[3]

[1]*Çanakkale Onsekiz Mart University, Vocational School of Health Services Çanakkale, TÜRKIYE*
[2]*Çanakkale Onsekiz Mart University, School of Graduate Studies, Department of Biology, Çanakkale, TÜRKIYE*
[3]*Çanakkale Onsekiz Mart University, Faculty of Science, Department of Biology, Çanakkale, TÜRKIYE*
ORCID ID: İbrahim UYSAL: https://orcid.org/0000-0002-7507-3322; Didem KURTUL: https://orcid.org/0000-0003-0778-5966;
Ceren Nur ÖZGÜL: https://orcid.org/0000-0002-1597-4321; Murat TOSUNOĞLU: https://orcid.org/0000-0002-9764-2477

Received: 20.09.2024 **Accepted:** 03.01.2025 **Published online:** 03.02.2025 **Issue published:** 30.06.2025

Abstract: Given the rapid loss of wetland ecosystems today, monitoring bird species and populations that can respond quickly to environmental changes is crucial for the effective tracking of wetland ecosystems. Additionally, wetland ecosystems are of critical importance for the life cycles and migratory movements of bird species. The aim of the study is to examine the monthly variations in bird species diversity in the wetland areas (Kavak Delta, Çardak Lagoon, Kumkale Delta, Suvla Salt Lake, and Umurbey Delta) surrounding the Çanakkale/Dardanelles Strait, located in the northeastern part of the Mediterranean basin, which plays a significant role in migration strategies for numerous bird species. Additionally, correlations between the habitat types and areas of these wetlands and their diversity indices were analyzed and updated species lists for the studied wetlands were compiled. The field studies were conducted monthly in 2023 using point and transect observation methods to assess species and population counts. Diversity indices were calculated using the number of species and individuals recorded monthly for each area. The relationship between the habitat types and the areas they cover in wetlands and the diversity indices was tested using Spearman's rho correlation analysis. A total of 184.068 birds belonging to 279 species, encompassing 22 orders and 61 families, were counted across all areas. In the wetland areas, species richness (Margalef index - M) ranged from 15.417 to 22.718 and species diversity (Shannon-Wiener Index - H') ranged from 1.819 to 2.416. The fact that the research areas lie along a significant migration route enhances species diversity and richness during migration periods. In Deltas where shallow surface waters predominate, more pronounced differences in diversity indices have been observed due to variations in seasonal water levels. A strong positive correlation was found between species richness and the size of wetlands, particularly Salt Marshes and Permanently Irrigated Lands, indicating the critical role of habitat size in supporting biodiversity. Seasonal water level fluctuations also significantly impacted diversity in delta regions. Given the global loss of wetlands, long-term research with standardized methods is crucial for understanding and protecting these vital ecosystems.

Keywords: Diversity index, ornitofauna, wetland ecosystems, correlation.

Çanakkale Boğazı Çevresindeki Sulak Alanlardaki Kuş Popülasyonlarının Analizi

Öz: Günümüzde sulak alan ekosistemlerinde yaşanan hızlı yok oluş göz önüne alındığında, yaşanan değişimlere hızlı tepki verebilen kuş türlerinin ve popülasyonlarının izlenmesi sulak alan ekosistemlerinin takibi açısından önem arz etmektedir. Aynı zamanda, sulak alan ekosistemleri de kuş türlerinin yaşam döngüsü ve göç hareketlilikleri açısından kritik öneme sahiptir. Çalışmanın amacı, çok sayıda kuş türünün göç stratejilerinde önemli rol oynayan Akdeniz havzasının kuzeydoğu kesiminde yer alan Çanakkale Boğazı çevresindeki sulak alanlardaki (Kavak Deltası, Çardak Lagünü, Kumkale Deltası, Suvla Tuz Gölü, Umurbey Deltası) kuş türü çeşitliliğindeki aylık değişimleri incelemektir. Ayrıca, bu sulak alanların habitat tipleri ve alanları ile çeşitlilik endeksleri arasındaki korelasyonlar analiz edilmiş ve incelenen sulak alanlar için güncellenmiş tür listeleri derlenmiştir. Saha çalışmaları, nokta ve transekt gözlem metodları kullanılarak 2023 yılında aylık olarak yürütülmüştür. Çeşitlilik endeksleri, her alan için aylık olarak kaydedilen tür ve birey sayıları kullanılarak hesaplanmıştır. Sulak alan alanlarındaki habitat tipleri ve kapsadıkları alanlar ile çeşitlilik indeksleri arasındaki ilişki, Spearman korelasyon analizi ile sınanmıştır. Tüm alanlarda 22 takım ve 61 familyayı kapsayan 279 kuş türüne ait toplam 184.068 birey sayılmıştır. Sulak alanlarda tür zenginliği (Margalef indeksi- M) 15.417 ile 22.718 arasında, tür çeşitliliği (Shannon-Wiener İndeksi- H') ise 1.819 ile 2.416 arasında değişmiştir. Araştırma alanlarının önemli bir göç yolu üzerinde yer alması, göç dönemlerinde tür çeşitliliğini ve zenginliğini artırmaktadır. Sığ yüzey sularının baskın olduğu deltalarda, mevsimsel su seviyelerindeki değişiklikler nedeniyle çeşitlilik indekslerinde daha belirgin farklılıklar gözlenmiştir. Tür zenginliği ile sulak alanların, özellikle tuzcul bataklıklar ve sürekli sulanan tarım alanlarının büyüklüğü arasında güçlü pozitif korelasyon bulunmuş olup, bu da biyolojik çeşitliliği desteklemede habitat büyüklüğünün kritik rolüne işaret etmektedir. Mevsimsel su seviyesi dalgalanmaları da delta bölgelerindeki çeşitliliği önemli ölçüde etkilemiştir. Sulak alanların küresel çapta kaybı göz önüne alındığında, bu hayatî ekosistemleri anlamak ve korumak için standart yöntemlerle uzun vadeli araştırmalar yapılması büyük önem taşıyor.

Anahtar kelimeler: Çeşitlilik indeksi, ornitofauna, sulak alan ekosistemi, korelasyon.

1. Introduction

Biodiversity is defined as the genetic, taxonomic, and ecosystem diversity of organisms in a specific area (Evans & Sheldon, 2008, Michel et al., 2020, Oliveira et al. 2019). According to this definition, species and populations serve as indicators of richness within an ecosystem. Wetlands, which constitute one of the most important ecosystems in

Corresponding author: uysalibrahim@comu.edu.tr

terms of biological diversity, provide habitat for numerous fauna and flora species (Dahl et al., 1991; Buckton, 2007; Sulaiman et al., 2015; Dauda et al., 2017; Harris, 1988; Richardson, 1994; Ghermandi et al., 2010; Gray et al, 2013; Murillo-Pacheco et al., 2018).

Therefore, wetlands are among the most important ecosystems on Earth for conserving biological diversity, sustaining ecosystem services, and managing water resources (Uysal & Uysal, 2022). However, since the beginning of the 20th century, a significant portion of wetlands worldwide has been under threat, mainly due to agricultural activities, global warming, anthropogenic pollution, and urbanization (Zedler & Kercher, 2005; Davidson, 2014; Çelik & Çelik, 2024). It is estimated that more than 50% of the total surface area of wetlands has been lost globally over the past century (Mitsch & Gosselink, 2007).

The most important group of wetland ecosystems comprises waterbirds and migratory birds. Waterbirds are highlighted as the primary vectors maintaining biotic connections between basins for aquatic plants and invertebrates and they are the organisms that respond most rapidly to changes in wetland ecosystems (Amezaga et al., 2002; Sulaiman et al., 2015). Therefore, monitoring their distributions, densities, and diversities provides information about their habitats (Sinav, 2019). Similarly, providing critical habitats such as wintering, resting, and nesting areas for migratory birds helps maintain ecosystem balance (Goudarzian & Erfanifard, 2017). In this context, studies have aimed to reveal the relationship between changes in wetland ecosystems and bird species diversity. Scientific research conducted by Arslan et al. (2023) in the Gediz Delta between 1835 and 2019 assessed changes in structure and composition based on average bird abundance using scientific studies, citizen science databases, and expert knowledge surveys. The findings indicated that changes in land cover and land use shape local bird communities. While agricultural practices have led to a decline in bird species in farmlands and grasslands, an increase in bird species diversity in coastal wetlands was observed due to effective conservation measures (Arslan et al., 2023). Nagy et al. (2022), on the other hand, utilized species distribution models to assess the exposure of waterbird species to climate change. They reported that, for most Palearctic migratory waterbird species, habitat losses in current stopover and wintering areas could largely be compensated for by newly emerging climatically suitable areas. However, they emphasized that climate change adaptation measures focusing solely on critical areas would be insufficient to offset the projected habitat losses (Nagy et al., 2022).

In order to monitor changes in wetland ecosystems, it is crucial to conduct bird species inventories and collect data using regular and standardized data collection methods. For this purpose, the comparison of monthly variations in bird species diversity in the wetland areas surrounding the Çanakkale Strait, which plays a significant role in migration strategies for numerous bird species in the northeastern Mediterranean basin, has been aimed. The study aims to test the relationship between similarity among areas, the extent of habitat types, and diversity indices by comparing monthly changes in bird species diversity across these areas.

2. Material and Method

2.1. Study Area

The research was conducted in five different wetland areas surrounding the Çanakkale Strait, which is one of the important bird migration routes in the Western Palearctic region and meets significant natural area criteria. The wetlands where the research was conducted include delta-type wetlands (Kavak Delta, Umurbey Delta, and Kumkale Delta), a lagoon-type wetland (Çardak Lagoon), and a salt lake and coastal wetland (Suvla Salt Lake). The locations of the wetland areas where the study was conducted are provided in Figure 1. Only a part of the Kavak Delta is designated as a Special Environmental Protection Area, while the remaining areas lack any protection status.

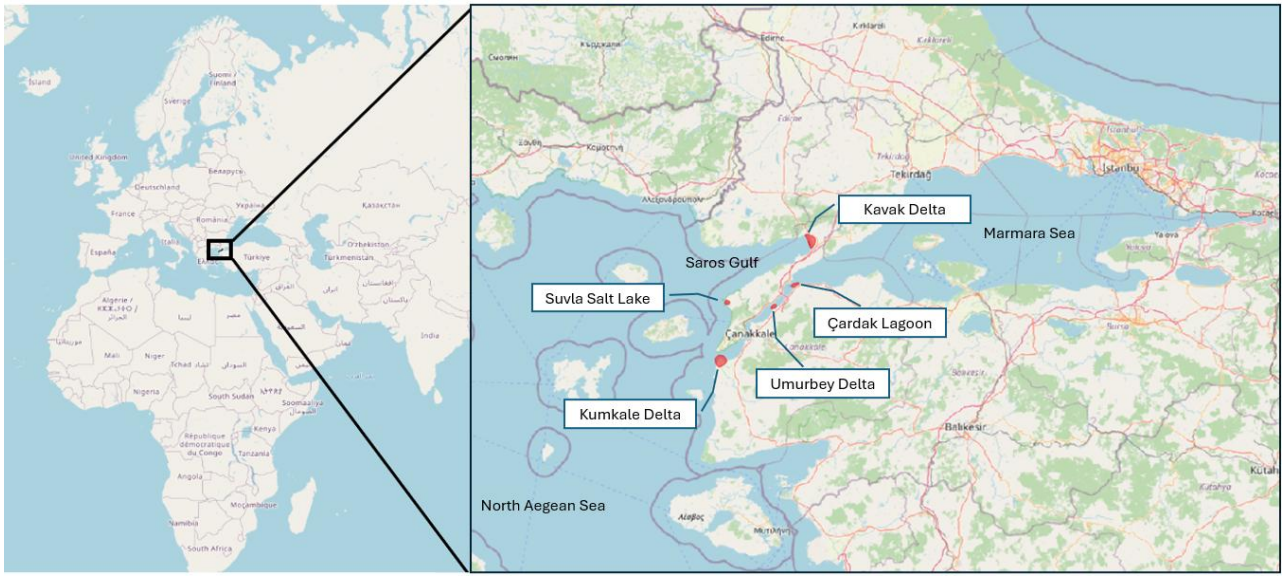

Figure 1. Locations of research sites.

Kavak Delta covers an area of approximately 5851.36 hectares and is characterized by coastal wetland features, including sandy and gravelly coastal dunes, saline and freshwater pools, and irrigated agricultural lands.

Umurbey Delta covers an area of approximately 450 hectares and is a coastal wetland area characterized by mountainous regions, plateau areas, and plains. It encompasses various habitat features such as dry and irrigated agricultural lands, water ponds, and wet meadows. Suvla Salt Lake covers an area of approximately 220 hectares. It comprises of different habitat types including saline marshes, rocky and dune areas, freshwater and brackish water bodies connected to the sea, and rocky areas in the northern part. Kumkale Delta covers an area of approximately 8.513.18 hectares. This coastal wetland area includes diverse habitat features such as dry and wet agricultural lands, saline and freshwater ponds, seasonal and temporary streams, and wet meadows. Çardak Lagoon, on the other hand, is approximately 1363.64 hectares in size and is characterized by a morphological coastal ridge and lagoon features. According to the Corine classification, the wetland areas consist of 14 different habitat types, with salt marshes being the largest habitat component. The areas covered by habitat types determined according to the Corine classification in hectares are provided in Table 1.

Table 1. Distribution and surface area (hectares/ha) of habitat types determined according to Corine classification in wetlands.

Habitat Type	Çardak Lagoon (ha)	Kumkale Delta (ha)	Kavak Delta (ha)	Umurbey Delta (ha)	Suvla Salt Lake (ha)
Total Area	1363.64	8513.18	5851.36	450	220
Salt Marshes	44.74	247.84	1185.74	90	
Non-irrigated Arable Land	38.7	2267.0	978.39	58.5	45.87
Permanently irrigated Land	-	5866.85	2842	8.80	-
Coastal Lagoons	134.99	-	3.55	206.71	
Rice Fields	-	-	60.38	-	-
Olive Groves	380.31	-	-	-	-
Complex Cultivation	79.26	-	-	-	-
Agriculture Land with Natural Vegetation	79.22	-	79.9	-	-
Coniferous Forest	252.39	-	-	-	-
Urban Fabric	102.46	-	44.89	42.33	-
Fruit Trees	290.27	-	-	144.52	-
Transitional Woodland / Shrub	14.46	-	739.96	68.6	-
Pastures	-	98.40	80.2	73.3	-
Beaches, Dunes, Sands	8.89	33.09	12.64	9.11	39.66

2.2. Sampling Method

Fieldwork was conducted in 2023 by visiting each area once a month using point count and transect observation methods as described by Bird and Bildstein (2007). Species and population counts in the areas were conducted using observation points determined to allow observation of the entire area, depending on the characteristics of the area, and the mobility level of the birds. Point count method was used for less mobile waterbirds, while transect (along a line) observation method was used for bird species with higher mobility. Conducting a perfect population count for bird species is quite challenging. This can be attributed to factors such as seasonal and daily bird movements in the areas, the dynamic nature of the area, and the hiding abilities of bird species. Therefore, data collection methods were standardized across all areas and data of sufficient size to allow statistical estimation were collected. Bird counts in all areas were initiated during the early morning hours when birds are most active for feeding and all counts were conducted by an equal number of observers to ensure equal effort in data collection. Additionally, to minimize errors in compiling bird species lists for the areas, data from other bird observers in the region were checked by consulting ebird.org and trakus.org databases and included in the research dataset.

2.3. Data Analysis

In comparing communities, it is essential to make the data obtained through standard data collection methods statistically comparable. One of the methods used for this purpose is the calculation of diversity indices. Index values are mathematical expressions of the ratio of bird species and individual numbers in an area obtained through mathematical operations (Odum & Barrett, 1971). Within the scope of the research, using the monthly counts of species and individuals obtained, diversity, species richness, and evenness indices for each area were calculated monthly. The following formulas were used: Shannon-Wiener diversity index (Shannon & Weaver, 1963) formula: $H' = - \Sigma pi \ln (pi)$; Margalef species richness index (Margalef, 1958) formula: $M = (S - 1) / \ln N$; Pielou index (Pielou, 1966) formula: $J = H' / Hmax = H' / \ln S$. Additionally, to calculate similarities between areas, the Jaccard index (Jaccard, 1901) and cluster analysis were applied. The relationship between habitat types and their areas covered in wetland areas and diversity indices was analyzed using Spearman's rho correlation analysis.

3. Results

The study investigated the monthly variations of bird species lists and diversity indices, as well as the relationship with habitat types, in five wetland areas around the Çanakkale Strait, which serves as a critical resting, feeding, breeding, and wintering area along an important migration route in the Western Palearctic zoogeographic region. Fieldwork conducted monthly in

five different wetland areas resulted in a total count of 184.068 birds belonging to 279 bird species, encompassing 22 orders and 61 families across all areas. Abundance was calculated considering the total number of species throughout the year in all wetland areas. Among the waterbird species dependent on wetlands, *Larus michahellis* with 6.4%, *Phoenicopterus roseus* with 4.7%, and *Tadorna ferruginea* with 2.97% were the most dominant species. The rarest species recorded only once included *Mergus merganser*, *Milvus milvus*, *Buteo lagopus*, *Grus grus*, *Pluvialis fulva, Gallinago media*, *Larus cachinnans*, *Larus armenicus*, *Clamator glandarius*, *Asio flammeus*, *Alaudala rufescens*, and *Lanius excubitor*. The most dominant species for Çardak Lagoon were *Calidris alpina* and *Larus ridibundus*; for Kumkale Delta, *Tadorna ferruginea* and *Larus michahellis*; for Kavak Delta, *Mareca penelope*, *Anas platyrhynchos*, *Calidris alpina*, and *Larus michahellis*; for Umurbey Delta, *Larus ridibundus*, *Larus michahellis*, and *Phylloscopus trochilus*; and for Suvla Salt Lake, *Phoenicopterus roseus*, *Tadorna ferruginea*, and *Tadorna tadorna* species.

3.1. Number of Species

As a result of the research, Çardak Lagoon recorded 162 species belonging to 19 orders and 44 families, Kumkale Delta recorded 234 species belonging to 22 orders and 55 families, Kavak Delta recorded 242 species belonging to 22 orders and 59 families, Umurbey Delta recorded 201 bird species belonging to 21 orders and 51 families, and Suvla Salt Lake recorded 155 bird species belonging to 20 orders and 44 families. The highest number of species observed monthly was 189 species in April at Kavak Delta, while the highest number of individuals was recorded in January with 16.842 individuals, again in Kavak Delta. The lowest number of species observed was 27 species in June at Çardak Lagoon and the lowest number of individuals was recorded in September with 247 individuals, also in Çardak Lagoon. When the counts conducted in all wetland areas were examined by month, the highest number of species was observed in April with 217 species and the highest number of individuals was counted in January with 24.100 individuals. The distributions of total species (S) and individuals (n) recorded based on monthly counts conducted in five wetland areas are presented in Table 2.

Table 2. Observed total species and individual numbers of wetlands by month.

Month	Çardak Lagoon		Kumkale Delta		Kavak Delta		Umurbey Delta		Suvla Salt Lake	
	S	N	S	n	S	n	S	n	S	n
January	89	2225	91	954	106	16842	68	1381	58	2698
February	74	3140	65	8425	91	6850	64	2515	67	2332
March	73	1591	102	1103	76	1105	102	1119	58	932
April	69	1486	160	2325	189	11986	155	5559	93	1950
May	66	617	131	4257	142	3480	125	1842	73	2083
June	27	776	50	418	76	696	73	730	40	666
July	52	848	73	479	59	1177	91	1329	49	1024
August	49	480	126	1792	149	6440	118	1689	53	493
September	47	247	136	3296	169	9668	120	2243	54	1974
October	33	378	130	2819	162	16801	97	1531	36	1175
November	91	2739	86	1019	113	7370	82	1157	31	719
December	71	2594	93	1570	105	11919	86	1273	73	5742
TOTAL	162	17121	234	28457	242	94334	201	22368	155	21788

*S: Total Number of Species, n: Total Number of Individuals

According to the criteria of the International Union for Conservation of Nature (IUCN) Red List, Version 2023/2 (International Union for Conservation of Nature, 2023), among the bird species identified, one species (*Stercorarius parasiticus*) is classified as Endangered at the European scale, 18 species are categorized as Vulnerable, indicating a high risk of extinction in the wild, and nine species are classified as Near Threatened, indicating potential future endangerment. These species belong to 14 orders and 20 families. At the order level, 39% of species in the endangered category belong to the Charadriiformes order and 16% belong to the Anseriformes order. Shallow water birds are species observed in river deltas, estuaries, lagoons, nearshore freshwater habitats, and the sea, being dependent on wetlands for part of their life cycles. These birds can be classified as flamingos, swans, geese, ducks, grebes, pelicans, herons, gulls, and terns. Of the species recorded and classified in the endangered category within the scope of the study, 81.6% are waterbird species. Lists of species endangered at the European and global scales according to IUCN Red List criteria and their regional statuses based on wetland areas are provided in Table 3.

3.2. Diversity Indexes

Within the scope of the study, the total number of species and individuals recorded in the wetland areas over one year was evaluated along with species richness, diversity, and evenness of species distribution. Diversity indices graphics in wetlands are given Figure 2. The Margalef index represents species richness, varying depending on the number of species and has no limit value. The area with the highest species richness in the study was Kumkale Delta (D: 22.718). The number of species in an area is directly related to habitat diversity and Kumkale Delta

recorded the highest number of habitat types among the wetland areas surveyed. The Shannon-Wiener Index (H') represents species diversity and as the value increases, the diversity of species in the area also increases. The index generally ranges between 0 and 5. Among the study areas, Kavak Delta exhibited the highest species diversity (H': 2.416). The Pielou Index provides information about the balance of species distribution, ranging from 0 to 1, with a value close to 1 indicating a balanced distribution among species within the community. Across all the wetland areas surveyed in the study, values ranged from 0.357 to 0.466 based on the total observation data collected over one year.

Table 3. List of endangered bird species detected in wetlands according to IUCN Red List criteria (v.2023/2).

Species	Common Name	IUCN (Europe)	IUCN (Global)	Kumkale Delta	Kavak Delta	Çardak Lagoon	Umurbey Delta	Suvla Salt Lake
Podiceps auritus	Horned Grebe	NT	VU	-	Wv	Wv	-	-
Podiceps nigricollis	Black-necked Grebe	VU	LC	Wv, r	Wv	Wv	Wv	Wv
Pelecanus crispus	Dalmatian Pelican	LC	NT	T	Wv	T	T	Wv
Puffinus yelkouan	Yelkouan Shearwater	VU	VU	T	T	T	T	T
Cygnus columbianus	Tundra Swan	VU	LC	-	Wv	-	-	-
Aythya ferina	Common Pochard	VU	VU	Wv	Wv,t	Wv	Wv	-
Aythya nyroca	Ferruginous Duck	LC	NT	Wv, r	Wv	Wv	Wv	-
Aythya fuligula	Tufted Duck	NT	LC	T	Wv,t	-	T	-
Mergus serrator	Red-breasted Merganser	NT	LC	-	Wv	Wv	-	Wv
Oxyura leucocephala	White-headed Duck	VU	EN	T	-	-	T	-
Circus macrourus	Pallid Harrier	LC	NT	T	T	-	T	T
Falco vespertinus	Red-footed Falcon	VU	VU	T	T	-	T	-
Falco columbarius	Merlin	VU	LC	Wv	Wv	Wv	-	Wv
Coturnix coturnix	Common Quail	NT	LC	T	T	-	T	-
Fulica atra	Common Coot	NT	LC	R, Wv	Wv	Wv	R, Wv	T
Tetrax tetrax	Little Bustard	VU	NT	T	Wv	-	-	-
Haematopus ostralegus	Eurasian Oystercatcher	VU	NT	T	T,yz	Sv	T	T
Vanellus vanellus	Northern Lapwing	VU	NT	Wv	Wv	T	T	T
Calidris canutus	Red Knot	LC	NT	T	T	T	-	-
Calidris ferruginea	Curlew Sandpiper	VU	NT	T	T	T	T	T
Limicola falcinellus	Broad-billed Sandpiper	VU	LC	T	T	T	T	T
Philomachus pugnax	Ruff	NT	LC	T	Wv,t	T	T	T
Gallinago gallinago	Common Snipe	VU	LC	Wv	Wv	Wv	Wv	Wv
Limosa limosa	Black-tailed Godwit	NT	NT	T	T	-	T	-
Limosa lapponica	Bar-tailed Godwit	LC	NT	T	T	-		
Numenius arquata	Eurasian Curlew	NT	NT	Wv	Wv	Wv	Wv	Wv
Tringa totanus	Common Redshank	VU	LC	R	R	R	R	R
Stercorarius parasiticus	Arctic Jaeger	EN	LC	-	T	-	-	-
Chroicocephalus genei	Slender-billed Gull	VU	LC	Wv	Wv	Wv	Wv	Wv
Ichthyaetus audouinii	Audouin's Gull	VU	VU	Wv	Wv	-	-	Wv
Streptopelia turtur	European Turtle-dove	VU	VU	Sv	T	T	T	-
Lanius senator	Woodchat Shrike	NT	NT	Sv	-	Sv	Sv	Sv
Apus apus	Common Swift	LC	NT	T	T	T	-	-
Corvus frugilegus	Rook	VU	LC	T	-	-	-	-
Turdus iliacus	Redwing	LC	NT	-	Wv	-	-	-

In the wetland areas where the study was conducted, the highest species diversity (Shannon-Wiener Indices) was observed in May (H': 2.659) in Kavak Delta, while species richness (Margalef Index) was recorded in April (M: 20.512) in Kumkale Delta. Species richness values were found to increase during the spring migration period (April, May, June) and the autumn migration period (September, October) in Kavak Delta, Kumkale Delta, and Umurbey Delta. In Suvla Salt Lake, species richness increases during the spring migration period (March, April) and winter period (December, February), while in Çardak Lagoon, it increases during the spring migration period and winter period (May, November, January). The lowest species richness values were calculated in July, the breeding season, across all areas. Monthly variations in species richness are given Figure 3.

Diversity indices are quantitative measures reflecting the number of different species and how evenly individuals are distributed among these species. Typically, the value of a diversity index increases as the number of species and evenness increase. For instance, communities where numerous species are evenly distributed are considered the most diverse, while those with fewer species and dominance of a single species are considered the least diverse. Although a decrease in diversity was observed in August in Kavak Delta and in June in Kumkale Delta, these periods coincide with the breeding season for bird species. In Kumkale Delta, the lowest diversity across all areas was recorded in February, likely due to the dominance of a single species, the starling (*Sturnus vulgaris*), which accounted for 8000 individuals recorded in the area. Monthly variations in species diversity are given Figure 4.

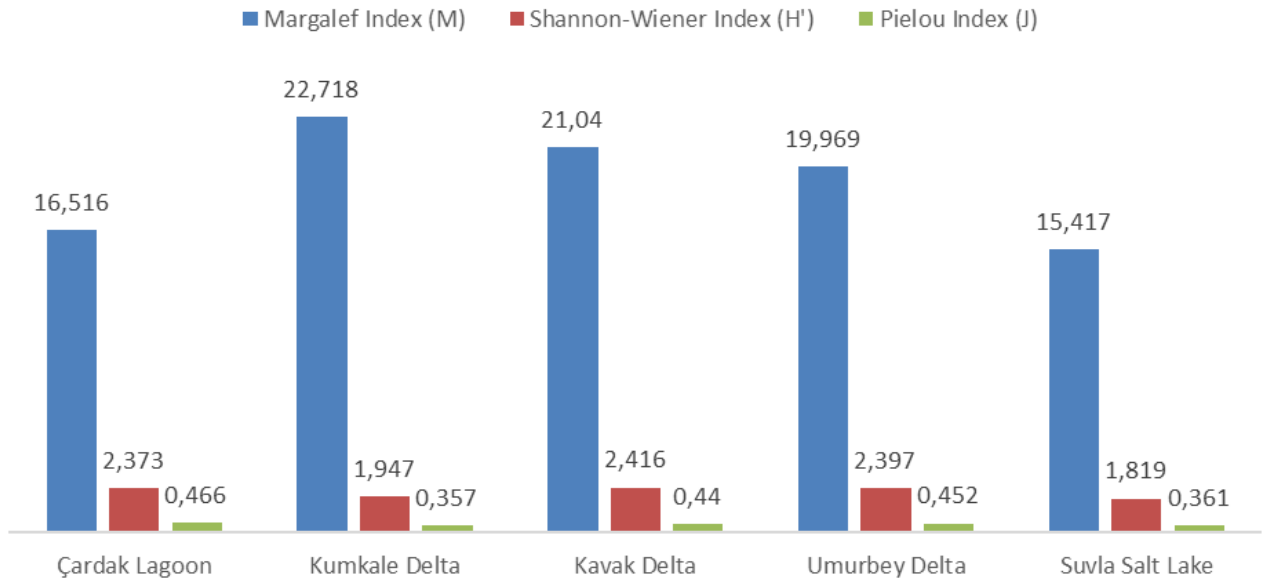

Figure 2. Diversity indices in wetlands.

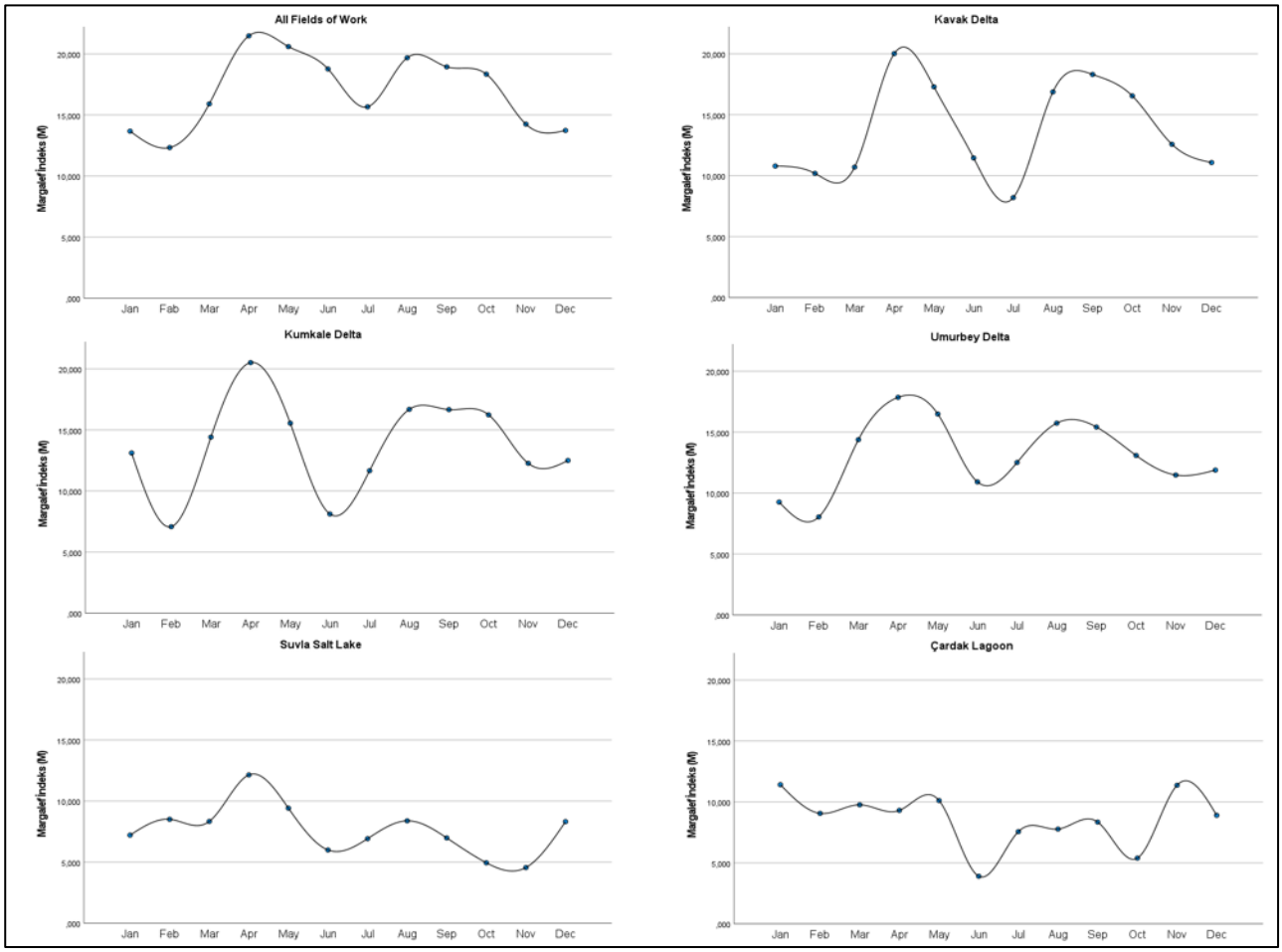

Figure 3. Monthly variations in species richness (Margalef Index).

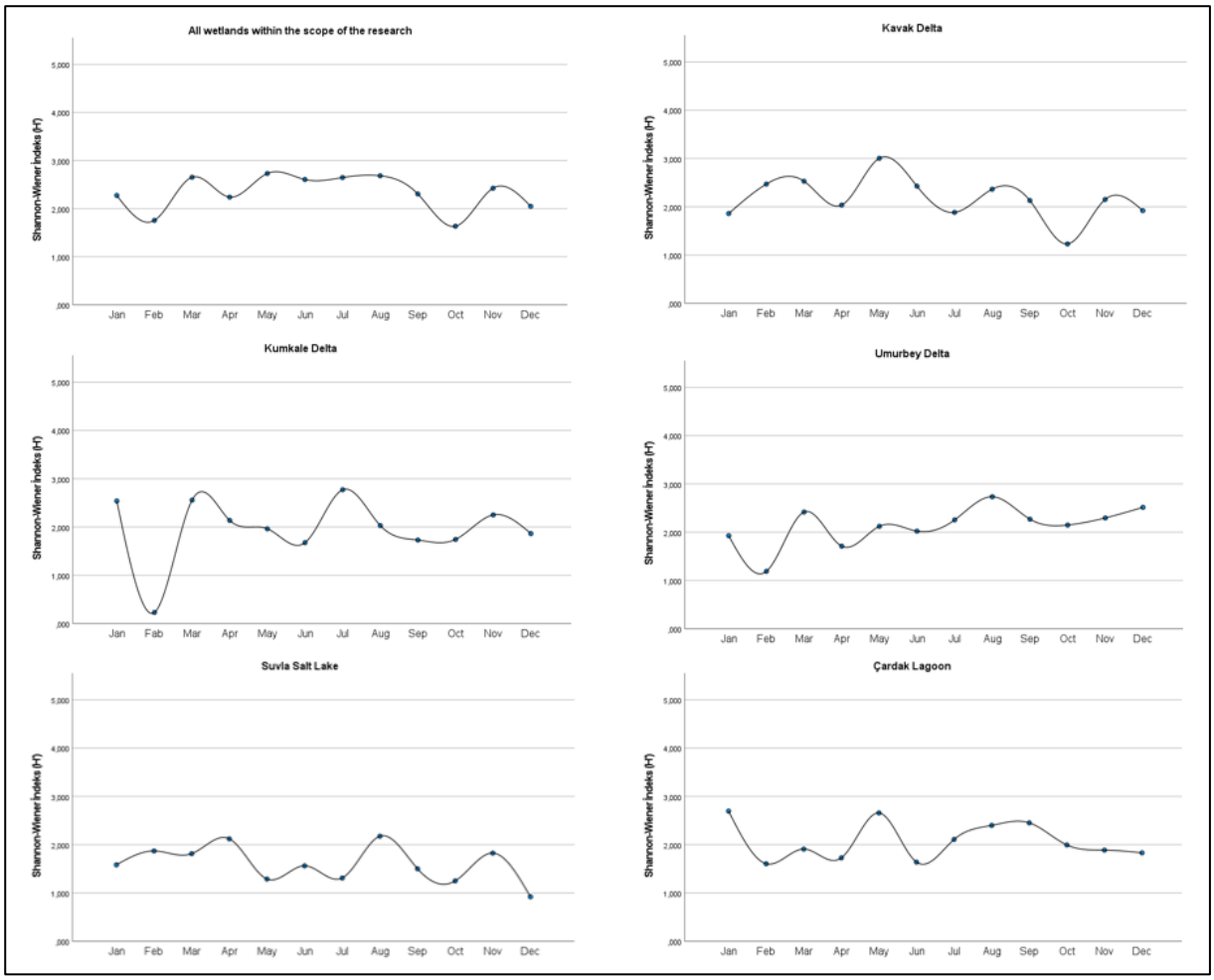

Figure 4. Monthly variations in species diversity (Shannon-Wiener Indices).

3.3. Similarity Index

The dendrogram resulting from the hierarchical clustering analysis based on species compositions in the wetlands is presented in Figure 5. The dendrogram illustrates the relationships between wetlands in terms of their similarity and distance, forming clusters. It can be observed that Kumkale Delta and Kavak Delta are the most similar wetlands, forming a cluster with Umurbey Delta, while Çardak Lagoon and Suvla Salt Lake, although less similar to each other, form a separate cluster. Hierarchical cluster analysis dendrogram are given Figure 5.

3.4. Correlation Analysis Results

According to the results of the Spearman's rho correlation analysis conducted to examine the relationship between species lists of wetland areas, the total recorded abundance of individuals, calculated diversity indices, and the sizes (hectares) of habitat types present in the wetlands, the following correlations were observed: Species richness (Margalef Index) showed a strong positive correlation with the total size of the wetland area as well as the sizes of salt marshes, permanently irrigated land, and pasture areas. Species diversity (Shannon-Wiener index) exhibited a strong positive correlation with the size of Transitional Woodland/Shrub habitats. The Pielou index revealed a strong negative correlation with the size of beaches, dunes, and sands habitats. Correlation between diversity indices and wetland habitat types are given Table 4.

4. Discussion

In the monthly counts conducted in the wetland areas within the scope of the research, the highest number of species was observed in April with 92 species, while the highest number of individuals, totaling 10.991 individuals, was observed in January. Fieldwork conducted once a month in five different wetland areas resulted in a total count of 184.068 birds belonging to 279 bird species within 22 orders and 61 families across all areas. Standard data collection methods should be used for comparing communities and the obtained data should be made statistically comparable. One of the methods used for this purpose is the calculation of diversity indices. In the study conducted by Uysal and Uysal (2021), investigating the monthly diversity indices of waterbirds in Suvla Salt Lake, it was found that the highest species diversity was in February (H': 2.377). Similarly, in the present study, the highest species diversity (H': 1.871) was observed in February, although the diversity index showed a declining trend. In a study conducted by Dauda et al. (2017) in the Ramsar site Uchali wetland in Pakistan, comparisons were made with previous studies conducted in the area, revealing that the number of bird species supported by the wetland area was significantly lower in the recent past (1991) compared to the number of bird species supported by the same wetland area. When evaluated together with previous studies conducted in the same area, it was found that there was an annual decrease of 6.59 species. The study conducted in the wetland areas surrounding the

Çanakkale Strait, which forms one of the important bird migration routes in the Mediterranean basin, provides data for future monitoring studies. These data along this important migration route can provide insights into the changes in bird species diversity across a wide region.

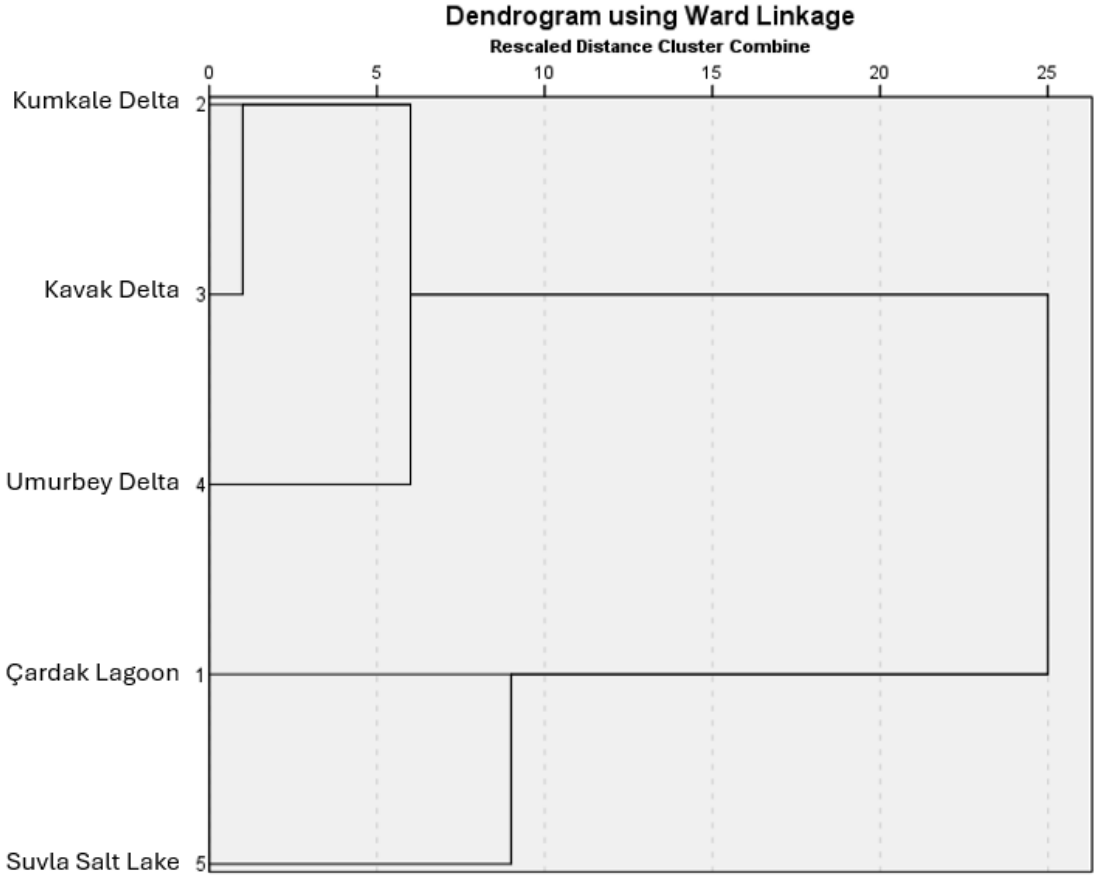

Figure 5. Hierarchical cluster analysis dendrogram.

Table 4. Correlation between diversity indices and wetland habitat types.

Habitat size (hectare)	Margalef Index (M)	Shannon -Wiener Index (H')	Pielou Index (J)
Total Area	**.900***	.300	-.300
Salt Marshes	**.900***	.700	-.200
Non-irrigated Arable Land	**.900**	.200	-.700
Permanently irrigated Land	**.975****	.308	-.564
Coastal Lagoons	-.103	.667	.872
Rice Fields	.354	.707	.000
Olive Groves	-.354	.000	.707
Complex Cultivation	-.354	.000	.707
Agriculture Land with Natural Vegetation	.112	.671	.447
Coniferous Forest	-.354	.000	.707
Urban Fabric	-.103	.667	.872
Fruit Trees	-.335	.224	.894
Transitional Woodland / Shrub	.205	**.975****	.564
Pastures	**.975****	.308	-.564
Beaches, Dunes, Sands	.000	-.600	**-.900***

**. Correlation is significant at the 0.01 level.

*. Correlation is significant at the 0.05 level.

To highlight the adverse effects of wetland losses on biodiversity and sustainability at a global scale, there is a need for model organisms. Bird species are living organisms capable of quickly responding to sudden and adverse changes in their habitats and they provide significant ecosystem services. With their ability to rapidly

relocate in response to environmental changes, bird species can serve as indicator species and model organisms for monitoring the sustainable and healthy structure of ecosystems, unlike other animal groups.

To be able to compare different wetland areas and track changes in their ecosystems, it is necessary to make an inventory of species and conduct regular counts. The effects of global warming and increasing anthropogenic pressures around wetlands, such as disturbances in the water regime and wetland losses, are accelerating the extinction rate of some species, which are vital components of these ecosystems. In recent years, researchers' trends towards assessing and conserving biological diversity draw attention to this issue (Guo et al., 2003). The combined effects of land-use changes and climate change lead to biodiversity loss, community homogenization, and a decline in ecosystem functioning (Sekercioglu et al. 2008; Newbold et al., 2019; Rastandeh & Pedersen, 2018; Zhao et al., 2016; Northrup et al., 2019; Bateman et al. 2020). The Çanakkale Strait, located in the northeastern part of the Mediterranean basin, serves as an important migration corridor for numerous bird species. This underscores the ornithological importance of the wetlands surrounding the Çanakkale Strait. Diversity and similarity indices enable the standardization of data for comparing bird communities across different areas. Within the scope of this study, monthly variations in bird species diversity in the wetlands around the Çanakkale Strait were investigated. Additionally, correlations between the habitat types and areas of these wetlands and their diversity indices were analyzed and updated species lists for the studied wetlands were compiled.

In previous studies conducted in the wetland areas where the research was carried out, there were no data available on bird species lists. However, with the current study, updated bird species lists have been compiled. In the study conducted by Özcan et al. (2009) in Kavak Delta, between 2005 and 2007, 130 bird species belonging to 14 orders and 40 families were listed. Through monthly counts and bird observation data collected regularly within the scope of the research, the distribution of 242 species belonging to 22 orders and 59 families was determined in Kavak Delta. In the postgraduate thesis study conducted by Samsa (2012) in Çardak Lagoon between 2008 and 2011, 102 species belonging to 15 orders and 35 families were identified. In the research conducted, 162 species belonging to 19 orders and 44 families were identified in Çardak Lagoon. In the postgraduate thesis study conducted by Şengül (2012) in Kumkale Delta between 2011 and 2012, 120 bird species belonging to 14 orders and 39 families were identified. However, in the research, 234 bird species belonging to 22 orders and 55 families were identified in Kumkale Delta. In the study conducted by Uyman and Tosunoğlu (2019) in Umurbey Delta, 182 bird species belonging to 20 orders and 49 families were recorded. However, in the research, 201 bird species belonging to 21 orders and 51 families were identified in Umurbey Delta. In the study conducted by Uysal and Uysal (2021) in Suvla Salt Lake, 154 bird species belonging to 20 orders and 44 families were identified through monthly observations between 2017-2020. However, in the research completed with monthly counts in 2023, 155 bird species belonging to 20 orders and 44 families were recorded in Suvla Salt Lake. The increase in species numbers observed in the current study compared to the previous studies is believed to be related not to the increase in bird species diversity in the area but rather to the regular monthly observations conducted in the field. Globally, the decline in population sizes and ranges of numerous species continues rapidly. In recent years, observed changes in the distribution of many species are primarily attributed to ongoing rapid climate change and large-scale habitat loss (Sekercioglu et al. 2008; Davidson, 2014; Northrup et al., 2019). Additionally, there is a northward shift in the distribution of waterbird species due to the impact of global warming (Hickling et al., 2006; Chen & Zhou, 2011). On the other hand, the increase in species numbers observed in the study areas compared to the previous literature data is thought to be associated with the standard observation methodology, namely, the conduct of monthly fieldwork and the increase in the number of bird observers, paralleled by the increase in data entered into national and international databases within the scope of citizen science.

It is noted that the relationship between wetlands and bird species is bidirectional, with wetlands playing an important role in shaping the richness of bird species (Skórka et al., 2006). The decrease in the number of bird species in wetlands can be attributed to fluctuations in the surface area and water level of the wetland. Studies in this regard have shown a positive relationship between the abundance of bird species and the water level of wetlands (Maclean et al., 2011; Sharma & Saini, 2012). Additionally, habitat diversity in wetlands is also associated with bird species diversity (Uysal & Uysal, 2022). Similarly, the sudden decrease in species diversity in wetlands is mainly attributed to habitat changes (Azizoğlu et al., 2023; Reif & Flousek, 2012; González & Farina, 2013; Russell et al., 2014). Among the 5 wetland areas where data was collected in the study, Çardak Lagoon stands out in terms of similarity as it is connected to the sea through the lagoon mouth and maintains water levels throughout the year. The species composition and diversity indices in these areas did not show significant differences compared to the other areas throughout the year. In Deltas where shallow surface waters are more abundant, there were more pronounced differences in diversity indices due to seasonal variations in water levels. In the study, a strong positive relationship was found between species richness (Margalef Index) and the total size of the wetland, salt marshes, permanently irrigated land, and pasture areas.

In all wetland areas where the research was conducted, the breeding seasons were found to be the periods with the lowest species diversity and richness. Pearce-Higgins et al. (2015) noted in their study in the UK that there were changes among important species groups during the breeding season (especially in June), winter (December- February), and summer (July and August) periods and that cold winters had a consistent negative impact on resident and short-distance migrant bird populations in the UK on a large scale. They mentioned that the populations of long-distance migrants were not affected by winter temperatures throughout the year but were strongly associated with rainfall in their wintering areas. Being located on an important migration route increases species diversity and richness during migration periods in our study area, while during the winter period, with species coming to winter from further north, species

diversity and richness increase. However, due to the impact of global warming, there has been a northward shift in the distribution of waterbird species (Hickling et al., 2006; Chen & Zhou, 2011) and since the early 20th century, a large part of wetlands worldwide has become the most threatened habitats due to the factors such as agricultural activities, global warming, anthropogenic pollution, and urbanization (Zedler & Kercher, 2005; Davidson, 2014).

The dendrogram derived from the hierarchical clustering analysis based on species compositions in the wetlands indicates that the Kumkale Delta and Kavak Delta exhibit the highest similarity, clustering together with the Umurbey Delta. In contrast, the Çardak Lagoon and Suvla Salt Lake, despite being less similar to each other, form a distinct cluster. Typically, in wetlands where the water table is close to the surface, the terrain is covered with shallow waters, water sources feeding the wetland are small, and the water level changes more rapidly seasonally or depending on temperatures. This rapid fluctuation in water level leads to faster changes in bird species populations within the wetland. Despite not being fed by freshwater sources in terms of wetland type, Çardak Lagoon and Suvla Salt Lake, due to their connection to the sea, relatively maintain their water levels and cover a larger area of saline and brackish water compared to other more deltaic wetlands. The differences in species compositions and diversity indices in these areas compared to other wetlands, and their relatively stable changes throughout the year, can be explained by this situation.

5. Conclusions

The study underscores the importance of standardized bird species monitoring to track ecosystem changes, particularly in the Çanakkale/Dardanelles Strait, a key migratory route in the Mediterranean. According to Kiziroğlu (2015), the number of bird species recorded in Turkey is 513. 54.5% of the bird species recorded in Turkey were observed in the wetlands where the study was conducted. This situation points to the ornithological importance of the Dardanelles and the surrounding wetlands, which are on an important migration route. Observing 279 species across 22 orders and 61 families, the research reveals high species richness and diversity, especially during migration periods. A strong positive correlation was found between species richness and the size of wetlands, particularly salt marshes and permanently irrigated lands, indicating the critical role of habitat size in supporting biodiversity. Seasonal water level fluctuations also significantly impacted diversity in delta regions. Given the global loss of wetlands, long-term research with standardized methods is crucial for understanding and protecting these vital ecosystems.

Ethics committee approval: Ethics committee approval is not required for this study.

Conflict of interest: The authors declare that there is no conflict of interest.

Author Contributions: Conception – İ.U., M.T.; Design – İ.U.; Supervision – İ.U., M.T.; Data Collection and Processing – İ.U., D.K., C.N.Ö., M.T.; Analysis Interpretation – İ.U., D.K., C.N.Ö.; Literature Review – – İ.U., D.K., C.N.Ö.; Writing – – İ.U., D.K., C.N.Ö., M.T.; Critical Review – – İ.U., D.K.

References

Amezaga, J.M., Santamaría, L., & Green, A.J. (2002). Biotic wetland connectivity—supporting a new approach for wetland policy. *Acta oecologica*, 23(3), 213-222. https://doi.org/10.1016/S1146-609X(02)01152-9.

Arslan, D., Ernoul, L., Béchet, A., Döndüren, Ö., Siki, M., & Galewski, T. (2023). Using literature and expert knowledge to determine changes in the bird community over a century in a Turkish wetland. *Marine and Freshwater Research*, 74(3), 220–233. https://doi.org/10.1071/MF21332.

Azizoglu, E., Kara, R., & Celik, E. (2023). A statistical approach on distribution and seasonal habitat use of waterfowl and shorebirds in Çıldır Lake (Ardahan, Türkiye). *Environmental Science and Pollution Research*, 30(31), 77371-77384.

Bateman, B.L., Taylor, L., Wilsey, C., Wu, J., LeBaron, G.S., & Langham, G. (2020). Risk to North American birds from climate change-related threats. *Conservation Science and Practice*, 2(8), e243.

Bird, D.M. & Bildstein, K.L. (2007). Raptor Research and Management Techniques. Hancock House Publisher. Surrey, Canada.

Buckton, S. (2007). Managing wetlands for sustainable livelihoods at Koshi Tappu. *Danphe*, 16(1), 12-13.

Chen, J., & Zhou, L. (2011). Guild structure of wintering waterbird assemblages in shallow lakes along Yangtze River in Anhui Province, China. *Shengtai Xuebao/Acta Ecologica Sinica*, 31(18), 5323-5331.

Çelik, M. A., & Çelik, E. (2024). Are Urbanisation and Biodiversity Antithetical? A Bibliometric Analysis. *Coğrafya Dergisi*, (48), 121-135.

Dahl, T.E., Johnson, C.E. & Frayer, W.E. (1991). Wetlands, status and trends in the conterminous United States mid-1970's to mid-1980's. US Fish and Wildlife Service.

Dauda, T.O., Baksh, M.H., & Shahrul, A.M.S. (2017). Birds' species diversity measurement of Uchali Wetland (Ramsar site) Pakistan. *Journal of Asia-Pacific Biodiversity*, 10(2), 167-174. https://doi.org/10.1016/j.japb.2016.06.011

Davidson, N.C. (2014). How much wetland has the world lost? Long-term and recent trends in global wetland area. *Marine and Freshwater Research*, 65(10), 934-941. https://doi.org/10.1071/MF14173

Evans, S.R., & Sheldon, B.C. (2008). Interspecific patterns of genetic diversity in birds: correlations with extinction risk. *Conservation Biology*, *22*(4), 1016-1025.

Ghermandi, A., Van Den Bergh, J.C., Brander, L.M., De Groot, H.L., & Nunes, P.A. (2010). Values of natural and human-made wetlands: A meta-analysis. *Water Resources Research*, 46(12). https://doi.org/10.1029/2010WR009071

González, A.L., & Fariña, J.M. (2013). Changes in the abundance and distribution of black-necked swans (*Cygnus melancoryphus*) in the Carlos Anwandter Nature Sanctuary and Adjacent Wetlands, Valdivia, Chile. *WATERBIRDS: The International Journal of Waterbird Biology*, 36(04), 507-514. http://www.bioone.org/doi/full/10.1675/063.036.0408

Goudarzian, P., & Erfanifard, S.Y. (2017). The efficiency of indices of richness, evenness and biodiversity in the investigation of species diversity changes (case study: migratory water birds of Parishan international wetland, Fars province, Iran). *Biodiversity International Journal*, 1(2), 41-45. https://doi.org/10.15406/bij.2017.01.00007

Gray, M.J., Hagy, H.M., Nyman, J.A., & Stafford, J.D. (2013). Management of wetlands for wildlife. In: Anderson MG, Davis CA (eds) *Wetland techniques: Volume 3: Applications and management*. Springer, Dordrecht, 121–180.

Guo, Y., Gong, P., & Amundson, R. (2003). Pedodiversity in the United States of America. *Geoderma*, 117(1-2), 99-115. https://doi.org/10.1016/S0016-7061(03)00137-X.

Harris, L.D. (1988). The nature of cumulative impacts on biotic diversity of wetland vertebrates. *Environmental Management*, 12, 675-693. https://doi.org/10.1007/BF01867545.

Hickling, R., Roy, D.B., Hill, J.K., Fox, R., & Thomas, C.D. (2006). The distributions of a wide range of taxonomic groups are expanding polewards. *Global change biology*, 12(3), 450-455. https://doi.org/10.1111/j.1365-2486.2006.01116.x.

International Union for Conservation of Nature (2023). The IUCN Red List of Threatened Species. Version 2023-2. Retrieved from https://www.iucnredlist.org.

Jaccard, P. (1901). Etude comparative de la distribution florale dans une portion des Alpes et du Jura. *Bulletin de la Soci´et´e Vaudoise des Sciences Naturelles*, 37(1), 547–579.

Kiziroğlu, İ. (2015). Türkiye Kuşları Cep Kitabı (The pocket book for birds of Turkey). İnkılap Kitabevi. Ankara, Türkiye.

Maclean, I.M., Wilson, R.J., & Hassall, M. (2011). Predicting changes in the abundance of African wetland birds by incorporating abundance–occupancy relationships into habitat association models. *Diversity and Distributions*, 17(3), 480-490. https://doi.org/10.1111/j.1472-4642.2011.00756.x.

Michel, N.L., Whelan, C.J., & Verutes, G.M. (2020). Ecosystem services provided by Neotropical birds. *The Condor*, 122(3).

Mitsch, W.J. & Gosselink, J.G. (2007). Wetland ecosystems Wilet J. & Sons Ed., New York, 4th ed, pp. 256.

Murillo-Pacheco, J., López-Iborra, G.M., Escobar, F., Bonilla-Rojas, W.F., & Verdú, J.R. (2018). The value of small, natural and man-made wetlands for bird diversity in the east Colombian Piedmont. *Aquatic Conservation, Marine and Freshwater Ecosystems*, 28(1), 87-97. https://doi.org/10.1002/aqc.2835.

Nagy, S., Breiner F.T., Anand, M., F. T. Breıner, S. H. M. Butchart, E. Fluet-Chouınard, M. Flörke, A. Guısan, L. Hılarıdes, et al. 2022. Climate change exposure of waterbird species in the African-Eurasian flyways. Bird Conservation International. 2022, 32(1), 1-26. doi: https://doi.org/10.1017/S0959270921000150

Newbold, T., Adams, G.L., Robles, G.A., Boakes, E.H., Ferreira, G.B., Chapman, A.S., Outhwaite, C.L. (2019). Climate and land-use change homogenise terrestrial biodiversity, with consequences for ecosystem functioning and human well-being. *Emerging Topics in Life Sciences*, 3, 207–219.

Odum, E.P. & Barrett, G.W. (1971). Fundamentals of ecology. Saunders Philadelphia.

Oliveira, J.D., Almeida, S.M., Florencio, F.P., Pinho, J.B., Oliveira, D.M., Ligeiro, R., & Rodrigues, D.J. (2019). Environmental structure affects taxonomic diversity but not functional structure of understory birds in the southwestern Brazilian Amazon. *Acta Amazonica*, 49, 232-241.

Özcan, H., Akbulak, C., Kelkit, A., Tosunoğlu, M., & İsmet, U. (2009). Ecotourism potential and management of kavak delta (northwest turkey). *Journal of Coastal Research*, 25(3), 781-787. https://doi.org/10.2112/08-1068.1.

Pearce-Higgins, J.W., Eglington, S.M., Martay, B., & Chamberlain, D.E. (2015). Drivers of climate change impacts on bird communities. *Journal of Animal Ecology*, 84(4), 943-954. https://doi.org/10.1111/1365-2656.12364.

Pielou, E.C. (1966). The measurement of diversity in different types of biological collections. *Journal of Theoretical Biology,* 13, 131-144.

Rastandeh, A., & Pedersen, Z.M. (2018). A spatial analysis of land cover patterns and its implications for urban avifauna persistence under climate change. *Landscape Ecology*, 33, 455–474.

Reif, J., & Flousek, J. (2012). The role of species' ecological traits in climatically driven altitudinal range shifts of central European birds. *Oikos*, 121(7), 1053-1060. https://doi.org/10.1111/j.1600-0706.2011.20008.x.

Richardson, C.J. (1994). Ecological functions and human values in wetlands: a framework for assessing forestry impacts. *Wetlands*, 14, 1-9. https://doi.org/10.1007/BF03160616.

Russell, I.A., Randall, R.M., & Hanekom, N. (2014). Spatial and temporal patterns of waterbird assemblages in the Wilderness Lakes Complex, South Africa. *WATERBIRDS: The International Journal of Waterbird Biology*, 1-18. https://doi.org/10.1675/063.037.0104.

Samsa, Ş. (2012). Çardak (Çanakkale/Türkiye) Lagünü Avifaunası (309626). Retrieved from https://tez.yok.gov.tr/UlusalTezMerkezi/tezSorguSonucYeni.jsp

Shannon, C.E. & Weaver, W. (1963). The Mathematical Theory of Communication, Urbana, University of Illinois Press, Urbana, USA, pp. 117.

Sharma, K.K., & Saini, M. (2012). Impact of anthropogenic pressure on habitat utilization by the waterbirds in Gharana Wetland (reserve), Jammu (J&K, India). *International Journal of Environmental Sciences*, 2(4), 2050-2062.

Sinav, L. (2019). Türkiye'deki Kuş Türü Zenginliğinin Coğrafi Varyasyon Deseni (589924). Retrieved from https://tez.yok.gov.tr/UlusalTezMerkezi/tezSorguSonucYeni.jsp

Skórka, P., Martyka, R., & Wójcik, J.D. (2006). Species richness of breeding birds at a landscape scale: which habitat type is the most important? *Acta Ornithologica*, 41(1), 49-54. https://doi.org/10.3161/068.041.0111.

Sulaiman, I.M., Abubakar, M.M., Ringim, A.S., Apeverga, P.T., & Dikwa, M.A. (2015). Effects of wetlands type and size on bird diversity and abundance at the Hadejia-Nguru wetlands, Nigeria. *International Journal of Research Studies in Zoology*, 1(1), 15-21.

Margalef, R. (1958). Information theory in ecology. *General Systems,* 3, 36-71.

Northrup, J.M., Rivers, J.W., Yang, Z., & Betts, M.G. (2019). Synergistic effects of climate and land-use change influence broad-scale avian population declines. *Global Change Biology*, 25, 1561–1575.

Sekercioglu, C. H., Schneider, S. H., Fay, J. P., & Loarie, S. R. (2008). Climate change, elevational range shifts, and bird extinctions. *Conservation Biology*, 22, 140–150.

Şengül, E. (2012). Kumkale Deltası' nın Avifaunası (326628). Retrieved from https://tez.yok.gov.tr/UlusalTezMerkezi/tezSorguSonucYeni.jsp

Uyman, M., & Tosunoğlu, M. (2019). Diversity of Bird Species in Umurbey Delta (Çanakkale/Turkey). 1st International Symposium on Biodiversity Research, Çanakkale, Turkey, 2–4 May 2019. pp. 342-355.

Uysal, İ., & Uysal, İ. (2021). Suvla Tuz Gölü (Çanakkale/Türkiye)'nün Ornithofaunası ve Su Kuşları Çeşitlilik Göstergeleri'nin Aylık Değişimi. *Environmental Toxicology and Ecology*, 1(1), 14-26.

Uysal, İ., & Uysal, İ. (2022). Evaluation of different wetland preferences of wintering waterbird species in Çanakkale, Turkey. *Turkish Journal of Biodiversity*, 5(1), 17-29. https://doi.org/10.38059/biodiversity.1034415

Zhao, Q., Silverman, E., Fleming, K., & Boomer, G. S. (2016). Forecasting waterfowl population dynamics under climate change - Does the spatial variation of density dependence and environmental effects matter? *Biological Conservation*, 194, 80–88.

Zedler, J.B., & Kercher, S. (2005). Wetland resources: status, trends, ecosystem services, and restorability. *Annual Review of Environment and Resources*, 30(1), 39-74. https://doi.org/10.1146/annurev.energy.30.050504.144248

Commagene Journal of Biology

Al-Jubouri & Al-Khazali, (2025) *Comm. J. Biol.* 9(1), 28-32.
DOI: 10.31594/commagene.1587687

e-ISSN 2602-456X

Research Article/Araştırma Makalesi

Investigation of Scorpion Stings in Nineveh Province, Northern Iraq, for the Period 2022-2023

Mohammed Abdul Karim AL-JUBOURI, Azhar Mohammed AL-KHAZALI

Department of Science, College of Basic Education, University of Sumer, Dhi Qar, IRAQ
ORCID ID: Mohammed Abdul Karim AL-JUBOURI: https://orcid.org/0009-0007-8928-292X,
Azhar Mohammed AL-KHAZALI: https://orcid.org/0000-0001-7268-696X

Received: 19.11.2024 **Accepted:** 04.02.2025 **Published online:** 13.02.2025 **Issue published:** 30.06.2025

Abstract: Scorpion stings are a challenging health problem in many hot and dry regions worldwide, including Iraq. Although studies on the epidemiology of scorpions in Iraq are rare, the northern areas, especially Nineveh province, have not witnessed comprehensive epidemiological studies related to these poisonous arachnids. This research is the first study in this region, providing detailed information on scorpion stings in Nineveh province during 2022 and 2023. The current study included 327 cases of scorpion stings recorded during 2022 and 2023 in Nineveh province, northern Iraq. Of the recorded cases, 185 (57.56%) were males and 142 (43.42%) were females. The data showed that the age group most exposed to scorpion stings is people aged between 15-49 years, as this group represented 70.34% of the total recorded cases, indicating that the socially and economically active group is most exposed to the risks associated with scorpions. It was also determined that the highest number of scorpion stings occurred in the summer months, highlighting the relationship between high temperatures and increased scorpion activity. These results indicate the need to take preventive and advisory measures directed at the most vulnerable groups, especially during the hot months.

Keywords: Epidemiology, scorpionism, stings, Mosul, venom.

2022-2023 Döneminde Kuzey Irak Ninova İli'ndeki Akrep Sokmalarının Araştırılması

Öz: Akrep sokmaları, Irak da dahil olmak üzere dünya çapında birçok sıcak ve kuru bölgede önemli bir sağlık sorunudur. Irak'taki akreplerin epidemiyolojisi üzerine yapılan çalışmalar nadir olmasına rağmen, özellikle kuzey bölgeleri ve özellikle de Ninova vilayeti, bu zehirli araknitler ile ilgili kapsamlı epidemiyolojik çalışmalar yapılmamıştır. Bu araştırma, bu bölgede yapılan ilk çalışma olup, 2022 ve 2023 yıllarında Ninova vilayetinde meydana gelen akrep sokmaları hakkında ayrıntılı bilgiler sunmaktadır. Mevcut çalışma, 2022 ve 2023 yıllarında Irak'ın kuzeyindeki Ninova vilayetinde kaydedilen 327 akrep sokması vakasını içermektedir. Kayıtlı vakaların 185'i (%57.56) erkek, 142'si (%43.42) ise kadındır. Veriler, akrep sokmalarına en çok maruz kalan yaş grubunun 15-49 yaş aralığında olduğunu ve bu grubun toplam kayıtlı vakaların %70.34'ünü oluşturduğunu göstermektedir. Bu durum, sosyal ve ekonomik olarak aktif grubun akreplerle ilişkili risklere en çok maruz kalan kesim olduğunu göstermektedir. Ayrıca, en fazla akrep sokması vakasının yaz aylarında meydana geldiği belirlenmiş olup, yüksek sıcaklıklar ile akrep aktivitesi arasındaki ilişkiyi ortaya koymaktadır. Bu sonuçlar, özellikle sıcak aylarda en savunmasız gruplara yönelik önleyici ve bilgilendirici tedbirlerin alınması gerektiğini göstermektedir.

Anahtar kelimeler: Epidemiyoloji, akrep sokmaları, Musul, zehir.

1. Introduction

Scorpions are venomous arthropods belonging to the arachnid order and are adapted to survive in a wide range of habitats such as tropical and temperate rainforests as well as grasslands, savannas, caves, and even snow-capped mountains (Leeming, 2003).

Scorpions are known for their stings and venom; humans often consider them dangerous and even deadly creatures. More than 1.2 million scorpion stings occur annually worldwide, mainly in tropical and subtropical regions (Ebrahimi et al., 2017). While all scorpion species possess venom, their level of danger is often exaggerated and some species can be dangerous to certain groups such as children, the elderly, and individuals with weak immune systems. However, most of the 1.270 to 1.300 known scorpion species worldwide are of no medical significance (Ren & West, 2024). There are 50 species of scorpions with venom dangerous to humans and the Buthidae family of scorpions is considered the most toxic group (Ali & Ali, 2015). In typical cases, a scorpion sting results in pain, numbness, and swelling, while in severe cases, a scorpion sting may lead to severe pain, to serious illness or even death depending on the degree of toxicity of the venom (James et al., 2006). Nonetheless, scorpion stings are responsible for around 3.000 deaths globally each year (Chippaux, 2012). Worldwide, numerous epidemiological studies have been conducted on scorpion stings, particularly in Middle Eastern countries, including Iraq's neighboring countries such as Turkey (Ozkan et al., 2006), Iran (Dehghani & Fathi, 2012), and Saudi Arabia (Jarrar & Al-Rowaily, 2008). Locally, there are limited epidemiological studies on scorpion stings in Iraq, including Kachel (2020) study on scorpion fauna and scorpionism in a district in Duhok province, northern Iraq, followed by Hussein and Ahmed (2021), which addressed the epidemiological and clinical aspects of scorpion stings in the Kurdish region. Nineveh province is one of the most prominent provinces in northern Iraq as it enjoys a unique geographical location that connects diverse natural environments from the agricultural plains in the center to the mountainous regions in the north. The province's hot

Corresponding author: azhararach@gmail.com

and dry climate also contributes to the reproduction of many living organisms, including scorpions. Although scorpion stings represent a major health challenge in Iraq, epidemiological studies on this phenomenon in Nineveh, especially in rural and northern regions, are still rare. Despite the presence of six known scorpion species in this province, five of which belong to the Buthidae family and one to the Scorpionidae family (Kachel et al., 2021), research on scorpion epidemiology remains insufficient in most regions of Iraq, including Nineveh province, where epidemiological studies are still largely lacking. Accordingly, this study aims to provide information and data on the epidemiology of scorpion stings in this province during a specific period. This study is part of a master's thesis by the first author. It is the first of its kind in this region, providing detailed information about cases of scorpion stings in Nineveh province during 2022 and 2023.

2. Material and Method

2.1. Study Area

Nineveh Province is located in the northwestern part of Iraq at the following geographical coordinates: °36°13'46.47" N, °42°14'10.48" E (Fig. 1)., bordered to the north by Dohuk Province, to the south by Salah al-Din Province, to the east by Kirkuk and Erbil Provinces, and the west by the Syrian Arab Republic. The Tigris River runs through the governorate from north to south, dividing it into two almost equal parts: eastern and western, known locally as the left and right coast. The province's topography is characterized by its geographical diversity, as it includes three main regions: mountainous areas in the north, hills in the center, and extended plateaus with winding terrain in the south.

Figure 1. Map of Iraq showing the study area (Nineveh province).

2.2. Data collection and statistical analysis

The data for this study were collected from the medical records in five public hospitals in three districts along the right side of Mosul City, Nineveh Province, for the period between January 2022 and December 2023 (Table 1). The data collection focused on basic demographic information (e.g., age, gender, area of residence), with no exploration into clinical or therapeutic details. The data were statistically analyzed using SPSS (version 24) and descriptive analysis to summarize demographic data using frequencies and percentages, the t-test for the comparison of means between two independent groups and the ANOVA test for the comparison of means among more than two groups.

Table 1. Coordinates of the locations of hospitals from which data on scorpion stings were collected in Nineveh Governorate for the years 2022 and 2023.

Data Collection Site	Coordinates	
Al-Qayyarah General Hospital	35°48'14.38"N	43°17'36.41"E
Al-Jumhuri General Hospital	36°20'27.07"N	43° 7'7.78"E
Mosul General Hospital	36°19'23.23"N	43° 7'24.68"E
Tal Afar General Hospital	36°23'7.76"N	42°27'14.90"E
Al-Baaj Hospital	36° 2'34.32"N	41°43'0.07"E

3. Results

A total of 327 scorpion sting cases were recorded by five public hospitals located on the right side of Nineveh province during the study period, with the highest number of scorpion stings recorded during the study period in 2023, amounting to 186 cases, while the lowest number of cases was 141 during 2022 (Table 2).

Table 2. Seasonal average of scorpion stings in Nineveh province for 2022 and 2023.

Year	Seasons				Total
	Spring	Summer	Autumn	Winter	
2022	24	76	39	2	141
2023	22	89	71	4	186
Total	46	165	110	6	327
Percentage %	14.06	50.45	33.63	1.83	

Seasonally, the highest number of scorpion stings was recorded during the summer during the study period, amounting to 165 cases (50%) of all recorded cases, followed by the fall season, with 110 cases (33%) of all recorded cases, the spring season recorded 46 cases (14%) of the total cases, while the lowest number of injuries was during the winter season, amounting to 6 cases (1.83) of the total cases (Fig. 2). Monthly, August recorded the highest number of scorpion stings with 79 cases (41 males, 38 females) and 24% of the total number of stings. February recorded the lowest number of scorpion stings with 3 cases (2 males, 1 female) and approximately 1% of the total number of stings (Table 3) (Fig. 3). Most cases of scorpion stings were in patients aged between 15 and 49 years, with 70% of all cases, most of them males (Table 4). While the rate of infection in the age group less than five years was 4% of all cases, most of them males, while no cases were recorded in the age group less than one year. By reviewing the notes recorded in the documents of the emergency department of the public hospitals from which the data for our current results were collected, it was noted that most of the recorded cases of scorpion stings belong to patients whose place of residence is rural rather than urban but the place of residence was not recorded in all the hospitals studied; thus, we were unable to refer to it in our results in the form of precise numbers.

Based on the available data, a comprehensive statistical analysis was conducted to understand the distribution of scorpion stings injuries. The descriptive analysis included calculating the arithmetic mean, median, and standard deviation of the number of stings. The results showed that the average number of stings in 2023 was higher than in 2022 (46.50 vs. 35.25), with a standard

deviation of 34.50 and 29.34, respectively. A t-test was used to compare the average number of stings between males and females, with the results showing no statistically significant difference (0.2834) t-test. In addition, an analysis of variance (ANOVA) was used to compare the average number of stings between different seasons, with the results showing a statistically significant difference of 0.0456. The total number of stings was calculated, with 327 injuries. Pearson's correlation coefficient was also used to measure the relationship between age and number of stings with results showing a strong positive correlation (r = 0.85).

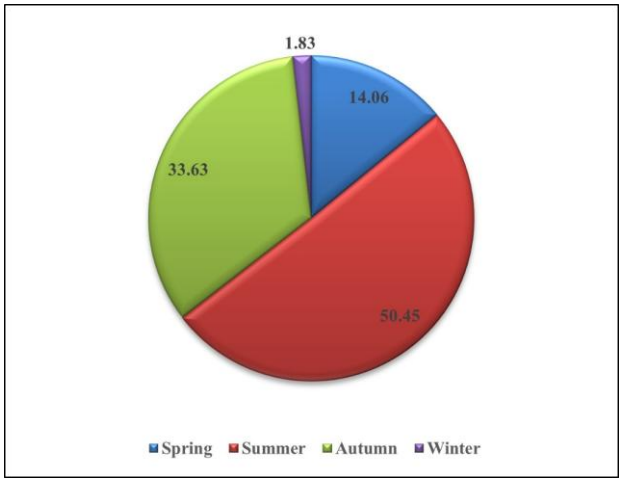

Figure 2. Percentages of the average number of scorpion stings by season in Nineveh province for 2022 and 2023.

Table 3. Monthly scorpion sting cases reported in Nineveh province for 2022 and 2023.

Age (Years)	Male	Female	Total	Percentage %
Less than 1	0	0	0	0
1 to 4	11	3	14	4.28
5 to 14	35	23	58	17.73
15 to 49	132	98	230	70.34
Over 50	7	18	25	7.65
Total	185	142	327	100

Table 4. Age distribution for scorpion stings in Nineveh province for 2022 and 2023.

Month	Male	Female	Total	Percentage %
January	3	1	4	1.22
February	2	1	3	1
March	5	3	8	2.44
April	2	5	7	2.14
May	16	15	31	9.48
June	14	9	23	7
July	36	23	59	18
August	41	38	79	24.15
September	30	19	49	14.98
October	22	18	40	12.24
November	13	7	20	6.12
December	1	3	4	1.23
Total	185	142	327	100

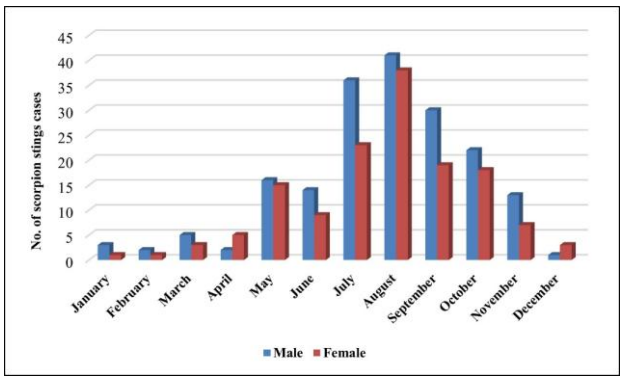

Figure 3. Monthly scorpion sting cases reported in Nineveh province for 2022 and 2023.

4. Discussion

Scorpionism represents a significant public health issue in various regions worldwide due to the high incidence and severity of envenomations, which are often challenging for healthcare systems to manage, or sometimes due to both factors simultaneously. Recent studies have identified seven regions at high risk of scorpionism: North Saharan Africa, Sahelian Africa, South Africa, the Near and Middle East, South India, Mexico, and southern Latin America east of the Andes (Chippaux & Goyffon, 2008). Scorpion stings are one of the most important health problems in Iraq, including the northern provinces, specifically Nineveh Province. The results of our current study showed that 327 cases of scorpion stings were recorded in public medical centers in this province during the two years of study (2022-2023). The highest number of cases of infection was during the summer, accounting for 50% of the total number of infections. This is consistent with the results of Hussen and Ahmed (2021), who studied the epidemiological and clinical aspects of scorpion stings in the Kurdish Region of Iraq, where they recorded the highest number of infections during the summer, accounting for 52.54%. It is also consistent with the results of Kachel (2020), who studied the epidemiology of scorpions in the city of Zakho in Dohuk Province, northern Iraq, where the highest number of infections was recorded during the summer months (July and August). Despite the limited number of scorpion stings recorded in the present study, as well as their geographical limitation, they affect approximately 2.5 billion people at risk (Chippaux & Goyffon, 2008). Summer in Nineveh province is characterized by significantly high temperatures, as daily temperatures may exceed 45 degrees Celsius in some areas. Scorpions are cold-blooded animals, which means that their temperature is greatly affected by the surrounding environment. In hot weather, scorpions are at their peak activity, as they emerge from their hiding places in search of food (usually small insects or rodents) and reproduce more. Scorpions also tend to seek shelter in dark, cool places during the hot hours of the day but they are more active at night, increasing the likelihood of being stung in the evening or late at night.

The results of the current study showed a significant discrepancy between scorpion stings in males (185, 56.57%) and females (142, 43.42%) among patients whose information was recorded in public hospitals during the study period. This is in complete agreement with the studies of Kachel (2020) and Hussen and Ahmed (2021),

which were conducted in some areas of the Kurdish Region of Iraq. However, these results are not consistent with Furtado et al. (2016) who found that the highest incidence of scorpion stings occurred in females in the state of Serra, northeastern Brazil. Also, in Ramhormoz, southwestern Iran, Karami et al. (2013) indicated that the number of scorpion stings in females was higher than in males.

Studying the age distribution of scorpion stings in patients who have been exposed is of great importance in understanding and analyzing the epidemiological consequences of scorpions in a region through identifying the most vulnerable groups, analyzing the severity of poisoning, improving treatment strategies, drawing up preventive policies, and studying the epidemiological factors more accurately. This in turn contributes to improving medical planning and reducing the number of injuries and deaths resulting from scorpion stings. The results of our study showed that the highest number of scorpion stings was in patients aged between 15-49 years, which is completely consistent with the results of Kachel (2020). It does not agree with the results of Furtado et al. (2016), who stated that most of the victims of scorpion stings are women aged between 20-29 years. The observations recorded in the results of the current study showed that most cases of scorpion stings were due to patients living in the countryside, which is consistent with what Celis et al. (2007) stated that the risk of injury is certainly higher in rural areas than in cities.

The results of the statistical analysis of the distribution of scorpion sting injuries showed that the average number of stings in 2023 was higher than in 2022, with a large standard deviation indicating a significant variation in the number of stings between time periods. This variation could be attributed to environmental factors or changes in scorpion activity. On the other hand, the t-test showed no statistically significant difference between the average number of stings in males and females, indicating that gender does not play a major role in increasing the likelihood of scorpion stings in this sample. Analysis of variance (ANOVA) showed a statistically significant difference between the average number of stings in different seasons, confirming that seasons play an important role in determining infection rates. In addition, Pearson's correlation coefficient showed a strong positive association between age and the number of stings, with the age group from 15 to 49 years being the most affected.

5. Conclusion

The study results indicate that scorpion stings are a significant health problem in Nineveh Governorate, northern Iraq, with 327 stings recorded during 2022 and 2023. The study showed that the age group most susceptible to scorpion stings is the 15-49 age group, which represents 70.34% of cases, reflecting the greater exposure of socially and economically active individuals at risk. It was also found that males constitute the largest proportion of those infected (57.56%), which may reflect their greater exposure due to outdoor activities in rural areas. Moreover, the study revealed a clear association between high temperatures in the summer months and increased stings, which calls for taking special preventive measures during these hot periods. Given the limited epidemiological studies in Iraq in general, this study stands out as a fundamental contribution to documenting the phenomenon of scorpion stings in the Nineveh province, which calls for further ongoing research in this area to ensure improved prevention and treatment strategies. Therefore, the importance of directing awareness campaigns targeting the most vulnerable groups is highlighted, in addition to the need to provide appropriate preventive measures to reduce the health risks associated with this phenomenon.

Ackowledgement: This manuscript is part of a master's thesis project by the first author and supervised by the second author.

Ethics committee approval: Ethics committee approval is not required for this study.

Conflict of interest: The authors declare that there is no conflict of interest.

Author Contributions: Conception – A.M.Al-K.; Design – M.A.K.Al-J.; Supervision – A.M.Al-K.; Fund – M.A.K.Al-J.; Materials – M.A.K.Al-J.; Data Collection and Processing – M.A.K.Al-J.; Analysis Interpretation – A.M.Al-K.; Literature Review – A.M.Al-K.; Writing – M.A.K.Al-J.; Critical Review – A.M.Al-K.

References

Ali, N., & Ali, O. M. (2015). Scorpion sting in different regions of Sudan: Epidemiological and clinical survey among university students. *International Journal of Bioinformatics and Biomedical Engineering*, 1(2), 147-152.

Celis, A., Gaxiola-Robles, R., Sevilla-Godínez, E., de Orozco Valerio, M.J., & Armas, J. (2007). Tendencia de la mortalidad por picaduras de alacrán en México, 1979–2003. *Revista Panamericana de Salud Pública,* 6, 373–380.

Chippaux, J.P. (2012). Emerging options for the management of scorpion stings. *Drug Design, Development and Therapy*, 6, 165–173. https://doi.org/10.2147/DDDT.S24754

Chippaux, J.P., & Goyffon, M. (2008). Epidemiology of scorpionism: A global appraisal. *Acta Tropica,* 107(2), 71–79.

Dehghani, R., & Fathi, B. (2012). Scorpion sting in Iran: A review. *Toxicon*, 60, 919-33. https://doi.org/10.1016/j.toxicon.2012.06.002

Ebrahimi, V., Hamdami, E., Moemenbellah-Fard, M. D. & Jahromi, S. E. (2017). Predictive determinants of scorpion stings in a tropical zone of south Iran: Use of mixed seasonal autoregressive moving average model. *Journal of Venomous Animals and Toxins including Tropical Diseases,* 23(39). https://doi.org/10.1186/s40409-017-0129-4

Furtado, S. da S., Belmino, J.F.B., Diniz, A.G.Q., & Leite, R. de S. (2016). Epidemiology of scorpion envenomation in the state of Ceará, Northeastern Brazil. R*evista do Instituto de Medicina Tropical de São Paulo*, 58, 15. https://doi.org/10.1590/S1678-9946201658015

Hussen, F.S.H. & Ahmed, S.T (2021). Epidemiological and Clinical Aspects of Scorpion Stings in Kurdistan Region of Iraq. *Polish Journal of Environmental Studies*, 30(1), 629-634. https://doi.org/10.15244/pjoes/122840

James, W.D. & Berger, T.G. (2006). Andrews' Diseases of the Skin: Clinical dermatology (p. 455). Saunders Elsevier.

Jarrar, B., & Al-Rowaily, M. (2008). Epidemiological aspects of scorpion stings in Al-Jouf Province, Saudi Arabia. *Annals of Saudi Medicine*, 28, 183–187. https://doi.org/10.5144/0256-4947.2008.183

Kachel, H.S. (2020). Scorpion Fauna and Scorpionism in Zakho Province of Northern Iraq. *Commagene Journal of Biology*, 4(1), 22-27. https://doi.org/10.31594/commagene.710923

Kachel, H.S., Al-Khazali, A.M., Hussen, F.S., & Yağmur, E.A. (2021). Checklist and review of the scorpion fauna of Iraq (Arachnida: Scorpiones). *Arachnologische Mitteilungen/Arachnology Letters*, 61, 1-10. https://doi.org/10.30963/aramit6101

Karami, K., Vazirianzadeh, B., Mashhadi, E., Hossienzadeh, M., & Moravvej, S. A. (2013). A five-year epidemiologic study on scorpion stings in Ramhormoz, South-West of Iran. *Pakistan Journal of Zoology*, 45(2), 469–474.

Leeming, J. (2003). Scorpions of Southern Africa. Struik Publishers. 96p.

Ozkan, O., Adigüzel, S., Yakiştiran, S., Cesaretli, Y. Orman, M., & Karaer, K. (2006). Androctonus crassicauda (Olivier 1807) scorpionism in the

Şanlıurfa provinces of Turkey. *Türki Acta Parasitologica Turcica*, 30, 239–245.

Rein, J. O., & West, K. M. (2024). The Scorpion Files: Scorpions of medical importance. Retrieved from https://www.ntnu.no/ub/scorpion-files/medical.php

Commagene Journal of Biology

Aydoğan Türkoğlu et al., (2025) *Comm. J. Biol.* 9(1), 33-41.
DOI: 10.31594/commagene.1590025

e-ISSN 2602-456X

Research Article/Araştırma Makalesi

Experimental and *In silico* Analysis of the Hypoxic Response of Human HTR1B Expression in Human Cell Lines and Its Ortholog Ser-4 Expression in *Caenorhabditis elegans*

Sümeyye AYDOĞAN TÜRKOĞLU[1]*, Canberk TOPRAK[2], Aysu BOZKURT[2], Fatma POYRAZLI[2]

[1]*Balikesir University, Faculty of Science and Literature, Department of Molecular Biology and Genetics, 10145 Balikesir, TÜRKIYE*
[2]*Balikesir University, Institute of Science, Department of Molecular Biology and Genetics, 10145 Balikesir, TÜRKIYE*
ORCID ID: Sümeyye AYDOĞAN TÜRKOĞLU: https://orcid.org/0000-0003-1754-0700; Canberk TOPRAK: https://orcid.org/0009-0000-0575-4360; Aysu BOZKURT: https://orcid.org/0000-0003-0165-528X; Fatma POYRAZLI: https://orcid.org/0000-0001-8069-6447

Received: 23.11.2024 **Accepted:** 24.02.2025 **Published online:** 10.03.2025 **Issue published:** 30.06.2025

Abstract: The relationship between serotonin receptors and cancer has been particularly investigated in recent years. Some studies suggest that serotonin receptors may promote the growth, spread, and metastasis of cancer cells. Serotonin also plays an important role in *C. elegans*. The simple nervous system of *C. elegans* provides an ideal system to study to understand the functions of neurons and neuromodulators. The Serotonin system is highly conserved evolutionarily in humans and *C. elegans*.

A decrease in oxygen levels in cells is called hypoxia and hypoxia promotes tumor growth and is associated with treatment resistance. The usability of *C. elegans* as a new model in the investigation of cancer-related genes in hypoxic studies is important. For this purpose, hypoxic conditions were created in two different models (human cell lines (HUVEC and PC-3) and *C. elegans*) and the expression changes of serotonin receptors HTR1B and its ortholog Ser-4 were examined. Bioinformatic analyses showed that these two genes were 87% similar and affected similar cellular signaling pathways. The expression of HTR1B was increased in the HUVEC cell line at 48 and 72 hours under hypoxic conditions. A hypoxic response was observed in the PC-3 cell line at 48 hours. The expression of Ser-4, the HTR1B *C. elegans* ortholog gene, was also increased in hypoxia at 1 hour.

The effects of the HTR1B gene on various cell lines play a critical role in understanding the complex dynamics of the serotonergic system. In conclusion, the effects of the HTR1B gene on various cell lines constitute an important step in understanding the functionality of this gene in cancer and its potential therapeutic uses.

Keywords: Serotonin, HTR1B, Ser-4, HUVEC, PC-3, *C. elegans*, cancer, hypoxia.

İnsan HTR1B İfadesinin İnsan Hücre Hatlarında ve Ortoloğu Ser-4'ün *Caenorhabditis elegans*'da Hipoksik Koşullarda Cevabının Deneysel ve *In silico* İncelenmesi

Öz: Serotonin ve serotonin reseptörleri ile kanser arasındaki ilişki son yıllarda özellikle araştırılmıştır. Bazı çalışmalar, serotonin reseptörlerinin kanser hücrelerinin büyümesini, yayılmasını ve metastazını destekleyebileceğini ileri sürmektedir. Serotonin ayrıca *C. elegans*'ta önemli bir rol oynar. Bu organizmada serotonin, sinir sistemi ve diğer dokulardaki çeşitli fizyolojik süreçlerin düzenlenmesinde kullanılan bir nörotransmitter olarak işlev görür. *C. elegans*, serotonin sisteminin evrimsel olarak oldukça korunduğunu ve insanlarda benzer biyolojik işlevlere sahip olduğunu göstermektedir.

Hücrelerdeki oksijen seviyelerinde azalmaya hipoksi denir ve bazı klinik çalışmalar hipoksinin tümör büyümesini desteklediğini ve tedavi direnciyle ilişkili olduğunu göstermiştir. HIF, oksijen seviyelerindeki değişikliklere yanıt olarak gen ekspresyonunu düzenler ve hipoksi koşulları altında hücrelerin yanıt verdiği DNA'nın belirli bölgelerine bağlanarak gen ekspresyonunu etkiler. Hipoksik çalışmalarda kanserle ilişkili genlerin araştırılmasında yeni bir model olarak *C. elegans*'ın kullanılabilirliği önemlidir. Bu amaçla iki farklı modelde (insan hücre hatları (HUVEC ve PC-3) ve *C. elegans*) hipoksik koşullar oluşturuldu ve son yıllarda kanserle ilişkili olduğu belirlenen serotonin reseptörleri HTR1B ve onun ortologu Ser-4'ün ekspresyon değişiklikleri incelendi. Yapılan biyoinformatik analizlerde bu iki genin %87 benzer olduğu ve benzer hücresel sinyal yollarını etkilediği görülmüştür. HTR1B'nin hipoksik koşullarda 48 ve 72. saatlerde HUVEC hücre hattında ekspresyonunun normal koşullara kıyasla arttığını bulduk. PC-3 hücre hattında ise 48. saatte hipoksik yanıt gözlendi. HTR1B *C. elegans* ortolog geni olan Ser-4'ün ekspresyonu da 1. saatte hipokside artmıştır.

HTR1B geninin çeşitli hücre hatları üzerindeki etkileri, serotoninerjik sistemin karmaşık dinamiklerini anlamada kritik bir rol oynamaktadır. Sonuç olarak, HTR1B geninin çeşitli hücre hatları üzerindeki etkileri, bu genin kanserdeki işlevselliğini ve potansiyel terapötik kullanımlarını anlamada önemli bir adım oluşturmaktadır.

Anahtar kelimeler: Serotonin, HTR1B, Ser-4, HUVEC, PC-3, *C. elegans*, kanser, hipoksi.

1. Introduction

Serotonin ($C_{10}H_{12}N_2O$ and 5-hydroxytryptamine) is a neurotransmitter that plays an important role in the central nervous system and other body tissues. It is synthesized by the raphe nuclei in nerve cells and by the enterochromaffin cells in tissues such as the intestine. It is particularly important in regulating many processes such as mood, sleep, appetite, sexual activity, learning, memory, and social behavior (Kitson, 2007; Veenstra-

Corresponding author: sumeyye_ayd@hotmail.com

WanderWelee et al., 2000). Therefore, a deficiency or imbalance of serotonin can contribute to depression, anxiety, sleep disorders, and other mental health problems.

Serotonin synthesis begins with tryptophan, an amino acid taken in through food. In the liver, it is metabolized by the enzyme tryptophan hydroxylase (TPH1) to an intermediate product called 5-hydroxytryptophan (5-HTP). 5-hydroxytryptophan (5-HTP), which is formed as a result of the metabolism of tryptophan by the enzyme tryptophan hydroxylase, is then converted to 5-HTP by another enzyme, amino acid decarboxylase (AADC). This reaction occurs in the areas where tryptophan hydroxylase functions (skin, intestine, and pineal gland). 5-HTP is then converted to the molecule 5-hydroxytryptamine, called serotonin, by another enzyme, amino acid decarboxylase (Veenstra-WanderWelee et al., 2000).

Serotonin metabolism is a key process in how this chemical is produced, broken down, and used in the body. Imbalances in serotonin can contribute to a range of mental health problems, and therefore research on serotonin is important in understanding the physiology and pathology of such disorders and is critical to their treatment. Serotonin receptors are found in various tissues throughout the body and receive serotonin signals, causing cellular responses (Walther et al., 2003).

Serotonin is broken down by an enzyme called monoamine oxidase (MAO). MAO breaks down serotonin molecules and removes them from the body. This metabolic process is important in keeping serotonin levels balanced (Smith et al., 2020). Additionally, medications that increase serotonin reuptake, such as selective serotonin reuptake inhibitors (SSRIs), can also affect serotonin metabolism, which is used to treat conditions such as depression (David & Gardier, 2016).

The relationship between serotonin and serotonin receptors has been particularly investigated in recent years. Serotonin can have an effect on the cell through its receptors. It is important to understand the functions of serotonin and its cellular effects because recent studies have shown that serotonin is effective not only in physiological conditions but also in pathophysiological processes such as cancer. Studies show that serotonin receptors can be found in cancer cells and may play a role in cancer development. For example, some studies suggest that serotonin receptors may promote the growth, spread, and metastasis of cancer cells. However, the relationship between serotonin and cancer is quite complex and not fully understood. Serotonin has been shown to have a potential effect on cancer cell proliferation, invasion, spreading, and tumor angiogenesis (Balakrishna et al., 2021). Different receptor subtypes mediate the effect of serotonin in prostate cancer at different tumor stages (Dizeyi et al., 2004). An in vitro study using an androgen-independent cell line demonstrated that serotonin has a dose-dependent stimulatory effect on cell proliferation (Siddiqui et al., 2006). Serotonin shows its effects through different types of receptors found on pre-synaptic and post-synaptic cell membranes. These receptors are 5-Hydroxytryptamine receptors (5-HTR1-5-HTR7). Serotonin function may vary depending on the region and receptor. Serotonin signaling promotes tumor progression by stimulating the proliferation of cancer cells and inhibiting apoptosis via the MAPK and PI3K/Akt signaling axis (Karmakar et al., 2021).

Caenorhabditis elegans (*C. elegans*) is a microscopic nematode (roundworm) species. *C. elegans* is considered a very important model organism in the scientific world because these worms are easily genetically modified, reproducing rapidly, transparent, and have contributed to the understanding of many basic biological processes with their simple structure and completely sequenced genome (Savaş et al., 2018; Riddle et al., 1997).

Serotonin also plays an important role in *C. elegans*. In this organism, serotonin functions as a neurotransmitter used in the regulation of various physiological processes in the nervous system and other tissues. In *C. elegans*, serotonin is secreted from nerve cells and plays a role in synaptic transmission. *C. elegans* is a model organism used in studies of the functioning of the nervous system and the regulation of behavioral responses. Serotonin plays an important role in various processes in this organism, such as behavioral regulation, movement control, development, and aging. The simple nervous system of *C. elegans* provides an ideal system to study to understand the functions of neurons and neuromodulators (White et al., 1986; Dag et al., 2023). However, studies on *C. elegans* show that the serotonin system is highly conserved evolutionarily and has similar biological functions in humans (Fig. 1.) In the *C. elegans* serotonin pathway, serotonin is synthesized by tryptophan hydroxylase (TPH1) and degraded by an enzyme homologous to monoamine oxidase (MAOA). Therefore, studies on *C. elegans* can also provide important clues in research aimed at understanding and treating human health and diseases. The Ser-4 gene, the human HTR1B *C. elegans* ortholog, is a part of the serotonin receptors and these receptors play an important role in locomotor activity. Serotonin and serotonin receptors, such as Ser-4, may have a role in the functions of cells that regulate development and food sensing. This may affect postembryonic development and food-seeking behavior in *C. elegans* (Gürel et al., 2012).

Oxygen plays a critical role in the energy metabolism of cells. Anabolic processes, signaling pathways, and enzymatic reactions are dependent on ATP produced by mitochondrial oxidative phosphorylation and glycolysis. However, decreased oxygen levels in cells are called hypoxia and are especially common in solid tumors. In hypoxic conditions, tumor cells adapt to genetic changes and some clinical studies have shown that hypoxia promotes tumor growth and contributes to treatment resistance (Türkoğlu et al., 2021; Türkoğlu & Kockar, 2016).

The molecular mechanism of hypoxia is governed by a key protein called Hypoxia-Inducible Factor (HIF). HIF regulates gene expression in response to changes in oxygen levels. In particular, HIF-1α affects gene expression by binding to specific regions of DNA to which cells respond under hypoxia conditions. This mechanism can affect the survival strategies of tumor cells, causing them to behave aggressively in a hypoxic environment (Türkoğlu et al., 2021).

Caenorhabditis elegans can exhibit various physiological and genetic responses when exposed to hypoxic environments. These responses provide

researchers with clues to understand how the worms' metabolism and gene expression change under hypoxic stress (Nystul et al., 2003; Miller & Roth, 2009). In addition, *C. elegans* lifespan is extended by hypoxia (Rascón & Harrison, 2010; Leiser et al., 2013). However, understanding the defense mechanisms of *C. elegans* against hypoxia may contribute to the development of potential therapeutic strategies for the treatment or prevention of hypoxia-related diseases in humans.

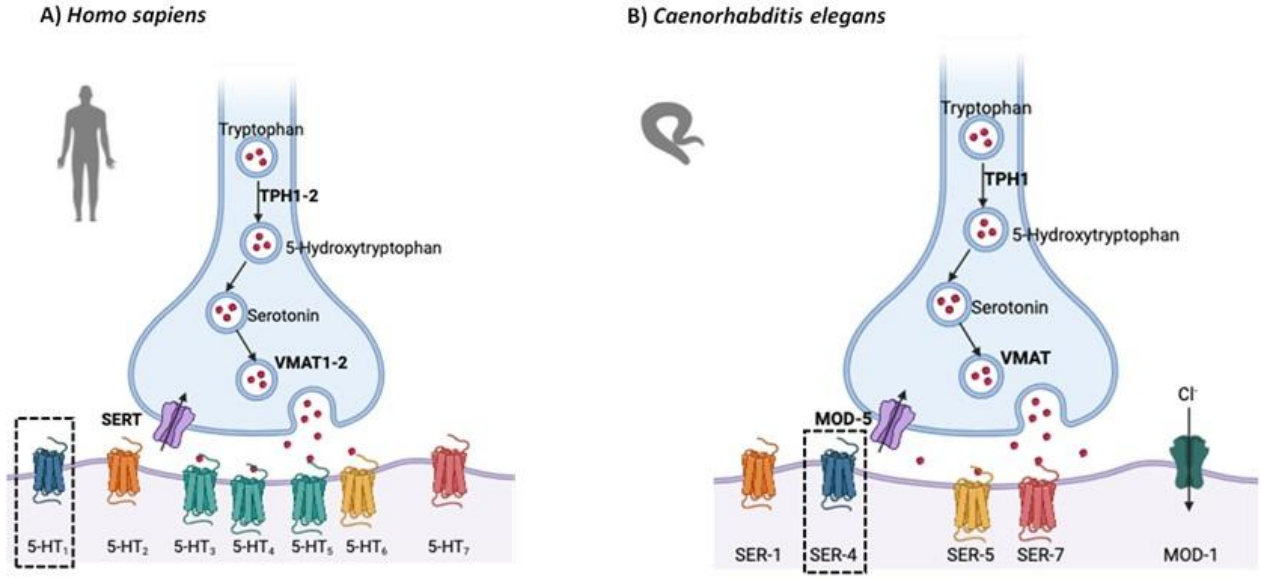

Figure 1. Human (A) and *C. elegans* (B) serotonin pathway (Curran & Chalasani, 2012).

Caenorhabditis elegans is a valuable model organism used in hypoxia research and studying the physiological and genetic responses of this worm under hypoxic conditions plays an important role in basic science and medical research. Especially considering that the cancer microenvironment is hypoxic, the usability of *C. elegans* as a new model in the investigation of cancer-related genes is important. Serotonin, which acts on cells through its receptors, is effective not only in physiological conditions but also in pathophysiological processes such as cancer. Studies on its effect on cancer are associated with changes in the expression of serotonin receptors. In this context, in our study, hypoxic conditions were created in two different models and the expression changes of serotonin receptors HTR1B and its ortholog Ser-4, which have been identified to be associated with cancer in recent years, were examined.

2. Material and Method

2.1. Cell Culture

Human vein endothelial cell line (HUVEC) and Prostate Cancer Cell Line (PC-3) were cultured using a routine passaging method in DMEM (Sigma, Dulbecco's Modified Eagle's Medium) containing 10% FCS (Fetal Calf Serum). Cells were incubated at 37°C in an environment containing 5% CO_2.

2.2. Cultivation of *C. elegans*

First, for the preparation of NGM (Nematode Growth Medium), 2.5 g peptone, 3 g NaCl, and 20 g agar were weighed and mixed with one liter of pure water and the mixture was autoclaved at 121°C for 15 minutes and then cooled to 55°C. 1 mL cholesterol, 1 mL 1M $MgSO_4$, 25 mL 1.5M KH_2PO_4, and 1 mL 1M $CaCl_2$ were added to the cooled mixture and mixed until the medium became homogeneous and poured into petri dishes and allowed to solidify. For the cultivation of E. coli OP50 strain, LST (Lauryl Sulfate Broth) 9.125 g Lauryl Sulfate Broth was weighed on a precision balance and mixed with 250 mL of pure water. The mixture was autoclaved at 121°C for 15 minutes and cooled to 37°C. A colony of E. coli was seeded into the cooled mixture and kept in a shaking incubator at 37°C for 24 hours. 400µL of *E. coli* OP50 strain was spread onto the solidified *C. elegans* medium and allowed to dry.

2.3. Creation of Hypoxic Model

The HUVEC and PC-3 cell lines were seeded in 25 cm^2 flasks with 2,000,000 cells. Control groups that were not treated with any substance were labeled as normoxia and experimental groups were treated with 150 µM $CoCl_2$ and were labeled as hypoxic experimental groups for 24, 48, and 72 hours (Türkoğlu & Köçkar 2016). To examine the hypoxic effect, cell pellets were taken at 24, 48, and 72 hours and stored at -80^{0}C before RNA isolation.

For *C. elegan's* hypoxic experiment, embryos were removed from adult *C. elegans* with hypochlorite and L1 stage organisms were obtained 16 hours later. The worms were then kept on NGM plates for 3 days. To create the *C. elegans* hypoxic model, sodium sulfite solution was prepared in M9 buffer at a concentration of 1 g/L. Worms were washed with the prepared M9 buffer after 3 days and the plates were transferred to 15 mL falcons and incubation was provided at different time intervals. At the end of incubation, the organisms were transferred to new NGM plates and waited for 24 hours for recovery.

2.4. Total RNA Isolation and cDNA Synthesis

For cell lines, RNA isolation was performed according to the previous studies. 1µg of RNA was used as a template to obtain cDNA according to the protocol. cDNAs were checked using Hb2 microglobulin primers for HUVEC and PC-3 cells (Poyrazlı et al., 2024; Türkoğlu et al., 2020). CDC primers were used for *C. elegans* control PCR analysis (Control PCR, Fig. 2A).

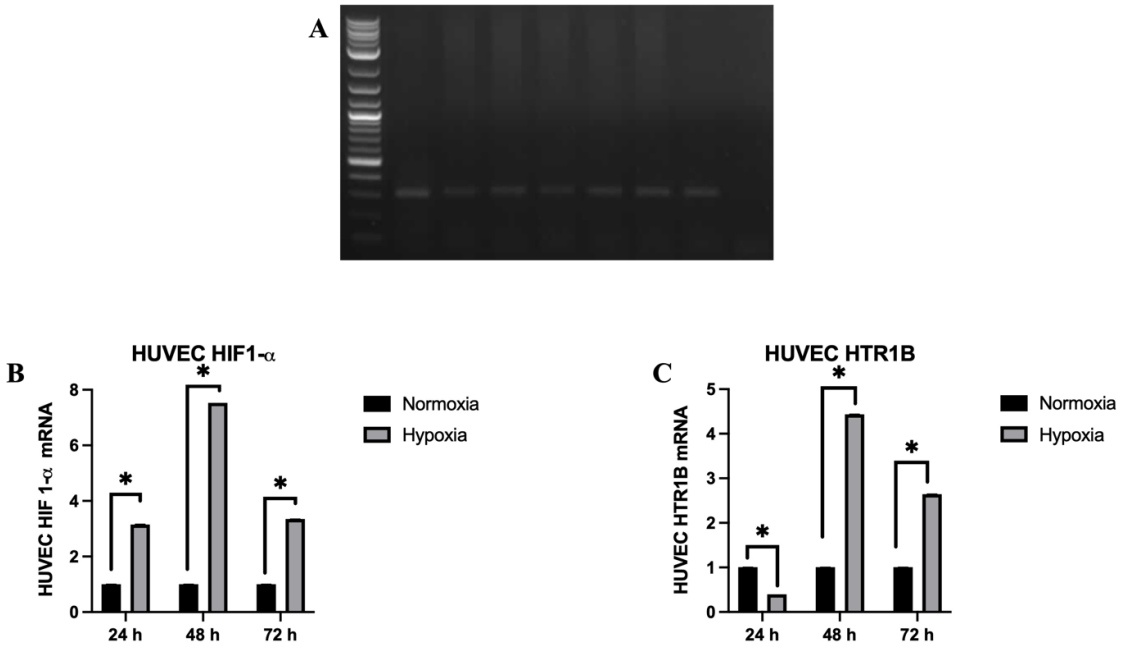

Figure 2. Expression of HIF1-α and HTR1B in HUVEC cell line (24, 48 and 72 hours); A: HB2 HUVEC control PCR image (M: 1 kb marker, 1: 24 h Normoxia, 2: 24 h Hypoxia, 3: 48 h Normoxia, 4: 48 h Hypoxia, 5: 72 h Normoxia, 6: 72 h Hypoxia, 7: Positive Control, 8: Negative Control), B: HIF1-α Expression, C: HTR1B Expression.

Caenorhabditis elegans were washed with M9 buffer and collected from the media. Then, the living organisms were placed in a falcon tube and the M9 on them was aspirated. Fresh M9 was added and the falcon tube was kept on ice. The living organisms were placed in the tubes and centrifuged to form a pellet. After the supernatant was removed, Trizol was added and the tubes were quickly frozen by throwing them into liquid nitrogen and RNA isolation was performed according to the protocol (Riccio, 2019). cDNAs were checked using CDC primers for *C. elegans* (Control PCR, Fig. 3A).

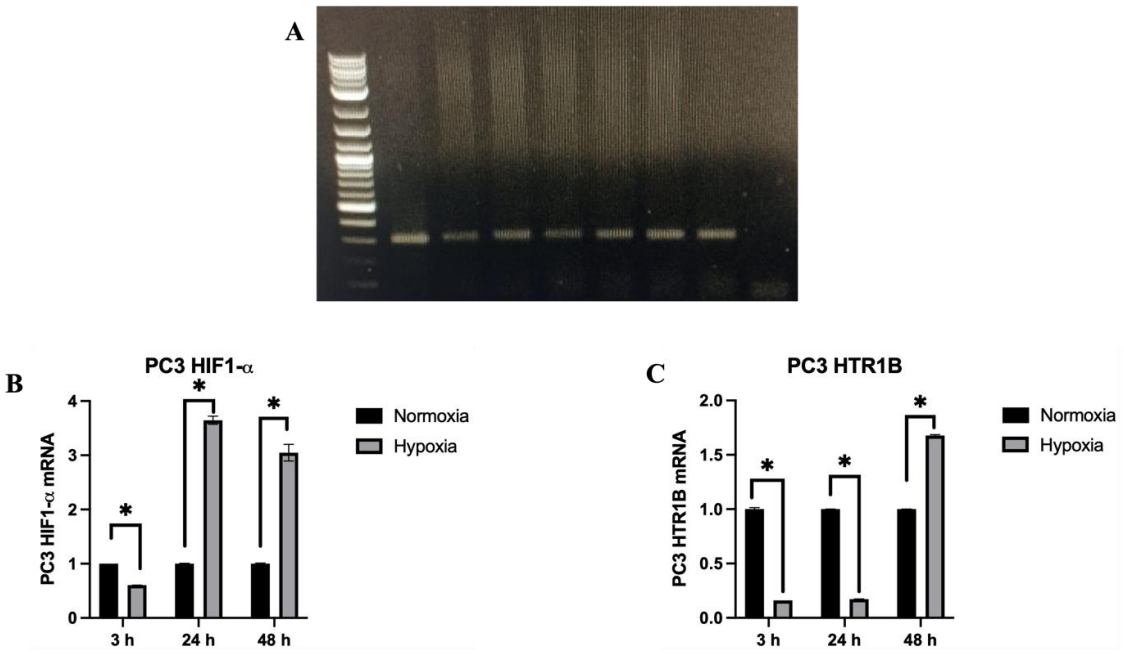

Figure 3. Expression of HIF1-α and HTR1B in PC3 cell line (24, 48 and 72 hours); A: HB2 PC3 control PCR image (M: 1 kb marker, 1: 3 h Normoxia, 2: 3 h Hypoxia, 3: 24 h Normoxia, 4: 24 h Hypoxia, 5: 48 h Normoxia, 6: 48 h Hypoxia, 7: Positive Control, 8: Negative Control), B: HIF1-α Expression, C: HTR1B Expression.

2.5. Real-Time PCR

To determine the HTR1B and Ser-4 mRNA expression, Real-Time PCR (Light Cycler 485 (Roche Diagnostic)) was performed by using 0.5 µl (100 ng/µl) for each of the forward and reverse primers, 6.25 µl RealQ Plus 2x Master Mix Green (Ampliqon) and 4.25 µl dH2O in a volume of 1µl from the obtained cDNAs. The experiments established with these cDNAs were performed in 3 repetitions and the Ct values were evaluated according to the LIVAK method.

2.6. Bioinformatics Analyses

The sequence of the human HTR1B gene (NM_000863.3)

and the *C. elegans*, Ser-4 (NM_065051.8) sequences were accessed from the website http://www.ncbi.nlm.nih.gov/. Primers were designed using Blast and OligodT Analyzer programs. In this context, the designed primers for the HTR1B gene are forward 5′-AAGAAGAAACTCATGGCCGCTAGGG-3′ reverse 5′-GGGGTTGATGAGGGAGTTGAGATAG-3′ and for the Ser-4 gene, forward 5′-CAGGTTTTCTCCACAGCGAC-3′ reverse 3′-CTTGATTCATTGTGGCGTGGA-5′ and the annealing temperatures are 55ºC. HTR1B and Ser-4 aa sequences were compared with NCBI and Bioedit Programme (Fig. 4).

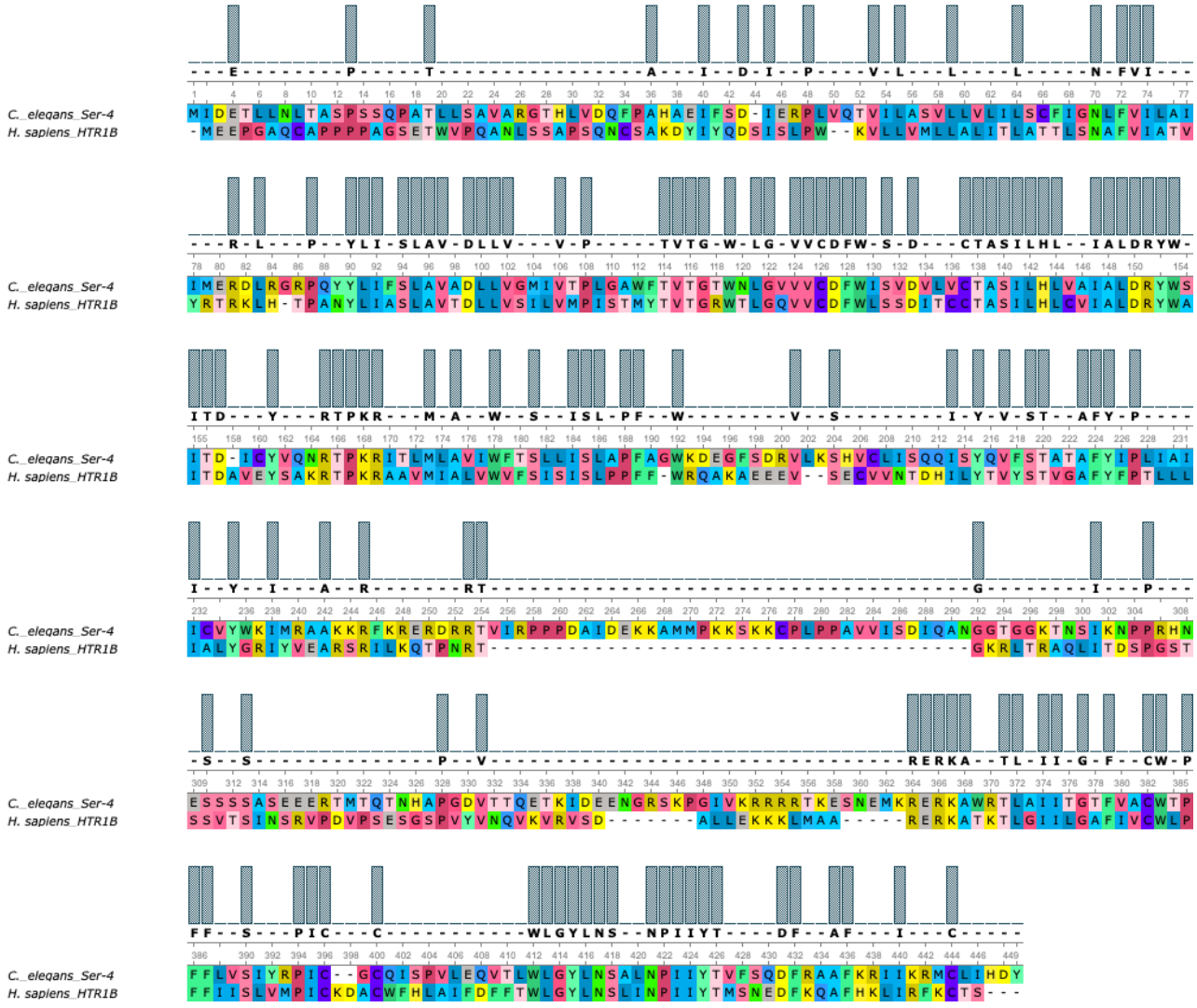

Figure 4. Bioinformatic comparison of *H. sapiens* HTR1B and *C. elegans* ser-4 amino acid sequence.

STRING database was used to draw the associated protein network diagram of HTR1B and Ser-4 genes and then analysis was performed with the KEGG database to display the basic biological processes they are involved in (Figs. 5-6).

Statistical analysis

Determination of HIF-1α, HTR1B, and Ser-4 mRNA levels were performed in cell lines and *C. elegans* in independent experiments at different time periods. HIF-1α and HTR1B levels were normalized by comparing with hβ2 and averaged from three replicate groups. Ser-4 levels were normalized with CDC42 and averaged from three replicate groups. Ct values obtained from Real Time PCR were analyzed according to LIVAC method. The results were graphed using the GraphPad Prism 8 program and evaluated statistically with One Way Anova in the program ($p<0.05$* was considered significant). The experiment was carried out in 3 repetitions.

3. Results

3.1. Similarities of HTR1B and ser-4 Genes

Human and *C. elegans* serotonin synthesis and signaling pathways are quite similar. As can be seen in Figure 1, serotonin is synthesized from the amino acid tryptophan via TPH enzymes in both organisms. Storage, release, and reuptake mechanisms are also quite similar. There are also similarities in terms of the receptors that initiate the effect of serotonin, which is very important in these signaling pathways, in cells. In particular, human HTR1b and its *C. elegans* ortholog Ser-4, which are among the active receptors, were compared in terms of gene and amino acid similarity.

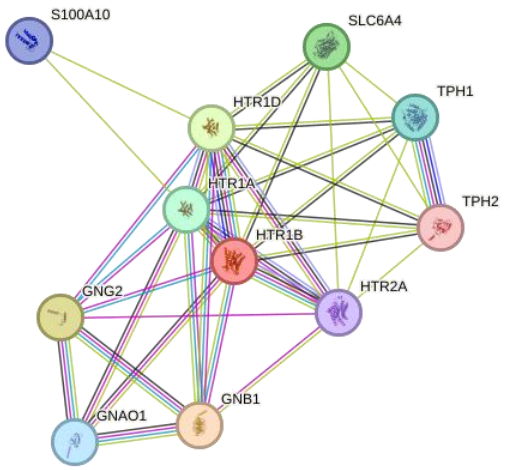

Figure 5. Pathway analysis of the HTR1B gene (HTR1B: 5-hydroxytryptamine receptor 1B, GNB1: Guanine nucleotide-binding protein G(I)/G(S)/G(T) subunit beta-1, GNG2: Guanine nucleotide-binding protein G(I)/G(S)/G(O) subunit gamma-2, HTR1D: 5-hydroxytryptamine receptor 1D, SLC6A4: Sodium-dependent serotonin transporter, HTR1A: 5-hydroxytryptamine receptor 1A, TPH1: Tryptophan hydroxylase 1, GNAO1: Guanine nucleotide-binding protein G(o) subunit alpha, S100A10: Protein S100-A10, HTR2A: 5-hydroxytryptamine receptor 2A, TPH2: Tryptophan hydroxylase 2.)

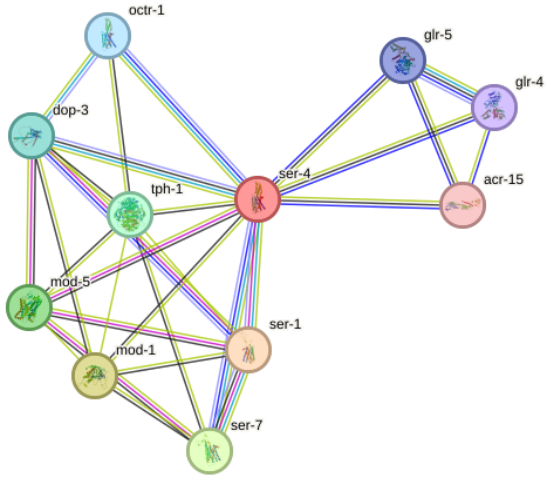

Figure 6. Pathway analysis of the ser-4 gene (ser-4: G_PROTEIN_RECEP_F1_2 domain-containing protein, ser-1: G_PROTEIN_RECEP_F1_2 domain-containing protein, mod-1: Serotonin-gated chloride channel, ser-7: G_PROTEIN_RECEP_F1_2 domain-containing protein, mod-5: Transporter, tph-1: BH4_AAA_HYDROXYL_2 domain-containing protein, dop-3: Dopamine receptor 3, octr-1: G_PROTEIN_RECEP_F1_2 domain-containing protein, glr-5: GLutamate Receptor family, glr-4: GLutamate Receptor family, acr-15: Acetylcholine Receptor.)

The similarity of *Homo sapiens* HTR1B and *C. elegans* Ser-4 genes were analyzed using both the UGENE program and NCBI blast programs. The similarity rate of HTR1B and Ser-4 aa sequence were compared and 87% aa identity was found (Fig. 4). It is seen from the Figure that the similarity between the 81st and 192nd amino acids is highly conserved.

3.2. HTR1B and HIF1-α Expression in HUVEC and PC-3 Cell Lines

Firstly, to confirm the hypoxic condition in the selected cell lines, the expression of HIF1-α, the main regulatory transcription factor of the hypoxic condition, was analyzed with Real-Time PCR. As seen in Figure 7, the expression of HIF1-α increased in hypoxic conditions at 24, 48, and 72 hours and it was confirmed that hypoxia occurred in HUVEC cell line. The expression of the serotonin receptor gene HTR1B under hypoxic conditions was also analyzed. HTR1B is regulated in hypoxic conditions at 48 and 72 hours and its expression increases compared to normal conditions in HUVEC cell line (Fig. 2). In the PC-3 cell line, no hypoxic response occurred at 3 hours. It can be observed in Figure 3 that hypoxia occurred at 24 and 48 hours. When the HTR1B mRNA level was examined at these time periods, an increase was detected at 72 hours compared to normal conditions.

3.3. Ser-4 and CeHIF Expression in *C. elegans*

To confirm whether our *C. elegans* hypoxic model was formed, this time *C. elegans* CeHIF expression was analyzed with Real-Time PCR. As shown in Figure 7, CeHIF expression could not be detected in all time periods. CeHIF expression increased only at 1 hour and the chemical hypoxia model was confirmed at 1 hour in *C. elegans*. When the expression of Ser-4, the HTR1B *C. elegans* ortholog gene, was examined, it was shown that its expression increased at 1 hour depending on the hypoxic condition.

3.4. Pathways in which the HTR1B Gene is Involved and Genes It Interacts with

HTR1B is an important receptor in serotonin metabolism. As a result of pathway analysis studies conducted with the String program, it was seen that the HTR1B gene was associated with Serotonergic synapse, folate biosynthesis, tryptophan metabolism, taste transmission, GABAergic synapse, morphine addiction, circadian entrainment, cAMP signaling pathway, and neuroactive Ligand-Receptor interaction pathways. It also plays a role in the cancer pathway together with the GNG2 gene it interacts with.

3.5. Pathways in Which Ser-4 Gene Takes Part and Genes it Interacts with

As a result of the analyses, it was observed that the Ser-4 gene takes part in the Neuroactive Ligand-Receptor interaction, calcium signaling pathway, and axon regeneration pathways. The genes selected in both models were found to be related to the G protein-coupled receptor signaling pathway, cellular response to dopamine, chemical synaptic transmission, cellular response to chemical stimulation, regulation of multicellular organism processes, serotonin binding, G protein-coupled serotonin receptor activity, neurotransmitter receptor activity, and GPCR ligand binding signaling pathways.

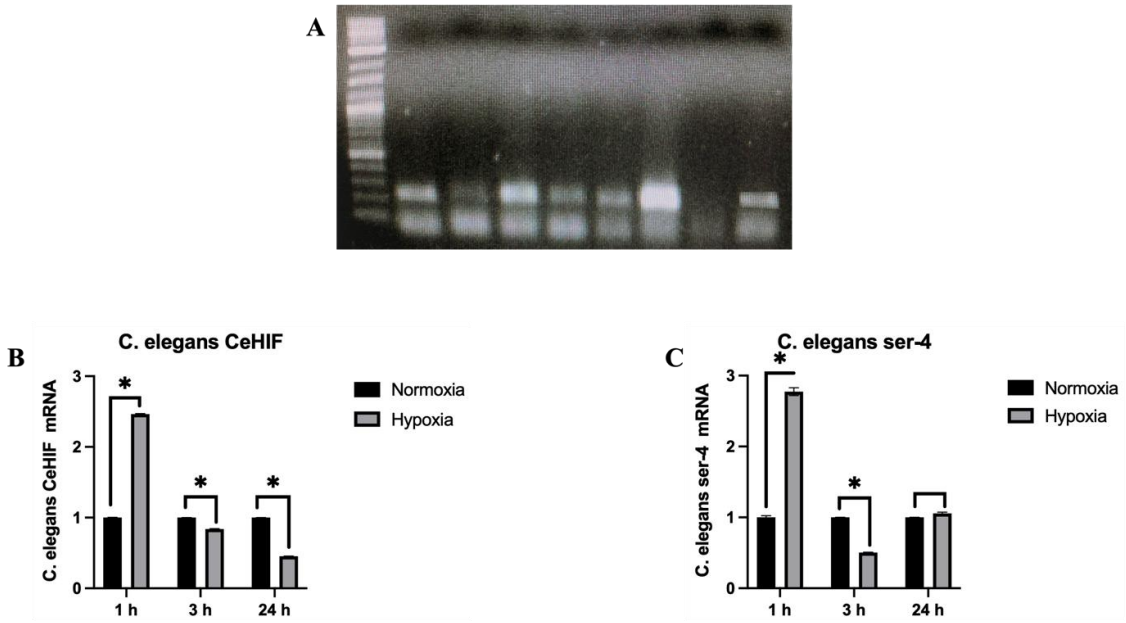

Figure 7. *C. elegans* CeHIF and ser-4 expression (1, 3 and 24 hours); A: CDC-42 *C. elegans* control PCR image (M: 1 kb marker, 1: 1-hour Normoxia, 2: 1-hour Hypoxia, 3: 3 hours Normoxia, 4: 3 hours Hypoxia, 5: 24 hours Normoxia, 6: 24 hours Hypoxia, 7: Negative Control, 8: Positive Control), B: cEHIF Expression, C: Ser-4 Expression.

4. Discussion and Conclusion

In recent years, studies on the potential roles of serotonin and serotonin receptors in cancer treatment have provided important findings. In studies conducted with prostate cancer cell lines, it was observed that hormone-independent DU145 and PC3 cell lines were more sensitive to 5-HT1A, 5-HT2B, and 5HT4 antagonists compared to androgen-dependent LNCaP cell lines. In particular, 5-HT1B receptor antagonists NAN-190 and SB224289 induce apoptosis in PC3 cell lines, indicating that they may have potential in the treatment of prostate cancer (Sarrouilhe et al., 2015).

Studies on the effects of serotonin and its receptors, especially 5-HT1A and 5-HT1B, on bladder cancer cell growth emphasize that these receptors have potential for treatment. It is thought that serotonin administration promotes cell growth in the HT1376 cell line with dose changes and may play a role in bladder cancer progression. In addition, 5-HT1B receptor antagonists, which significantly inhibit cell growth in the HT1376 cell line, suggest that this receptor may be a potential target in bladder cancer (Sarrouilhe et al., 2015).

In studies conducted with Small Cell Lung Carcinoma (SCLC), the effect of serotonin and its receptors on cell proliferation was examined and although the 5-HT1 antagonist methysergide was shown to be a potential treatment for SCLC, the 5-HT1D agonist sumatriptan was shown to increase SCLC proliferation. More studies should be conducted to elucidate the effect of serotonin and its receptors on SCLC (Sarrouilhe et al., 2015).

In the antagonist studies on colorectal cancer, Y25130 for 5-HT3 is seen as a potential target for treatment because it has a strong apoptotic effect. The effect of sulforaphane, which reduces the expression of serotonin receptors 5-HT1A, 5-HT2C 5-HT3, and SERT, on colorectal cancer is shown. Immunohistochemical analyses in colorectal cancer show that the 5-HT1B receptor needs to be investigated further (Sarrouilhe et al., 2015).

Cholangiocarcinoma is a type of cancer that occurs in the bile duct. Studies in this cancer show that serotonin receptors play an important role. Experiments have found that cholangiocarcinoma cell lines express all serotonin receptors and down-regulate 5-HT1B, 1F, 2B, 3C, and 7 and up-regulate all other receptors compared to the H69 cell line (Sarrouilhe et al., 2015).

Studies on serotonin and serotonin receptors in breast cancer have shown that serotonin signal imbalance plays a role in the onset and progression of breast cancer through disruption of the epithelial homeostatic system. In the MCF-7 cell line, 5-HT2A has been shown to have a proliferation-promoting property when serotonin levels increase. However, the increase in the expression of TPH1, which plays a role in serotonin biosynthesis, is associated with changes in tumor progression. However, immunohistochemical analyses do not show that 5-HT1A, 5-HT1B, and 5-HT2B receptors are associated with tumor grade (Sarrouilhe et al., 2015).

The most common form of liver cancer is hepatocellular carcinoma (HCC) and the role of the serotonin system, especially the receptors, in the development and prognosis of liver cancer is being studied significantly. In studies where different concentrations of serotonin were applied to Huh7 and HepG2 cell lines, cell survival and proliferation were increased. In the same cell lines, 5-HT1B and 5-HT2B antagonists (SB216641 and LY272015) were shown to have strong cytotoxic effects. Thus, serotonin receptors are thought to be of great importance in the treatment of hepatocellular cancer (Sarrouilhe et al., 2015).

In the study conducted with carcinoid tumors, typical bronchopulmonary NET cell line (NCI-H727), atypical bronchopulmonary NET cell line (NCI-H720), small intestine NET cell line (KRJ-I), and functional human pancreatic carcinoid cell line (BON) were used. As a result of the studies, exogenously added serotonin increased cell proliferation in four human carcinoid cell lines in a concentration-dependent manner. It was shown that the

proliferative effect of serotonin on carcinoid cells was mediated by 5-HT1A, 1B, and 5-HT2. This suggests that serotonin promotes the growth of carcinoid cells in an autocrine manner. In addition, the tumor growth-regulating effects of serotonin-release inhibitors such as Sandostatin LAR® demonstrate the potential of this mechanism in terms of treatment. In conclusion, these findings support that serotonin-related pathways may be therapeutic targets for carcinoid tumors (Sarrouilhe et al., 2015).

The effects of the HTR1B gene on various cell lines play a critical role in understanding the complex dynamics of the serotonergic system. In conclusion, the effects of the HTR1B gene on various cell lines constitute an important step in understanding the functionality and potential therapeutic uses of this gene. More comprehensive studies of HTR1B in various disease models may contribute to the development of the targeted treatment strategies.

The Ser-4 gene, the human HTR1B *C. elegans* ortholog, is part of the serotonin receptors and these receptors play an important role in locomotor activity. Serotonin activates these receptors, slowing down movement (Gürel et al., 2012). Serotonin may also affect the immune system of *C. elegans*. The function of serotonin receptors, such as Ser-4, is to regulate G-protein communication in serotonin epithelial cells and may affect the immune system response to infections (Anderson et al. 2013). Serotonin and serotonin receptors, such as Ser-4, may have a role in the functions of cells that regulate development and food sensing. This may affect postembryonic development and food-seeking behavior (Gürel et al., 2012).

In our study, the expression of serotonin receptor HTR1B was compared in both healthy human endothelial cells and prostate cancer cell line PC-3 cells, which are observed to be more sensitive to 5-HT1A, 5-HT2B, and 5HT4 antagonists due to hypoxia, an important mechanism for cancer microenvironment. The response of the Ser-4 gene, which was revealed to be %87 similar in bioinformatic analyses performed by us in *C. elegans*, which is planned to be a model in cancer studies related to serotonin, to hypoxia was also investigated. It was observed that HTR1B and Ser-4 were studied in both human cell line models and *C. elegans*, responded to hypoxia. HIF-1 binding site was detected in TF binding regions of the promoter regions of the genes. In the literature, no studies have been found on the chemical hypoxia model of this gene in HUVEC and PC-3 cell lines under hypoxic conditions and the *C. elegans* ortholog of this gene, Ser-4. Investigating the responses of these genes to hypoxic conditions and revealing their similarities in humans and *C. elegans* provides new information about serotonin and its metabolism in the evolutionary process. It also showed that hypoxia, a cancer-related condition, should be addressed in the creation of therapeutic protocols in different cancer cell types where these genes are effective. All these results indicate that further regulation studies are needed to reveal the status of serotonin metabolism in cancer. The effects of the HTR1B gene on various cell lines play a critical role in understanding the complex dynamics of the serotonergic system. In conclusion, the effects of the HTR1B gene on various cell lines constitute an important step in understanding the functionality of this gene and its potential therapeutic uses. In our study, the selected genes were examined at the mRNA level. Examining the response of these genes at the protein level and also at the promoter level can provide information about whether there are changes in different gene regulation steps of the hypoxic response. A more comprehensive examination of HTR1B in various disease models may contribute to the development of the targeted treatment strategies.

Ackowledgement: This work was supported by Health Institutes of Türkiye (TUSEB) project (TUSEB 2023-A4-04 38374).

Ethics committee approval: Ethics committee approval is not required for this study.

Conflict of interest: The authors declare that there is no conflict of interest.

Author Contributions: Conception – S.A.T.; Supervision – S.A.T.; Fund – S.A.T.; Materials – S.A.T.; Data Collection and Processing – S.A.T., C.T., A.B., F.P.; Analysis Interpretation – S.A.T., C.T., A.B., F.P.; Literature Review – S.A.T., C.T., A.B., F.P.; Writing – S.A.T., C.T.; Critical Review – S.A.T., C.T.

References

Anderson, A., Laurenson-Schafer, H., Partridge, F.A., Hodgkin, J., & McMullan, R. (2013). Serotonergic chemosensory neurons modify the *C. elegans* immune response by regulating G-protein signaling in epithelial cells. *PLoS pathogens*, 9(12), e1003787. https://doi.org/10.1371/journal.ppat.1003787

Balakrishna, P., George, S., Hatoum, H., & Mukherjee, S. (2021). Serotonin Pathway in Cancer. *International Journal of Molecular Sciences*, 22(3), 1268. https://doi.org/10.3390/ijms22031268

Curran, K.P., & Chalasani, S.H. (2012). Serotonin circuits and anxiety: what can invertebrates teach us? *Invertebrate Neuroscience*, 12, 81-92. https://doi.org/10.1007/s10158-012-0140-y

Dag, U., Nwabudike, I., Kang, D., Gomes, M.A., Kim, J., Atanas, A.A., ... & Flavell, S.W. (2023). Dissecting the functional organization of the *C. elegans* serotonergic system at whole-brain scale. *Cell*, 186(12), 2574-2592. https://doi.org/10.1016/j.cell.2023.04.023

David, D.J., & Gardier, A.M. (2016). Les bases de pharmacologie fondamentale du système sérotoninergique: application à la réponse antidépressive. *L'encéphale*, 42(3), 255-263. https://doi.org/10.1016/j.encep.2016.03.012

Dizeyi, N., Bjartell, A., Nilsson, E., Hansson, J., Gadaleanu, V., Cross, N., & Abrahamsson, P.A. (2004). Expression of serotonin receptors and role of serotonin in human prostate cancer tissue and cell lines. *Prostate*, 59(3), 328-36. https://doi.org/10.1002/pros.10374

Gürel, G., Gustafson, M.A., Pepper, J.S., Horvitz, H.R., & Koelle, M.R. (2012). Receptors and other signaling proteins required for serotonin control of locomotion in *Caenorhabditis elegans*. *Genetics*, 192(4), 1359-1371. https://doi.org/10.1534/genetics.112.142125

Karmakar, S., & Lal, G. (2021). Role of serotonin receptor signaling in cancer cells and anti-tumor immunity. *Theranostics*, 11(11), 5296. https://doi.org/10.7150/thno.55986

Kitson, S.L. (2007). 5-hydroxytryptamine (5-HT) receptor ligands. *Current pharmaceutical design*, 13(25), 2621-2637. https://doi.org/10.2174/138161207781663000

Leiser, S.F., Fletcher, M., Begun, A., & Kaeberlein, M. (2013). Life-span extension from hypoxia in *Caenorhabditis elegans* requires both HIF-1 and DAF-16 and is antagonized by SKN-1. *Journals of Gerontology Series A: Biomedical Sciences and Medical Sciences*, 68(10), 1135-1144. https://doi.org/10.1093/gerona/glt016

Miller, D.L., & Roth, M.B. (2009). *C. elegans* are protected from lethal hypoxia by an embryonic diapause. *Current Biology*, 19(14), 1233-1237. https://doi.org/10.1016/j.cub.2009.05.066

Nystul, T.G., Goldmark, J.P., Padilla, P.A., & Roth, M.B. (2003). Suspended animation in *C. elegans* requires the spindle checkpoint. *Science*, 302(5647), 1038-1041. https://doi.org/10.1126/science.1089705

Poyrazlı, F., Okuyan, D., Köçkar, F., & Türkoğlu, S.A. (2024). Hypoxic Regulation of the KLK4 Gene in two Different Prostate Cancer Cells Treated with TGF-β. *Cell Biochemistry and Biophysics*, 82(3), 2797-2812. https://doi.org/10.1007/s12013-024-01396-5

Rascón, B., & Harrison, J.F. (2010). Lifespan and oxidative stress show a non-linear response to atmospheric oxygen in Drosophila. *Journal of Experimental Biology*, 213(20), 3441-3448. https://doi.org/10.1242/jeb.044867

Riccio, C. (2019). Extracting total RNA from *Caenorhabditis elegans* using phase-lock gel separation tubes. https://doi.org/10.17504/protocols.io.5sug6ew

Riddle, D.L., Blumenthal, T., Meyer, J.B., & Priess, J.R. (1997). *C. elegans* II, 2nd edition''. Cold Spring Harbor Mongraph Series 1222pp.

Sarrouilhe, D., Clarhaut, J., Defamie, N., & Mesnil, M. (2015). Serotonin and cancer: what is the link?. *Current molecular medicine*, 15(1), 62-77. https://doi.org/10.2174/1566524015666150114113411

Siddiqui, E.J., Shabbir, M., Mikhailidis, D.P., Thompson, C.S., & Mumtaz, F.H. (2006). The role of serotonin (5-hydroxytryptamine1A and 1B) receptors in prostate cancer cell proliferation. *J Urol.*, 176(4 Pt 1), 1648-53. https://doi.org/10.1016/j.juro.2006.06.087

Savaş, N., Öğüt, S., & Olgun, A. (2018). Toksikolojik Araştirmalarda Alternatif Bir Organizma: *Caenorhabditis elegans* (*C. elegans*). *Adnan Menderes Üniversitesi Sağlık Bilimleri Fakültesi Dergisi*, 2(2), 99-106.

Smith, C., Smith, M., Cunningham, R., & Davis, S. (2020). Recent advances in Antiemetics: New formulations of 5-HT: 3: Receptor antagonists in adults. *Cancer Nursing*, 43(4), E217-E228. https://doi.org/10.1097/NCC.0000000000000694

Turkoglu, S.A., & Kockar, F. (2016). SP1 and USF differentially regulate ADAMTS1 gene expression under normoxic and hypoxic conditions in hepatoma cells. *Gene*, 575(1), 48-57. https://doi.org/10.1016/j.gene.2015.08.035

Türkoğlu, S.A., Dayi, G., & Köçkar, F. (2020). Upregulation of PSMD4 gene by hypoxia in prostate cancer cells. *Turkish Journal of Biology*, *44*(5), 275-283. https://doi.org/10.3906/biy-2002-71

Türkoğlu, S.A., Poyrazlı, F., Babacan, D., & Köçkar, F. (2021). Hipoksi ve kanser. *Journal of Advanced Research in Natural and Applied Sciences*, 7(3), 450-463. https://doi.org/10.28979/jarnas.930938

Veenstra-VanderWeele, J., Anderson, G.M., & Cook Jr, E.H. (2000). Pharmacogenetics and the serotonin system: initial studies and future directions. *European journal of pharmacology*, 410(2-3), 165-181 https://doi.org/10.1016/S0014-2999(00)00814-1

Walther, D.J., Peter, J.U., Bashammakh, S., Hörtnagl, H., Voits, M., Fink, H., & Bader, M. (2003). Synthesis of serotonin by a second tryptophan hydroxylase isoform. *Science*, 299(5603), 76. https://doi.org/10.1126/science.1078197

White, J.G., Southgate, E., Thomson, J.N., & Brenner, S. (1986). The structure of the nervous system of the nematode *Caenorhabditis elegans*. *Philos Trans R Soc Lond B Biol Sci*, 314(1165), 1-340. https://doi.org/10.1098/rstb.1986.0056

Commagene Journal of Biology

Erdoğan et al., (2025) *Comm. J. Biol.* 9(1), 42-48.
DOI: 10.31594/commagene.1644311

e-ISSN 2602-456X

Research Article/Araştırma Makalesi

Evaluation of the Effect of Thymol on the Cytotoxicity of Cetuximab in Lung Cancer Cells

Ayşe ERDOĞAN*, Ekin HAZNEDAR, Mehmet BAŞER

Alanya Alaaddin Keykubat University, Faculty of Engineering, Department of Genetic and Bioengineering, Alanya, Antalya, TÜRKIYE
ORCID ID: Ayşe ERDOĞAN: http://orcid.org/0000-0001-7616-7673; Ekin HAZNEDAR: http://orcid.org/0009-0009-4895-0471; Mehmet BAŞER: http://orcid.org/0009-0006-8827-0444

Received: 21.02.2025 **Accepted:** 28.03.2025 **Published online:** 18.04.2025 **Issue published:** 30.06.2025

Abstract: The treatment of lung cancer continues to be a significant challenge for many oncologists and their patients. Treatment using epidermal growth factor receptor inhibitors is connected to a positive outcome. Cetuximab, a chimeric monoclonal antibody targeting the epidermal growth factor receptor (EGFR), in conjunction with monoterpene phenol thymol, is recommended for the treatment of lung cancer. While a mild acne-like skin rash is quite frequent in patients using cetuximab, a severe rash is rare. The goal of the current study was to assess whether thymol could enhance the anticancer effectiveness of cetuximab in A-549, non-small cell lung cancer (NSCLC) cell line. We found that the combination of cetuximab and thymol synergistically suppressed cell proliferation by inducing membrane damaging, oxidative stress, and apoptosis in A-549 cells. Taken together, our results indicate that the combination of thymol and cetuximab could improve anticancer responses and may notably enhance treatment outcomes in NSCLC.

Keywords: Cetuximab, carvacrol, lung cancer, synergistic anticancer effect, apoptosis.

Timol'ün Akciğer Kanseri Hücrelerinde Cetuximab'ın Sitotoksisitesi Üzerindeki Etkisinin Değerlendirilmesi

Öz: Akciğer kanserinin tedavisi, birçok onkolog ve hasta için önemli bir zorluk olmaya devam etmektedir. Epidermal büyüme faktörü reseptörü inhibitörleri kullanarak yapılan tedaviden olumlu bir sonuçlar alınmaktadır. Epidermal büyüme faktörü reseptörünü (EGFR) hedefleyen bir kimerik monoklonal antikor olan cetuximab, monoterpen fenol timol ile birlikte, akciğer kanserinin tedavisi için önerilmektedir. Cetuximab kullanan hastalarda hafif akne benzeri cilt döküntüsü oldukça sık görülürken, şiddetli döküntü nadir görülmektedir. Mevcut çalışmanın amacı, timolün cetuximabın A-549, küçük hücreli olmayan akciğer kanseri (NSCLC) hücre dizisindeki antikanser etkinliğini artırıp artırmayacağını değerlendirmektir. Cetuximab ve timol kombinasyonunun A-549 hücrelerinde zar hasarını, oksidatif stresi ve apoptozu uyararak hücre proliferasyonunu sinerjik bir şekilde baskıladığını bulduk. Bir arada değerlendirildiğinde, bulgularımız timol ve cetuximab kombinasyonunun antikanser yanıtların iyileştirilebileceğini ve NSCLC'deki tedavi sonuçlarının önemli ölçüde arttırılabileceğini göstermektedir.

Anahtar kelimeler: Cetuximab, karvakrol, akciğer kanseri, sinerjik antikanser etki, apoptoz.

1. Introduction

Lung cancer has the highest incidence rate among men worldwide, resulting in approximately 1.2 million deaths annually. Lung and prostate cancer are among the most common cancers in men in terms of incidence (Parkin et al., 2005). Lung cancer, originating from bronchial epithelium, is a type of cancer that has a very high incidence rate in men and women between the ages of 60 and 70. The incidence rate in young adults (under 50 years old) is quite low, ranging from 5-10%. Because it affects both men and women, it is recognized as the leading cause of cancer-related deaths worldwide. Smoking is the primary cause of lung cancer (Alar & Şahin, 2012; Ergelen & Çimşit, 2000). Due to existing medical treatments, the average 5-year survival rate for patients is 16% (Üstüner & Entok, 2019). Lung cancer is divided into two primary categories. These two groups are named non-small cell lung cancer and small cell lung cancer (Işıtmangil, 2013). Non-small cell lung cancer (NSCLC) makes up 80% of all lung cancer cases. Choosing the appropriate treatment method for NSCLC is of great importance. Surgical intervention is applied to the disease if diagnosed in early stages. In advanced stages, chemotherapy and radiotherapy treatments are applied. The survival rate in these patients is very low and their condition is poor (Balta et al., 2013; Ceylan et al., 2009). A-549 cells used in our study are non-small cell lung cells. A-549 cells are a monolayer of cells that adhere to the culture flask and can be propagated in these flasks. A-549 cells have a hypotriploid structure and contain the tumor suppressor P53 gene (Ding et al., 2008).

Cetuximab is a drug that belongs to a group of medications called monoclonal antibodies. Monoclonal antibodies are proteins that selectively recognize and bind to substances referred to as antigens. Cetuximab is a chimeric monoclonal IgG1 antibody, produced in mammalian cells, that attaches to the extracellular active site of EGFR (Cai et al., 2020). Thus, cetuximab blocks the ligand-mediated (RAS) activation of EGFR and induces antibody-dependent cellular cytotoxicity. When

Corresponding author: ayse.erdogan@alanya.edu.tr

cetuximab binds to EGFR, it prevents the phosphorylation and activation of kinases associated with the receptor, such as MAPK and PI3K/Akt. In this way, it inhibits cell growth and induces apoptosis, thereby preventing the development of cancer invasion and metastasis. Cetuximab is commonly associated with skin toxicity, occurring in 80% of cases. It appears on the face, neck, scalp, chest, and upper back. Patients usually experience mild to moderate rashes, with severe rashes being uncommon. This situation emphasizes the importance of developing alternative treatment approaches to minimize the side effects associated with cetuximab-based therapies.

Thymol, chemically referred to as 2-isopropyl-5-methylphenol, is a transparent crystalline monoterpene phenol. It is a secondary metabolite present in species of thyme. Used in traditional medicine for centuries, it has demonstrated a range of pharmacological effects, such as antioxidant, free radical neutralizing, anti-inflammatory, pain-relieving, antispasmodic, antibacterial, antifungal, disinfectant, and anticancer properties (Nagoor Meeran et al., 2017). Thymol has also lowered the levels of byproducts of lipid degradation in plasma, including thiobarbituric acid reactive substances (TBARS), lipid hydroperoxides (LOOH), and conjugated dienes (CDs). It has also been reported that thymol, due to its potent antioxidant properties, boosts the levels of non-enzymatic antioxidants like vitamin C, vitamin E, and GSH in plasma (Nagoor Meeran & Prince, 2012; Javed et al., 2019).

This study aimed to identify the most effective combination concentrations by combining different concentrations of cetuximab, a drug used in targeted therapy for A-549, NSCLC cell line, with non-cytotoxic concentrations of thymol to minimize the side effects of cetuximab.

2. Material and Method

2.1. Chemicals and drugs

Cetuximab used in the experiments was mixed with the medium in suitable ratios for dilution. Thymol is available for purchase with a purity of 99% (CDH, CAS-No: 89-83-8). The caspase activity kit was sourced from Elabscience Biotechnology Co., Ltd, USA. The kit used to measure Lactate Dehydrogenase Activity was acquired commercially from Sigma-Aldrich (St. Louis, MO, USA).

2.2 .Cell Lines and cultivation

A-549 cell line (human non-small cell lung cancer (NSCLC)) used in our experiments was obtained from the American Type Culture Collection (ATCC) and cultured under appropriate conditions. The cells were cultured in Roswell Park Memorial Institute 1640 medium (RPMI 1640) along with other components in appropriate proportions. Once the cells reached an adequate density (over 75%) in the culture vessel, experimental groups were established, and then cetuximab (<IC_{50}) and the natural monoterpenic phenol (thymol) (<IC_{50}) were administered to the cells for 48 h.

2.3. Cell viability test

After the cells in the flask were treated with trypsin, they were quantified and transferred into 96-well plates, with 10,000 cells per well. The cytotoxic effects of cetuximab (500-4000 µg/mL) and thymol (25-400 µg/mL) on A-549 cells were assessed over a 48 h period. Additionally, the cells were exposed to cetuximab (<IC_{50}) and thymol (<IC_{50}) simultaneously for 48 h. The cytotoxic effects of the treatments were assessed using the 3-(4,5-dimethylthiazol-2-yl)-2,5-diphenyltetrazolium bromide (MTT) assay. In this assay, mitochondrial dehydrogenases metabolize tetrazolium salts like MTT to produce a blue formazan dye, which is then used to assess cytotoxicity. The test reagents were introduced into the culture medium and the samples were then incubated at 37°C for 2 h. The plates were incubated for 1 h after adding solubilizing/stop solutions (dimethyl sulfoxide) to each well.

The optical density of each sample was recorded at 490 nm (Mosmann, 1983). Each concentration was replicated in eight wells.

The concentrations below IC_{50} (<IC_{50}) were determined separately for cetuximab and thymol. The combination treatments were then carried out using the calculated IC values (<IC_{50}). Based on the cytotoxicity results, the optimal combination concentration was identified after applying cetuximab (<IC_{50}) and thymol (<IC_{50}) together. The optimal combination concentrations were also applied in other ongoing experiments. The combination index (CI) was calculated to assess whether the co-treatment of cetuximab and thymol in cells produced additive, synergistic, or antagonistic effects (Huang et al., 2014). Cells treated with only the medium or 0.1% DMSO were regarded as the control group.

2.4. Lactate dehydrogenase (LDH) activity test

LDH activity was measured after exposing A-549 cells to cetuximab alone (IC_{30}) and combination of cetuximab (IC_{30}) with thymol (IC_{10}) concentrations, which demonstrated the most significant cytotoxic effects, for 48 h. LDH activity changes were assessed to evaluate whether either treatment induced membrane damage in lung cancer cells. LDH activity in each sample was analyzed using the protocol provided in the commercially available kit (MAK066, Sigma-Aldrich). The equation used to determine LDH activity is provided below.

LDH Activity = The amount of NADH that occurs between the first and last measurement (nmol) × Sample Dilution Factor/Reaction Time× Sample volume (mL)

2.5. Glutathione peroxidase (GPx) enzyme activity

After exposing the cells treated with cetuximab only (IC_{30}) and the combination of cetuximab (IC_{30}) and thymol (IC_{10}), which demonstrated the strongest cytotoxic effects, for a duration of 48 h, the supernatant from the cell culture was collected for assessment of GPx activity. GPx activity was evaluated using tert-butyl hydroperoxide as the substrate, following the specified method (Flohe & Gunzler, 1984). Protein concentration was measured using Bradford assay, with bovine serum as the standard (Bradford, 1976). The tests were conducted in three replicates.

2.6. Caspase-3 enzyme activity

Caspase-3 activity was evaluated after A-549 cells were exposed to cetuximab (IC_{30}) individually and together with thymol (IC_{10}), the concentrations that showed the highest cytotoxic effects, for 48 h. Apoptotic enzyme performance was assessed by utilizing the colorimetric Caspase-3 Activity Assay Kit (Elabscience), following kit's

instructions, after treating the cells with cetuximab alone and in combination with thymol. The plates were examined at 405 nm using a well plate spectrophotometer. The experiments were conducted in triplicate and the results are presented as units per milligram of protein.

2.7. Analysis of data

The findings from the replicates were pooled and presented as the mean ± standard deviation (SD). A statistical analysis using ANOVA was conducted. One-way ANOVA was employed to evaluate if there were notable differences between the averages of three or more independent groups for a particular variable. Tukey multiple comparisons tests were applied. Quantitative importance was accepted at $p<0.05$. Statistical assessments were carried out using Minitab software (http://www.minitab.com/products), version 13.0.

3. Results

3.1. Evaluation of the cell-damaging effects of cetuximab solitary and in partnership with thymol

Cytotoxic effects can be measured by analyzing the suppression of cancer cell growth and the triggering of cell death through different pathways. For this purpose, we used the MTT test, which is among the widely used cell viability tests in our experiments. In this research we explored the combination of cetuximab and thymol, the possible synergistic impact of both compounds on cancer cell survival was assessed.

A reduction in cell viability was noted in A-549 cells handled with several doses of cetuximab and thymol for 48 h, with a corresponding increase in concentration. When A-549 cells were put through diverse doses of thymol, changing from 25 to 400 µg/mL, IC_{10}, IC_{20}, IC_{30}, IC_{40}, and IC_{50} values were determined to be 27 µg/mL, 77 µg/mL, 127 µg/mL, 177 µg/mL, and 227 µg/mL, sequentially (Fig. 1).

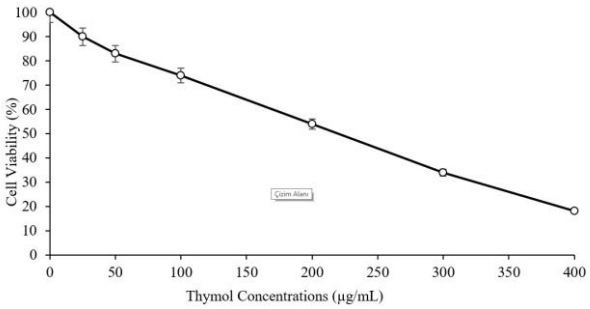

Figure 1. The cytotoxic influence of thymol on A-549 cells

When A-549 cells were subjected to multiple concentrations of cetuximab, starting at 500 and going up to 4000 µg/mL, IC_{10}, IC_{20}, IC_{30}, IC_{40}, and IC_{50} values were assessed as 174 µg/mL, 472 µg/mL, 770 µg/mL, 1067 µg/mL, and 1365 µg/mL, in the same order (Fig. 2).

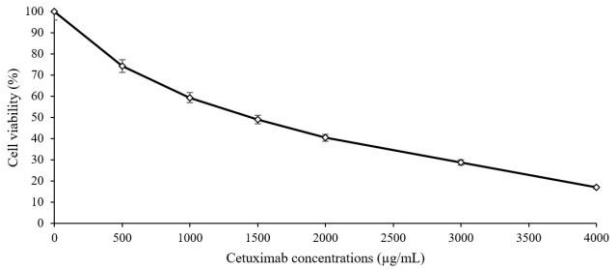

Figure 2. The cytotoxic effect of cetuximab on A-549 cells

By evaluating the cell viability in cells treated in conjunction alongside cetuximab ($<IC_{50}$) and thymol ($<IC_{50}$) and calculating the combination index (CI) value, it was determined that the most potent combination doses were IC_{30} for cetuximab and IC_{10} for thymol (Fig. 3). The combined effect of IC_{30} cetuximab and IC_{10} thymol treatment on A-549 cells was proven to be synergistic through CI value of 1.38 that was calculated.

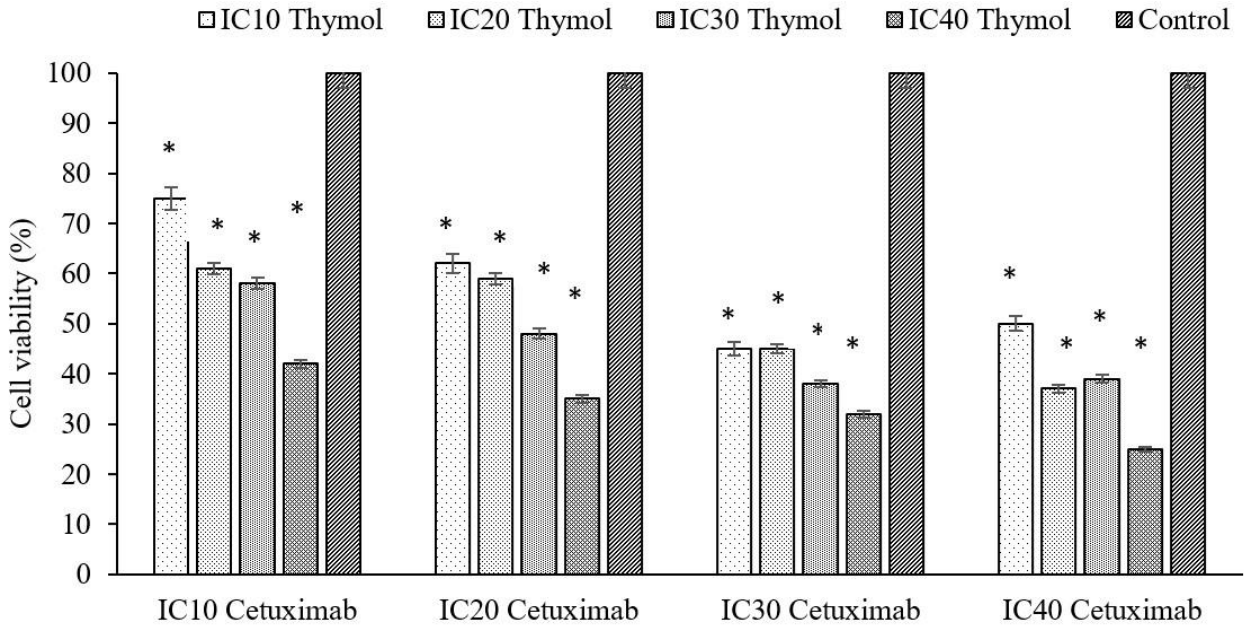

Figure 3. The joint cetuximab's cell-damaging effects (IC10, IC20, IC30, IC40) and thymol (IC10, IC20, IC30, IC40) on A-549 cells for 48 h were assessed. The results are displayed as the survival ratio relative to the reference group (cells exposed solely to the medium, devoid of treatment). The findings are shown as the average of three standalone experiments, each alongside three replicates, ± standard deviation (SD). *Notably different from the control (untreated cells) ($p<0.05$).

3.2. Assessment of the membrane disrupting effect of cetuximab alone and in combination with thymol

Lactate dehydrogenase (LDH) is essential for converting lactate to pyruvate in anaerobic metabolism. LDH is often used as a biomarker in medical diagnostics, particularly to assess tissue damage or cell injury. LDH activity is typically measured using a spectrophotometric method, which monitors changes in absorbance as the enzyme catalyzes the conversion of lactate to pyruvate (or vice versa). This method relies on detecting the changes in light absorbance at specific wavelengths, which is proportional to the enzyme's activity (Kaja et al., 2017).

LDH release is commonly applied in cell culture studies to assess cell viability and cytotoxicity. When cells are damaged or killed, LDH leaks out of the cells and into the culture medium. Measuring LDH levels in the medium can indicate the degree of cell damage. In summary, LDH activity measurement is a versatile and widely used tool in both clinical and research settings to assess cell viability, tissue damage, and disease progression (Parhamifar et al., 2019).

After A-549 cells were exposed to cetuximab at IC_{30} concentration and to combination of IC_{30} cetuximab + IC_{10} thymol (the most potent cytotoxic concentration combinations) for 48 h, LDH enzyme activity changes were assessed. Cetuximab and thymol were applied to the cells for a duration of 48 h and it was observed that LDH enzyme activity was elevated in comparison to the control. In A-549 cells administered with cetuximab at IC_{30} level, LDH enzyme activity was observed to increase approximately 2.1 times in relation to the control group. When cetuximab and thymol were implemented simultaneously, LDH activity rose by roughly 3.3 times in comparison to the control (Fig.4).

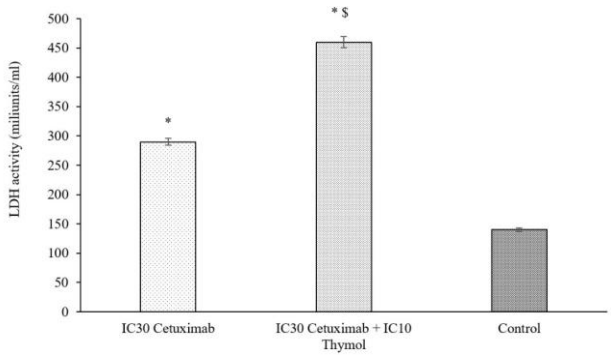

Figure 4. Alterations in LDH activity following treatment with cetuximab alone and in combination with thymol. *Markedly disparate from the control ($p<0.05$). $Significantly distinct from cetuximab solitary treatment ($p<0.05$). One unit of LDH activity is specified as the quantity of enzyme that accelerates the reduction of lactate to pyruvate, generating 1.0 µmol of NADH in a minute at 37 °C.

3.3. Examination of the influence of cetuximab alone and alongside thymol on glutathione peroxidase activity

Glutathione peroxidase (GPx) plays a key role in defending cells against oxidative harm by breaking down hydrogen peroxide (H_2O_2) and organic peroxides into benign substances, requiring glutathione (GSH) as a cofactor. Evaluating GPx activity is an essential method for assessing oxidative stress and the antioxidant potential within cells (Pei et al., 2023).

After A-549 cells underwent treatment with cetuximab alone and in conjunction with thymol for 48 hours, GPx activity changes were measured to evaluate the potential of the treatments to trigger oxidative stress. Approximately 2.8 -fold increase in GPx activity was observed with cetuximab treatment alone, relative to the controls. The combined treatment (IC_{30} cetuximab + IC_{10} thymol) was found to induce 4-fold greater boost in GPx activity compared to the controls. The rise in GPx activity observed after both cetuximab treatment alone and the combined treatment, relative to the controls, was established as statistically significant ($p<0.05$) (Fig. 5). Induction of oxidative stress was more pronounced with the combined treatment than with cetuximab treatment alone.

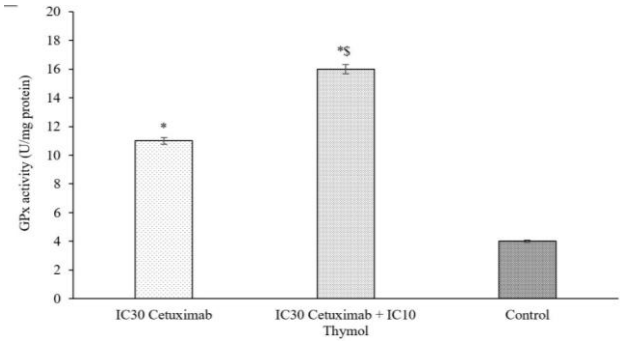

Figure 5. The influence of methotrexate treatment alone and in combination with carvacrol on glutathione peroxidase (GPx) activity. *Significantly distinct from control ($p<0.05$). $Markedly different from cetuximab monotherapy ($p<0.05$).

3.4. Investigation of the apoptotic response to cetuximab alone and along with thymol

Caspase-3 is a critical enzyme involved in the process of apoptosis or programmed cell death.

It is classified under the caspase family, a collection of cysteine-aspartic proteases that play essential roles in controlling cell death and inflammation. Specifically, caspase-3 is categorized as an "effector caspase," meaning it executes the final steps of apoptosis by breaking down key cellular components (McComb et al., 2019).

In cancer research, caspase-3 activity can indicate the effectiveness of chemotherapy or targeted therapies that induce apoptosis in cancer cells.

Our study involved measuring caspase-3 enzyme activity after 48 h of incubation with cetuximab alone and combined with thymol to assess the apoptotic impact of both treatments. It was revealed that the combination of IC_{30} cetuximab and IC_{10} thymol (the most effective cytotoxic concentrations) led to a more pronounced apoptotic response than cetuximab treatment alone. The caspase-3 activity recorded after the combined treatment was approximately 1.65 times more than the caspase-3 activity recorded after cetuximab treatment alone (Fig. 6). In addition, the augmentation in caspase-3 activity following the combination therapy was markedly different from the augmentation in caspase-3 activity following cetuximab treatment alone ($p<0.05$). Both treatments induced a statistically significant boost in caspase-3 activity versus the control group.

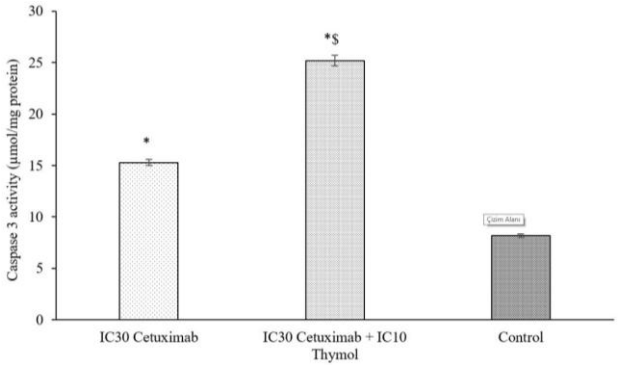

Figure 6. Impact of cetuximab alone and in combination with thymol on caspase-3 enzyme activity. *Significantly distinct from control ($p<0.05$). $ Notably distinct from cetuximab single care ($p<0.05$).

4. Discussion

EGFR inhibitors, particularly cetuximab, are becoming more widely used due to their lower systemic side effects, enhanced survival rates, and improved overall well-being for individuals with cancer. Cetuximab is employed in the treatment of colorectal, head and neck, pancreatic, and lung cancers. Hence, it is essential to gain a clearer understanding of the processes behind EGFRI-associated skin toxicities and their management (Peréz-Soler & Saltz, 2005; Lacouture, 2006; Albanell et al., 2002). Cetuximab is a composite monoclonal antibody composed of human and mouse components that selectively bind to the epidermal growth factor receptor (EGFR), blocking the attachment of epidermal growth factor and other signaling molecules through competition. Interacting with EGFR prevents phosphorylation and activation process of kinases tied to the receptor, leading to cell growth inhibition and programmed cell death. At present, there is an absence of definitive instructions for preventing and managing the cutaneous toxicities associated with epidermal growth factor receptor blockers. Conversely, the utilization of EGFR inhibitors is rising not just in head and neck cancer but also in colon and lung cancers (Bonner et al., 2006; Lacouture, 2006; Jacot et al., 2004; Lacouture et al., 2006; Chung et al., 2005).

At present, combination therapies are gaining increasing attention in various cases and have been designed to enhance effectiveness, minimize side effects, and overcome drug resistance in the treatment of cancer patients. Recent developments show that combination therapy offers several benefits over traditional treatments and presents a promising strategy to mitigate harmful effects by lowering the drug dosage (Anitha et al., 2016). Thus, it is crucial to prioritize the search for more targeted combination therapies that cause fewer harmful effects on normal cells. Among these, the incorporation of natural products is on the rise. When used alongside various cancer-fighting agents derived from plant-based sources, cetuximab has been found to enhance the occurrence of apoptosis in human cancer cells across several experimental models. Examining the combined impact of thymol and cetuximab on cancer cells is crucial to understand whether thymol has an effect on EGFR-targeted treatments. Although research on this combination is scarce, some studies propose that thymol could affect cell cycle regulation or boost immune responses.

No studies have been conducted on the combined cytotoxic and apoptotic effects of cetuximab and thymol treatment on A-549 cells. In this study, lung cancer cells treated with both cetuximab and thymol exhibited more extensive membrane damage and enhanced apoptotic effects compared to those treated with cetuximab alone. Our study is the first to show that thymol increases the cytotoxic impact of cetuximab at low concentrations ($<IC_{50}$) in lung cancer cells. In our study, higher concentrations of cetuximab and thymol led to a reduction in cancer cell viability. When cetuximab ($<IC_{50}$) was combined with different concentrations of thymol ($<IC_{50}$), we identified the optimal combined concentration that amplified cytotoxicity in A-549 cells. As a result, the co-administration of cetuximab and thymol demonstrated a stronger cytotoxic effect on A-549 cells compared to cetuximab alone. Lower concentrations of thymol may have exerted stronger cytotoxic effects on A-549 cells when combined with cetuximab, potentially due to their ability to more efficiently activate the cell's antioxidant mechanisms. LDH enzyme activity was measured following the treatment of A-549 cells with IC_{30} cetuximab alone and in combination with IC_{10} thymol, which demonstrated the highest cytotoxic effect over 48 h period. The results indicated that LDH enzyme activity was higher in A-549 cells exposed to the combination treatment compared to those treated with cetuximab alone. Our LDH activity results are consistent with the cell viability findings. In our study, both cetuximab alone and in combination with thymol were observed to increase GPx activity in A-549 cells. This effect is attributed to cetuximab, either by itself or in combination with thymol, inducing oxidative stress through the production of reactive oxygen species. Additionally, cetuximab treatment, both individually and alongside thymol, led to an increase in caspase-3 activity, resulting in a more pronounced apoptotic response. Based on our results, the combination of cetuximab and thymol triggered a higher level of apoptosis in the cells compared to cetuximab alone.

Park and colleagues (2010) noted significant anti-tumor effects when cetuximab was combined with genistein, a naturally occurring isoflavonoid in soybeans, in mouse models with an oral squamous cell carcinoma (OSCC) xenograft. Cetuximab when combined alongside docetaxel, a taxoid sourced from the foliage of the European yellow tree, was able to suppress the growth of non-small cell lung cancer PC9/G2 cells both *in vitro* and *in vivo* (Zhang et al., 2014).

Leeman-Neill and colleagues (2009) highlighted that guggulsterone, a natural compound used in traditional Indian medicine, enhances the inhibitory effects of cetuximab on cell proliferation in head and neck squamous cell carcinoma (HNSCC). The combination of cetuximab with oridonin, a potent compound derived from *Rabdosia rubescens*, is an effective strategy for inducing a joint antitumor effect against laryngeal squamous cell carcinoma (LSCC), both *in vitro* and *in vivo*. This study also explored the mechanisms behind the observed synergy between the two treatments. Throughout the entire experimental phase, no significant side effects were

observed in the treatment groups. The findings suggest that the combined use of cetuximab and oridonin has a strong anticancer effect on LSCC, primarily through the reduction of p-EGFR levels. The concurrent treatment using oridonin and cetuximab inhibited EGFR phosphorylation, leading to significant apoptosis both *in vitro* and *in vivo*. LSCC cells treated alongside oridonin and cetuximab exhibited superior levels of Fas, FasL, and engaged caspase-8 compared to cells treated with oridonin alone (Cao et al., 2016). Natural products, due to their minimal side effects on normal cells, offer an optimal strategy when used alongside the approved drug 5-fluorouracil to more precisely target colorectal cancer cells. This combination helps improve therapeutic outcomes and enhances patients' quality of life. In particular, the promising anticancer natural compound withaferin-A, when combined with 5-fluorouracil, is being evaluated for its synergistic anti-tumor effects in colorectal cancer cells. The goal is to improve the drug combination's efficacy, reduce the required dosage, and minimize side effects on normal cells. In this study, detailed analysis revealed that the combination treatment significantly reduces cell viability in colorectal cancer cells and exhibits a robust combination index. This not only lowers the required dosage but also shows strong effectiveness and a safe toxicity profile in normal colon cells. The combination treatment reduced cell viability at lower doses compared to when withaferin-A or 5-fluorouracil was used alone. Drug index analysis further confirmed that the combination produces a highly potent synergistic effect, enhances drug efficacy, and demonstrates a safe toxicity profile in normal colon cells (Alnuqaydan et al., 2020). Ambrož and colleagues (2017) showed that a sesquiterpene extracted from *Myrica rubra* enhances the effectiveness of doxorubicin in both sensitive and resistant cancer cells. In another study, it was shown that the coalition of cetuximab and honokiol manifested a strong antiproliferative impression on cetuximab-resistant clones both *in vitro* and *in vivo* (Alnuqaydan et al., 2020).

5. Conclusions

The current study demonstrates that the combination of thymol and cetuximab produces synergistic effects on inhibiting cell growth by inducing membrane damage, leading increase in GPx activity, and apoptotic effect. In conclusion, while cetuximab has a well-established role in cancer treatment, research on the combined use of cetuximab and timol is limited. However, there is potential for timol to enhance the effects of cetuximab. Further preclinical and clinical studies are necessary to determine whether timol provides a synergistic effect when combined with cetuximab in cancer treatment.

Ackowledgement: The authors wish to thanks to Alanya Alaaddin Keykubat University for providing the necessary facilities to conduct this study. The author would like to thank Alanya Alaaddin Keykubat University Scientific Research Projects Unit (2023-02-07-LAP01) for financial support of this work.

Ethics committee approval: Ethics committee approval is not required for this study.

Conflict of interest: The authors declare that there is no conflict of interest.

Author Contributions: Conception – A.E.; Design – A.E.; Supervision – A.E.; Fund – Alanya Alaaddin Keykubat University; Materials – A.E.; Data Collection and Processing – A.E., E.H., M.B.; Analysis Interpretation – A.E.; Literature Review – A.E.; Writing – A.E.; Critical Review – A.E.

References

Alar, T., & Şahin, E.M. (2012). Akciğer kanseri: birinci basamakta tanı, tedavi ve korunma Lung cancer: Diagnosis, treatment and prevention in primary care. *Smyrna Tıp Dergisi*, 68-74.

Albanell, J., Rojo, F., Averbuch, S., Feyereislova, A., Mascaro, J.M., Herbst, R., … & Baselga, J. (2002). Pharmacodynamic studies of the epidermal growth factor receptor inhibitor ZD1839 in skin from cancer patients: histopathologic and molecular consequences of receptor inhibition. *Journal of Clinical Oncology*, 20, 110-124. https://doi.org/10.1200/jco.20.1.110

Alnuqaydan, A.M., Rah, B., Almutary, A.G., & Chauhan, S.S. (2020). Synergistic antitumor effect of 5-fluorouracil and withaferin-A induces endoplasmic reticulum stress-mediated autophagy and apoptosis in colorectal cancer cells. *American Journal of Cancer Research*, 10(3), 799.

Ambrož, M., Matoušková, P., Skarka, A., Zajdlová, M., Žáková, K., & Skálová, L. (2017). The effects of selected sesquiterpenes from myrica rubra essential oil on the efficacy of doxorubicin in sensitive and resistant cancer cell lines. *Molecules*, 22(6), 1021. https://doi.org/10.3390/molecules22061021

Anitha, A., Maya, S., Sivaram, A.J., Mony, U., & Jayakumar, R. (2016). Combinatorial nanomedicines for colon cancer therapy. *Wiley Interdisciplinary Reviews: Nanomedicine and Nanobiotechnology*, 8, 151-159. https://doi.org/10.1002/wnan.1353

Balta, B.Z., Üre, Ö.S., Erturan, S., & Aydin, G. (2013). Prognostic factors in advanced-stage non-small cell lung cancer. *Haseki Tip Bulteni*, 51(2), 56-60. https://doi.org/10.4274/Haseki.848

Bonner, J.A., Harari, P.M., Giralt, J., Azarnia, N., Shin, D.M., Cohen, R.B., … & Ang, K.K. (2006). Radiotherapy plus cetuximab for squamous-cell carcinoma of the head and neck. *New England Journal of Medicine*, 354, 567-578. https://doi.org/10.1056/NEJMoa053422

Bradford, M.M. (1976). A rapid and sensitive method for the quantization of microgram quantities of protein utilizing the principle of protein dye binding. *Analytical Biochemistry*, 72, 248-254. https://doi.org/10.1006/abio.1976.9999

Cai, W.Q., Zeng, L.S., Wang, L. ., Wang, Y.Y., Cheng, J.T., Zhang, Y., … & Xin, H.W. (2020). The latest battles between EGFR monoclonal antibodies and resistant tumor cells. *Frontiers in Oncology*, 10, 1249. https://doi.org/10.3389/fonc.2020.01249

Cao, S., Xia, M., Mao, Y., Zhang, Q., Donkor, P.O., Qiu, F., & Kang, N. (2016). Combined oridonin with cetuximab treatment shows synergistic anticancer effects on laryngeal squamous cell carcinoma: involvement of inhibition of EGFR and activation of reactive oxygen species-mediated JNK pathway. *International Journal of Oncology*, 49(5), 2075-2087. https://doi.org/10.3892/ijo.2016.3696

Ceylan, K.C., Arpat, A.H., & Kaya, Ş.Ö. (2009). Küçük hücreli dışı akciğer kanserinde klinik ve patolojik evrelemenin karşılaştırılması. *Dr. Suat Seren Göğüs Hastalıkları ve Cerrahisi Eğitim Araştırma Hastanesi, Göğüs Cerrahisi*, 14.

Chung, K.Y., Shia, J., Kemeny, N.E., Shah, M., Schwartz, G.K., Tse, A., … & Saltz, L.B. (2005). Cetuximab shows activity in colorectal cancer patients with tumors that do not express the epidermal growth factor receptor by immunohistochemistry. *Journal of Clinical Oncology*, 23, 1803-1810. https://doi.org/10.1200/jco.2005.08.037

Ding, L., Getz, G., Wheeler, D.A., Mardis, E.R., McLellan, M.D., Cibulskis, K., … & Wilson, R.K. (2008). Somatic mutations affect key pathways in lung adenocarcinoma. Nature, 455(7216), 1069-1075. https://doi.org/10.1038/nature07423

Ergelen, R., & Çimşit, N.Ç. (2000). Akciğer tümörü. *Türk Toraks Derneği*, 178-188. https://doi.org/10.5152/tcb.2013.30

Flohe, L., & Gunzler, W.A. (1984). Glutathione peroxidase. *Methods in Enzymology*, 105, 115-121. https://doi.org/10.1016/S0076-6879(84)05015-1

Huang, F., Wu, X.N., Chen, J.I.E., Wang, W.X., & Lu, Z.F. (2014). Resveratrol reverses multidrug resistance in human breast cancer doxorubicin-resistant cells. *Experimental and Therapeutic Medicine*, **7**, 1611-1616. https://doi.org/10.3892/etm.2014.1662

Işıtmangil, G.A. (2013). Akciğer kanser immünoterapisinde yeni stratejiler. *Haydarpaşa Numune Eğitim ve Araştırma Hastanesi Tıp Dergisi*, 53(3), 168-177.

Jacot, W., Bessis, D., Jorda, E., Ychou, M., Fabbro, M., Pujol, J. L., & Guillot, B. (2004). Acneiform eruption induced by epidermal growth factor receptor inhibitors in patients with solid tumours. *British Journal of Dermatology*, 151(1), 238-241. https://doi.org/10.1111/j.1365-2133.2004.06026.x

Javed, H., Azimullah, S., Meeran, M.F., Ansari, S.A., & Ojha, S. (2019). Neuroprotective effects of thymol, a dietary monoterpene against dopaminergic neurodegeneration in rotenone-induced rat model of Parkinson's disease. *International Journal of Molecular Sciences*, 20(7), 1538. https://doi.org/10.3390/ijms20071538

Kaja, S., Payne, A.J., Naumchuk, Y., & Koulen, P. (2017). Quantification of lactate dehydrogenase for cell viability testing using cell lines and primary cultured astrocytes. *Current Protocols in Toxicology*, 72, 2-26. https://doi.org/10.1002/cptx.21

Lacouture, M.E. (2006). Mechanisms of cutaneous toxicities to EGFR inhibitors. *Nature Reviews Cancer*, 6(10), 803-812. https://doi.org/10.1038/nrc1970

Lacouture, M.E., Basti, S., Patel, J., & Benson, A.3rd (2006). The SERIES clinic: an interdisciplinary approach to the management of toxicities of EGFR inhibitors. *The Journal of Supportive Oncology*, 4(5), 236-238.

Leeman-Neill, R.J., Wheeler, S.E., Singh, S.V., Thomas, S.M., Seethala, R.R., Neill, D.B., … & Grandis, J.R. (2009). Guggulsterone enhances head and neck cancer therapies via inhibition of signal transducer and activator of transcription-3. *Carcinogenesis*, 30, 1848-1856. https://doi.org/10.1093/carcin/bgp211

McComb, S., Chan, P. ., Guinot, A., Hartmannsdottir, H., Jenni, S., Dobay, M.P., Bourquin, J.P., & Bornhauser, B.C. (2019). Efficient apoptosis requires feedback amplification of upstream apoptotic signals by effector caspase-3 or-7. *Science Advances*, 5, eaau9433. https://doi.org/10.1126/sciadv.aau9433

Mosmann, T. (1983). Rapid colorimetric assay for cellular growth and survival: Application to proliferation and cytotoxicity assays. *Journal of Immunological Methods*, 65, 55-63. https://doi.org/10.1016/0022-1759(83)90303-4

Nagoor Meeran, M.F., & Stanely Mainzen Prince, P. (2012). Protective effects of thymol on altered plasma lipid peroxidation and nonenzymic antioxidants in isoproterenol induced myocardial infarcted rats. *Journal of Biochemical and Molecular Toxicology*, 26, 368-373. https://doi.org/10.1002/jbt.21431

Nagoor Meeran, M.F., Javed, H., Al Taee, H., Azimullah, S., & Ojha, S.K. (2017). Pharmacological properties and molecular mechanisms of thymol: prospects for its therapeutic potential and pharmaceutical development. *Frontiers in pharmacology*, 8, 380. https://doi.org/10.3389/fphar.2017.00380

Parhamifar, L., Andersen, H., & Moghimi, S.M. (2019). Lactate dehydrogenase assay for assessment of polycation cytotoxicity. *Nanotechnology for Nucleic Acid Delivery: Methods and Protocols*, 291-299. https://doi.org/10.1007/978-1-4939-9092-4_18

Park, S.J., Kim, M.J., Kim, Y.K., Kim, S.M., Park, J.Y., & Myoung, H. (2010). Combined cetuximab and genistein treatment shows additive anti-cancer effect on oral squamous cell carcinoma. *Cancer Letters*, 292(1), 54-63. https://doi.org/10.1016/j.canlet.2009.11.004

Parkin, D.M., Bray, F., Ferlay, J., & Pisani, P. (2005). Global cancer statistics. *CA: A Cancer Journal for Clinicians*, 55(2), 74-108. http://doi.org/10.3322/canjclin.55.2.74

Pei, J., Pan, X., Wei, G., & Hua, Y. (2023). Research progress of glutathione peroxidase family (GPX) in redoxidation. *Frontiers in Pharmacology*, 14, 1147414. https://doi.org/10.3389/fphar.2023.1147414

Peréz-Soler, R., & Saltz, L. (2005). Cutaneous adverse effects with HER1/EGFR-targeted agents: is there a silver lining?. *Journal of Clinical Oncology*, 23(22), 5235-5246. https://doi.org/10.1200/jco.2005.00.6916

Üstüner, C., & Entok, E. (2019). Experimental animal models for lung cancer. *Nuclear Medicine Seminars*, 5, 40-48. https://doi.org/10.4274/nts.galenos.2019.0006

Zhang, L., Li, X.F., Tand, L., Zhao, Y.M., & Zhou, C.C. (2014). The effects of cetuximab in combination with docetaxel for the acquired resistance to EGFR-TKI in non-small cell lung cancer cells. *Tumor*, 34, 584-590.

Commagene Journal of Biology

Ellibeş-Gökkaya et al., (2025) *Comm. J. Biol.* 9(1), 49-58.
DOI: 10.31594/commagene.1632392

e-ISSN 2602-456X

Research Article/Araştırma Makalesi

Alterations Induced by Nano-Polystyrene Administration in Biological Parameters of Host-Endoparasitoids (*Galleria mellonella* and *Pimpla turionellae*) and Host Hemocyte Counts

Tuğba Nur ELLİBEŞ-GÖKKAYA[1], Zülbiye DEMİRTÜRK[1], Fevzi UÇKAN *[1], Serap MERT[2,3,4]

[1]*Department of Biology, Faculty of Science-Art, Kocaeli University, Kocaeli, TÜRKİYE*
[2]*Center for Stem Cell and Gene Therapies Research and Practice, Kocaeli University, Kocaeli, TÜRKİYE*
[3]*Department of Polymer Science and Technology, Kocaeli University, Kocaeli, TÜRKİYE*
[4]*Department of Chemistry and Chemical Processing Technology, Kocaeli University, Kocaeli, TÜRKİYE*
ORCID ID: Tuğba Nur ELLİBEŞ-GÖKKAYA: https://orcid.org/0000-0002-1265-9844; Zülbiye DEMİRTÜRK: https://orcid.org/0000-0002-3107-4278; Fevzi UÇKAN: https://orcid.org/0000-0001-9304-4296 ; Serap MERT: https://orcid.org/0000-0001-5939-5295

Received: 03.02.2025 **Accepted:** 11.04.2025 **Published online:** 26.05.2025 **Issue published:** 30.06.2025

Abstract: Plastic pollution is one of the biggest threats to the environment and human health. Micro and nanoplastics are encountered in many areas of our daily lives and may accumulate in organisms, causing reduced life span, genotoxicity, and altered metabolism. Plastic pollution around the environment may lead to reductions in insect biodiversity and populations. It may also lead to the collapse of food webs and ecosystems of organisms that feed on them in the food chain. Therefore, the effects of nano-polystyrene (PSs) on the life cycle, biological characteristics, total hemocyte count (THCs) of the host, and hemocyte types of the model organism *Galleria mellonella* and its endoparasitoid *Pimpla turionellae* were investigated. Nano-PSs were produced according to the single emulsion solvent evaporation method and larval feeds were prepared with solutions of different concentrations. These diets were given to the larvae until they developed. The developmental time of the host-larvae fed with nano-PS-containing diets and the parasitoids that emerged using the pupae of these larvae as hosts were shortened. While the host adult weight and size increased, the weight of the parasitoid decreased. Dose-dependent decreases in THCs were observed. Prohemocyte, plasmatocyte, oenocytoid, and spherulocyte counts decreased, while granulocyte counts increased. Furthermore, the changes in the biology of the host exposed to nano-PSs indirectly affected the endoparasitoids. In addition, this study emphasizes that nanoplastic toxicity in honey-bees is generally ignored and that the consumption of bee products may pose potential hazards to human health. This reveals the crucial role of taking necessary precautions in beekeeping.

Keywords: Cellular immunity, greater wax moth, life cycle, nano-plastic, parasitoid wasp.

Nano-Polistiren Uygulamasının Konak-Endoparazitoitlerin (*Galleria mellonella* ve *Pimpla turionellae*) Biyolojik Parametrelerinde ve Konak Hemosit Sayılarında Oluşturduğu Değişiklikler

Öz: Plastik kirliliği çevre ve insan sağlığı açısından en büyük tehditlerden biridir. Mikro ve nanoplastikler, günlük yaşamımızın birçok alanında karşımıza çıkmaktadır ve organizmalarda birikerek yaşam süresinin azalmasına, genotoksisiteye ve metabolizmanın değişmesine neden olabilmektedir. Çevredeki nanoplastik kontaminasyonu, böcek biyoçeşitliliğindeki ve popülasyonlarındaki azalmalara neden olabilir. Aynı zamanda besin zincirinde onlarla beslenen canlıların besin ağlarının ve ekosistemlerin çökmesine yol açabilir. Bu nedenle nano-polistiren (PS)'lerin model organizma *Galleria mellonella* ve endoparazitoiti *Pimpla turionellae*'nın yaşam döngüsüne, biyolojik özelliklerine, konağın toplam hemosit sayısına (THS) ve hemosit tiplerine etkileri incelendi. Nano-PS'ler tekli emülsiyon çözücü buharlaştırma yöntemine göre üretildi ve farklı konsantrasyonlarda solüsyonları ile larval besinler hazırlandı. Bu besinler, larvalara gelişinceye kadar verildi. Nano-PS içeren besinlerle beslenen konak larvaların ve bu larvaların pupalarını konak olarak kullanarak ortaya çıkan parazitoitlerin gelişim süreleri kısaldı. Konak ergin ağırlığı ve boyutları artarken, parazitoitin ağırlığı azaldı. THS'de doza bağlı azalmalar görüldü. Prohemosit, plazmatosit, önositoid ve sferülosit sayısının azaldığı, granülosit sayısının ise arttığı görüldü. Ayrıca nano-PS'lerle beslenen konağın biyolojisindeki değişiklikler, endoparazitoitleri dolaylı olarak etkiledi. Öte yandan bu çalışma ile bal arılarında nanoplastik toksisitesinin genellikle göz ardı edildiği ve arı ürünlerinin tüketilmesinin insan sağlığı için potansiyel tehlikeler yaratabileceği vurgulanmaktadır. Bu durum, arıcılıkta gerekli önlemlerin alınmasının önemini ortaya koymaktadır.

Anahtar kelimeler: Hücresel bağışıklık, büyük balmumu güvesi, yaşam döngüsü, nano-plastik, parazitoit yaban arısı.

1. Introduction

The high persistence of plastic wastes in ecosystems due to their high resistance to degradation and their interactions with living organisms has been a concern for the last century. Plastic materials accumulated in terrestrial and aquatic ecosystems have the potential to easily enter organisms by breaking down into micro and nanoplastics due to some factors such as sunlight, biodegradation, hydrolysis, photooxidation, mechanical abrasion, salinity, and temperature (Kögel et al., 2020; Murphy et al., 2016; Oliveira et al., 2019; Parenti et al., 2020). In comparison to large plastic wastes, micro and nanoplastics may create more risk as they are more likely to pass through biological boundaries, accumulate in tissues, or get into the food chain (Hu & Palić, 2020; Muhammad et al., 2021).

Corresponding author: fevzi.uckan@kocaeli.edu.tr

Meanwhile, there is increasing concern about the pollution that microplastics may cause (Rothen-Rutishauser et al., 2021). The influences of plastic particles in terrestrial ecosystems have been almost underestimated compared to the aquatic ecosystems (Awet et al., 2018; El Kholy & Al Naggar, 2023; Muhammad et al., 2021; Wang et al., 2021). Insects both encompass a large part of the ecosystem and play an essential role in the ecosystem. Recently, it has been emphasized that there has been a significant decline in insect species due to micro/nanoplastic pollution (Shen et al., 2023). Plastic pollution in a terrestrial ecosystem may create serious problems owing to atmospheric cycling and transport to distant areas such as glaciers. Hence, it may adversely affect insects, plants and animals, food chains, ecosystems, and subsequently human-related activities that depend on these factors that may occur (Muhammad et al., 2021; Toussaint et al., 2019; Wang et al., 2021). Furthermore, the studies on the intake of plastic particles and their impacts on terrestrial organisms remain quite scarce and have only been considered in the last few years (Parenti et al., 2020; Wang et al., 2020). Among plastic particles, micro-sized particles have been particularly emphasized and their impacts on terrestrial ecosystems have recently been demonstrated (Deng et al., 2021; Dolar et al., 2022; Dolar et al., 2021; El Kholy & Al Naggar, 2023; Kalman et al., 2023; Kholy & Naggar, 2022; Zhang et al., 2023). For this reason, it is extremely critical to determine the effects of nanoplastics on living organisms, in particular insects.

Among plastic materials, polystyrene (PS) polymers are recognized as one of the most globally used plastics in the production of disposable cutlery, egg cups, spectacle frames, food packaging, and building insulation (Deng et al., 2021; El Kholy & Al Naggar, 2023; Long et al., 2017). When the wide range of usage areas is considered, it is unlikely to be unaffected by chemical, mechanical, and direct/indirect toxic potential impacts (Kim & An, 2019; Kögel et al., 2020; Muhammad et al., 2021). In recent years, it has been stated that some terrestrial organisms, notably *Bombyx mori* (Muhammad et al., 2024; Muhammad et al., 2021; Parenti et al., 2020; Wang et al., 2023), *Drosophila melanogaster* (Aloisi et al., 2024; El Kholy & Al Naggar, 2023; Kholy & Naggar, 2022; Tu et al., 2023; Urbisz et al., 2024), *Galleria mellonella* (Demirtürk et al., 2024), *Eisenia fetida* (Wang et al., 2019), *Aphylla williamsoni* (Guimarães et al., 2021), *Apis mellifera,* and *Apis cerana* (Deng et al., 2021; Wang et al., 2021), *Chironomus riparius* (Martin-Folgar et al., 2024), *Chironomus kiinensis* (Zhang et al., 2023), and *Tenebrio molitor* (Peng et al., 2024) may uptake micro and nano PSs from the environment; accumulate in the intestine, adipose tissue, ovary, and hemolymph; cause substantial changes in weight, development, and life span; cause necrosis and apoptosis; suppress the immune system; display neurotoxic effects; increase susceptibility to viral infection; and cause DNA damage. However, studies on the biological development of PS NPs in terrestrial insects are deficient and information on the aggregation effect of PS NPs in the food chain is limited (Wang et al., 2023).

Honey-bees are highly valued species that provide pollination services for the production of a wide variety of agricultural crops (Calderone, 2012). The greater wax moth *Galleria mellonella* L. (Lepidoptera: Pyralidae) is the world's most severe pest of honey-bees worldwide. They infest stored wax combs and bee colonies, causing extensive damage. Additionally, when the apiary is queenless or exposed to pesticides, the hive suddenly weakens and problems arise (Gounari et al., 2024). Apart from these, potential adverse biological and cellular effects can be seen on the host *G. mellonella* directly exposed to nanoplastics, especially PS NPs. On the other hand, these host species may interact indirectly with honey-bees by parasitism and their endoparasitoids *Pimpla turionellae,* and even by invading combs and may have adverse effects on their biological processes such as survival and lifespan. Also, host hemocytes, which are critical in the insect immune system and are involved in the defense against parasitoid invasion, may weaken the immune system by affecting its vitality and function with the effect of nanoplastics. Conversely, nanoplastic parasitoids may also have the ability to successfully parasitize the host. Nanoplastics released into the environment may carry potential risks for non-target organisms, including useful insects such as honey-bees. For instance, PS and three other different plastic microparticles were detected in bee species from fields in six different provinces of China (Deng et al., 2021). Insight into the specific effects on *G. mellonella* and *P. turionellae* helps to assess broader ecological consequences, informing guidelines for the use/management of nanoplastics in pest management and other applications. Hence, in the present study, nano-PSs were manufactured and administered to the larvae of *G. mellonella*, a model greater wax moth host, mixed with their diet. Subsequently, changes in the life cycle, weight, and length of *G. mellonella* and its endoparasitoid *P. turionellae* were analyzed. Differences in total and differential hemocyte counts in *G. mellonella* larval hemolymph were determined. In addition, multivariate correlation and principal component analysis were performed to determine the correlation between biological features. The same analyses were also performed for the types of hemocytes of *G. mellonella.*

2. Material and Method

2.1. Host and endoparasitoid

The greater wax moth *G. mellonella* was reared in the laboratory at 25 ± 2°C, 60 ± 2% relative humidity, and 24 h in the dark. Host larvae were fed a synthetic diet containing honeycomb, honey, glycerin, bran, and distilled water (Bronskill, 1961; Sak et al., 2006). The host endoparasite *P. turionellae* was cultured at 25 ± 5°C, 60 ± 5% relative humidity, and 12 h light/12 h dark. Endoparasitoid species were fed with sterile cotton wool soaked in honey solution (30%, V: V) diluted with distilled water and pupal hemolymph of *G. mellonella* (two pupae for five females) three times a week.

2.2. Preparation of polystyrene nanoparticles

Demirtürk et al. (2024) optimized the single emulsion solvent evaporation (w/o) method to prepare PS NPs. In brief; 20 mg of weighed PS pellets (Sigma Aldrich, MW: 35,000 g/L, density: 1.06 g/mL at 25°C) were dissolved in 2 mL of dichloromethane and 4 mL of 0.75% poly(vinyl alcohol) (PVA) (Sigma Aldrich, Mowiol® 4-88, MW: 31,000 g/L) was added to form an oil-in-water emulsion (o/w). The emulsion was sonicated (Bandelin Sonopuls HD 2070.2) for 4 min and 0.75% PVA was added. The organic solvent was removed by stirring for 3 h. The particles were

then centrifuged at 15,000 × g (Gyrozen 1580R, Seoul, Korea) and washed twice with distilled water. The properties of the NPs formed are given in the previous study (Demirtürk et al., 2024). Various doses of solutions (50, 100, 500, and 1000 ppm) of the obtained NPs were prepared. The solutions were prepared by adding the amount of water specified in the diet of the larvae. The larvae were fed with NP-containing food until they developed from early instars to final instars (~25 days).

2.3. Host and endoparasitoid biology

We recorded the time required to complete the larval, pupal, and adult stages of *G. mellonella*, as well as the adult weights and lengths. Pupae were parasitized by reproductively mature *P. turionellae* females. Afterwards, the emergence time, longevity, weight, and size data of *P. turionellae* adult parasitoids were regularly observed and recorded (Uçkan et al., 2011).

2.4. Hemolymph collection

The last instars of host larvae (0.21 ± 0.01 g) were randomly selected from the experimental groups to determine total and differential hemocyte counts. The larvae were anesthetized on ice for five minutes and sterilized with 70% ethanol. Under sterile conditions, the hind leg of the larvae was punctured and hemolymph samples were taken with a micropipette (Eppendorf, St. Louis, MO) (Altuntaş et al., 2012).

2.5. Total and Differential hemocyte counts

To detect the effects of NPs on circulating total hemocyte counts (THCs), the protocol recommended by Altuntaş et al. (2012) was applied. In short, 3 µL hemolymph was obtained and transferred to microcentrifuge tubes containing 27 µL anticoagulant solution. From the obtained cell suspension, 10 µL of hemolymph was removed and transferred to a Neubauer slide. Hemocytes were counted under 60 × magnification under phase-contrast microscopy (Nikon Eclipse Ti-U phase contrast microscopy). Results were expressed as THCs × 10^6 cells/mL hemolymph (Altuntaş et al., 2012).

The Giemsa staining protocol was used for differential hemocyte counts (DHCs) (Uçkan & Sak, 2010). In summary, 5 µl of hemolymph was spread on a sterile slide, dried, and fixed in methanol:acetic acid (3:1) for five min. The slides were stained in Giemsa stain solution (3 mL Giemsa, 57 mL PBS) for 10 min. The slides were then washed with distilled water and PBS and dried. DHCs in the prepared slides were examined under phase-contrast microscopy. For DHCs, 500 cells from a single larva were counted on each slide and the results are given as cells/500 prohemocytes, granulocytes, plasmatocytes, oenocytoids, and spherulocytes. Hemocyte types were defined by using the morphological characters described by Uçkan and Sak (2010).

2.6. Multivariate correlation and principal component analysis

Multivariate correlation analysis (MCA) was applied to detect the correlation between the nine biological features of *G. mellonella* and *P. turionellae* obtained. Principal component analysis (PCA) was used to analyze the proximity between different factors on five important biological features related to development. MCA and PCA were also applied to determine the correlation between the five types of hemocytes of *G. mellonella* and larval development.

2.7. Statistical Analysis

SPSS analysis software program (IBM SPSS Statistics, Version 27.0. IBM Corp.) was used for statistical analyses. Normal distribution analysis between groups was performed using Levene's test. For data sets that did not show normal distribution, the data were first normalized by taking the square root of the data. All data obtained from the experiments and the determined standard errors were expressed as mean and the results were shown as mean ± standard error. ANOVA (One-Way Analysis of Variance) was used when the means were homogeneous and Tukey's HSD (Tukey's Honestly Significant Difference) test was used to determine significant differences. The Kruskall Wallis test was used for nonparametric data. Dunn's post hoc test was used if the mean data were not homogenous. In all statistical analyses, the p-value was taken as 0.05 ($p < 0.05$). OriginLab OriginPro 2024 SR1 v.10.1.0.178 software was used in MCA and PCA analyses. In MCA analyses, the symbols ** and * indicate extreme significance at $p < 0.01$ and statistical significance at $p < 0.05$, respectively.

3. Results

3.1. Biological Features of host-endoparasitoid

All doses of PS NP reduced the larval development time of *G. mellonella* in a dose-dependent manner (degree of freedom 1 (df1), df2 = 4.70, F = 33.92, sig = 0.001, Table 1). Pupal development time showed the first effect at a 100 ppm PS NP dose and this time decreased with increasing dose (df1, df2 = 4.70, F = 74.82, sig = 0.001, Table 1). The most effective dose of PS NP that shortened adult longevity was 50 ppm; however, adult longevity was also shortened at other doses (df1, df2 = 4.70, F = 29.88, sig = 0.001, Table 1). The most statistically significant increase in *G. mellonella* adult weights was observed at the 500 ppm PS NP dose (df1, df2 = 4.70, F = 4.90, sig = 0.002, Table 1). Moreover, statistically significant increases in *G. mellonella* adult size were detected in the 500 and 1000 ppm groups (df1, df2 = 4.70, F = 20.34, sig = 0.001, Table 1).

Adult emergence time of *P. turionellae* at 50 and 100 ppm were similar to each other, while adults grown at doses of 500 and 1000 ppm were also similar to each other. In general, adult emergence time decreased at all doses (df1, df2 = 4.70, F = 35.74, sig = 0.001, Table 2). Interestingly, while the 1000 ppm dose had no change in adult parasitoid longevity compared to the control, the other NP doses decreased adult longevity. Specifically, the 50 ppm NP dose was the most effective group (df1, df2 = 4.70, F = 27.98, sig = 0.001, Table 2). In contrast, similar decreases in *P. turionellae* adult weights were detected in all PS NP groups but no significant differences in size were noticed (df1, df2 = 4.70, F = 5.59, sig = 0.001; df1, df2 = 4.70, F = 1.55, sig = 0.198, Table 2).

3.2. Multivariate correlation and principal component analysis for biological parameters

Pearson's r correlation coefficient was applied to inspect the relation between the detected data. The results in Figure 1 showed that there were significant positive

Table 1. Polystyrene nanoparticles (PS NPs)-associated changes in larval, pupal development, adult longevity (day), adult weight (mg), and size (mm) of *Galleria mellonella*

Groups	Larval Development (day)*	Pupal Development (day)*	Adult Longevity (day)*	Adult Weight (mg)*	Adult Size (mm)*
Control	28.0 ± 0.25 ^{a}	16.0 ± 0.22 ^{a}	16.0 ± 0.33 ^{a}	79.2 ± 0.29 ^{a}	12.6 ± 0.18 ^{a}
50 ppm	26.5 ± 0.23 ^{b}	15.1 ± 0.27 ^{a}	12.2 ± 0.22 ^{c}	79.6 ± 0.25 ^{a}	12.2 ± 0.11 ^{a}
100 ppm	25.7 ± 0.20 ^{b}	14.0 ± 0.21 ^{b}	13.1 ± 0.27 ^{bc}	80.1 ± 0.27 ^{ab}	12.5 ± 0.16 ^{a}
500 ppm	24.7 ± 0.30 ^{c}	12.0 ± 0.23 ^{c}	14.0 ± 0.22 ^{b}	80.0 ± 0.35 ^{b}	14.0 ± 0.18 ^{b}
1000 ppm	24.0 ± 0.25 ^{c}	11.1 ± 0.23 ^{c}	13.8 ± 0.20 ^{b}	80.3 ± 0.31 ^{ab}	13.4 ± 0.16 ^{b}

*All data for each group are represented as "Means ± Standard Errors". In each group, the mean of 15 individuals was given and 3 replicates were analyzed. The means in each experimental group followed by the same letter are not significantly dissimilar but different letters (a-c) are statistically significant (Tukey's HSD, $p < 0.05$).

Table 2. Polystyrene nanoparticles (PS NPs)-associated changes in adult emergence time, longevity (day), adult weight (mg), and size (mm) of *Pimpla turionellae*

Groups	Adult Emergence Time (day)*	Adult Longevity Time (day)*	Adult weight (mg)*	Adult size (mm)*
Control	21.6 ± 0.19 ^{a}	23.7 ± 0.11 ^{a}	17.7 ± 0.11 ^{a}	10.7 ± 0.11 ^{a}
50 ppm	20.6 ± 0.15 ^{b}	21.9 ± 0.18 ^{c}	17.4 ± 0.13 ^{ab}	10.5 ± 0.13 ^{a}
100 ppm	20.4 ± 0.13 ^{b}	22.3 ± 0.12 ^{cb}	16.9 ± 0.15 ^{b}	10.4 ± 0.13 ^{a}
500 ppm	19.3 ± 0.12 ^{c}	22.6 ± 0.12 ^{b}	17.0 ± 0.16 ^{b}	10.6 ± 0.13 ^{a}
1000 ppm	19.6 ± 0.12 ^{c}	23.2 ± 0.11 ^{a}	17.0 ± 0.16 ^{b}	10.3 ± 0.12 ^{a}

*All data for each group are represented as "Means ± Standard Errors". In each group, the mean of 15 individuals was given and 3 replicates were analyzed. The means in each experimental group followed by the same letter are not significantly dissimilar but different letters (a-c) are statistically significant (Tukey's HSD, $p < 0.05$).

correlations between Host Larval Development (HLD), Host Pupal Development (HPD), Host Adult Longevity (HAL), Host Adult Weight (HAW), Host Adult Size (HAS), Endoparasitoid Adult Emerge Time (EAET), Endoparasitoid Adult Longevity (EAL), Endoparasitoid Adult Weight (EAW), and Endoparasitoid Adult Size (EAS) at 0.05 and 0.01 levels. The color and size of the circles shown in Figure 1 indicate the correlation coefficient between the two parameters. HLD was positively correlated with HPD, EAET, EAW, and EAS 89.9%, 74.9%, 31.9%, and 31.5%, respectively, whereas it was negatively correlated with HAW and HAS 78.0% and 66.7%, respectively ($p < 0.01$). It was also found that HLD was not correlated with HAL and EAL. HPD was strongly positively correlated with EAET and EAW 75.5% and 40.7%, ($p < 0.01$), weakly positively correlated with EAS 26.6% ($p < 0.05$), and strongly negatively correlated with HAW and HAS 82.2% and 66.9% ($p < 0.01$), respectively. On the other hand, HPD was not correlated with HAL and EAL. HAL showed a strong positive correlation with HAS and EAL with 50.4% and 61.2% ($p < 0.01$), respectively, a weak positive correlation with EAW with 23.0% ($p < 0.05$), and no correlation with HAW and EAS. HAW exhibited a 73.4% strong positive correlation with HAS, whereas it exhibited a 67.8% and 49.5% strong negative correlation with EAET and EAW, respectively ($p < 0.01$). At the same time, EAL and EAS were not correlated with EAW. HAS was strongly negatively correlated ($p < 0.01$) with EAET (61.6%) and EAW (30.9%) but not with EAL and EAS. EAET was positively correlated with 44.3% EAW ($p < 0.01$) but not with EAL and EAS. EAL was positively correlated with EAW by 45.1% ($p < 0.01$) but not with EAS. On the other hand, no correlation was observed between EAW and EAS (Fig. 1).

Varimax rotated PCA revealed that the first two principal components (PC1 and PC2) greater than 1 explained 84.61% of the data variability (Kaiser-Meyer-Olkin test value = 0.66, Fig. 2A). PC1 accounted for 52.50% and PC2 accounted for 32.12% (Fig. 2B). HLD 95.02%, HPD 95.17%, and EAET 89.02% were positively correlated with PC 1, while HAL 89.60% and EAL 89.78% were positively correlated with PC 2 (Fig. 2B). Two factors can explain 90.4% of the variance of the HLD variable, 90.6% of the variance of the HPD variable, 80.4% of the variance of the HAL variable, 80.4% of the variance of the EAET variable, and 81.4% of the variance of the EAL variable. As shown in Figure 2B, three development-related variables (HLD, HPD, and EAET) loaded the highest on the first component and two variables (HAL and EAL) loaded the highest on the second component.

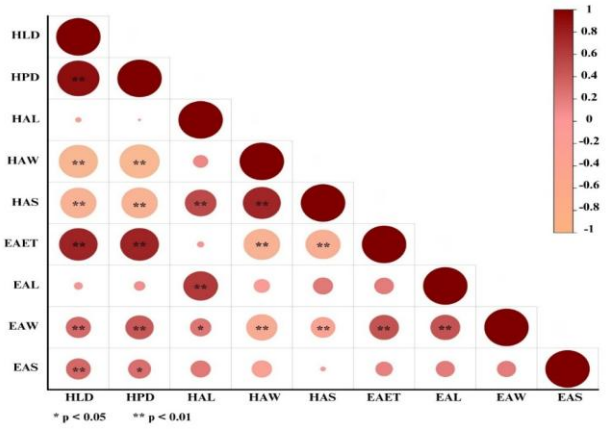

Figure 1. Correlation coefficient plot between nine biological parameters in host *Galleria mellonella* and endoparasitoid *Pimpla turionellae*. Host Larval Development (day) = HLD, Host Pupal Development (day) = HPD, Host Adult Longevitiy (day) = HAL, Host Adult Weight (mg) = HAW, Host Adult Size (mm) = HAS, Endoparasitoid Adult Emergence Time (day) = EAET, Endoparasitoid Adult Longevitiy (day) = EAL, Endoparasitoid Adult Weight (mg) = EAW, Endoparasitoid Adult Size (mm) = EAS

3.3. Total and Differential Hemocyte Counts

THCs in *G. mellonella* larvae statistically decreased at all PS NP doses (df1, df2 = 4.70, F = 127.5, sig = 0.001, Fig. 3). In the control group, THCs were determined as 40 ± 0.33 × 10^{6} cells/mL. At the lowest concentrations of 50 and 100

ppm NP, THCs reduced to 32.4 ± 0.64 and 29.6 ± 0.69 × 10^6 cells/mL, respectively. In the 500 and 1000 ppm NP groups, which constituted the highest concentrations, THCs declined by 26.6 ± 0.44 and 24.8 ± 0.42 × 10^6 cells/mL, respectively (Fig. 3).

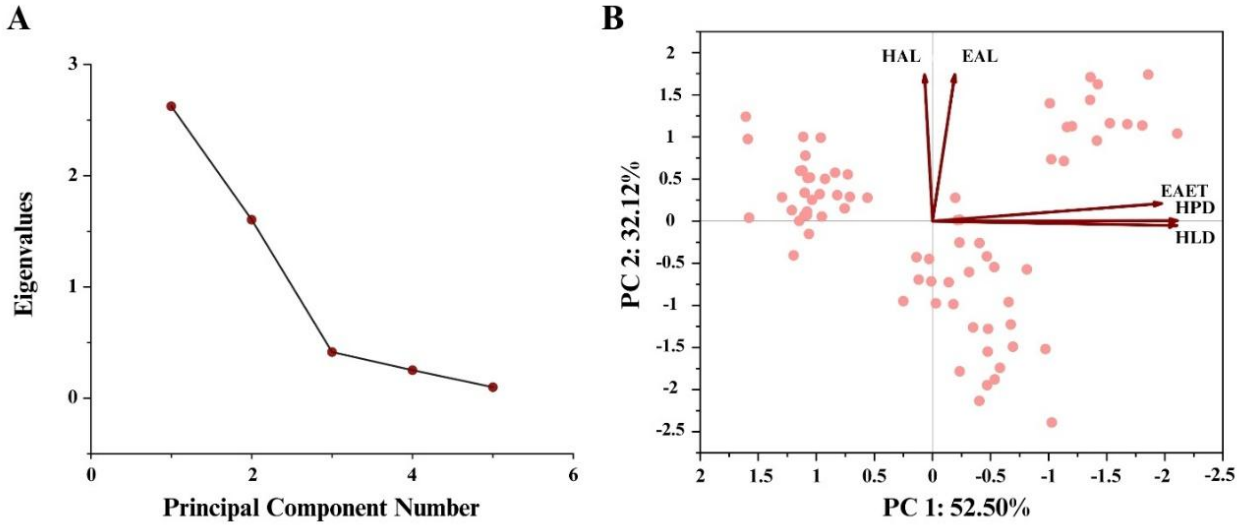

Figure 2. Principal Component Analysis (PCA) on all developmental variables measured in *Galleria mellonella* larvae exposed to Nano-PS, A) Scree plot of all variables, B) Proximity of developmental parameters to components. Host Larval Development (day) = HLD, Host Pupal Development (day) = HPD, Host Adult Longevity (day) = HAL, Endoparasitoid Adult Emerge Time (day) = EAET, Endoparasitoid Adult Longevity (day) = EAL

Changes in DHCs (cells/500) of *G. mellonella* larvae associated with PS NPs are given in Figure 4. Significant increases in granulocyte counts were observed in all groups of PS NP concentrations (df1, df2 = 4.70, F = 192.05, sig = 0.00 < 0.001). Granulocyte counts were 27.66 ± 191 cells/500 in the control group. The mean values of granulocyte count from low to high concentrations were 36.77 ± 1.00, 48.69 ± 0.99, 55.57 ± 1.03, and 58.45 ± 0.64 cells/500, respectively. On the contrary, plasmatocyte counts were significantly diminished at all concentrations compared to the control (df1, df2 = 4.70, F = 89.82, sig = 0.00 < 0.001). Significant changes were observed in each experimental group, while 55.88 ± 1.22 cells/500 in the control group. Plasmatocyte cells constituted 52.84 ± 0.98, 42.42 ± 1.06, 38.09 ± 0.91, and 33.81 ± 0.76 cells/500 of the total hemocyte population at all concentrations (50, 100, 500, and 1000 ppm) of *G. mellonella* larvae, respectively. Similarly, significant decreases in prohemocyte, oenocytoid, and spherulocyte counts were observed at all concentrations (df1, df2 = 4.70, F = 46.63, sig = 0.00 < 0.001; df1, df2 = 4.70, F = 53.05, sig = 0.00 < 0.001; df1, df2 = 4.70, F = 35.96, sig = 0.00 < 0.001, respectively).

3.4. Multivariate correlation and principal component analysis for hemocytes

Pearson's r correlation coefficient was applied to inspect the relation between the detected data. The data in Table 3 and Figure 4 showed highly significant positive correlations between prohemocytes, granulocytes, plasmatocytes, oenocytoids, and spherulocytes at the 0.01 level. The darker the color and the larger the size of the circles shown in Figure 4, the correspondingly bigger correlation coefficient and the greater correlation. A negative correlation was observed between granulocytes, other hemocytes, and larval development.

Table 3. Pearson's r correlation coefficient matrix among the detected differential hemocyte counts and larval development

Correlations	Prohemocytes	Granulocytes	Plasmatocytes	Oenocytoids	Spherulocytes	Larval Development
Prohemocytes	1					
Granulocytes	-0.790**	1				
Plasmatocytes	0.660**	-0.967**	1			
Oenocytoids	0.825**	-0.832**	0.700**	1		
Spherulocytes	0.816**	-0.781**	0.602**	0.853**	1	
Larval Development	0.796**	-0.882**	0.828**	0.795**	0.729**	1

**Correlation between differential hemocyte counts and larval development are significant at the 0.01 level.

PCA for differential hemocyte counts revealed that only one principal component (PC) explained 82.71% of the data variability (Kaiser-Meyer-Olkin test value = 0.49). Prohemocytes correlated with 90.0%, granulocytes with 96.1%, plasmatocytes with 86.4%, oenocytoids with 92.7%, and spherulocytes with 89.2%. A single factor (Component 1 = 'related to hemocyte types') can explain 81.0% of the variance of prohemocytes, 92.4% of the variance of granulocytes, 74.7% of the variance of plasmatocytes, 86.0% of the variance of oenocytoids, and 79.5% of the variance of spherulocytes. We therefore extracted a principal component comprising the five types of hemocytes identified in our analysis.

4. Discussion

Insects are an extremely valuable part of ecosystems and have a strong influence on the survival of the entire biosphere (Outhwaite et al., 2022). Hitherto, a remarkable

decline in insect species and populations globally has been documented owing to microplastic-induced toxicity (Shen et al., 2023) rather than insecticides (Shafiq ur, 2009). Microplastics may adversely affect insect survival, reproduction, development, and gut microbiota (Shen et al., 2023). Besides, nanoplastic-induced toxicity findings, which have a smaller structure, constitute a very new research area. As a result of the idea that nano-sized plastics can be taken into the body and penetrate tissues and cells more easily, we planned our study on the model *G. mellonella*. Our research was carried out based on the hypothesis that the counts of hemocytes involved in the development, longevity, growth, and immune system in insects may change/impair their function. *P. turionellae*, the endoparasitoid of *G. mellonella*, which is harmful to honeycombs and creates a major challenge in beekeeping by affecting honeybee colonies, is responsible for maintaining the ecological balance. Thus, here we first manufactured nano PSs, then determined the biological effects of PS NPs with an approximate size of 275 nm on these host-parasitoid species and on host hemocytes.

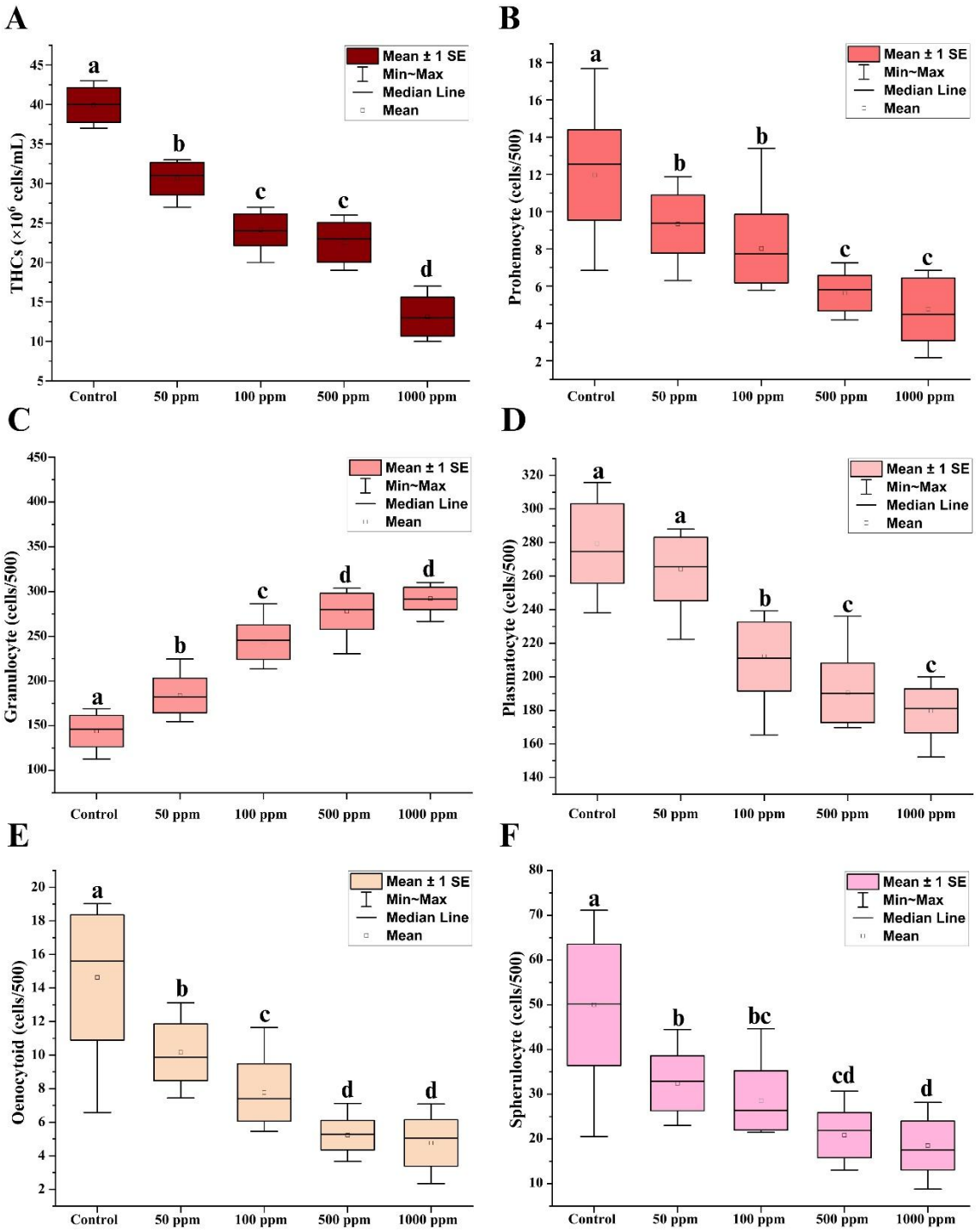

Figure 3. Influence of Polystyrene nanoparticles (PS NPs) on, A) total hemocyte counts (×10⁶ cells/mL), B) prohemocyte, C) granulocyte, D) plasmatocyte, E) oenocytoid, and F) spherulocyte counts (cells/500) in the hemolymph *Galleria mellonella* larvae. Dissimilar letters (a-d) in the control and experimental groups represent statistically significant differences (Tukey's HSD $p < 0.001$ for THCs, prohemocytes, granulocytes, plasmatocytes, and spherulocytes; Kruskall Wallis for oenocytoids). Data are indicated as "Means ± Standard Errors" of three replicates using five larvae in one replicate

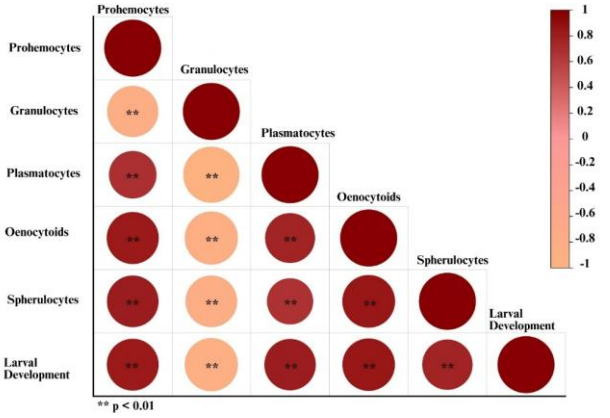

Figure 4. Correlation coefficient plot between differential hemocyte counts and larval development in *Galleria mellonella*

Terrestrial organisms such as *B. mori* (Muhammad et al., 2021; Parenti et al., 2020; Wang et al., 2023), *D. melanogaster* (Aloisi et al., 2024; El Kholy & Al Naggar, 2023; Tu et al., 2023), and *A. williamsoni* (Guimarães et al., 2021) may intake micro and nano PSs from the environment and accumulate them in the body cavity, intestine, intestinal lumen, midgut epithelium, Malpighian tubules, adipose tissue, and larval tissues such as ovary, head, digestive system, and hemolymph. Accordingly, it is concluded that plastic pollutants may easily enter and retain organisms and may be transported through the intestinal barrier to larval tissues. The data obtained in the literature on insect development are highly variable. Parenti et al. (2020) fed *Bombyx mori* larvae an artificial diet containing non-fluorescent 716 nm and fluorescent 533 nm PS NP (0.25 mg/0.5 g diet) and concluded that it did not cause changes in larval mortality, cycle time, adult emergence, and body weight. Under the researchers' experimental conditions, PS NPs were shown not to alter individual and population fitness of *B. mori* (Parenti et al., 2020). Likewise, PS NPs (50–100 nm, 2.22 × 10^{10}/mL, acute exposure) administered to *B. mori* had no significant effect on larval body mass or survival (Muhammad et al., 2021). Further, in *B. mori*, environmental concentrations of PS MNPs (0.25 to 1.0 µg/mL, 91.92 nm, 5.69 µm, 9.7 µm) increased body weight without affecting survival but did not cause significant changes in the development time and life span (Muhammad et al., 2024). In the present study, *G. mellonella* adult weights and adult sizes increased at high doses, while *P. turionellae* adult weights decreased similarly in all groups but no significant change in size was detected. The existence and accumulation of PS NPs in adipose tissue are probably due to the lipophilic properties of PS NPs. Accumulation of NPs in adipose tissue may enhance the weight and size of the organism as seen in *B. mori* (Muhammad et al., 2024) and *G. mellonella*. These findings suggest that chronic exposure to micro and nano PSs may affect host energy homeostasis and induce weight gain in organisms. In addition, PS NP treatment diminished the larval and pupal development time of *G. mellonella* and adult emergence time of *P. turionellae* in a dose-dependent manner. The concentration at which adult longevity reduced the most was the lowest concentration (50 ppm) in both *G. mellonella* and *P. turionellae*. The impacts of PS NP treatment on *G. mellonella* and *P. turionellae* exhibit interesting differences when compared to the impacts on *B. mori* in the literature. While Parenti et al. (2020) and Muhammad et al. (2021) did not reveal any significant effect of PS NPs in these species, our findings revealed meaningful reductions in developmental times. These results suggest that the effects of PS NPs may vary between species and that even low concentrations may be harmful. The idea that plastic pollution has a negligible but potential effect on the development of some insect species becomes relevant. At the same time, this evidence suggests that PS NPs have a unique effect on insect physiology, potentially by accelerating metabolic processes or through toxicological stress promoting faster development as a survival response.

Recent developmental studies in terrestrial organisms have indicated that, in parallel with the present findings, developmental time is more likely to be reduced in insects. For instance, adverse effects such as growth retardation and body weight loss have been described in *B. mori* fed with feed containing fluorescent PS NP (Wang et al., 2023). In *D. melanogaster* fed with food treated with PS-MPs (2 µm) at different concentrations (0.005, 0.05, 0.5 µg/mL), life span was shorter in males than females (Kholy & Naggar, 2022). The same researchers found that 7 days of acute treatment of adult D. melanogaster with almost all concentrations of PS MP significantly diminished survival of both male and female flies (El Kholy & Al Naggar, 2023). Micro (1.0-1.9 µm, 0.4-0.6 µm) and nano (0.04-0.06 µm) sized PS particles have been studied to reduce survival and alter the structure of the midgut, ovary, and testis in *D. melanogaster* (Urbisz et al., 2024). This impact was found to be sex-dependent, with male flies being more susceptible (Urbisz et al., 2024). In *D. melanogaster* fed with fluorescent PS NPs (100 µm) for prolonged periods, a reduction in larval-pupal development time and a reduction in the weight of male and female adults were determined (Aloisi et al., 2024). Also in another study, it was shown that the number of egg production and hatching rate of *D. melanogaster* were significantly reduced with delayed development after 5 days of exposure to PS NPs (100 nm; 1, 10, 50, and 100 mg/L) (Tu et al., 2023). Moreover, Martin-Folgar et al. (2024) have stated that PS NPs (30 nm, 24 h acute exposure) impeded the expression of genes involved in the endocrine system and development in *C. riparius* (Diptera) larvae. An almost 90% survival rate was found in larvae (Martin-Folgar et al., 2024). Results showed important declines in larval and pupal development of *G. mellonella* and *P. turionellae* in a dose-dependent manner. The adverse effects seen in Wang et al. (2023), El Kholy and Al Naggar (2023), and Kholy and Naggar (2022) studies further highlight the toxic effects of PS NPs in different organisms, while the sex-linked sensitivity described by Urbisz et al. (2024) also highlights the potential effects of PS NP exposure on ecosystem dynamics. Additionally, the effects of experimental conditions such as NP size and exposure times on the results are crucial to understanding the reasons for different findings. Thereby, examining the long-term effects of PS NPs on population fitness will also help to develop a more comprehensive understanding of this issue.

In insects, it is also very critical to obtain data on the immune system related to the effects of PS NPs and MPs such as accumulation in tissues, development, weight, growth, life span, and survival. For instance, it was emphasized that exposure to PS NPs in *B. mori* suppressed the immune response and rendered the host defenseless

(Muhammad et al., 2021). PS NPs have been demonstrated to diminish the activity of superoxide dismutase (Muhammad et al., 2021; Parenti et al., 2020) and glutathione transferase (Muhammad et al., 2021) which are crucial in antioxidant defense in the same organism. In general, it was concluded that PS NPs and MPs trigger cellular and oxidative stress and cause REDOX imbalance in *D. melanogaster*, *A. williamsoni*, *C. riparius* (Guimarães et al., 2021; Martin-Folgar et al., 2024; Urbisz et al., 2024). Besides, concentration-dependent impacts of PS on the cellular structure of midgut cells in *D. melanogaster*, indicative of cell necrosis and apoptosis, have been demonstrated (El Kholy & Al Naggar, 2023; Kholy & Naggar, 2022). In the study, we determined the responses of *G. mellonella* hemocytes, which are effective in cellular immune defense in insects, against PS NPs. Granulocytes increased dose-dependently, whereas other types of hemocytes and THCs decreased. Our data are similar in conjunction with our previous findings of cellular encapsulation responses (Demirtürk et al., 2024). Since encapsulation reactions against PS NPs entering the host as a foreign substance are realized with the help of host granulocytes. Granulocytes attach to the surface of PS NPs, disintegrate, and deposit their granules on the NPs in a thick layer. Plasmatocytes also mediate this defense mechanism. Even in this process, REDOX interactions may become dysregulated, and oxidative stress, apoptosis, and necrosis may occur. The decreases in THCs and DHCs also suggest that these NPs may weaken the insect's immune defenses, making them more susceptible to pathogens and parasites. This may have wider implications for insect health and survival in environments contaminated with nanoplastics. On the other hand, the changing developmental duration and immune responses of the host *G. mellonella* as well as the changing adult lifespan and weight of *P. turionellae* suggest a complex interaction in which the parasitoid may be indirectly affected by host exposure to PS NPs. Such a relation is critical for understanding the ecosystem dynamics and potential cascading effects in food webs.

Micro- and nanoplastics are an emerging threat to biodiversity and ecological conservation but little is known about their possible effects on pollinator species (Deng et al., 2021; Hu et al., 2019). Four types of MP, including polystyrene (PS), were identified in 66.7% of honey-bee samples (*Apis mellifera* and *Apis cerana*) collected from fields in six provinces in China. In a study conducted to measure how the application of PS MPs (0.5, 5, and 50 µm) for 21 days affected the proliferation of Israeli acute paralysis virus, it was revealed that PS was ingested, accumulated in the midgut, and increased the susceptibility of bees to viral infection. It has also been documented that PS, mainly the smallest sizes, damages the midgut tissue, which is then transferred to the hemolymph, Malpighian tubules, and trachea (Deng et al., 2021). Considering the ecological and economic significance of honey-bees, it is extremely important to expand similar studies on *Apis mellifera* to directly assess how PS NPs affect their development, immune responses, and overall health. However, bees and bee products as biological indicators of environmental pollution have been indicated as an economic alternative method for monitoring pollutants (Voget, 1989). Within this scope, bees and bee products may be considered to be effective in monitoring plastic pollution. Understanding the similarities and differences between the responses of *G. mellonella* and honey-bees to nanoplastics may help to predict the findings and develop specific guidelines for beekeeping. Further, how PS NPs affect pollination efficiency and hive health, bee behavior, foraging patterns, and the nutritional quality of pollen and nectar are also of interest.

With the results, it was determined that PS NPs caused shortening in the life cycle of *G. mellonella* and *P. turionellae*, and significant declines in the total and differential hemocyte counts of the host species. Data highlighted the possibility of transfer of nano PSs along the food chain in terrestrial ecosystems. Simultaneously, it demonstrates the potential of using the wax moth as a model of fully metamorphosed insects to investigate the biological impact of PS NPs on conspecific terrestrial animals and indirectly on the endoparasitoid *P. turionellae* to which NP toxicity can be transferred. The positive correlation of host larval and pupal development with endoparasitoid emergence time provides new information about the developmental toxicity of PS NPs due to host-parasitoid interaction. In addition, the data obtained will be useful for the assessment of environmental risks associated with PS NPs or potential adverse impacts on people and emphasizes the neglected nanoplastic toxicity in honey-bees affected by anthropogenic pollution and the potential hazards to human health from ingestion of bee products. The insights gained from studies of *G. mellonella* and *P. turionellae* may be translated into practical applications in beekeeping, providing knowledge about the health and sustainability of bee populations and their critical role in pollination and agriculture. Consequently, the study contributes to being able to fill the knowledge gaps on insect development at different doses of PS NPs.

Ackowledgement: This study is the MSc thesis of Tuğba Nur ELLİBEŞ GÖKKAYA. We are grateful to Ezgi ÇOĞAL for her experimental help. Hemocytes data were presented as a poster at the 7th International Marmara Science Congress-IMASCON in 2021. This study was supported by the Kocaeli University Scientific Research Projects Coordination Department under Grant Number: FYL-2021-2345.

Ethics committee approval: Ethics committee approval is not required for this study.

Conflict of interest: The authors declare that there is no conflict of interest.

Author Contributions: Conception – T.N.E.G., Z.D., F.U., S.M.; Design – T.N.E.G., Z.D., F.U., S.M.; Supervision – T.N.E.G., Z.D., F.U., S.M.; Fund – Kocaeli University; Materials – T.N.E.G., Z.D., F.U., S.M.; Data Collection and Processing – T.N.E.G., Z.D., F.U., S.M.; Analysis Interpretation – T.N.E.G., Z.D., F.U., S.M.; Literature Review – T.N.E.G., Z.D., F.U., S.M.; Writing – T.N.E.G., Z.D., F.U., S.M.; Critical Review – T.N.E.G., Z.D., F.U., S.M.

References

Aloisi, M., Grifoni, D., Zarivi, O., Colafarina, S., Morciano, P., & Poma, A.M.G. (2024). Plastic Fly: What *Drosophila melanogaster* Can Tell Us about the Biological Effects and the Carcinogenic Potential of Nanopolystyrene. *International Journal of Molecular Sciences*, 25(14), 7965. https://doi.org/10.3390/ijms25147965

Altuntaş, H., Kılıç, A.Y., Uçkan, F., & Ergin, E. (2012). Effects of Gibberellic Acid on Hemocytes of *Galleria mellonella* L. (Lepidoptera: Pyralidae). *Environmental Entomology*, 41(3), 688-696. https://doi.org/10.1603/en11307

Awet, T.T., Kohl, Y., Meier, F., Straskraba, S., Grün, A.L., Ruf, T., … & Emmerling, C. (2018). Effects of polystyrene nanoparticles on the microbiota and functional diversity of enzymes in soil. *Environmental Sciences Europe*, 30(1), 11. https://doi.org/10.1186/s12302-018-0140-6

Bronskill, J. (1961). A cage to simplify the rearing of the greater wax moth, *Galleria mellonella* (Pyralidae). *Journal of the Lepidopterists' Society*, 15(2), 102-104.

Calderone, N.W. (2012). Insect Pollinated Crops, Insect Pollinators and US Agriculture: Trend Analysis of Aggregate Data for the Period 1992–2009. *PLOS ONE*, 7(5), e37235. https://doi.org/10.1371/journal.pone.0037235

Demirtürk, Z., Uçkan, F., & Mert, S. (2024). Interactions of alumina and polystyrene nanoparticles with the innate immune system of *Galleria mellonella*. *Drug and Chemical Toxicology*, 47(5), 483-495. https://doi.org/10.1080/01480545.2023.2217484

Deng, Y., Jiang, X., Zhao, H., Yang, S., Gao, J., Wu, Y., … & Hou, C. (2021). Microplastic Polystyrene Ingestion Promotes the Susceptibility of Honeybee to Viral Infection. *Environmental Science & Technology*, 55(17), 11680-11692. https://doi.org/10.1021/acs.est.1c01619

Dolar, A., Drobne, D., Dolenec, M., Marinšek, M., & Jemec Kokalj, A. (2022). Time-dependent immune response in *Porcellio scaber* following exposure to microplastics and natural particles. *Science of the Total Environment*, 818, 151816. https://doi.org/10.1016/j.scitotenv.2021.151816

Dolar, A., Selonen, S., van Gestel, C.A.M., Perc, V., Drobne, D., & Jemec Kokalj, A. (2021). Microplastics, chlorpyrifos and their mixtures modulate immune processes in the terrestrial crustacean *Porcellio scaber*. *Science of The Total Environment*, 772, 144900. https://doi.org/10.1016/j.scitotenv.2020.144900

El Kholy, S., & Al Naggar, Y. (2023). Exposure to polystyrene microplastic beads causes sex-specific toxic effects in the model insect *Drosophila melanogaster*. *Scientific Reports*, 13(1), 204. https://doi.org/10.1038/s41598-022-27284-7

Gounari, S., Goras, G., & Thrasyvoulou, A. (2024). *Dibrachys cavus*, a promising parasitoid in the biological control of the greater wax moth (*Galleria mellonella*). *Journal of Apicultural Research*, 63(2), 323-328. https://doi.org/10.1080/00218839.2021.2008707

Guimarães, A.T.B., de Lima Rodrigues, A.S., Pereira, P.S., Silva, F.G., & Malafaia, G. (2021). Toxicity of polystyrene nanoplastics in dragonfly larvae: An insight on how these pollutants can affect bentonic macroinvertebrates. *Science of The Total Environment*, 752, 141936. https://doi.org/10.1016/j.scitotenv.2020.141936

Hu, D., Shen, M., Zhang, Y., Li, H., & Zeng, G. (2019). Microplastics and nanoplastics: would they affect global biodiversity change? *Environmental Science and Pollution Research*, 26(19), 19997-20002. https://doi.org/10.1007/s11356-019-05414-5

Hu, M., & Palić, D. (2020). Micro- and nano-plastics activation of oxidative and inflammatory adverse outcome pathways. *Redox Biology*, 37, 101620. https://doi.org/10.1016/j.redox.2020.101620

Kalman, J., Muñiz-González, A.B., García, M.Á., & Martínez-Guitarte, J.L. (2023). *Chironomus riparius* molecular response to polystyrene primary microplastics. *Science of the Total Environment*, 868, 161540. https://doi.org/10.1016/j.scitotenv.2023.161540

Kholy, S.E., & Naggar, Y.A. (2022). Polystyrene Microplastic Beads Caused Cellular Alterations in midgut cells and Sex-Specific Toxic Effects on Survival, Starvation Resistance, and Excretion of the Model Insect *Drosophila melanogaster*. *Research Square*. https://doi.org/10.21203/rs.3.rs-1977878/v1

Kim, S.W., & An, Y.J. (2019). Soil microplastics inhibit the movement of springtail species. *Environment International*, 126, 699-706. https://doi.org/10.1016/j.envint.2019.02.067

Kögel, T., Bjorøy, Ø., Toto, B., Bienfait, A.M., & Sanden, M. (2020). Micro- and nanoplastic toxicity on aquatic life: Determining factors. *Science of The Total Environment*, 709, 136050. https://doi.org/10.1016/j.scitotenv.2019.136050

Long, M., Paul-Pont, I., Hégaret, H., Moriceau, B., Lambert, C., … & Soudant, P. (2017). Interactions between polystyrene microplastics and marine phytoplankton lead to species-specific hetero-aggregation. *Environmental Pollution*, 228, 454-463. https://doi.org/10.1016/j.envpol.2017.05.047

Martin-Folgar, R., Sabroso, C., Cañas-Portilla, A.I., Torres-Ruíz, M., González-Caballero, M.C., Dorado, H., … & Morales, M. (2024). DNA damage and molecular level effects induced by polystyrene (PS) nanoplastics (NPs) after *Chironomus riparius* (Diptera) larvae. *Chemosphere*, 346, 140552. https://doi.org/10.1016/j.chemosphere.2023.140552

Muhammad, A., Zhang, N., He, J., Shen, X., Zhu, X., Xiao, J., … & Shao, Y. (2024). Multiomics analysis reveals the molecular basis for increased body weight in silkworms (*Bombyx mori*) exposed to environmental concentrations of polystyrene micro- and nanoplastics. *Journal of Advanced Research*, 57, 43-57. https://doi.org/10.1016/j.jare.2023.09.010

Muhammad, A., Zhou, X., He, J., Zhang, N., Shen, X., Sun, C., … & Shao, Y. (2021). Toxic effects of acute exposure to polystyrene microplastics and nanoplastics on the model insect, silkworm *Bombyx mori*. *Environmental Pollution*, 285, 117255. https://doi.org/10.1016/j.envpol.2021.117255

Murphy, F., Ewins, C., Carbonnier, F., & Quinn, B. (2016). Wastewater Treatment Works (WwTW) as a Source of Microplastics in the Aquatic Environment. *Environmental Science & Technology*, 50(11), 5800-5808. https://doi.org/10.1021/acs.est.5b05416

Oliveira, M., Almeida, M., & Miguel, I. (2019). A micro(nano)plastic boomerang tale: A never ending story? *TrAC Trends in Analytical Chemistry*, 112, 196-200. https://doi.org/10.1016/j.trac.2019.01.005

Outhwaite, C.L., McCann, P., & Newbold, T. (2022). Agriculture and climate change are reshaping insect biodiversity worldwide. *Nature*, 605(7908), 97-102. https://doi.org/10.1038/s41586-022-04644-x

Parenti, C.C., Binelli, A., Caccia, S., Della Torre, C., Magni, S., Pirovano, G., & Casartelli, M. (2020). Ingestion and effects of polystyrene nanoparticles in the silkworm *Bombyx mori*. *Chemosphere*, 257, 127203. https://doi.org/10.1016/j.chemosphere.2020.127203

Peng, B.Y., Xu, Y., Zhou, X., Wu, W.M., & Zhang, Y. (2024). Generation and Fate of Nanoplastics in the Intestine of Plastic-Degrading Insect (*Tenebrio molitor* Larvae) during Polystyrene Microplastic Biodegradation. *Environmental Science & Technology*, 58(23), 10368-10377. https://doi.org/10.1021/acs.est.4c01130

Rothen-Rutishauser, B., Bogdanovich, M., Harter, R., Milosevic, A., & Petri-Fink, A. (2021). Use of nanoparticles in food industry: current legislation, health risk discussions and public perception with a focus on Switzerland. *Toxicological & Environmental Chemistry*, 103(4), 423-437. https://doi.org/10.1080/02772248.2021.1957471

Sak, O., Uçkan, F., & Ergin, E. (2006). Effects of cypermethrin on total body weight, glycogen, protein, and lipid contents of *Pimpla turionellae* (L.) (Hymenoptera: Ichneumonidae). *Belgian Journal of Zoology*, 136(2006), 53-58.

Shafiq ur, R. (2009). Evaluation of malonaldialdehyde as an index of chlorpyriphos insecticide exposure in *Apis mellifora*: Ameliorating role of melatonin and α-tocopherol against oxidative stress. *Toxicological & Environmental Chemistry*, 91(6), 1135-1148. https://doi.org/10.1080/02772240802542617

Shen, J., Liang, B., & Jin, H. (2023). The impact of microplastics on insect physiology and the indication of hormesis. *TrAC Trends in Analytical Chemistry*, 165, 117130. https://doi.org/10.1016/j.trac.2023.117130

Toussaint, B., Raffael, B., Angers-Loustau, A., Gilliland, D., Kestens, V., Petrillo, M., … & Van den Eede, G. (2019). Review of micro- and nanoplastic contamination in the food chain. *Food Additives & Contaminants*, Part A, 36(5), 639-673. https://doi.org/10.1080/19440049.2019.1583381

Tu, Q., Deng, J., Di, M., Lin, X., Chen, Z., Li, B., … & Zhang, Y. (2023). Reproductive toxicity of polystyrene nanoplastics in *Drosophila melanogaster* under multi-generational exposure. *Chemosphere*, 330, 138724. https://doi.org/10.1016/j.chemosphere.2023.138724

Uçkan, F., Öztürk, Z., Altuntaş, H., & Ergin, E. (2011). Effects of Gibberellic Acid (GA3) on Biological Parameters and Hemolymph Metabolites of the Pupal Endoparasitoid *Pimpla turionellae* (Hymenoptera: Ichneumonidae) and its Host *Galleria mellonella* (Lepidoptera: Pyralidae). *Journal of the Entomological Research Society*, 13(3), 1-14.

Uçkan, F., & Sak, O. (2010). Cytotoxic effect of cypermethrin on *Pimpla turionellae* (Hymenoptera: Ichneumonidae) larval hemocytes. https://doi.org/10.5053/ekoloji.2010.753

Urbisz, A.Z., Małota, K., Chajec, Ł., & Sawadro, M.K. (2024). Size-dependent and sex-specific negative effects of micro- and nano-sized polystyrene particles in the terrestrial invertebrate model *Drosophila melanogaster*. *Micron*, 176, 103560. https://doi.org/10.1016/j.micron.2023.103560

Voget, M. (1989). Bees and beeproducts as biological indicators of environmental contamination: An economical alternative way of monitoring pollutants. *Toxicological & Environmental Chemistry*, 20-21(1), 199-202. https://doi.org/10.1080/02772248909357376

Wang, J., Coffin, S., Sun, C., Schlenk, D., & Gan, J. (2019). Negligible effects of microplastics on animal fitness and HOC bioaccumulation in earthworm *Eisenia fetida* in soil. *Environmental Pollution*, 249, 776-784. https://doi.org/10.1016/j.envpol.2019.03.102

Wang, K., Li, J., Zhao, L., Mu, X., Wang, C., Wang, M., … & Wu, L. (2021). Gut microbiota protects honey bees (*Apis mellifera* L.) against

polystyrene microplastics exposure risks. *Journal of Hazardous Materials*, 402, 123828. https://doi.org/10.1016/j.jhazmat.2020.123828

Wang, W., Ge, J., Yu, X., & Li, H. (2020). Environmental fate and impacts of microplastics in soil ecosystems: Progress and perspective. *Science of The Total Environment*, 708, 134841. https://doi.org/10.1016/j.scitotenv.2019.134841

Wang, Z.J., Zhang, Y.H., Gao, R.Y., Jia, H.B., Liu, X.J., Hu, Y.W., … & Zhang, J.P. (2023). Polystyrene Nanoparticle Uptake and Deposition in Silkworm and Influence on Growth. *Sustainability*, 15(9), 7090. https://doi.org/10.3390/su15097090

Zhang, J., Ma, C., Xia, X., Li, Y., Lin, X., Zhang, Y., & Yang, Z. (2023). Differentially Charged Nanoplastics Induce Distinct Effects on the Growth and Gut of Benthic Insects (*Chironomus kiinensis*) via Charge-Specific Accumulation and Perturbation of the Gut Microbiota. *Environmental Science & Technology*, 57(30), 11218-11230. https://doi.org/10.1021/acs.est.3c02144

Commagene Journal of Biology

Kurt & Yıldırım Doğan, (2025) *Comm. J. Biol.* 9(1), 59-63.
DOI: 10.31594/commagene.1648391

e-ISSN 2602-456X

Research Article/Araştırma Makalesi

First Molecular Data for the Genus *Kovalius* (Opiliones: Sclerosomatidae: Leiobuninae) and their Phylogenetic Relationships

Pınar KURT[1]*, Nalan YILDIRIM DOĞAN[2]

[1]*Gümüşhane University, Vocational School of Health Services, Department of Medical Services and Techniques, Gümüşhane, TÜRKİYE.*
[2]*Erzincan Binali YILDIRIM University, Science and Art Faculty, Department of Biology, Erzincan, TÜRKİYE*
ORCID ID: Pınar KURT: https://orcid.org/0000-0002-0202-9320; Nalan YILDIRIM DOĞAN : https://orcid.org/0000-0002-5344-5367

Received: 27.02.2025 **Accepted:** 14.04.2025 **Published online:** 26.05.2025 **Issue published:** 30.06.2025

Abstract: *Kovalius* (Opiliones: Sclerosomatidae: Leiobuninae) is a small genus of harvestmen described by Tchemeris, 2023. The first description of *Kovalius logunovi* was made from Russia and it was subsequently recorded from Türkiye on the basis of the morphological data. The use of morphological data alone for the identification of taxa and determination of their relationships may lead to limitations and difficulties in some cases. As a result, the use of molecular data in addition to the morphological data in the identification of new taxa and determination of phylogenetic relationships increases the reliability of studies. In this study, the mitochondrial 16S rRNA gene region of the *Kovalius logunovi* species was examined for the first time and a sequence of approximately 408 bp was obtained. Based on these data, the phylogenetic relationships of the species with similar species were revealed.

Keywords: 16S rRNA, *Kovalius logunovi*, phylogenetic tree, Türkiye.

Kovalius (Opiliones: Sclerosomatidae: Leiobuninae) Cinsinin İlk Moleküler Verileri ve Filogenetik İlişkileri

Öz: *Kovalius* (Opiliones: Sclerosomatidae: Leiobuninae) Tchemeris tarafından 2023 yılında tanımlanan küçük bir otbiçen cinsidir. *Kovalius logunovi*'nin ilk tanımı Rusya'dan yapılmış ve daha sonra morfolojik verilere dayanarak Türkiye'den kaydedilmiştir. Taksonların tanımlanması ve ilişkilerinin belirlenmesi için sadece morfolojik verilerin kullanılması bazı durumlarda sınırlamalara ve zorluklara yol açabilir. Sonuç olarak, yeni taksonların tanımlanmasında ve filogenetik ilişkilerin belirlenmesinde morfolojik verilere ek olarak moleküler verilerin de kullanılması çalışmaların güvenilirliğini artırmaktadır. Bu çalışmada *Kovalius logunovi* türünün mitokondriyal 16S rRNA gen bölgesi ilk kez çalışılmış ve yaklaşık 408 bp'lik bir dizi elde edilmiştir. Bu verilere dayanarak türün benzer türlerle olan filogenetik ilişkileri ortaya konmuştur.

Anahtar kelimeler: 16S rRNA, *Kovalius logunovi*, filogenetik ağaç, Türkiye.

1. Introduction

The genus *Kovalius* Tchemeris, 2023 is monotypic genus of the family Sclerosomatidae Simon, 1879 subfamily Leiobuninae Banks, 1893 that is distributed in Russia and Türkiye (Tchemeris, 2023; Kurt, 2024). It has been recognized that only one species (*Kovalius logunovi* Tchemeris, 2023) of the genus *Kovalius* is extant.

The genus *Kovalius* was described for the first time from the Sokolova cave in the NW Caucasus, Russia. In 2024, the genus was recorded from Türkiye for the first time. Furthermore, the genitalia of female individuals were also described for the first time. Both studies were on the basis of morphological data and no data was available on the molecular characteristics of the genus (Tchemeris, 2023; Kurt, 2024).

Mitochondrial DNA has become the most widely used molecular marker in animal systematics in recent years, playing an important role in the revolution in molecular systematics. Fragments of mtDNA markers, so-called DNA barcodes, have been developed to facilitate species identification and accelerate DNA-based taxonomy. For mitochondrial (mt) DNA analysis, conserved genes such as 16S rRNA, Cyt b or cytochrome oxidase subunit I (COI) are usually used. The 16S rRNA gene is approximately 1500 base pairs (bp) in length, although this can vary between 500 bp, 800 bp, and 1500 bp depending on the primer combinations utilized. It is frequently utilized as a DNA barcode region in various taxonomic groups, including gastropods, hydrozoans, amphibians, and Pholcid spiders (Wang et al., 2018; Chan et al., 2022).

In this study, the molecular characteristics of the genus *Kovalius* are presented for the first time. It also reveals the phylogenetic relationships of the species with other members of similar species based on 16S rRNA gene regions.

2. Material and Method

2.1. Material examined and morphological analyses

In this study, harvestmen samples were collected by hand and forceps from the Kürtün district of Gümüşhane province, Turkey in 2020 and stored in 70% ethyl alcohol. Samples were identified by Dr. Kemal KURT (Gümüşhane University, Türkiye) based on morphological data. A detailed description of the species is given in Tchemeris (2023) and Kurt (2024).

Corresponding author: pinarkurt29@gmail.com

2.2. Molecular analysis

Samples were washed with distilled water, dried and the body and legs were crushed. DNA was extracted according to the manufacturer's instructions using the GeneAll Exgene Tissue Kit (Korea). The 16S rRNA gene was amplified using the primers 16Sa 5′-CGCCTGTTTATCAAAAACAT-3′ (Xiong & Kocher, 1991); 16Sb 5′-CTCCGGTTTGAACTCAGATCA-3′ (Edgecombe et al., 2000).

The polymerase chain reaction was conducted in a complete volume of 20 µl, comprising: 3 µl of DNA template, 8 µl of master mix (2x) (master mix: 10X buffer, 2.5 mM dNTP, 25 mM $MgCl_2$, Taq polymerase), 1 µl of all primer and 7 µl of sterile destilled water.

The amplification conditions comprised an initial denaturation step for a duration of 5 minutes at a temperature of 95°C. This was followed by 40 cycles of denaturation for 30 seconds at 95°C, annealing for 30 seconds at a temperature of 49-50°C, elongation for 30 seconds at 72°C and a final extension step at 72°C for a duration of 5 minutes. These amplification conditions were implemented as outlined in the GeneAll protocol (Seoul, Korea). The PCR products obtained were evaluated by gel electrophoresis in 1% agarose and DNA was extracted in pure form using a gel extraction kit (GeneAll Gel SV).

2.3. Phylogenetic analysis

Nucleotide sequences were edited using the software CodonCode Aligner ver.5.0.2 (CodonCode Corporation, Dedham, MA). The data were queried through the GenBank database using the Basic Local Alignment Search Tool (BLAST) algorithm (Altschul et al., 1990). GenBank accession numbers for sequences used in the present study are provided in Table 1. Phylogenetic analyses were performed using neighbor-joining (NJ) and Bayesian inference (BI) methods (Figs. 1-2). To construct a neighbor-joining (NJ) tree using the P-distance model MEGA 12 version was used for analyses on 1000 bootstrap replicates (Saitou & Nei, 1987; Nei & Kumar, 2000; Kumar et al., 2024).

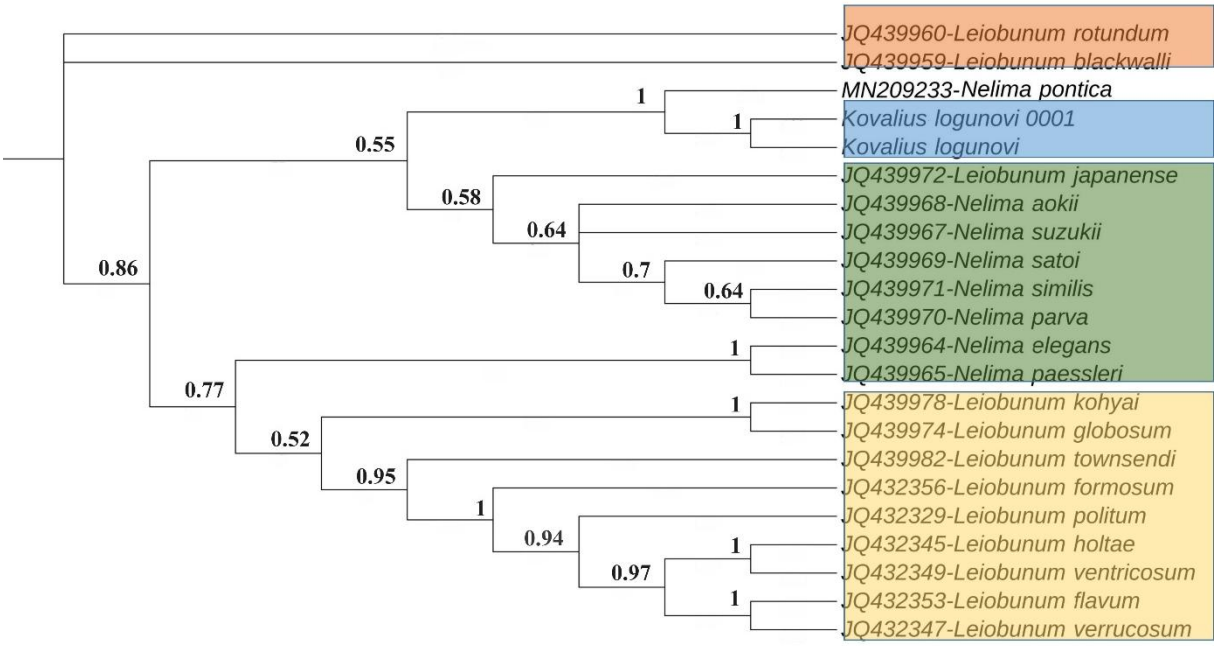

Figure 1. A phylogenetic tree was inferred through Bayesian analysis (BI) based on the sequences of the 16S rRNA gene region.

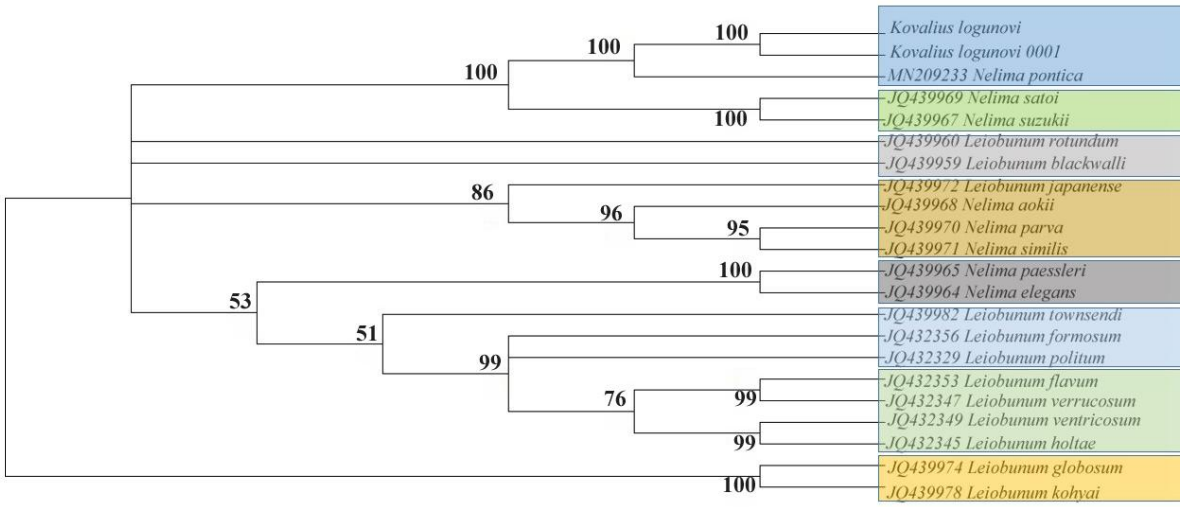

Figure 2. A phylogenetic tree was inferred through Neighbour-joining (NJ) based on the sequences of the 16S rRNA gene region.

Analyses were performed on NGPhylogeny.frserver using Multiple Alignment (Clustal Omega), Alignment Curation (Noisy); Tree Inference (Mr Bayes) (Lemoine et al., 2019). The sequences were aligned with Clustal Omega alignment tool (Sievers et al., 2014); then, sequences were alignment curated with Noisy (commandline: cutoff=0.80, distance=HAMMING, missing=N, nogap=0, noconstant=0, ordering=nnet, shuffles=1000, smooth=1, seqtype=D) (Dress et al., 2008). We performed phylogenetic reconstruction for concatenated 16S rRNA alignment using Bayesian inference (BI) analyses. The BI analysis was run in MrBayes ver. 3.2.7 (Huelsenbeck & Ronquist, 2001).

In the BI analysis, the following settings were used: (Nst =6; Rates= Equal; Setting number of generations to 100000; sample frequency to 500; check-pointing frequency to 100000; burnin fraction to 0.25; number of chains=4; number of runs=1). The best-fit evolutionary model (GTR+G+I) selected according to the Akaike information criterion AIC (Akaike, 1998) in the MEGA 12 version. The analyses were performed using NGPhylogeny.frserver (Lemoine et al., 2019). Phylogenetic trees were visualized using ITOL v5 (Letunic & Bork, 2021). Mean genetic distances (p-distances) between sequences were determined with MEGA 12 version (Kumar et al., 2024).

3. Results and Discussion

A fragment of 408 bp from the 16S rRNA gene was sequenced. The mean frequencies for Adenine (A), Thymine (T), Cytosine (C), and Guanine (G) were 37, 32, 20, and 11%, respectively. The mean nucleotide frequencies were higher and more significant in the A + T ratio than in the C + G ratio (Table 2).

Table 1. GenBank sequence accession numbers of the species used in this study.

Species name	Sequence accession numbers	References
Leiobunum blackwalli	JQ439959	Hedin et al., 2012
Leiobunum flavum	JQ432353	Burns et al., 2012
Leiobunum formosum	JQ432356	Burns et al., 2012
Leiobunum globosum	JQ439974	Hedin et al., 2012
Leiobunum holtae	JQ432345	Burns et al., 2012
Leiobunum japanense	JQ439972	Hedin et al., 2012
Leiobunum kohyai	JQ439978	Hedin et al., 2012
Leiobunum politum	JQ432329	Burns et al., 2012
Leiobunum rotundum	JQ439960	Hedin et al., 2012
Leiobunum townsendi	JQ439982	Hedin et al., 2012
Leiobunum ventricosum	JQ432349	Burns et al., 2012
Leiobunum verrucosum	JQ432347	Burns et al., 2012
Nelima aokii	JQ439968	Hedin et al., 2012
Nelima elegans	JQ439964	Hedin et al., 2012
Nelima paessleri	JQ439965	Hedin et al., 2012
Nelima parva	JQ439970	Hedin et al., 2012
Nelima pontica	MN209233	Doğan & Kurt, 2019
Nelima satoi	JQ439969	Hedin et al., 2012
Nelima similis	JQ439971	Hedin et al., 2012
Nelima suzukii	JQ439967	Hedin et al., 2012

Table 2. Length of base pairs and nucleotide frequencies of the region of the 16S rRNA gene

	T(U)	C	A	G	Base pair length
Kovalius logunovi 0001	38	10	32	20	408
Kovalius logunovi	38	10	32	20	408
Nelima pontica	40	8	32	20	333
Leiobunum blackwalli	33	17	41	8	413
Leiobunum flavum	31	22	36	11	412
Leiobunum formosum	30	22	36	11	411
Leiobunum verrucosum	31	22	36	11	412
Leiobunum japanense	30	21	39	9	412
Leiobunum politum	28	24	35	13	412
Leiobunum ventricosum	29	22	36	12	412
Leiobunum holtae	30	22	36	12	412
Nelima parva	30	21	40	9	416
Leiobunum globosum	28	23	38	10	409
Leiobunum kohyai	28	24	38	10	411
Leiobunum townsendi	33	19	38	10	409
Leiobunum rotundum	35	17	39	9	410
Nelima similis	30	20	40	10	414
Nelima satoi	33	20	39	8	402
Nelima aokii	31	19	41	9	415
Nelima suzukii	32	21	38	9	400
Nelima paessleri	31	22	38	10	413
Nelima elegans	31	22	38	9	412
Avg.	32	20	37	11	389

P-distance, used in phylogenetic tree construction, expresses the ratio of nucleotide differences between sequences. It helps to determine evolutionary relationships in phylogenetic trees and shows the relationship of species based on genetic similarity. While genetic distances between closely related species are small, large genetic differences occur at high genetic distances (Kaleshkumar et al., 2015; Alyamani, 2024). P-distances vary from 0.01% to 0.71% between the opilionid species used in the study. The distance value was 0.36% overall. Genetic distances ranged from 0.01 to 0.70% between *Kovalius logunovi* species and other species. The lowest genetic distance to species of *Kovalius logunovi* was found between species of *Nelima pontica* (0.22) while the highest genetic distance was found between species of *Leiobunum politum* (0.70). The minimum genetic distance is between *K. lounovi* and *N. pontica*, indicating that they have a close relationship (Table 3).

The genus *Kovalius* Tchemeris, 2023 is morphologically similar to the genus *Nelima* Roewer, 1910. However, it is morphologically distinguished from *Nelima* by the structure of the penis, ovipositor, and the prominent apophysis of patellae and tibiae on pediplap. The genus *Nelima* Roewer, 1910 is comprised of two species, *N. pontica* Charitonov, 1941 and *N. doriae* (Canestrini, 1871), within the geographical areas of Türkiye and the NW Caucasus (Kurt, 2014; Tchemeris, 2023). The database at the National Centre for Biotechnology (NCBI) contains data on the 16S rRNA gene region of the *N. pontica* species. However, no such data is available for the *N. doriae* species.

Table 3. Genetic distances (p-distance) based on partial 16S rRNA sequences.

	1	2	3	4	5	6	7	8	9	10	11	12	13	14	15	16	17	18	19	20	21	22
Kovalius logunovi 0001																						
Kovalius logunovi	0.01																					
Nelima pontica	0.22	0.23																				
Leiobunum blackwalli	0.66	0.66	0.67																			
Leiobunum flavum	0.69	0.69	0.69	0.18																		
Leiobunum formosum	0.68	0.68	0.67	0.19	0.09																	
Leiobunum verrucosum	0.69	0.69	0.69	0.18	0.01	0.10																
Leiobunum japanense	0.66	0.67	0.68	0.19	0.21	0.21	0.20															
Leiobunum politum	0.70	0.70	0.70	0.21	0.09	0.11	0.10	0.22														
Leiobunum ventricosum	0.68	0.69	0.69	0.20	0.05	0.09	0.06	0.21	0.11													
Leiobunum holtae	0.68	0.69	0.69	0.20	0.06	0.09	0.06	0.21	0.11	0.00												
Nelima parva	0.67	0.68	0.68	0.18	0.20	0.21	0.20	0.16	0.21	0.20	0.20											
Leiobunum globosum	0.69	0.69	0.71	0.21	0.22	0.21	0.22	0.21	0.21	0.20	0.20	0.22										
Leiobunum kohyai	0.68	0.68	0.69	0.22	0.21	0.20	0.21	0.21	0.21	0.20	0.20	0.22	0.05									
Leiobunum townsendi	0.68	0.69	0.69	0.17	0.15	0.14	0.15	0.20	0.16	0.16	0.16	0.19	0.22	0.21								
Leiobunum rotundum	0.68	0.68	0.66	0.16	0.21	0.20	0.21	0.22	0.23	0.22	0.21	0.23	0.23	0.23	0.19							
Nelima similis	0.67	0.67	0.68	0.17	0.21	0.20	0.20	0.15	0.22	0.20	0.20	0.08	0.22	0.22	0.20	0.21						
Nelima satoi	0.59	0.59	0.61	0.62	0.61	0.63	0.61	0.61	0.62	0.61	0.61	0.63	0.63	0.63	0.61	0.61	0.63					
Nelima aokii	0.67	0.67	0.67	0.17	0.18	0.17	0.19	0.15	0.19	0.19	0.19	0.10	0.21	0.22	0.17	0.21	0.11	0.62				
Nelima suzukii	0.59	0.59	0.58	0.62	0.61	0.63	0.61	0.62	0.63	0.63	0.63	0.62	0.65	0.65	0.61	0.59	0.62	0.26	0.62			
Nelima paessleri	0.68	0.68	0.69	0.19	0.16	0.16	0.16	0.18	0.17	0.17	0.17	0.18	0.19	0.20	0.16	0.21	0.18	0.62	0.17	0.61		
Nelima elegans	0.68	0.68	0.69	0.19	0.16	0.16	0.16	0.19	0.18	0.17	0.17	0.19	0.20	0.20	0.17	0.20	0.19	0.62	0.18	0.61	0.04	

The p-distances and high bootstrap values obtained in this study indicate a stronger similarity between the genus *Kovalius* and the genus *Nelima* than between the other genera (Figs. 1-2). This finding provides further support for the molecular and morphological data and thus contributes to our understanding of taxonomic relationships within the indicated group.

Ackowledgement: We are grateful to Prof. Dr Kemal KURT (Gümüşhane University, Turkey) for the collection and identification of harvester specimens for this study.

Ethics committee approval: Ethics committee approval is not required for this study.

Conflict of interest: The authors declare that there is no conflict of interest.

Author Contributions: Conception – P.K., N.Y.D.; Design – P.K., N.Y.D.; Data Collection and Processing – P.K; Analysis Interpretation – P.K., N.Y.D.; Literature Review – P.K., N.Y.D.; Writing – P.K., N.Y.D.; Critical Review – P.K., N.Y.D.

References

Akaike, H. (1998) Information theory and an extension of the maximum likelihood principle. *In*: Parzen, E., Tanabe, K. &Kitagawa, G. (Eds.), *Selected Papers of Hirotugu Akaike*. Springer, New York, New York, pp. 199–213.

Altschul, S.F., Gish, W., Miller, W., Myers, E.W., & Lipman, D.J. (1990). Basic local alignment search tool. *Journal of molecular biology*, 215(3), 403-410.

Alyamani, N.M. (2024). Mitochondrial 16S rRNA gene as a molecular marker in the phylogenetic relationships of some Rabbitfishes species (Siganidae: Perciformes). *Open Veterinary Journal*, 14(8), 1936.

Burns, M., Hedin, M., & Shultz, J.W. (2012). Molecular phylogeny of the leiobunine harvestmen of eastern North America (Opiliones: Sclerosomatidae: Leiobuninae). *Molecular Phylogenetics and Evolution*, 63(2), 291-298.

Chan, K.O., Hertwig, S.T., Neokleous, D.N., Flury, J.M., & Brown, R.M. (2022). Widely used, short 16S rRNA mitochondrial gene fragments yield poor and erratic results in phylogenetic estimation and species delimitation of amphibians. *BMC Ecology and Evolution*, 22(1), 37.

Doğan, N.Y., & Kurt, P. (2019). DNA barcoding and phylogenetic analysis of *Nelima pontica* Charitonov, 1941 (Opiliones: Sclerosomatidae) based on mitochondrial COI and 16S rRNA genes. *Acta Biologica Turcica*, 33(1), 8-11.

Dress, A.W., Flamm, C., Fritzsch, G., Grünewald, S., Kruspe, M., Prohaska, S.J., & Stadler, P.F. (2008). Noisy: identification of problematic columns in multiple sequence alignments. *Algorithms for Molecular Biology*, 3, 1-10.

Edgecombe, G.D., Wilson, G.D.F., Colgan, D.J., Gray, M.R., & Cassis, G. (2000). Arthropodcladistics: combined analysis of histone H3 and U2 snRNA sequences andmorphology. *Cladistics*, 16, 155-203.

Hedin, M., Tsurusaki, N., Macías-Ordóñez, R., & Shultz, J.W. (2012). Molecular systematics of sclerosomatid harvestmen (Opiliones, Phalangioidea, Sclerosomatidae): geography is better than taxonomy in predicting phylogeny. *Molecular Phylogenetics and Evolution*, 62(1), 224-236.

Huelsenbeck, J.P., & Ronquist, F. (2001). MRBAYES: Bayesian inference of phylogenetic trees. *Bioinformatics*, 17(8), 754-755.

Kaleshkumar, K., Rajaram, R., Vinothkumar, S., Ramalingam, V., & Meetei, K.B. (2015). Note DNA barcoding of selected species of pufferfishes (Order: Tetraodontiformes) of Puducherry coastal waters along south-east coast of India. *Indian Journal of Fisheries,* 62(2), 98–103.

Kumar, S., Stecher, G., Suleski, M., Sanderford, M., Sharma, S., & Tamura, K. (2024). MEGA12: Molecular Evolutionary Genetic Analysis version 12 for adaptive and green computing. *Molecular Biology and Evolution*, 41(12), msae263.

Kurt, K. (2014). Updated checklist of harvestmen (Arachnida: Opiliones) in Turkey. *Archives of Biological Sciences*, 66(4), 1617-1631.

Kurt, K. (2024). A New Harvestman Genus Record for Turkey: *Kovalius* Tchemeris, 2023 (Opiliones Sclerosomatidae, Leiobuninae). *Entomological News*, 131(4), 186-192.

Lemoine, F., Correia, D., Lefort, V., Doppelt-Azeroual, O., Mareuil, F., Cohen-Boulakia, S., & Gascuel, O. (2019). NGPhylogeny. fr: new generation phylogenetic services for non-specialists. *Nucleic acids research*, 47(W1), W260-W265.

Letunic, I., & Bork, P. (2021). Interactive Tree of Life (iTOL) v5: an online tool for phylogenetic tree display and annotation. *Nucleic Acids Research,* 49(W1), W293–W296.

Nei, M., & Kumar, S. (2000). *Molecular evolution and phylogenetics*. Oxford university press.

Saitou, N., & Nei, M. (1987). The neighbor-joining method: a new method for reconstructing phylogenetic trees. *Molecular biology and evolution*, 4(4), 406-425.

Sievers, F., Wilm, A., Dineen, D., Gibson, T. J., Karplus, K., Li, W., ..., & Higgins, D. G. (2011). Fast, scalable generation of high-quality protein multiple sequence alignments using Clustal Omega. *Molecular systems biology*, 7(1), 539.

Tchemeris, A.N. (2023). *Kovalius* - a new genus of cave-dwelling harvestmen from the Caucasus (Opiliones: Sclerosomatidae: Leiobuninae). *Zootaxa*, 5227(4), 486-494.

Wang, Z.L., Yang, X.Q., Wang, T.Z., & Yu, X. (2018). Assessing the effectiveness of mitochondrial COI and 16S rRNA genes for DNA barcoding of farmland spiders in China. *Mitochondrial DNA Part A*, 29(5), 695-702.

Xiong, B., & Kocher, T. D. (1991). Comparison of mitochondrial DNA sequences of seven morphospecies of black flies (Diptera: Simuliidae). *Genome*, 34(2), 306-311.

Commagene Journal of Biology

Ali & Kackel, (2025) *Comm. J. Biol.* 9(1), 64-70.
DOI: 10.31594/commagene.1651651

e-ISSN 2602-456X

Research Article/Araştırma Makalesi

Scorpion Fauna of Duhok Province, Iraq, with New Records for the Country (Arachnida: Scorpiones)

Farhad ALI*, Hamid KACKEL

University of Zakho, College of Science, Department of Biology, Duhok, IRAQ
ORCID ID: Farhad ALI: https://orcid.org/0000-0002-8645-6564; Hamid KACKEL: https://orcid.org/0000-0002-7231-8267

Received: 05.03.2025 **Accepted:** 18.04.2025 **Published online:** 26.05.2025 **Issue published:** 30.06.2025

Abstract: This study of scorpion fauna was conducted in the Duhok province of northern Iraq, from June to October 2024. In this survey 273 specimens were collected from different districts, representing six species: *Androctonus* sp., *Hottentotta saulcyi* (Simon, 1880), *Orthochirus fomichevi* (Kovařík, Yağmur, Fet & Hussen, 2019), *Compsobuthus matthiesseni* (Birula, 1905), *Scorpio kruglovi* (Birula, 1910), *and Mesobuthus faiki* (Yağmur, Kovařík & Fet, 2024). *Hottentotta saulcyi* was the most abundant species (35.9% of total individuals) followed by *Orthochirus fomichevi* 29.7%. *Compsobuthus matthiesseni*, *Mesobuthus faiki*, *Androctonus* sp. and *Scorpio kruglovi*, were less frequent (less than 16 % each). A significant finding was the first-time documentation of *Mesobuthus faiki* in Duhok province, marking it a new record for Iraq.

Keywords: Scorpion diversity, distribution, identification, *Mesobuthus faiki*, Buthidae.

Irak'ın Duhok ilinin Akrep Faunası ve Ülke İçin Yeni Kayıtlar (Arachnida: Scorpiones)

Öz: Bu çalışma Irak'ın kuzeyinde yer alan Duhok ilinde akrep faunasının belirlenmesi için 2024 yılı Haziran ile Ekim ayları arasında yürütülmüştür. Bu araştırmada farklı ilçelerden toplam 273 örnek toplanmış ve altı türe ait bireyler belirlenmiştir. Bunlar: *Androctonus* sp, *Hottentotta saulcyi* (Simon, 1880), *Orthochirus fomichevi* (Kovařík, Yağmur, Fet & Hussen, 2019), *Compsobuthus matthiesseni* (Birula, 1905), *Scorpio kruglovi* (Birula, 1910) ve *Mesobuthus faiki* (Yağmur, Kovařík & Fet, 2024). *Hottentotta saulcyi* en bol bulunan türdür ve toplam bireylerin %35,9'unu oluşturmuştur, onu %29,7 ile *Orthochirus fomichevi* takip etmiştir. *Compsobuthus matthiesseni, Mesobuthus faiki, Androctonus* sp. ve *Scorpio kruglovi* ise daha az sıklıkta (%16'dan az) gözlemlenmiştir. Bu çalışma kapsamında *Mesobuthus faiki*'nin Duhok ilinde ilk kez rapor edilmesi, türün Irak için yeni bir kayıt olarak kaydedilmesi açısından önemli bir bulgudur.

Anahtar kelimeler: Akrep çeşitliliği, dağılış, tanımlama, *Mesobuthus faiki*, Buthidae.

1. Introduction

Scorpions, classified within the arachnid order Scorpiones, are of considerable medical importance. According to current taxonomic data, there are 2,865 recognized scorpion species distributed worldwide. Of these, the venom of approximately 30 species is considered medically significant due to its potential to cause serious harm to humans (Prendini & Wheeler, 2005; Rein, 2025).

Scorpion stings are a significant global public health issue, with approximately 1.2 million cases and 3,250 deaths recorded annually. Mexico, Colombia, and Iran report particularly high numbers of stings (Bawaskar & Bawaskar, 2012; Shahsavarinia et al., 2017). Epidemiological studies on scorpion stings in Iraq are limited. However, recent unofficial reports from the Iraqi Ministry of Health indicate a substantial incidence of scorpion envenomation, influenced by regional, climatic, and environmental factors. A study conducted in 2019 and 2020 in the Duhok, Erbil, and Sulaymaniyah provinces revealed that Duhok experienced the highest rate of scorpion stings compared to the other two provinces. Recent investigations into the scorpion fauna of these three provinces have identified 10 species (Hussen et al., 2022).

A recent review of Iraqi scorpion fauna indicates a composition of 20 species, categorized into 13 genera across five families: Buthidae, Euscorpiidae, Hemiscorpiidae, Iuridae, and Scorpionidae. The Buthidae family constitutes the predominant group, encompassing 16 species, which represents 80 % of the total recorded species. In contrast, each of the remaining families is represented by a single species (Kachel et al., 2021; Lourenço, 2022). Several scorpion species in Iraq are known only from single locality records, often based on a limited number of specimens, sometimes a single individual. This apparent restriction in geographical distribution may stem from insufficient scientific field surveys rather than genuine ecological limitations. The species *A. crassicauda* (Olivier, 1807), *C. matthiesseni*, *H. mesopotamicus* (Lourenço and Qi, 2007), *H. salucyi*, *O. fomichevi*, and *S. kruglovi* have been previously documented in Duhok (Hussen & Ahmed, 2020; Kachel, 2020; Kachel et al., 2021; Hussen et al., 2022). Consequently, this study aims to conduct a comprehensive field survey across various districts of Duhok province to construct a geographical distribution map illustrating the diversity of scorpion species within the city.

2. Material and Method

The study area is situated within the Duhok province in northern Iraq, a mountainous region sharing borders with Turkey and Syria. Geographically, it is located between 36°40' and 37°20' North latitude and 43°20' and 44°10' East

Corresponding author: farhad.ali@staff.uoz.edu.krd

longitude. Scorpion specimens were collected from June to October 2024 across seven districts within the Duhok Governorate: Zakho, Sumel, Duhok, Amedi, Shekhan, Akre, and Bardarash (Fig. 1). Collection methodologies encompassed searching under rocks and flooding burrows with water, as well as nocturnal UV flashlight detection. Following collection, specimens were transported to the Zoology Laboratory at the University of Zakho and individually preserved in 80-95% ethanol within small plastic boxes.

Figure 1. Maps showing the geographical outline of (A) Iraq and (B) Duhok province districts.

Species identification was conducted following the taxonomic keys and methodologies established by Levy and Amitai (1980) and Kovařík (2007). Whole specimen photographs were captured using a Canon EOS 7D camera, with image stacking performed via Helicon Focus software. The focus stacking technique was adapted from the Canon-Cognisys system as recommended by Brecko et al. (2014). Measurements were taken by a digital caliper (INGCO, China) for large specimens, whereas for small specimens, ToupView software was used to measure specimens' images which were taken by an ocular digital camera, the brand and origin of which are unspecified, attached to an AmScope stereomicroscope. Statistical analyses were performed by Microsoft Excel 2010 and SPSS v26 software. Geographical distribution of each species was constructed separately by ArcGIS pro v3.0.1 software.

3. Results

3.1. Scorpion fauna relative abundance (RA)

A total of 273 scorpion specimens were collected, comprising 161 males (58.97%) and 112 females (41.03%). Taxonomic analysis revealed the presence of six species belonging to two families: Buthidae and Scorpionidae. The most abundant species were *Hottentotta saulcyi*, representing 35.9% of the total collection, followed by *Orthochirus fomichevi* (29.7%) and *Scorpio kruglovi* (15.0%). The remaining species, *Compsobuthus matthiesseni*, *Mesobuthus faiki*, and *Androctonus* sp., were found in relatively lower numbers, accounting for 10.3%, 5.5%, and 3.6 % of the specimens, respectively (Fig. 2).

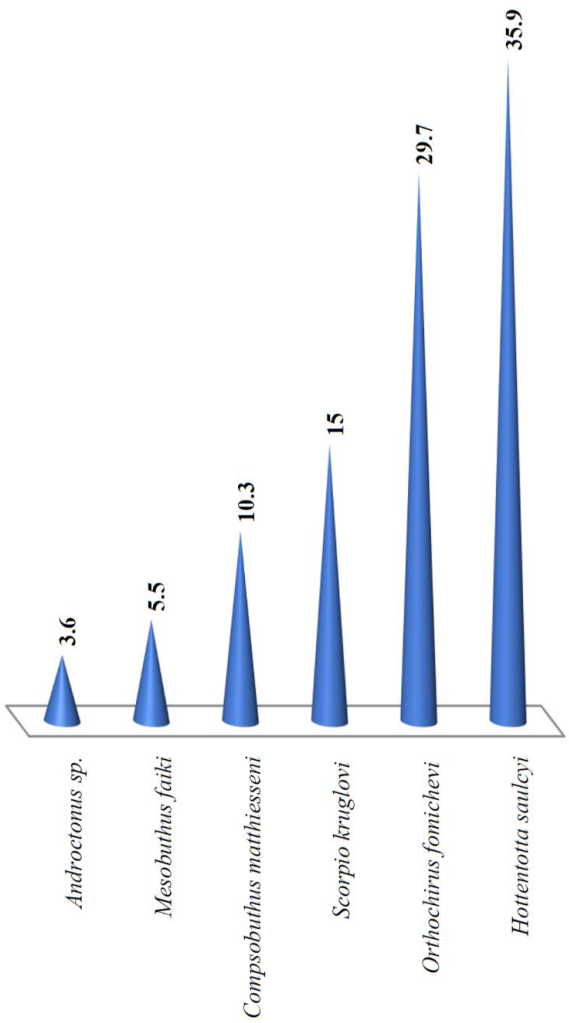

Figure 2. Relative abundance of scorpion species recorded in Duhok Province, Iraq.

3.2. Taxonomy

3.2.1. Family Buthidae C. L. Koch, 1837

The Buthidae family is recognized as the largest family of scorpions, encompassing nearly half of the global diversity of scorpion species (Štundlová et al., 2022). In this study, a total of 232 specimens were identified as belonging to this family, representing 85% of all specimens collected. These specimens included five species: *M. faiki*, *Androctonus* sp., *H. saulcyi*, *O. fomichevi* and *C. matthiesseni*. Key distinguishing features of the Buthidae family include a triangular sternum and pedipalp-patella that lack ventral trichobothria (Amr & El-Oran, 1994; Polis, 1990).

3.2.1.1. *Mesobuthus faiki* Yağmur, Kovařík & Fet, 2024 (Fig. 3e and 4)

Type material examined. Iraq, Duhok province, Duhok district, Zewka Kandala, 37°02'36.2"N 43°10'22.7"E, 1024 m a.s.l, 3♂1♀; Duhok district, Nizarke, 36°50'20.7"N 43°04'03.5"E, 659 m a.s.l, 3♂1♀; Amedi district, Barash, 37°00'23.6"N 43°15'49.5"E, 1357 m a.s.l, 7♂.

Measurements. Total length 37.09 - 45.82 mm (average: ♂ 41.74 mm, ♀ 38.34 mm), prosoma 4.14 - 4.82 mm (average: ♂ 4.46 mm, ♀ 4.50 mm), mesosoma 10.32 - 12.85 mm (average: ♂ 11.85 mm, ♀ 11.37 mm), metasoma and telson 22.63 - 28.20 mm (average: ♂ 25.43 mm, ♀ 22.47 mm). Pectines 21-26 in males and 18-19 in females.

Figure 3. General Overview of Scorpion Species in Duhok province, northern Iraq; A. *Hottentotta saulcyi*; B. *Androctonus* sp.; C. *Scorpio kruglovi*; D. *Orthochirus fomichevi*; E. *Mesobuthus faiki*; and F. *Compsobuthus matthiesseni*. Species are organized according to total body length.

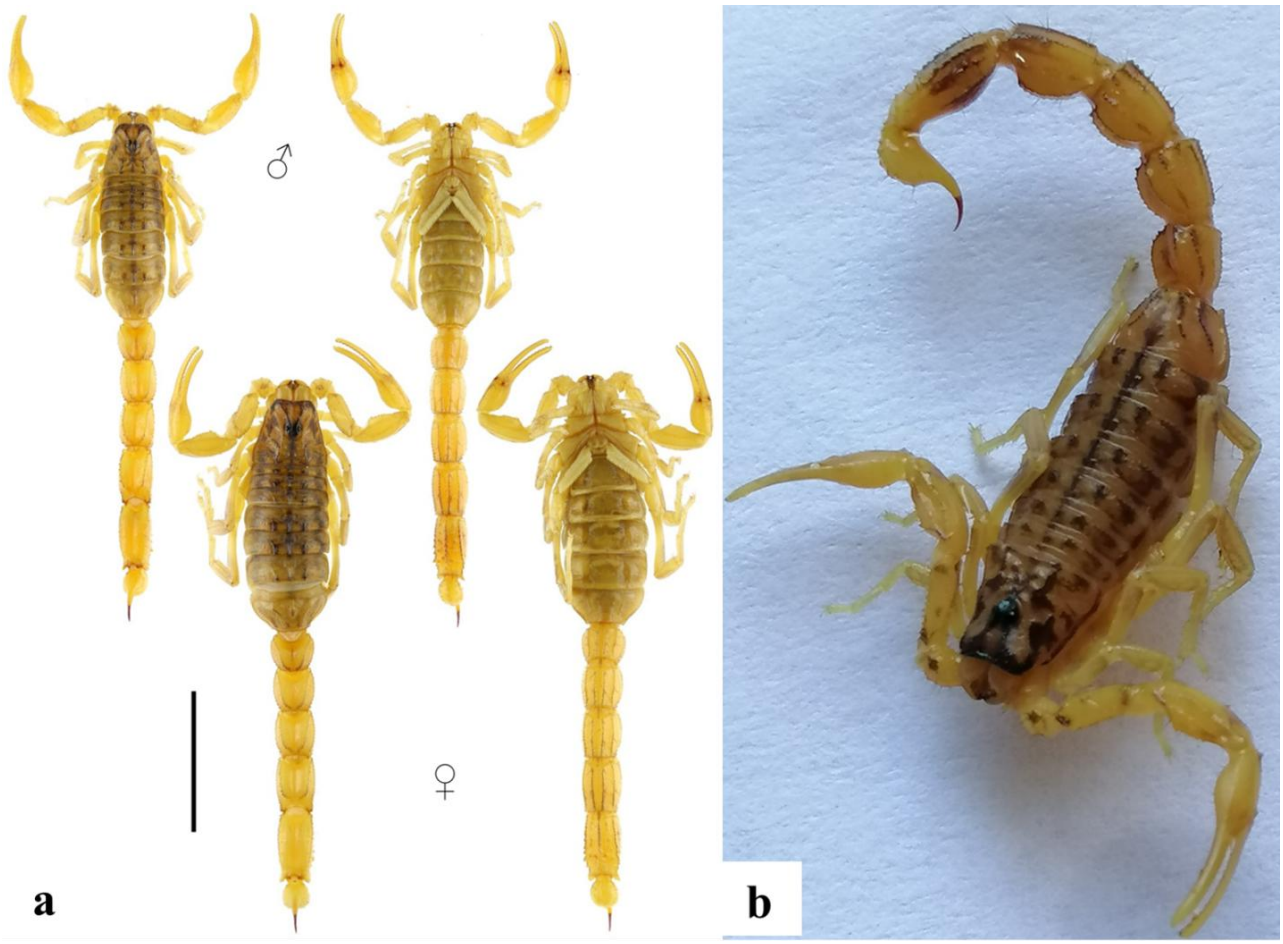

Figure 4. Whole *Mesobuthus faiki* of Iraq photographs with; A. Professional Canon EOS 7D camera, with image stacking performed via Helicon Focus software Top male Bottom female B. Normal mobile phone camera dorsal view.

Comments. During this study, fifteen *M. faiki* specimens were collected, representing 5.5% of the total sample. The sex ratio was skewed towards males, with thirteen specimens identified as male and two as female. All

specimens exhibited a yellow body color, with the carapace and mesosoma displaying darker pigmentation, particularly in females. Brown patches were observed on the carapace, and five longitudinal dark stripes were present on mesosomal tergites I-VI. The metasoma was yellow, with carinae exhibiting increased darkness towards the posterior end. Carapace carinae exhibited a lyre-shaped configuration, in which central-lateral and posterior-median carinae were joined. Notably, metasomal segment V carinae, especially the ventrolateral carinae, displayed uneven denticles, with the posterior denticles being significantly larger. The telson was bulbous and exhibited ventral roughness. Fixed finger of pedipalp-chela with trichobothrium *db* proximal to *est*. The pedipalp-chela movable finger presented four subterminal denticles. Sexual dimorphism was evident in the pedipalp chela, with males exhibiting a prominent scalloping, facilitating differentiation from females.

3.2.1.2. *Androctonus* sp. (Fig. 3b)

Type material examined. Iraq, Duhok province, Sumel district, Asihe, 37°01'05.3"N 42°42'22.5"E, 692 m a.s.l., 2♂1♀; Duhok district, Avrike, 36°50'06.1"N 43°08'14.1"E 868 m a.s.l., 1♀; Shekhan district, Atrush, 36°51'07.7"N 43°21'54.3"E, 1014 m a.s.l., 1♀; Bardarash district, Kawnabak, 36°29'25.0"N 43°37'57.7"E, 430 m a.s.l., 3♂2♀.

Measurements. Total length 63.03 - 81.55 mm (average: ♂ 75.13 mm, ♀ 72.74 mm), prosoma 7.44 - 9.45 mm (average: ♂ 8.67 mm, ♀ 8.53 mm), mesosoma 18.42 - 24.39 mm (average: ♂ 22.17 mm, ♀ 22.14 mm), metasoma and telson 37.17 - 47.71 mm (average: ♂ 44.29 mm, ♀ 42.06 mm). Pectines 31-34 in males and 25-27 in females.

Comments. A total of ten specimens were collected during this study, constituting 3.6% of the overall sample. The specimens comprised an equal sex ratio, with five identified as males and five as females. The general body coloration was dark brown, except for the distal portions of the pedipalp-chela fingers and leg tarsomere II, which exhibited a yellow hue. Notably, these specimens displayed distinct characteristics that differentiate them from *Androctonus crassicauda*, leading to their provisional classification as *Androctonus* sp. Further investigation is necessary to ascertain whether these specimens represent a previously unrecognized species within the fauna of Duhok and Iraq.

3.2.1.3. *Hottentotta salucyi* (Simon, 1880) (Fig. 3a)

Type material examined. Iraq, *Duhok province*, Zakho District, Karne, 37°12'30.0"N 42°39'19.0"E, 559 m a.s.l., 26♂14♀; Zakho district, Khrababk, 37°08'30.6"N 42°45'02.1"E, 526 m a.s.l., 2♂1♀; Zakho district, Salka, 37°06'50.8"N 42°39'05.7"E, 573 m a.s.l., 2♂2♀; Zakho district, Betas, 37°04'02.6"N 42°42'06.1"E, 675 m a.s.l., 1♂; Zakho district, Khelakh, 37°07'29.5"N 42°36'44.0"E, 480 m a.s.l., 2♀; Zakho district, Shinava, 37°06'40.7"N 42°30'37.4"E, 513 m a.s.l., 3♂5♀; Zakho district, Batifa, 37°10'53.9"N 42°59'57.3"E, 605 m a.s.l., 1♂; Duhok district, Zewka kandala, 37°02'36.2"N 43°10'22.7"E, 1024 m a.s.l., 5♂3♀; Duhok district, Alkishk, 37°00'53.8"N 43°11'47.0"E, 1037 m a.s.l., 2♀; Shekhan district, Shekhan, 36°40'31.3"N 43°20'31.4"E, 433 m a.s.l., 2♂; Shekhan district, Atrush, 36°51'07.7"N 43°21'54.3"E, 1014 m a.s.l., 1♂3♀; Amedi district, Sheladiz, 37°02'09.6"N 43°46'41.4"E, 623m a.s.l., 1♂; Akre District, Bashqal Agha, 36°44'43.1"N 43°55'11.3"E, 711 m a.s.l., 1♀; Bardarash district, Dusara, 36°25'24.6"N 43°31'47.3"E, 310 m a.s.l., 7♂14♀.

Measurements. Total length 75.35 - 115.65 mm (average: ♂ 92.51 mm, ♀ 86.08 mm), prosoma 8.18 - 11.30 mm (average: ♂ 9.25 mm, ♀ 9.39 mm), mesosoma 22.98 - 34.97 mm (average: ♂ 28.10 mm, ♀ 27.04 mm), metasoma and telson 44.19 - 69.38 mm (average: ♂ 55.15 mm, ♀ 49.65 mm). Pectines 28-34 in males and 24-28 in females.

Comments. A total of ninety-eight specimens were collected during this study, accounting for 35.9% of the overall sample, thereby establishing this species as the most abundant and widely distributed in the region. Among the collected specimens, 51 were identified as males and 47 as females. Males can be distinguished from females by their narrower mesosoma and a metasomal segment I that is longer than wide, whereas females have a broader mesosoma and a metasomal segment I that is slightly wider than long. *Hottentotta saulcyi* specimens were predominantly located in rocky habitats, where they were observed resting on rocks at night. Notably, this species exhibited the highest level of aggression among all captured specimens. The general body coloration was yellowish-brown, with the chelicerae, anterior portion of the carapace, metasomal segment V, and telson displaying black pigmentation; metasomal segments III and IV may also appear black. The body surface was characterized by moderate hairiness. Additionally, sternite VII exhibited a pentacarinate structure (Amiri et al., 2024).

3.2.1.4. *Orthochirus fomichevi* Kovařík, Yağmur, Fet & Hussen, 2019 (Fig. 3d)

Type material examined. Iraq, Duhok province, Zakho district, Shahida, 37°08'01.1"N 42°40'24.0"E, 506 m a.s.l., 2♂2♀; Zakho district, Khrababk, 37°08'30.6"N 42°45'02.1"E, 526 m a.s.l., 1♂3♀; Zakho district, Salka, 37°06'50.8"N 42°39'05.7"E, 573 m a.s.l., 2♂3♀; Zakho district, Betas, 37°04'02.6"N 42°42'06.1"E, 675 m a.s.l., 1♂; Zakho district, Dubanik, 37°02'30.2"N 42°50'19.9"E, 709 m a.s.l., 4♂3♀; Sumel district, Sumel, 36°50'31.3"N 42°51'52.8"E, 446 m a.s.l., 6♂2♀; Sumel district, Esmahil Ava, 36°57'25.3"N 42°38'12.9"E, 504 m a.s.l., 13♂11♀; Duhok district, Nizarke, 36°50'20.7"N 43°04'03.5"E, 659 m a.s.l, 6♂7♀; Shekhan district, Atrush, 36°51'07.7"N 43°21'54.3"E, 1014 m a.s.l., 7♂8♀.

Measurements. Total length 30.12 - 39.91 mm (average: ♂ 35.68 mm, ♀ 38.16 mm), prosoma 3.38 - 4.43 mm (average: ♂ 3.93 mm, ♀ 4.32 mm), mesosoma 8.68 - 10.92 mm (average: ♂ 9.96 mm, ♀ 11.23 mm), metasoma and telson 18.06 - 24.68 mm (average: ♂ 21.79 mm, ♀ 22.61 mm). Pectines 21-23 in males and 17-20 in females.

Comments. A total of eighty-one specimens were collected during this study, representing 29.7% of the total sample and making it the second most widely distributed species in the region. Of the collected specimens, 42 were males and 39 were females. These scorpions were primarily found in plain areas with sparse vegetation. Among all captured species, *Orthochirus fomichevi* was noted as the most active yet non-aggressive species. This species can be distinguished from others by its granulate sternite VII with well-developed granulate carinae; a densely granulated mesial dorsal surface of metasomal segment V; and

smooth, non-granulate, punctate, and bumpy ventral and lateral surfaces of metasomal segments II–III (Kovařík et al., 2019). The overall body coloration was black, with the exception of the pedipalp-chela fingers and distal segments of the legs, which were yellow.

3.2.1.5. *Compsobuthus matthiesseni* (Birula, 1905) (Fig. 3f)

Type material examined. Iraq, Duhok province, Zakho district, Khrababk, 37°08'30.6"N 42°45'02.1"E, 526 m a.s.l., 1♂; Zakho district, Salka, 37°06'50.8"N 42°39'05.7"E, 573 m a.s.l., 5♂3♀; Zakho district, Betas, 37°04'02.6"N 42°42'06.1"E, 675 m a.s.l., 3♂1♀; Zakho district, Khelakh, 37°07'29.5"N 42°36'44.0"E, 480 m a.s.l., 1♂; Zakho district, Shinava, 37°06'40.7"N 42°30'37.4"E, 513 m a.s.l., 1♂; Zakho district, Batifa, 37°10'53.9"N 42°59'57.3"E, 605 m a.s.l., 1♀; Sumel district, Sumel, 36°50'31.3"N 42°51'52.8"E, 446 m a.s.l., 9♂; Duhok district, Nizarke, 36°50'20.7"N 43°04'03.5"E, 659 m a.s.l, 2♂; Duhok district, Zewka kandala, 37°02'36.2"N 43°10'22.7"E, 1024 m a.s.l., 1♂.

Measurements. Total length 32.39 - 44.98 mm (average: ♂ 37.81 mm, ♀ 34.60 mm), prosoma 3.32 - 4.11 mm (average: ♂ 3.63 mm, ♀ 3.85 mm), mesosoma 9.03 - 12.07 mm (average: ♂ 10.64 mm, ♀ 10.69 mm), metasoma and telson 20.04 - 28.80 mm (average: ♂ 23.54 mm, ♀ 20.05 mm). Pectines 21-24 in males and 19-20 in females.

*Comments***.** During the present study, twenty-eight specimens were collected, comprising 10.3% of the total sample. The collected specimens consisted of 23 males and 5 females. These scorpions were observed in plain areas characterized by sparse vegetation. The overall body coloration was yellow, with a slightly darker metasomal segment V. The pedipalp-chela fingers were elongated and lacked external accessory denticles. The pedipalp-chela movable finger presented four subterminal granules. Sexual dimorphism was evident, with males exhibiting a significantly longer metasoma compared to females.

3.2.2. Family Scorpionidae Latreille, 1802

The family Scorpionidae is an exclusively Old-World group that encompasses some of the largest extant scorpion species, reaching approximately 200 mm in length. In this study, a total of 41 specimens were identified as belonging to Scorpionidae, representing 15% of all collected specimens. These specimens were classified as a single species, *Scorpio kruglovi*. Diagnostic characteristics of the family Scorpionidae include a pentagonal sternum and a lateroapical margin of the tarsi produced into a rounded lobe (Amr & El-Oran, 1994; Polis, 1990).

3.2.2.1. *Scorpio kruglovi* Birula, 1910 (Fig. 3c)

Type material examined. Iraq, Duhok province, Zakho district, Sharanish, 37°13'53.2"N 42°50'35.8"E, 1076 m a.s.l., 4♀; Zakho district, Salka, 37°06'50.8"N 42°39'05.7"E, 573 m a.s.l., 6♂2♀; Zakho district, Dubanik, 37°02'30.2"N 42°50'19.9"E, 709 m a.s.l., 3♂1♀; Sumel district, Sumel, 36°50'31.3"N 42°51'52.8"E, 446 m a.s.l., 9♂; Duhok district, Alkishk, 37°00'53.8"N 43°11'47.0"E, 1037 m a.s.l., 1♂; Duhok district, Nizarke, 36°50'20.7"N 43°04'03.5"E, 659 m a.s.l, 1♂1♀; Duhok district, Avrike, 36°50'06.1"N 43°08'14.1"E 868 m a.s.l., 2♂1♀; Shekhan district, Atrush, 36°51'07.7"N 43°21'54.3"E, 1014 m a.s.l., 4♂1♀; Amedi district, Khanka, 37°10'34.9"N 43°20'28.9"E, 967 m a.s.l., 4♀; Akre district, Bashqal Agha, 36°44'43.1"N 43°55'11.3"E, 711 m a.s.l., 1♂.

Measurements. Total length 50.87 - 61.24 mm (average: ♂ 53.79 mm, ♀ 61.05 mm), prosoma 7.15 - 8.58 mm (average: ♂ 7.62 mm, ♀ 8.90 mm), mesosoma 16.65 - 21.47 mm (average: ♂ 18.46 mm, ♀ 22.63 mm), metasoma and telson 26.34 - 31.48 mm (average: ♂ 27.71 mm, ♀ 29.53 mm). Pectines 10-13 in males and 9-11 in females

*Comments***.** A total of forty-one specimens were collected during this study, accounting for 15% of the total specimens gathered. Among these, 27 were identified as male and 14 as female. Males can be readily distinguished from females by the presence of fine granules that cover the entire surface of tergites I-VI, while females exhibit a smooth and glossy appearance in this region. Additionally, males possess medially wrinkled sternites III-VI, contrasting with the smooth and shiny sternites observed in females (Abu Afifeh et al., 2024). The overall coloration of the specimens ranged from yellowish-brown to brown, with the legs consistently exhibiting a yellow hue. Notably, several specimens displayed a darker coloration in metasoma V compared to other segments.

These scorpions belong to a burrowing species, typically retreating into their burrows during daylight hours. Observations indicated that many specimens rested at the entrances of their burrows with their chelae exposed. They demonstrated a heightened sensitivity to ground vibrations, rapidly retreating into their burrows upon sensing nearby movement. This behavior suggests that a combination of methods including the use of UV flashlights, pouring water into their burrows, and shoveling proved to be more effective for capturing these scorpions. Some specimens were also successfully captured during daylight hours using similar techniques, albeit without the use of UV flashlights.

4. Discussion

Our study showed the presence of *Mesobuthus faiki* as a new record among scorpion species fauna of Duhok province and Iraq. In addition to the following species: *Androctonus* sp., *Hottentotta saulcyi*, *Orthochirus fomichevi*, *Compsobuthus matthiesseni* and *Scorpio kruglovi*. The same number of scorpion species in this study was reported from Duhok in previous investigations with few species variation (Hussen et al., 2022; Kachel et al., 2021). Previously, *H. mesopotamicus*, was identified by Lourenço and Qi (2007) in Duhok province, particularly Zakho district and also in a few previous studies in the same area (Kachel, 2020); therefore, we conclude that geographical record of this species might be a mistake. Here we were not able to investigate a few districts comprehensively because of the unstable political situation, distance from our research center and difficulties of sample collection.

The morphological characteristics and morphometric data obtained from our *M. faiki* specimens are largely consistent with the description of the *M. faiki* type specimen, which originates from the Gaziantep province in Türkiye (Yağmur et al., 2024). However, discernible differences were observed in comparison to the *M. mesopotamicus* specimen from the Mosul province (Kovařík et al., 2022) and *M. phillipsi* specimens documented in the Erbil province, adjacent to Duhok, Iraq (Hussen & Ahmed,

2020). The taxonomic classification of this genus within Iraq remains complex. Previous records from various provinces have recorded specimens to different species and subspecies level and names, suggesting a need for further taxonomic clarification via comprehensive molecular analyses (Kachel et al., 2021).

Our specimens *Androctonus* sp. has a distinctive pedipalps structure and coloration which are critical morphological characterization for accurate species identification and might be a new species for the country. *Androctonus* sp. also has the lowest abundance with limited geographical distribution and has only been reported in four districts of Duhok. The genus *Androctonus* in Iraq includes two species of significant medical importance, *Androctonus crassicauda* and the recently described *Androctonus sumericus* from Dhi Qar Province (Al-Khazali & Yağmur, 2023). In Iraq, *A. crassicauda* is widely distributed and has been recorded in twelve provinces including Duhok and is recognized for its potent venom, which poses a considerable health risk to humans (Keegan, 1980).

The other four recorded species in the present study and previously are *H. saulcyi, O. fomichevi, C. matthiesseni,* and *S. kruglovi* (Hussen et al., 2022). The most abundant and largest species recorded in this study was *H. saulcyi*, which was recorded in six districts of Duhok Province. Likely, *S. kruglovi* were recorded from six districts followed by *O. fomichevi* and *C. matthiesseni* with four and three district records, respectively. Our data of geographical distribution (Fig. 5) of these species agree with their previous geographical distribution based on the provinces in Iraq to a certain degree (Kachel et al., 2021) with slight variation in their abundance and percentage (Hussen et al., 2022). Therefore, educating health staff and communities with necessary knowledge on the morphology and ecology of the known scorpion species and particularly on the geographical distribution of dangerous and medically important scorpion species in Duhok might lead to significant reduction in the rate of scorpion stings and mortality.

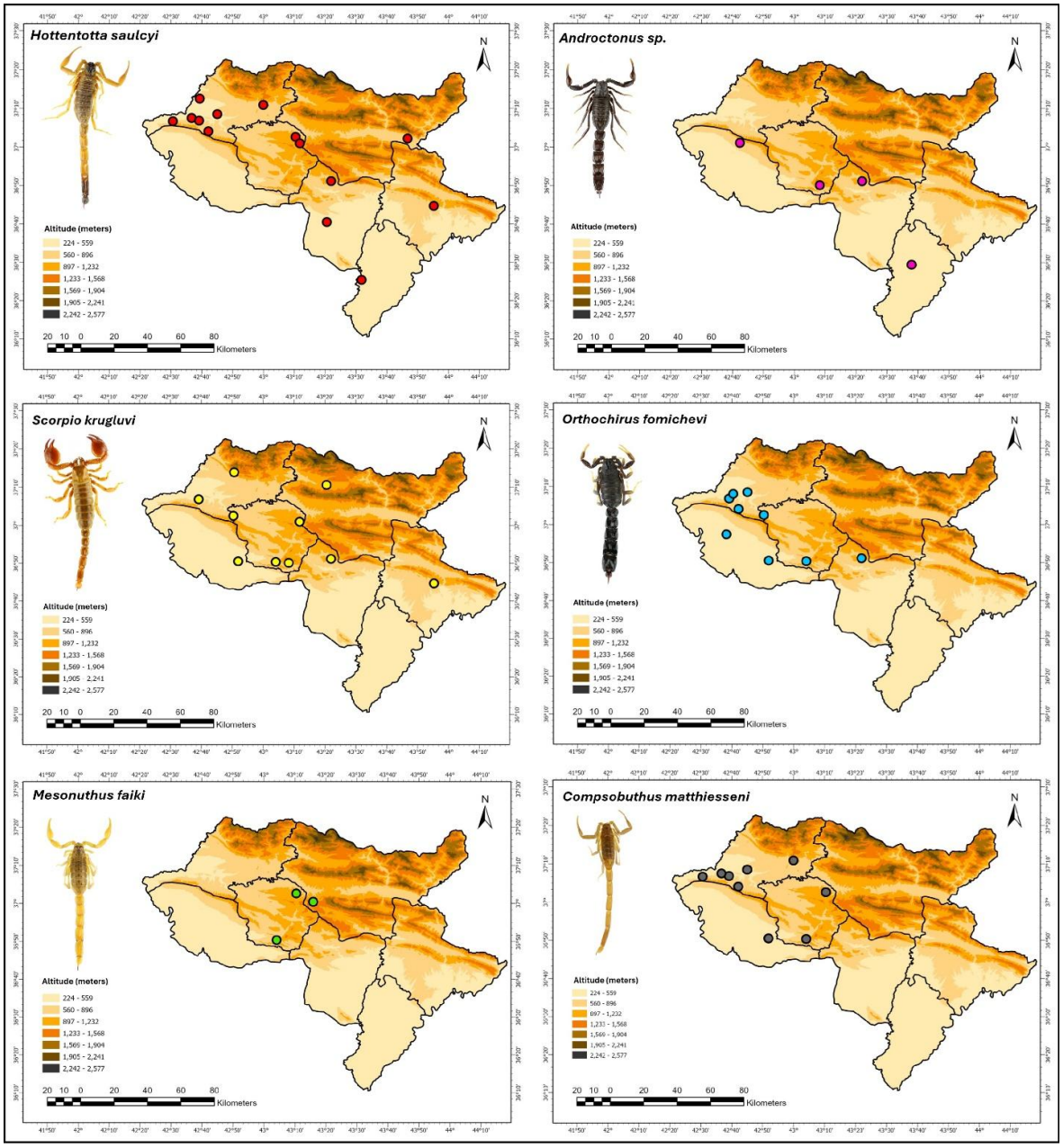

Figure 5. Show the district geographical distribution of the scorpion species of Duhok province, Iraq.

Ackowledgement: We would like to thank our friends and colleagues for their support in collecting samples, taking photographs, and offering scientific advice, including verifying species identities. Additionally, we appreciate the anonymous reviewers for their constructive scientific and technical comments.

Ethics committee approval: This study was performed in accordance with ethical standards of animal experiments. Legal research ethics committee approval permissions for the study were obtained from the Zakho University, Animal Experiments Local Ethics Committee (No: AEC-031).

Conflict of interest: The authors declare that there is no conflict of interest.

Author Contributions: Conception – H.K.; Design – F.A., H.K.; Supervision – H.K.; Fund – F.A.; Materials - F.A.; Data Collection and Processing – F.A.; Analysis Interpretation – F.A., H.K.; Literature Review – F.A., H.K.; Writing – F.A., H.K.; Critical Review – H.K.

References

Abu Afifeh, B., Yağmur, E.A., Al–Saraireh, M., & Amr, Z. (2024). Revision of the genus *Scorpio* in Jordan, with a description of a new genus and three new species (Scorpiones: Scorpionidae). *Euscorpius*, 2024(391), 1-66.

Al-Khazali, A.M., & Yağmur, E.A. (2023). *Androctonus sumericus* sp. nov., a new scorpion from Dhi Qar Province, Iraq (Scorpiones: Buthidae). *Zoology in the Middle East*, 69(4), 410-419. https://doi.org/10.1080/09397140.2023.2284016

Amiri, M., Prendini, L., Hussen, F.S., Aliabadian, M ,.Siahsarvie, R., & Mirshamsi, O. (2024). Integrative systematics of the widespread Middle Eastern buthid scorpion, *Hottentotta saulcyi* (Simon, 1880), reveals a new species in Iran. *Arthropod Systematics & Phylogeny*, 82, 323-341. https://doi.org/10.3897/asp.82.e98662

Amr, Z.S., & El-Oran, R. (1994). Systematics and distribution of scorpions (Arachnida, Scorpionida) in Jordan. *Italian Journal of Zoology*, 61(2), 185-190.

Bawaskar, H.S., & Bawaskar, P.H. (2012). Scorpion sting: update. *The journal of the association of physicians of India*, 60, 46-55.

Brecko, J., Mathys, A., Dekoninck, W., Leponce, M., VandenSpiegel, D., & Semal, P. (2014). Focus stacking: Comparing commercial top-end set-ups with a semi-automatic low budget approach. A possible solution for mass digitization of type specimens. *ZooKeys*, 464, 1-23. https://doi.org/https://doi.org/10.3897/zookeys.464.8615

Hussen, F., Kachel, H., Hama, G., Kachal, E., Slo, M., Hiwil, I., & Ahmed, A. (2022). Epidemiological characterizations, new localities, and a checklist of the known scorpions in the Kurdistan Region, Northern Iraq. *Journal of Arthropod-Borne Diseases*, 16(3), 251–261. https://doi.org/https://doi.org/10.18502/jad.v16i3.12042

Hussen, F.S., & Ahmed, S.T. (2020). New data of scorpion fauna, include two new records with identification key of scorpion species (Arachnida: Scorpiones) in Iraq. *Plant Archives*, 20(2), 6711-6725.

Kachel, H. (2020). Scorpion Fauna and Scorpionism in Zakho Province of Northern Iraq [Kuzey Irak Zakho İli Akrep Faunası ve Skorpionizmi]. *Commagene Journal of Biology*, 4(1), 22-27. https://doi.org/10.31594/commagene.710923

Kachel, H.S., Al-Khazali, A.M., Hussen, F.S., & Yağmur, E.A. (2021). Checklist and review of the scorpion fauna of Iraq (Arachnida: Scorpiones). *Arachnologische Mitteilungen: Arachnology Letters*, 61(1), 1-10 .

Keegan, H.L. (1980). *Scorpions of medical importance*.

Kovařík, F. (2007). A revision of the genus *Hottentotta* Birula, 1908, with descriptions of four new species (Scorpiones, Buthidae). *Euscorpius*, 2007(58), 1-107.

Kovařík, F., Fet, V., Gantenbein, B., Graham, M.R., Yağmur, E.A., Šťáhlavský, F., Poverennyi, N.M., & Novruzov, N.E. (2022). A revision of the genus *Mesobuthus* Vachon, 1950, with a description of 14 new species (Scorpiones: Buthidae). *Euscorpius*, 348, 1-189.

Kovařík, F., Yağmur, E.A., Fet, V., & Hussen, F.S. (2019). A review of *Orthochirus* from Turkey, Iraq, and Iran (Khoozestan, Ilam, and Lorestan Provinces), with descriptions of three new species (Scorpiones: Buthidae). *Euscorpius*, 2019(278), 1-31.

Levy, G., & Amitai, P. (1980). *Fauna Palaestina. Arachnida I: Scorpiones.*

Lourenço, W.R. (2022). A new subgenus and species of *Leiurus* Ehrenberg, 1828 from Iraq (Scorpiones: Buthidae). *Serket*, 18(4), 421-427.

Lourenço, W.R., & Qi, J.-X. (2007). Description of a new species of the genus *Hottentotta* Birula, 1908 (Scorpiones: Buthidae) from Iraq. *Zoology in the Middle East*, 41(1), 99-104.

Polis, G. A. (1990). *The biology of scorpions*.

Prendini, L., & Wheeler, W.C. (2005). Scorpion higher phylogeny and classification, taxonomic anarchy, and standards for peer review in online publishing. *Cladistics*, 21(5), 446-494.

Rein, J.O. (2025). *The Scorpion Files*. Trondheim: Norwegian University of Science and Technology. Retrieved from https://www.ntnu.no/ub/scorpion-files /

Shahsavarinia, K., Taghizadieh, A., Ghaffarzad, A., Shariati, A., & Rahmani, F. (2017). Epidemiological and clinical status of patients with scorpion sting: emergency department of Sina hospital in Tabriz-Iran. *Journal of emergency practice and Trauma*, 3(1), 18-21.

Štundlová, J., Šťáhlavský, F., Opatova, V., Stundl ,J., Kovařík, F., Dolejš, P., & Šmíd, J. (2022). Molecular data do not support the traditional morphology-based groupings in the scorpion family Buthidae (Arachnida: Scorpiones). *Molecular Phylogenetics and Evolution*, 173, 107511.

Yağmur, E.A., Kovařík, F., Fet, V., Kurt, R., Hussen, F. S., Al-Khazali, A.M., ... & Al-Fanharawi, A.A. (2024). New records of *Mesobuthus mesopotamicus* (Penther, 1912) in Iraq and *Mesobuthus faiki* sp. nov. from Turkey (Scorpiones: Buthidae). *Euscorpius*, 2024(388), 1-22.

Commagene Journal of Biology

Deveci et al., (2025) *Comm. J. Biol.* 9(1), 71-79.
DOI: 10.31594/commagene.1607811

e-ISSN 2602-456X

Research Article/Araştırma Makalesi

The Preliminary Study on Phytochemical Profile and Antioxidant and Cytotoxic Activities of Harmal (*Peganum harmala* L.)

Ebru DEVECI*[1], Bahar YILMAZ ALTINOK[2], Gülsen TEL-ÇAYAN[3]

[1]*Chemistry and Chemical Processing Technology Department, Technical Sciences Vocational School, Konya Technical University, Konya, TÜRKİYE*
[2]*Department of Bioengineering, Faculty of Engineering, Karamanoğlu Mehmetbey University, Karaman, TÜRKİYE*
[3]*Department of Chemistry and Chemical Processing Technologies, Muğla Vocational School, Muğla Sıtkı Koçman University, Muğla, TÜRKİYE*
ORCID ID: Ebru DEVECI: https://orcid.org/0000-0002-2597-9898; Bahar YILMAZ ALTINOK: https://orcid.org/0000-0002-6315-3018; Gülsen TEL-ÇAYAN: https://orcid.org/0000-0002-1916-7391

Received: 26.12.2024 **Accepted:** 22.04.2025 **Published online:** 26.05.2025 **Issue published:** 30.06.2025

Abstract: Harmal (*Peganum harmala* L.) is a perennial plant that has come to the fore with its medicinal use since ancient times. In this study, the phytochemical profile of the methanol extract of harmal was characterized by HPLC and total phenolic and flavonoid amounts were determined by spectrophotometric methods. Additionally, antioxidant and cytotoxic (HT-29 (human colon cancer line), HeLa (human cervical cancer line), and HEK-293 (human embryonic kidney 293)) activities were investigated. Among 20 different phytochemical compounds screened, the presence of catechin (2.65±0.01 mg/g), coumarin (0.96±0.01 mg/g), ascorbic acid (0.91±0.02 mg/g), protocatechuic acid (0.85±0.01 mg/g), gallic acid (0.60±0.01 mg/g), hesperidin (0.24±0.01 mg/g), ferulic acid (0.06±0.01 mg/g), rutin (0.04±0.01 mg/g), and *trans*-cinnamic acid (0.03±0.01 mg/g) were detected. Total phenolic amount was found as 63.80±0.13 µg GAE/mg extract and total flavonoid amount was found as 13.50±0.36 µg QE/mg extract. Harmal methanol extract showed varying degrees of antioxidant activity in $ABTS^{\bullet+}$ (IC_{50}: 353.67±1.10 µg/mL), $DPPH^{\bullet}$ (17.54±0.45%), CUPRAC (absorbance: 0.41±0.02), phosphomolybdenum ($A_{0.50}$: 99.11±0.02 µg/mL), and metal chelating (38.47±0.77%) assays. Harmal methanol extract was low cytotoxic active on HT-29 cell line (> 800 µg/mL) and near-positive control cytotoxic active on HeLa cell line (IC_{50}: 45.84±0.95 µg/mL). These findings highlight harmal as a valuable reserve in the search for natural antioxidant and cytotoxic (on HeLa cell line) agents, especially with respect to the research focusing on possible pharmaceutical and food additive applications.

Keywords: Plant, HT-29 cell line, Methanol extract, HeLa cell line, HEK-293 cell line, HPLC.

Üzerlik (*Peganum harmala* L.) Bitkisinin Fitokimyasal Profili, Antioksidan ve Sitotoksik Aktiviteleri Üzerine Ön Çalışma

Öz: Üzerlik (*Peganum harmala* L.), antik çağlardan beri tıbbi kullanımı ile ön plana çıkan çok yıllık bir bitkidir. Bu çalışmada, üzerliğin metanol ekstresinin fitokimyasal profili HPLC ile karakterize edildi ve toplam fenolik ve flavonoid miktarları spektrofotometrik yöntemlerle belirlendi. Ayrıca, üzerliğin antioksidan ve sitotoksik (HT-29 (insan kolon kanseri hattı), HeLa (insan servikal kanser hattı) ve HEK-293 (insan embriyonik böbrek 293)) aktiviteleri araştırıldı. Taranan 20 farklı fitokimyasal bileşik arasında kateşin (2,65±0,01 mg/g), kumarin (0,96±0,01 mg/g), askorbik asit (0,91±0,02 mg/g), protokateşik asit (0,85±0,01 mg/g), gallik asit (0,60±0,01 mg/g), hesperidin (0,24±0,01 mg/g), ferulik asit (0,06±0,01 mg/g), rutin (0,04±0,01 mg/g) ve *trans*-sinnamik asit (0,03±0,01 mg/g) varlığı belirlendi. Toplam fenolik madde miktarı 63,80±0,13 µg GAE/mg ekstre ve toplam flavonoid miktarı 13,50±0,36 µg QE/mg ekstre olarak bulundu. Üzerlik metanol ekstresi, $ABTS^{\bullet+}$ (IC_{50}: 353,67±1,10 µg/mL), $DPPH^{\bullet}$ (%17,54±0,45), CUPRAC (absorbans: 0,41±0,02), fosfomolibden ($A_{0,50}$: 99,11±0,02 µg/mL) ve metal kelatlama (%38,47±0,77) yöntemlerinde değişen derecelerde antioksidan aktivite gösterdi. Üzerlik metanol ekstresi HT-29 hücre hattında (> 800 µg/mL) düşük sitotoksik aktiviteye sahipken, HeLa hücre hattında (IC_{50}: 45,84±0,95 µg/mL) pozitif kontrole yakın sitotoksik aktivite gösterdi. Bu bulgular, üzerliğin özellikle olası ilaç ve gıda katkı maddesi uygulamalarına odaklanan araştırmalar açısından doğal antioksidan ve sitotoksik (HeLa hücre hattına karşı) ajanların arayışında değerli bir rezerv olduğunu ortaya koymaktadır.

Anahtar kelimeler: Bitki, HT-29 hücre hattı, Metanol ekstresi, HeLa hücre hattı, HEK-293 hücre hattı, HPLC.

1. Introduction

Plants are hidden gems of bioactive compounds with a wide range of bioactive properties. These bioactive compounds produced in plants because of normal metabolic pathways are generally classified as secondary metabolites (Altemimi et al., 2017). Throughout history, mankind has relied on plants, which are the center of bioactive compounds, to address and eliminate many diseases (Davis & Choisy, 2024). These therapeutic benefits of plants have led to their inclusion in both traditional and modern medical practices from ancient times to the contemporary health system today. Medicines obtained from medicinal plants have different chemical and biological properties that make them remarkable in the field (Balkrishna et al., 2024). Their increasing global recognition is related to their capacity to supply natural solutions for diseases and contribute to the progress of health care. In determining the potential of a plant, not only the nutritional importance of that plant but also its medicinal properties should be properly recognized, thus providing a valuable contribution to general health and

Corresponding author: edeveci@ktun.edu.tr

disease prevention (Alves & Rosa, 2007). Extraction of bioactive components of plants provides raw materials for the pharmaceutical and cosmetic industries. Biomedical research is based on comprehensive studies on the phytochemical profile and biological mechanisms of plant species or specific compounds found in plants. Thus, the research conducted is extremely important in identifying new biological resources that can be used for disease prevention and therapeutic interventions (Hasan et al., 2024).

Cancer is one of the leading causes of death worldwide. Despite great efforts to discover effective chemotherapy drugs, there are still unsolved toxicity and selectivity problems (Chunarkar-Patil et al., 2024). The toxicity of modern chemotherapy and the resistance of cancer cells to anti-cancer agents lead to the search for new methods for the treatment or prevention of this insidious disease (Liu et al., 2024). Plants are the basic building blocks leading to the development of new anti-cancer drugs. In the last 20 years, more than a quarter of new drug molecules have been obtained from plant sources and the other quarter are their chemically modified derivatives (Grigalius & Petrikaite, 2017). Today, approximately half of the approved drugs are of natural origin (Asma et al., 2022).

Reactive oxygen species (ROS) is a collective term often used for unstable and reactive molecules derived from oxygen during cellular metabolism. Cells can produce ROS through various endogenous and exogenous mechanisms (Gu et al., 2024). Excessive ROS production leads to oxidative stress, which can have toxic effects on DNA, proteins, lipids, and other biomolecules, resulting in cell apoptosis or ferroptosis (Hayes et al., 2020). Furthermore, increased oxidative stress may contribute to tumor progression by directly oxidizing macromolecules or aberrant redox signaling resulting from oxidative stress, triggering tumor development (An et al., 2024). Studies have shown that high ROS levels may increase the risk of cancer when antioxidants are insufficient to protect cells from oxidative stress. In this context, the use of antioxidants in the treatment of cancer is an attractive strategy, as oxidative stress plays an important role in carcinogenesis and cancer progression (Ladas et al., 2004; Luo et al., 2022).

Harmal (*Peganum harmala* L.) belongs to *Zygophyllales* genus and Zygophyllaceae family. Harmal is a medicinal plant that grows naturally in South Asia and North Africa in general and used in traditional medicine as a decoction, powder and infusion for diarrhea, abortion, asthma, lumbago, and other ailments in Türkiye, Syria, Iran, Pakistan, India, Egypt, and Spain. This plant species is also known for its specific polyphenolic and alkaloid compounds (Asgarpanah & Ramezanloo, 2012). Antibacterial, antileishmanial, antiviral, antidiabetic, antitumor, antioxidant, insecticidal, cytotoxic, antifungal, hepatoprotective, and antinociceptive effects have been emphasized in earlier studies (Moloudizargari et al., 2013). This study was designed to investigate the phytochemical profile and bioactive properties of the methanol extract of harmal. For this purpose, the phytochemical profile of harmal was characterized by HPLC and the total amounts of phenolic and flavonoid were determined. In addition, antioxidant and cytotoxic activities of harmal were also tested.

2. Material and Method

2.1. Plant Material and Extraction

Harmal (*Peganum harmala* L.) was purchased from the local herbal market of Konya-Türkiye. The aerial parts of the plant sample, which were cut into small pieces, were extracted with methanol for 24 h at room temperature according to the maceration method. After the mixture was filtered, the residue was extracted with methanol 3 more times using the same method. All the methanol phases obtained were combined and evaporated in a rotary evaporator. Thus, methanol extract was obtained.

2.2. Phytochemical Profile

Phytochemical profile of harmal methanol extract was characterized by using HPLC. C_{18} column (5 µm, 250 mm × 4.6 mm i.d) (Ace Generix reverse phase) was preferred to sperate phytochemicals. The oven temperature was 30°C, solvent flow rate was 0.8 mL/min, and sample injection volume was 10 µL. The mobile phases consisted of 0.1% phosphoric acid in water (A) and acetonitrile (B). The elution gradient was as follows: 0-7 min, 0-17% B; 7-20 min, 17-15% B; 20-24 min, 15-20% B; 24-28 min, 20-25% B; 28-30 min, 25-30% B; 30-32 min, 30-40% B; 32-36 min, 40-50% B; 36-40 min, 50-70% B; 40-45 min, 70-17% B. Detection was operated via photodiode array detector (PDA) at 280 nm wavelength. Retention times and UV data were matched with commercial standards to identify the compounds. Three parallel analyses were practiced. The known concentrations of different standard compounds i.e. rutin, naringin, ascorbic acid, hesperidin, gallic acid, flavone, protocatechuic acid, catechin, *p*-hydroxy benzoic acid, vanillic acid, gentisic acid, *p*-coumaric acid, ferulic acid, *o*-coumaric acid, neohesperidin, resveratrol, quercetin, coumarin, *trans*-cinnamic acid, and alizarin were injected and calibration curves were obtained for the quantitative analysis of the phytochemical compounds (Deveci et al., 2023).

2.3. The Amounts of Total Phenolic and Total Flavonoid

Folin Ciocalteu assay was applied to experience of total phenolic amount of harmal methanol extract (Slinkard & Singleton, 1977). 1 mL harmal methanol extract, positive control or control solution, 46 mL distillated water, and 1 mL FCR were mixed. After 3 min, 3 mL Na_2CO_3 solution was added and the mixture was shaken for 2 h at room temperature. The absorbance was read at 760 nm. The result was given as µg gallic acid equivalent (GAE).

Aluminium nitrate assay was applied to experience of total flavonoid amount of harmal methanol extract (Park et al., 1997). 100 µL harmal methanol extract, positive control or control solution, 4.8 mL ethanol, 100 µL potassium acetate and 100 µL aluminium nitrate solution were added. The mixture was shaken for 40 min at room temperature. The absorbance was read at 415 nm. The result was given as µg quercetin equivalent (QE).

2.4. Antioxidant Activity

Antioxidant activity was investigated by DPPH$^{\bullet}$ and ABTS$^{\bullet+}$ scavenging, phosphomolybdenum, cupric reducing antioxidant capacity (CUPRAC), and metal chelating assays. Ascorbic acid, α-tocopherol, BHA, and

EDTA were used as positive controls. The results were presented as inhibition percentages (%) and absorbance at 800 µg/mL concentration, IC_{50} and $A_{0.50}$ values.

2.4.1. DPPH• Scavenging Activity

DPPH• scavenging assay was applied to experience of antioxidant activity of harmal methanol extract as stated in our prior study (Deveci et al., 2024). 40 µL harmal methanol extract, control or positive control solution and 160 µL DPPH• solution were mixed and the absorbance was read at 517 nm after 30 min.

2.4.2. ABTS•+ Scavenging Activity

ABTS•+ scavenging assay was applied to experience of antioxidant activity of harmal methanol extract as stated in our prior study (Deveci et al., 2024). 40 µL harmal methanol extract, control or positive control solution and 160 µL ABTS•+ solution were mixed and the absorbance was read at 734 nm after 10 min.

2.4.3. CUPRAC Activity

CUPRAC assay was applied to experience of antioxidant activity of harmal methanol extract as stated in our prior study (Deveci et al., 2024). 50 µL $CuCl_2$, 60 µL NH_4Ac buffer, 50 µL neocuproine, and 40 µL harmal methanol extract, control or positive control solution were mixed. The absorbance was read at 450 nm after 1 h.

2.4.4. Metal Chelating Activity

Metal chelating assay was applied to experience of antioxidant activity of harmal methanol extract as stated in our prior study (Deveci et al., 2024). 80 µL harmal methanol extract, control or positive control solution, 40 µL $FeCl_2$, and 80 µL ferene were mixed and the absorbance was read at 593 nm.

2.4.5. Phosphomolybdenum Reducing Antioxidant Power

Phosphomolybdenum assay was applied to experience of antioxidant activity of harmal methanol extract as stated in our prior study (Deveci et al., 2024). 300 µL harmal methanol extract, control or positive control solution and 3 mL the reagent solution (H_2SO_4, Na_3PO_4, $(NH_4)_6Mo_7O_{24}$) were incubated for 90 min at 95°C. When the mixture cooled to the room temperature, the absorbance was read at 695 nm.

2.5. Cytotoxic Activity

Alamar blue assay was applied to experience of cytotoxic activity of harmal methanol extract on HT-29 (human colon cancer line), HeLa (human cervical cancer line), and HEK-293 (human embryonic kidney 293) (Yılmaz, 2022). Cells previously stored at -80°C were thawed in a water bath, centrifuged, and then placed in the growth medium. In the incubation of the cells, DMEM (10% FBS, 1% penicillin-streptomycin, 0.01% gentamicin) and RPMI (10% FBS, 1% penicillin-streptomycin, 0.01% gentamicin) media were used in a 5% CO_2 atmosphere at 37°C. As a result of obtaining active cells that reached sufficient capacity, the cells were transferred to the transition media, washed with PBS, and the cells were separated from the surface by trypsinization. The obtained cell pellets were diluted in the appropriate medium and then transferred to fresh cell culture dishes. Cytotoxic activity was performed based on Alamar Blue assay. 37°C and 5% CO_2 environment was used in the incubation of cell lines seeded in 96-well plates. After removal of the growth medium, harmal methanol extract, control or positive control was added to each well and incubation continued. Alamar Blue® reagent was added after 18 h and incubated for 4 h. Absorbance was read at 570 nm and 600 nm. Cisplatin and doxorubicin were used as positive controls. The results were presented as cell growth (%) and IC_{50} values.

2.6. Statistical analysis

All results were the average of three parallel sample measurements and presented as the mean ± S.E. (standard error). Student's *t* test was used to analyze significant differences and *p* values <0.05 were accepted as significant.

3. Results

Phytochemical profile of harmal methanol extract was screened by HPLC. The HPLC chromatogram of the standards is given in Figure 1 and harmal methanol extract in Figure 2. Table 1 shows the analyzed and identified compounds. The presence of catechin (2.65±0.01 mg/g), coumarin (0.96±0.01 mg/g), ascorbic acid (0.91±0.02 mg/g), protocatechuic acid (0.85±0.01 mg/g), gallic acid (0.60±0.01 mg/g), hesperidin (0.24±0.01 mg/g), ferulic acid (0.06±0.01 mg/g), rutin (0.04±0.01 mg/g), and *trans*-cinnamic acid (0.03±0.01 mg/g) were detected in harmal methanol extract.

Total phenolic and flavonoid amounts of harmal methanol extract were spectrophotometrically tested. As seen in Table 2, when total phenolic amount was found as 63.80±0.13 µg GAE/mg extract, total flavonoid amount was found as 13.50±0.36 µg QE/mg extract.

Since antioxidants exhibit various mechanisms of action, five different methods (DPPH• and ABTS•+ scavenging, phosphomolybdenum, CUPRAC, metal chelating) were used here to better determine antioxidant activity. The results are given in Table 3. Harmal methanol extract was found as antioxidant active in all assays with IC_{50} value as 353.67±1.10 µg/mL in ABTS•+ scavenging assay, $A_{0.50}$ value as 99.11±0.02 µg/mL in phosphomolybdenum assay, absorbance as 0.41±0.02 in CUPRAC assay, inhibition values as 17.54±0.45% and 38.47±0.77% in DPPH• scavenging and metal chelating assays at 800 µg/mL, respectively.

Cytotoxic activity of harmal methanol extract was investigated according to Alamar blue assay. The cell growth values of HT-29, HeLa, and HEK-293 cell lines attained from treated different concentrations of harmal methanol extract and the positive controls are represented in Figure 3. The dose-dependent inhibition was obtained in all cancer lines. Table 4 shows the IC_{50} values for harmal methanol extract and positive controls. The cell growth value of harmal methanol extract was recorded as 59.51±2.24% on HT-29 cell line, 0.85±0.20% on HeLa cell line, and 88.33±1.26% on HEK-293 cell line at 800 µg/mL. When harmal methanol extract was found as very low active on HT-29 cell line with IC_{50} > 800 µg/mL, harmal methanol extract indicated near-positive control (IC_{50}: 31.02±0.05 µg/mL for cisplatin) cytotoxicity on HeLa cell line with IC_{50} of 45.84±0.95 µg/mL.

Table 1. Phytochemical profile (mg/g extract) of harmal methanol extract

Peak number	Compounds	Retention time (min)	Harmal
1	Ascorbic acid	3.372	0.91±0.02
2	Gallic acid	4.191	0.60±0.01
3	Protocatechuic acid	5.693	0.85±0.01
4	Catechin	6.518	2.65±0.01
5	*p*-Hydroxy benzoic acid	8.573	nd
6	Vanillic acid	9.722	nd
7	Gentisic acid	10.355	nd
8	*p*-Coumaric acid	17.214	nd
9	Rutin	19.084	0.04±0.01
10	Ferulic acid	20.223	0.06±0.01
11	Naringin	27.374	nd
12	*o*-Coumaric acid	28.686	nd
13	Neohesperidin	29.581	nd
14	Coumarin	30.805	0.96±0.01
15	Resveratrol	32.399	nd
16	Quercetin	34.732	nd
17	*trans*-Cinnamic acid	35.603	0.03±0.01
18	Hesperidin	36.702	0.24±0.01
19	Alizarin	38.661	nd
20	Flavone	40.769	nd

nd: Not detected.

Table 2. Total phenolic and flavonoid amounts of harmal methanol extract[a]

	Total phenolic amount (µg GAE/mg extract)[b]	Total flavonoid amount (µg QE/mg extract)[c]
Harmal	63.80±0.13	13.50±0.36

[a] Values state the means ± S.E. of three repetitions.

[b] GAE, gallic acid equivalents. Absorbance=0.0077[GAE (µg)]-0.007 (r^2, 0.9995).

[c] QE, quercetin equivalents. Absorbance=0.0154[QE (µg)]-0.0543 (r^2, 0.9998).

Table 3. Antioxidant activity of harmal methanol extract[a]

		Harmal	α-Tocopherol[e]	BHA[e]	Ascorbic acid[e]	EDTA[e]
$ABTS^{\bullet+}$	Inhibition (%)[b]	75.74±0.47	94.96±0.53	95.89±0.10	90.70±0.04	NT[f]
	IC_{50}[c]	353.67±1.10	38.51±0.54	11.82±0.18	5.24±0.18	NT[f]
$DPPH^{\bullet}$	Inhibition (%)[b]	17.54±0.45	96.12±0.42	96.05±0.08	89.65±0.03	NT[f]
	IC_{50}[c]	>800	37.20±0.41	19.80±0.36	6.68±0.94	NT[f]
CUPRAC	Absorbance[d]	0.41±0.02	2.93±0.16	3.50±0.04	3.42±0.01	NT[f]
	$A_{0.50}$[c]	>800	89.47±0.87	24.51±0.47	20.67±0.01	NT[f]
Phosphomolybdenum	Absorbance[d]	1.68±0.03	NT[f]	NT[f]	3.65±0.01	NT[f]
	$A_{0.50}$[c]	99.11±0.02	NT[f]	NT[f]	13.66±0.19	NT[f]
Metal chelating	Inhibition (%)[b]	38.47±0.77	NT[f]	NT[f]	NT[f]	96.30±0.11
	IC_{50}[c]	>800	NT[f]	NT[f]	NT[f]	3.50±0.44

[a] Values represent the means ± S.E. of three parallel measurements ($p < 0.05$); [b] Inhibition (%) at 800 µg/mL concentration; [c] Results were given as µg/mL; [d] Absorbance at 800 µg/mL concentration; [e] Positive controls; [f] NT: not tested.

Table 4. Cytotoxic activity of harmal methanol extract[a]

	HT-29[b]	HeLa[b]	HEK-293[b]
Harmal	>800	45.84±0.95	>800
Cisplatin[c]	14.75±0.87	31.02±0.05	NT[d]
Doxorubicin[c]	15.56±0.96	19.78±0.02	NT[d]

[a] Values represent the means ± S.E. of three parallel measurements ($p < 0.05$); [b] IC_{50} results were given as µg/mL; [c] Positive controls; [d] NT: not tested.

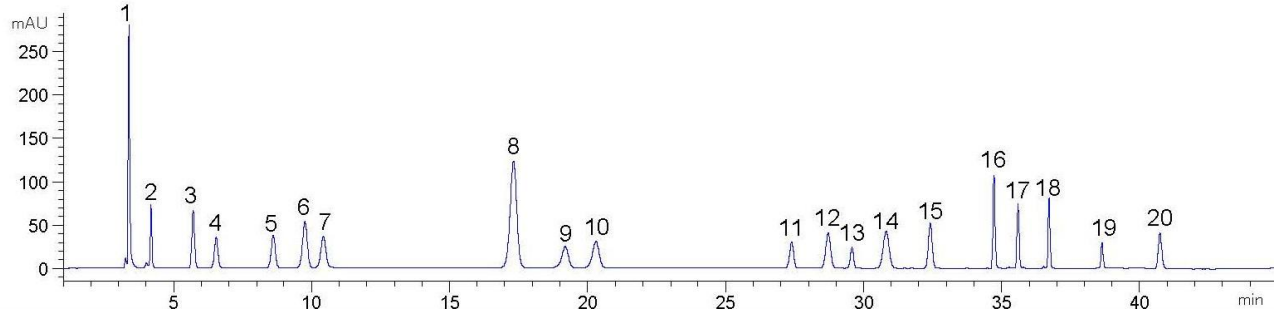

Figure 1. HPLC chromatogram of the standards

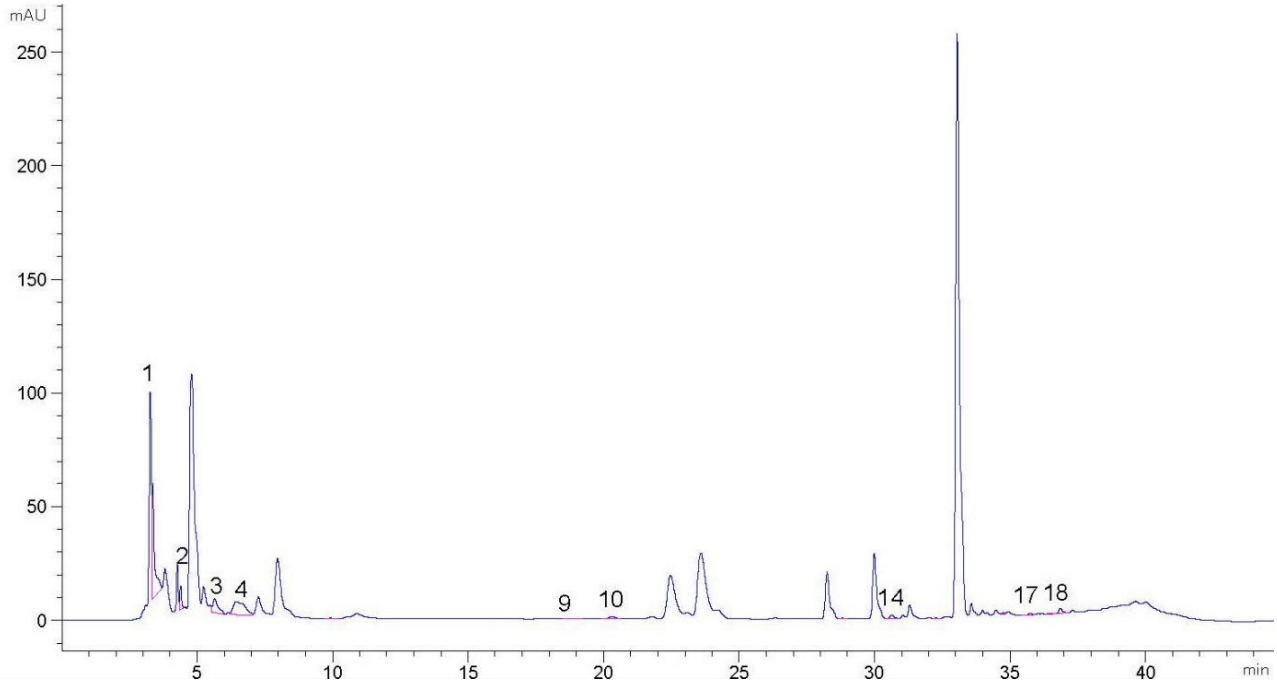

Figure 2. HPLC chromatogram of harmal methanol extract

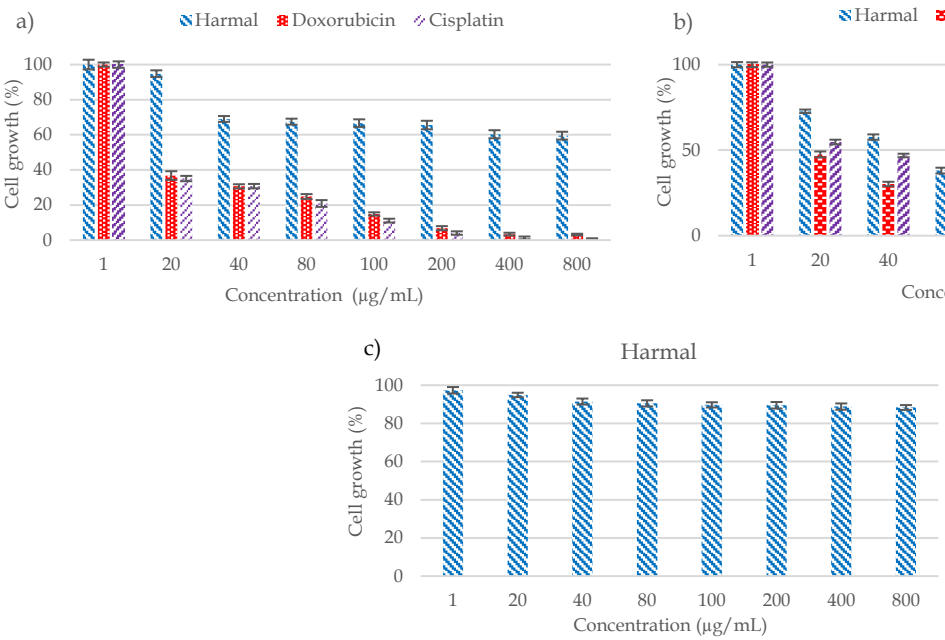

Figure 3. The cell growth values (%) of harmal methanol extract a) HT-29 cell line b) HeLa cell line c) HEK-293 cell line

4. Discussion

Phytochemical profile of harmal methanol extract was screened by HPLC. Among 20 phytochemical compounds analyzed, the presence of catechin, coumarin, ascorbic acid, protocatechuic acid, gallic acid, hesperidin, ferulic acid, rutin, and *trans*-cinnamic acid were detected. As

similar to our findings, gallic acid (0.02%), ascorbic acid (2.84%), quercetin (14.82%), butylated hydroxytoluene (0.41%), chlorogenic acid (0.26%), kaempferol (0.66%), hesperidin (2.04%), folic acid (3.33%), β-carotene (0.32%), naringenin (0.27%), hydroxy coumarin (0.10%), coumaric acid (70.61%), vanillin (1.77%), maleic acid (2.25%), and benzoic acid (0.23%) were identified in the butanol extract of harmal seeds from Algeria by UPLC-ESI-MS-MS (Kemel et al., 2024). In line with the results here, gallic acid (4.660 ppm), quercetin (2.747 ppm), caffeic acid (12.280 ppm), vanillic acid (13.253 ppm), chlorogenic acid (15.847 ppm), syringic acid (16.740 ppm), *p*-coumaric acid (17.767 ppm), *m*-coumaric acid (20.580 ppm), ferulic acid (22.280 ppm), cinnamic acid (25.133 ppm), and sinapic acid (26.060 ppm) were revealed as the phenolic acids in the leaves of harmal (Punjap-Pakistan) water extract by HPLC (Nazir et al., 2024). The synergic mixture (a mixture containing water, ethanol, acetone, chloroform, and hexane extracts) of harmal leaves from Pakistan was characterized by HPLC. Consistent with our results, the presence of ascorbic acid (261.97 µg/mL), caftaric acid (258.47 µg/mL), rosmeric acid (270.12 µg/mL), kaempferol (255.33 µg/mL), gallocatechin (270.03 µg/mL), caffeic acid (263.30 µg/mL), 3,4-*O*-dicaffeoylquinic acid (264.59 µg/mL), chrysin (268.14 µg/mL), catechin (270.17 µg/mL), chlorogenic acid (276.46 µg/mL), sinapic acid hexoside (327.41 µg/mL), kaempferol-*O*-dirhamnoside (494.80 µg/mL), chicoric acid (448.52 µg/mL), orientin (803.10 µg/mL), chebulic acid (503.83 µg/mL), malvidin-3-*O*-glucoside (538.18 µg/mL), and di-*O*-methyl ellagic acid (515.47 µg/mL) were observed (Kamran et al., 2024). Protocatechuic (51.6 mg/100 g), hydrocaffeic (199.4 mg/100 g), caffeic (20.6 mg/100 g), and rosmarinic (18.9 mg/100 g) acids, and luteolin-7-glucoside (713.5 mg/100 g) were characterized in the methanol extract of harmal leaves (from Saudi Arabia) by LC (Elansary et al., 2020a). In a different study on harmal seeds from Türkiye, interestingly, catechin (1.32 µg/g), luteolin (0.20 µg/g), and naringenin (0.38 µg/g) were identified in harmal hexane extract; only epicatechin (9.41 µg/g) in harmal ethanol extract; epicatechin (67.34 µg/g), naringin (0.17 µg/g), luteolin (0.1 µg/g), and naringenin (0.58 µg/g) in harmal water extract by HPLC (Gür et al., 2018). The basis of the differences between the findings here and the literature are not only the changes in the collection areas of the plant but also the agricultural, geographical, and seasonal factors that affect the phytochemical composition (Liu et al., 2022).

Phenolic compounds constitute the most important phytochemical compound class of plants due to the scavenging effects of hydroxyl groups on free radicals. These properties of phenolic compounds directly contribute to the antioxidant activities of plants (Tosun et al., 2009). Total phenolic and flavonoid amounts of harmal methanol extract were spectrophotometrically tested. When total phenolic amount of harmal methanol extract was found as 63.80±0.13 µg GAE/mg extract, total flavonoid amount was found as 13.50±0.36 µg QE/mg extract. The current findings are consistent with those of Mazandarani et al. (2012), who found 61.55 mg GAE/g extract of total phenolic content and 42.21 mg QE/g extract of total flavonoid content in the ethanol extract of harmal seeds from Iran. The study of Abbas et al. (2021) showed that harmal fruits from Pakistan had higher amounts of total phenolic compounds in dichloromethane (106.0 mg GAE/g), methanol (371.4 mg GAE/g), and 70% methanol (142.3 mg GAE/g) extracts and lower amounts of total flavonoid compounds in dichloromethane (0.31 mg QE/g), methanol (1.3 mg QE/g), and 70% methanol (0.81 mg QE/g) extracts than our findings. The higher amounts of total phenolic (144.97, 197.23, 237.23, and 111.25 µg GAE/mg, respectively) and flavonoid (43.62, 57.98, 82.58, and 22.36 µg QE/mg, respectively) compounds were reported in the methanol extract and butanol, ethyl acetate, and chloroform fractions of harmal seeds from Algeria (Nait Marzoug et al., 2023).

Herein, antioxidant activity of harmal methanol extract was analyzed by five different complementary methods (DPPH$^{\bullet}$ scavenging, ABTS$^{\bullet+}$ scavenging, CUPRAC, phosphomolybdenum, and metal chelating methods). Harmal methanol extract was found to be a high antioxidant active in all assays. Coumarins have been included in pharmaceutical products with their versatile antithrombotic, anti-inflammatory, antioxidant, antimicrobial, antiviral, anti-cancer, and neuroprotective pharmacological profiles and in perfumes and food products with their odor and flavor enhancing profiles (Elmusa & Elmusa, 2024). Coumarins have been reported to be promising super antioxidants for many synthetic antioxidant drugs, especially those that act by stopping DNA oxidation and scavenging radicals (Wang et al., 2020). Catechin is an important active antioxidant compound that acts by stopping reactive oxygen species, increasing antioxidant enzymes, inhibiting pro-enzymes involved in oxidative stress or chelating metals, in addition to its other bioactive abilities (Sheng et al., 2023). Ascorbic acid is a promising nutraceutical found naturally in plants and foods, exhibiting a wide range of medical or health benefits. It is a powerful antioxidant that protects cell membranes, DNA, and tissues from oxidative damage. Ascorbic acid interacts with free oxygen ions, superoxide ions, and hydroxyl ions with free radical properties, thereby stopping the formation of inflammation, carcinogens, and other factors that aggravate photoaging in the skin. It plays a critical role in maintaining health and fighting diseases and infections, especially with its prominent antioxidant properties (Ali et al., 2024). Multifaceted *in vivo* and *in vitro* studies have emphasized that the excellent antioxidant activity of protocatechuic acid is based on its ability to increase endogenous antioxidant enzyme activity and radical scavenging (Zhang et al., 2021). This antioxidant activity exhibited by harmal may be the result of a synergy of the high amounts of these compounds and other compounds identified in its content. In previous literature studies, antioxidant effect of harmal was mainly examined according to the radical scavenging methods. The similar DPPH$^{\bullet}$ scavenging activity was stated in harmal aerial parts (from Tunisia) methanol extract with IC_{50} value of 6 mg/mL and moderate antioxidant activity was also described in harmal petroleum ether (IC_{50}: 1.25 mg/mL), chloroform (IC_{50}: 3.25 mg/mL), ethyl acetate (IC_{50}: 0.850 mg/mL), and butanol (IC_{50}: 0.350 mg/mL) extracts (Edziri et al., 2010). It has been informed that the ethanol extract of harmal seeds (from Iran) exhibited antioxidant activity in DPPH$^{\bullet}$ scavenging (IC_{50}: 53.64 mg/mL), reducing power (IC_{50}: 84.75 mg/mL) and total antioxidant capacity (IC_{50}: 17.34 mg/mL) assays, supporting our results (Mazandarani et al., 2012). Higher DPPH$^{\bullet}$ scavenging activity was reported

in harmal fruits (from Pakistan) dichloromethane (IC_{50}: 146 µg/mL), methanol (IC_{50}: 49 µg/mL), and 70% methanol (IC_{50}: 69 µg/mL) extracts. Also, in the same study, harmal dichloromethane, methanol, and 70% ethanol extracts were reported as antioxidant active in FRAP (IC_{50}: 9.2, 39, 19.2 µg/mL) and H_2O_2 (25, 66, 43 %) assays (Abbas et al., 2021). The higher antioxidant activity was reported by Kemel et al. (2024) who observed that the butanol extract of harmal seeds from Algeria had 8.09 µg/mL IC_{50} value in $ABTS^{\bullet+}$ scavenging assay, 30.87 µg/mL IC_{50} value in $DPPH^{\bullet}$ scavenging assay, and 216.1 µg/mL OD_{50} value in FRAP assay. The methanol extract and butanol, ethyl acetate and chloroform fractions of harmal seeds from Algeria were investigated for antioxidant activity by using eight different assays. Harmal methanol extract and fractions were described as higher antioxidant than our results in $DPPH^{\bullet}$ scavenging (IC_{50}: 92.02-187.57 µg/mL), $ABTS^{\bullet+}$ scavenging (IC_{50}: 10.22-35.02 µg/mL), CUPRAC ($A_{0.50}$: 90.57-187.39 µg/mL), reducing power ($A_{0.50}$: 87.83-158.07 µg/mL), phenanthroline ($A_{0.50}$: 3.78-6.45 µg/mL), galvinoxyl radical scavenging (IC_{50}: 45.93-305.59 µg/mL), β-carotene bleaching (IC_{50}: 27.21-70.93 µg/mL), and ferrous ion chelating (> 800 µg/mL) assays (Nait Marzoug et al., 2023).

Cytotoxic activity of harmal methanol extract was investigated on HT-29, HeLa, and HEK-293 cell lines according to Alamar blue assay. Harmal methanol extract was found to have near-positive control cytotoxic activity against HeLa cell line and very low cytotoxicity on HT-29 cell line. In addition, harmal methanol extract did not possess any cytotoxicity on HEK-293 cell line. The high amounts of catechin, coumarin, ascorbic acid, and protocatechuic acid were found in harmal methanol extract among 20 phytochemical compounds analyzed. It has been presented that catechin caused apoptosis in HeLa cell line and was highly cytotoxic with an IC_{50} value of 22.91 µg/mL (Rahmaddiansyah et al., 2022). Chuang et al. (2007) demonstrated significant cytotoxic effect of coumarin by causing morphological changes and apoptosis in HeLa cell line with an IC_{50} of 54.2 µM. Ascorbic acid has been shown to have cytotoxicity on HeLa cell line with 202.3 µg/mL IC_{50} value (Abdullah et al., 2021). IC_{50} value of protocatechuic acid was calculated as 40.58 µg/mL on HeLa cell line in the study of Elansary et al. (2020b). This significant cytotoxic activity of harmal can be attributed to the identified phytochemicals mentioned above. Similar to our results, harmal (from Algeria) ethanol extract was recorded as potent cytotoxic active on HeLa cell line with 0.028 mg/mL IC_{50} value. In the same study, harmal seeds aqueous (IC_{50}: 0.230 mg/mL) and decoction (IC_{50}:0.242 mg/mL) extracts were poorly cytotoxic active on HeLa cell line (Mounira et al., 2022). In the study of Khalid et al. (2024), the two different harmal leaves (from Palestinian) ethanol extracts containing 100 µL DMSO and 500 µL DMSO were revealed as low cytotoxic active on HT-29 cell lines with 1350 and 841 mg/mL IC_{50} values, respectively. Elansary et al. (2020a) reported that while cytotoxic activity of harmal leaves methanol extract on HT-29 cell line (IC_{50}: 49.05 µg/mL) was higher than our result, cytotoxic activity on HeLa cell line (IC_{50}: 43.86 µg/mL) was similar to our result. Also, harmal methanol extract was found to be not cytotoxic against HEK-293 cell line (IC_{50}: > 400 µg/mL). The cytotoxicity of harmal seeds (from Palestine) water extract was investigated on COLO205 (IC_{50}: 150.01 µg/mL) and Caco-2 (IC_{50}: 308.35 µg/mL) colorectal cancer cell lines, HeLa cell line (IC_{50}: 155.60 µg/mL), and HEK-293 cell line (IC_{50}: 5.68 µg/mL) by Jaradat et al. (2024). In a different investigation on harmal (from India), isolated compounds harmine, harmaline, vasicinone, and vasicine were found as cytotoxic active on HeLa cell line with IC_{50} values of 61.81, 243.53, 368.57, 335.81 µM, respectively and on HT-29 cell line with IC_{50} values of 45.55, 218.33, 281.24, 291.61 µM, respectively (Ayoob et al., 2017).

5. Conclusion

Through this study, we characterized the phytochemical profile of harmal methanol extract by HPLC and determined the total phenolic and flavonoid amounts. We also focused on antioxidant and cytotoxic activities. Among a total of 20 significant phytochemical compounds, the presence of catechin, coumarin, ascorbic acid, protocatechuic acid, gallic acid, hesperidin, ferulic acid, rutin, and *trans*-cinnamic acid were detected. Harmal methanol extract was found to be rich in total phenolics and flavonoids. Moreover, harmal methanol extract was determined to have valuable antioxidant and cytotoxic (on HeLa cell line) activities comparable to positive controls. Although the results obtained here clearly indicate the possibility of using harmal as a promising antioxidant and cytotoxic agent (especially for cervical cancer), studies on animals and human patients need to be conducted and validated. These results can provide important guidance and can be used as a basis for the development of disease-focused drug discovery. In this context, screening of different bioactive properties of harmal and examination of phytochemicals related to these bioactive properties are needed for further research.

Ethics committee approval: Ethics committee approval is not required for this study.

Conflict of interest: The authors declare that there is no conflict of interest.

Author Contributions: Conception – E.D., G.T.Ç.; Design – E.D., G.T.Ç.; Supervision – E.D., G.T.Ç.; Fund – E.D., G.T.Ç.; Materials – E.D., G.T.Ç., B.Y.A.; Data Collection and Processing – E.D., G.T.Ç., B.Y.A.; Analysis Interpretation – E.D., G.T.Ç., B.Y.A.; Literature Review – E.D., G.T.Ç.; Writing – E.D., G.T.Ç., B.Y.A.; Critical Review – E.D., G.T.Ç., B.Y.A.

References

Abbas, M.W., Hussain, M., Qamar, M., Ali, S., Shafiq, Z., Wilairatana, P., & Mubarak, M.S. (2021). Antioxidant and anti-inflammatory effects of *Peganum harmala* extracts: An *in vitro* and *in vivo* study. *Molecules*, 26, 6084. https://doi.org/10.3390/molecules26196084

Abdullah, H., Mamat, N., Zakaria, N.M., Yunan, N.I.F.M., Hisham, M.I.N., & Hapidin, H. (2021). Combination effect of tamoxifen and ascorbic acid treatment on breast cancer cells (MCF-7) and cervical cancer cells (HeLa). *Jurnal Sains Kesihatan Malaysia*, 19(2), 1-6. https://doi.org/114.10.17576/jskm-2021-1902-12

Ali, A., Riaz, S., Khalid, W., Fatima, M., Mubeen, U., Babar, Q., …, & Madilo, F.K. (2024). Potential of ascorbic acid in human health against different diseases: An updated narrative review. *International Journal of Food Properties*, 27, 493-515. https://doi.org/10.1080/10942912.2024.2327335

Altemimi, A., Lakhssassi, N., Baharlouei, A., Watson, D.G., & Lightfoot, D.A. (2017). Phytochemicals: Extraction, isolation, and identification of bioactive compounds from plant extracts. *Plants*, 6(4), 42. https://doi.org/10.3390/plants6040042

Alves, R.R., & Rosa, I.M. (2007). Biodiversity, traditional medicine and public health: Where do they meet?. *Journal of Ethnobiology and Ethnomedicine*, 3, 14. https://doi.org/10.1186/1746-4269-3-14

An, X., Yu, W., Liu, J., Tang, D., Yang, L., & Chen, X. (2024). Oxidative cell death in cancer: mechanisms and therapeutic opportunities. *Cell Death & Disease,* 15, 556. https://doi.org/10.1038/s41419-024-06939-5

Asgarpanah, J., & Ramezanloo, F. (2012). Chemistry, pharmacology and medicinal properties of *Peganum harmala* L. *African Journal of Pharmacy and Pharmacology*, 6(22), 1573-1580. https://doi.org/10.5897/AJPP11.876

Asma, S.T., Acaroz, U., Imre, K., Morar, A., Shah, S.R.A, Hussain, S.Z., … & Ince, S. (2022). Natural products/bioactive compounds as a source of anticancer drugs. *Cancers (Basel),* 14(24), 6203. https://doi.org/10.3390/cancers14246203

Ayoob, I., Hazari, Y.M., Lone, S.H., Rehman, S., Khuroo, M.A., Fazili, K.M., …, & Bhat, K.A. (2017). Phytochemical and cytotoxic evaluation of *Peganum harmala*: Structure activity relationship studies of harmine. *Chemistry Select,* 2, 2965-2968. https://doi.org/10.1002/slct.201700232

Balkrishna, A., Sharma, N., Srivastava, D., Kukreti, A., Srivastava, S., & Arya, V. (2024). Exploring the safety, efficacy, and bioactivity of herbal medicines: bridging traditional wisdom and modern science in healthcare. *Future Integrative Medicine*, 3(1), 35-49. https://doi.org/10.14218/FIM.2023.00086

Chuang, J.Y., Huang, Y.F., Lu, H.F., Ho, H.C., Yang, J.S., Li, T.M., …, & Chung, J.G. (2007). Coumarin induces cell cycle arrest and apoptosis in human cervical cancer HeLa cells through a mitochondria- and caspase-3 dependent mechanism and NF-κB down-regulation. *In Vivo*, 21(6), 1003-1009.

Chunarkar-Patil, P., Kaleem, M., Mishra, R., Ray, S., Ahmad, A., Verma, D., …, & Kumar, S. (2024). Anticancer drug discovery based on natural products: from computational approaches to clinical studies. *Biomedicines,* 12(1), 201. https://doi.org/10.3390/biomedicines12010201

Davis, C.C., & Choisy, P. (2024). Medicinal plants meet modern biodiversity science. *Current Biology,* 34, R158-R173. https://doi.org/10.1016/j.cub.2023.12.038

Deveci, E., Tel-Çayan, G., Çayan, F., Yılmaz Altınok, B., & Aktaş, S. (2024). Characterization of polysaccharide extracts of four edible mushrooms and determination of *in vitro* antioxidant, enzyme inhibition and anticancer activities. *ACS Omega,* 9, 25887-25901. https://doi.org/10.1021/acsomega.4c00322

Deveci, E., Yılmaz Altınok, B., & Tel-Çayan, G. (2023). A study on phytochemical composition, antioxidant, and anti-cancer activities of *Gingko biloba* L. *Commagene Journal of Biology,* 7(2), 99-106. https://doi.org/10.31594/commagene.1322069

Edziri, H., Mastouri, M., Mahjoub, M.A., Patrich, G., Matieu, M., Ammar, S., …, & Aouni, M. (2010). Antibacterial, antiviral and antioxidant activities of aerial part extracts of *Peganum harmala* L. grown in Tunisia. *Toxicological & Environmental Chemistry,* 92(7), 1283-1292. https://doi.org/10.1080/02772240903450736

Elansary, H.O., Szopa, A., Kubica, P., Ekiert, H., Al-Mana, F.A., & El-Shafei, A.A. (2020a). Polyphenols of *Frangula alnus* and *Peganum harmala* leaves and associated biological activities. *Plants (Basel)*, 9(9), 1086. https://doi.org/10.3390/plants9091086.

Elansary, H.O., Szopa, A., Kubica, P., El-Ansary, D.O., Ekiert, H., & Al-Mana, F.A. (2020b). *Malus baccata* var. *gracilis* and *Malus toringoides* Bark polyphenol studies and antioxidant, antimicrobial and anticancer activities. *Processes,* 8, 283. https://doi.org/10.3390/pr8030283

Elmusa, F., & Elmusa, M. (2024). Mini-review on coumarins: Sources, biosynthesis, bioactivity, extraction and toxicology. *Journal of the Turkish Chemical Society Section A: Chemistry,* 11, 933-944. https://doi.org/10.18596/jotcsa.1419322

Grigalius, I., & Petrikaite, V. Relationship between antioxidant and anticancer activity of trihydroxyflavones. *Molecules,* 22(12), 2169. https://doi.org/10.3390/molecules22122169

Gu, X., Mu, C., Zheng, R., Zhang, Z., Zhang, Q., & Liang, T. (2024). The cancer antioxidant regulation system in therapeutic resistance. *Antioxidants,* 13, 778. https://doi.org/10.3390/antiox13070778

Gür, M., Güder, A., Verep, D., Güney, K., Özkan, O.E., Seki, N., & Kandemirli, F. (2018). Some important plants for epilepsy treatment: Antioxidant activity and flavonoid compositions. *Iranian Journal of Science and Technology, Transactions A: Science,* 42, 1847-1857. https://doi.org/10.1007/s40995-017-0361-3

Hasan, R., Haque, M.M., Hoque, A., Sultana, S., Rahman, M.M., Shaikh, A.A., & Sarker, K.U. (2024). Antioxidant activity study and GC-MS profiling of *Camellia sinensis* Linn. *Heliyon,* 10, e23514 https://doi.org/10.1016/j.heliyon.2023.e23514

Hayes, J.D., Dinkova-Kostova, A.T., & Tew, K.D. (2020). Oxidative stress in cancer. *Cancer Cell,* 38, 167-197. https://doi.org/10.1016/j.ccell.2020.06.001

Jaradat, N., Hawash, M., Sharifi-Rad, M., Shakhshir, A., Sobuh, S., Hussein, F., …, & Ibrahim, A.N. (2024). Insights into free radicals scavenging, α-amylase inhibition, cytotoxic and antifibrotic activities unveiled by *Peganum harmala* extracts. *BMC Complementary Medicine and Therapies,* 24, 299. https://doi.org/10.1186/s12906-024-04602-2

Kamran, M.Z., Din, M., Sahu, M.R., Ahmad, J., Bilal, Bilal, M., Jamil, N., Yasir, M., & Kanwal, Q. (2024). Bioactivities of Cholistani harmal (*Peganum harmala*) with exploration of bioactive phytochemicals. *International Journal of Chemical and Biochemical Sciences,* 25(19), 105-116. https://doi.org/10.62877/12-IJCBS-24-25-19-12

Kemel, H., Benguedouar, L., Boudjerda, D., Menadi, S., Cacan, E., & Sifour, E. (2024). Phytochemical profiling, cytotoxic, anti-migration, and anti-angiogenic potential of phenolic-rich fraction from *Peganum harmala*: *in vitro* and *in ovo* studies. *Medical Oncology*, 41, 144. https://doi.org/10.1007/s12032-024-02396-4

Khalid, M., Al-Rimawi, F., Darwish, S., Salah, Z., Alnasser, S.M., Wedian, F., …, & Al-Mazaideh, G.M. (2024). Assessment of the anticancer, antimicrobial, and antioxidant activities of the *Peganum harmala* L. plant. *Natural Product Communications*, 2024, 19(6), 1-10. https://doi.org/10.1177/1934578X241260597

Ladas, E.J., Jacobson, J.S., Kennedy, D.D., Teel, K., Fleischauer, A., & Kelly, K.M. (2004). Antioxidants and cancer therapy: A systematic review. *Journal of Clinical Oncology,* 22(3), 517-528. https://doi.org/10.1200/JCO.2004.03.086

Liu, B., Zhou, H., Tan, L., Siu, K.T.H., & Guan, X.Y. (2024). Exploring treatment options in cancer: Tumor treatment strategies. *Signal Transduction and Targeted Therapy,* 9, 175. https://doi.org/10.1038/s41392-024-01856-7

Liu, W., Zhang, Z., Zhang, T., Qiao, Q., & Hou, X. (2022). Phenolic profiles and antioxidant activity in different organs of *Sinopodophyllum hexandrum*. *Frontiers in Plant Science,* 13, 1037582. https://doi.org/10.3389/fpls.2022.1037582

Luo, M., Zhou, L., Huang, Z., Li, B., Nice, E.C., Xu, J., & Huang, C. (2022). Antioxidant therapy in cancer: Rationale and progress. *Antioxidants,* 11, 1128. https://doi.org/10.3390/antiox11061128

Mazandarani, M., Sepehr, K.S., Baradaran, B., & Khuri, V. (2012). Autecology, phytochemical and antioxidant activity of *Peganum harmala* L. seed extract in North of Iran (Tash Mountains). *Journal of Medicinal Plants and By-products,* 2, 151-156. https://doi.org/10.22092/jmpb.2012.108479

Moloudizargari, M., Mikaili, P., Aghajanshakeri, S., Asghari, M.H., & Shayegh, J. (2013). Pharmacological and therapeutic effects of *Peganum harmala* and its main alkaloids. *Pharmacognosy Reviews,* 7, 199-212. https://doi.org/10.4103/0973-7847.120524

Mounira, D., Abdelouahab, D., Widad, F., Riadh, B.M., Farid, B., & Ahmed, B. (2022). Cytotoxic, antioxidant and antimicrobial activities of *Peganum harmala* L. extracts. *Biotechnologia Acta,* 15, 61-71. https://doi.org/10.15407/biotech15.01.061

Nait Marzoug, A., Khaldi, F., Ayari, A., Gali, L., & Gheid, A. (2023). Antioxidant and anticholinesterase effects of methanol extract, and consecutive fractions of *Peganum harmala* L. *Egyptian Journal of Chemistry*, 66(6), 431-440. https://doi.org/10.21608/ejchem.2022.151986.6663

Nazir, F., Nawaz-ur-Rehman, S., Khadim, S., Amber, S., Ameen, F., Ahmad, … & Iqbal, M. (2024). Analytical characterization, antioxidant, antiviral and antimicrobial potential of selected medicinal plants. *Natural Product Communications,* 19(9), 1-15. https://doi.org/10.1177/1934578X241274986

Park, Y.K., Koo, M.H., Ikegaki, M., & Contado, J.L. (1997). Comparison of the flavonoid aglycone contents of *Apis mellifera* propolis from various regions of Brazil. *Brazilian Archives of Biology and Technology,* 40, 97-106.

Rahmaddiansyah, R., Hasani, S., Zikrah, A.A., & Arisanty, D. (2022). The effect of gambier catechin isolate on cervical cancer cell death (HeLa cell lines). *Open Access Macedonian Journal of Medical Sciences,* 10(B), 1293-1297. https://doi.org/10.3889/oamjms.2022.8779

Sheng, Y., Sun, Y., Tang, Y., Yu, Y., Wang, J., Zheng, F., …, & Sun, Y. (2023). Catechins: Protective mechanism of antioxidant stress in atherosclerosis. *Frontiers in Pharmacology*, 14, 1144878. https://doi.org/10.3389/fphar.2023.1144878

Slinkard, K., & Singleton, V.L. (1977) Total phenol analyses: Automation and comparison with manual methods. *American Journal of Enology and Viticulture*, 28, 49-55.

Tosun, M., Ercisli, S., Sengul, M., Ozer, H., & Polat, T. (2009). Antioxidant properties and total phenolic content of eight *Salvia* species from Turkey. *Biological Research,* 41, 175-181. https://doi.org/10.4067/S0716-97602009000200005

Wang, G., Liu, Y., Zhang, L., An, L., Chen, R., Liu, Y., …, & Xue, Y. (2020). Computational study on the antioxidant property of coumarin-fused coumarins. *Food Chemistry,* 304, 125446. https://doi.org/10.1016/j.foodchem.2019.125446

Yılmaz, B. (2022). Release of nifedipine, furosemide, and niclosamide drugs from the biocompatible poly (HEMA) hydrogel structures. *Turkish Journal of Chemistry,* 46(5), 1710-1722. https://doi.org/10.55730/1300-0527.3474

Zhang, S., Gai, Z., Gui, T., Chen, J., Chen, Q., & Li, Y. (2021). Antioxidant effects of protocatechuic acid and protocatechuic aldehyde: Old wine in a new bottle. *Evidence-Based Complementary and Alternative Medicine,* 8, 6139308. https://doi.org/10.1155/2021/6139308

Commagene Journal of Biology

Güngörmez et al., (2025) *Comm. J. Biol.* 9(1), 80-85.
DOI: 10.31594/commagene.1662649

e-ISSN 2602-456X

Research Article/Araştırma Makalesi

Quercetin-Mediated Modulation of Tumor Suppressor miR-15a, miR-34a, and p53 Signaling in MCF-7 Breast Cancer Cells

Cigdem GUNGORMEZ*[1], Hatice GUMUSHAN AKTAS[2], Zeynep CELIK[2], Busra ERGIN[2]

[1]*Siirt University, Medicine Faculty, Medical Biology Department, Siirt, TÜRKIYE*
[2]*Harran University, Art and Science Faculty, Biology Department, Şanlıurfa, TÜRKIYE*
ORCID ID: Cigdem GUNGORMEZ: https://orcid.org/0000-0001-7867-5356; Hatice GUMUSHAN AKTAS: https://orcid.org/0000-0002-6650-184X; Zeynep CELIK: https://orcid.org/0000-0002-2142-4342; Busra ERGIN: https://orcid.org/0000-0003-0588-619X

Received: 21.03.2025 **Accepted:** 23.04.2025 **Published online:** 26.05.2025 **Issue published:** 30.06.2025

Abstract: Breast cancer remains one of the most prevalent types of cancer among women globally, contributing significantly to cancer-related mortality. Despite advancements in treatment, many cases continue to exhibit resistance to chemotherapy, radiotherapy, and hormonal therapies, often resulting in drug resistance, high recurrence rates, and severe side effects. Consequently, the role of the natural food components in cancer prevention and treatment is gaining increasing attention in modern medicine. This study focuses on quercetin, a phytochemical compound, and its effects on the breast cancer cell line MCF-7. Specifically, the study has investigated changes in the expression of miR-15a and miR-34a—microRNAs (miRNAs) known to regulate gene expression at the post-transcriptional level—and the *P53* gene, which is critically involved in apoptosis. The analysis was performed using quantitative polymerase chain reaction (qPCR) and Western blot techniques. The results demonstrated that quercetin treatment at concentrations of 40 µM and 80 µM led to a 1.34-fold and 2.73-fold increase in *P53* gene expression, respectively. Additionally, the tumor suppressor miRNA miR-15a showed expression changes of 1.48-fold and 1.69-fold at the same quercetin concentrations. Similarly, miR-34a expression levels increased by 1.23-fold and 1.39-fold at 40 µM and 80 µM, respectively. These findings suggest that dietary phytochemicals, such as quercetin, may have therapeutic potential by modulating miRNA expression and targeting the p53 pathway. In conclusion, quercetin emerges as a promising natural therapeutic agent for breast cancer, warranting further in vivo studies and clinical trials to confirm its efficacy and explore its potential as a part of combination therapies.

Keywords: Flavonoids, cancer, non-coding RNAs, P53

MCF-7 Meme Kanseri Hücrelerinde Tümör Baskılayıcı miR-15a, miR-34a ve p53 Sinyalizasyonunun Kuersetin Aracılı Modülasyonu

Öz: Meme kanseri, küresel olarak kadınlarda en yaygın kanser türlerinden biri olmaya devam etmekte ve kanserle ilişkili ölümlere önemli ölçüde sebep olmaktadır. Tedavideki gelişmelere rağmen, birçok vaka kemoterapi, radyoterapi ve hormonal tedavilere direnç göstermeye devam etmekte ve bu da sıklıkla ilaç direnci, yüksek tekrarlama oranları ve ciddi yan etkilerle sonuçlanmaktadır. Bu nedenle, doğal gıda bileşenlerinin kanser önleme ve tedavisindeki rolü modern tıpta giderek daha fazla ilgi görmektedir. Bu çalışma, bir fitokimyasal bileşik olan kuersetin ve meme kanseri hücre hattı MCF-7 üzerindeki etkilerine odaklanmaktadır. Çalışmada, özellikle, gen ifadesini transkripsiyon sonrası düzeyde düzenlediği bilinen mikroRNA'lar (miRNA) olan miR-15a ve miR-34a'nın ve apoptozda kritik rol oynayan *P53* geninin ifadesindeki değişiklikler araştırılmıştır. Analiz, kantitatif polimeraz zincir reaksiyonu (qPCR) ve Western blot teknikleri kullanılarak gerçekleştirilmiştir. Sonuçlar, 40 µM ve 80 µM konsantrasyonlarında kuersetin tedavisinin *P53* gen ekspresyonunda sırasıyla 1,34 kat ve 2,73 kat artışa yol açtığını göstermiştir. Ek olarak, tümör baskılayıcı miRNA miR-15a aynı kuersetin konsantrasyonlarında 1,48 kat ve 1,69 kat ekspresyon değişiklikleri olduğu saptanmıştır. Benzer şekilde, miR-34a ekspresyon seviyeleri sırasıyla 40 µM ve 80 µM'de 1,23 kat ve 1,39 kat artmıştır. Bu bulgular, kuersetin gibi diyet fitokimyasallarının miRNA ekspresyonunu düzenleyerek ve p53 yolunu hedefleyerek terapötik potansiyele sahip olabileceğini düşündürmektedir. Sonuç olarak, kuersetin meme kanseri için umut verici bir doğal terapötik ajan olarak ortaya çıkmakta ve etkinliğini doğrulamak ve kombinasyon terapilerinin bir parçası olarak potansiyelini keşfetmek için daha fazla in vivo çalışma ve klinik denemeyi gerektirmektedir.

Anahtar kelimeler: Flavonoidler, kanser, kodlama yapmayan RNAlar, P53

1. Introduction

Breast cancer continues to be a major global health challenge, accounting for approximately 30% of all cancer cases worldwide, as reported by Siegel et al. (2020). This alarming prevalence underscores the pressing need to develop innovative and effective therapeutic strategies. In recent years, flavonoids have emerged as a promising class of natural compounds, gaining significant attention due to their diverse biological activities and potential therapeutic applications. These natural polyphenolic compounds possess antioxidant, anti-inflammatory, anticancer, antidiabetic, antiviral, and antiallergic properties (Kopustinskiene et al., 2020). They have shown remarkable potential in cancer therapy by inhibiting tumor cell proliferation, inducing apoptosis, and suppressing angiogenesis (Tang et al., 2021).

Quercetin, a well-known flavonoid commonly found in fruits, vegetables, and medicinal plants, has been

Corresponding author: gungormezcigdem@gmail.com

extensively studied for its pharmacological effects, including antioxidant, anti-inflammatory, antimicrobial, and antitumor activities (Hashemzaei et al., 2017; Li et al., 2020; Rhman et al., 2022). Its anticancer properties, such as inhibiting cell proliferation, inducing apoptosis, and delaying cancer cell invasion and metastasis, make it an attractive candidate for therapeutic intervention (Wang et al., 2021). Given its favorable safety profile and pharmacological value, quercetin has garnered increasing research interest, with numerous studies exploring its potential applications as a chemopreventive and chemotherapeutic agent (Iqbal et al., 2018; Chen et al., 2022). Moreover, its lower toxicity and side effect profile compared to the synthetic drugs make it an appealing option in cancer treatment (Zhang et al., 2019). Emerging evidence suggests that quercetin can modulate metabolic functions through regulatory effects on transcription factors and critical proteins within cellular signaling pathways (Ezzati et al., 2020). Additionally, flavonoids have been shown to regulate non-coding microRNAs (miRNAs), which are essential in controlling gene expression and various cellular processes (Mansoori et al., 2020; Adinew et al., 2021). In particular, quercetin has demonstrated the ability to modulate the expression of functional genes through miRNA-associated regulatory pathways (Tao et al., 2015).

MicroRNAs (miRNAs) are small, non-coding RNAs that regulate gene expression through post-transcriptional gene silencing, playing crucial roles in development, proliferation, metabolism, and inflammation (Kawaguchi et al., 2017; O'Brien et al., 2018). The expression of miRNAs varies significantly under pathological conditions, including cancer, and is closely linked to patient survival (Misso et al., 2014; Zhang et al., 2019). Aberrant miRNA expression is often associated with treatment resistance in tumors, making miRNAs attractive therapeutic targets (Ferdin et al., 2010; Gungormez & Acar, 2019). Among tumor suppressor miRNAs, miR-15a plays a vital role as a tumor suppressor in various cancers, including breast cancer (Bandi et al., 2009; Erbes et al., 2015). In MCF-7 breast cancer cell lines, miR-15a demonstrated anticancer activity by inhibiting cell proliferation and promoting apoptosis (Calin et al., 2008; Zhang et al., 2021). It interacts with the *P53* tumor suppressor gene, enhancing p53 pathway activation and subsequently arresting the cell cycle and triggering programmed cell death (Muller et al., 2011) Notably, decreased miR-15a expression correlates with tumor progression and metastasis in breast cancer, highlighting its potential as both a diagnostic biomarker and a therapeutic target (Tang et al., 2012). Similarly, miR-34a has garnered considerable attention due to its pivotal role in cancer biology (Agarwal et al., 2015; Imani et al., 2018; Kang et al., 2015). It exerts anticancer effects by inducing apoptosis through p53 signaling pathways and inhibiting the epithelial-mesenchymal transition (EMT) process (Wang et al., 2021). Due to its regulatory functions and impact on apoptosis, miR-34a holds substantial therapeutic potential, particularly in breast cancer (Chen et al., 2022). Its relevance as a tumor suppressor molecule is underscored by its association with p53 dysfunction, epigenetic silencing, and genomic losses (Chang et al., 2007; Zhang et al., 2019).

This study aimed to explore the anticancer potential of quercetin on the MCF-7 breast cancer cell line, focusing on the synergistic roles of miR-15a, miR-34a, and *P53*. This research examines their coordinated effects in cancer biology and provides valuable insights into the therapeutic potential of natural compounds in combating breast cancer.

2. Material and Method

2.1. Dataset Selection

In this study, microarray data were obtained from the Gene Expression Omnibus (GEO) database (https://www.ncbi.nlm.nih.gov/gds/). The miRNA profiles were collected from three platforms: GPL570 (6 assays), GPL571 (8 assays), and GPL6244 (25 assays), with additional screening performed using the Affymetrix Human Gene 1.0 ST Array.

Based on the observed changes in the expression levels of miR-15a, miR-34a, and p53 in the sampled datasets, the study focused on analyzing ARR files from the GPL platform through TAC processing. Among the miRNA datasets with the highest overlap in expression levels, miR-15a and miR-34a were identified as the top two miRNAs, with expression values ranging between -1.5 and 2.5 on the scale. These findings provided critical guidance for the design and planning of the study.

2.2. Cell Culture and Treatments

The MCF-7 cell line, kindly provided by Prof. Dr. İlknur Keskin from Medipol University, was cultured in Dulbecco's Modified Eagle Medium/Nutrient Mixture F-12 (DMEM/F12) supplemented with 10% (v/v) fetal bovine serum and 1% (v/v) penicillin-streptomycin. The cells were maintained under standard conditions at 37°C in a humidified incubator with 5% CO_2. The culture medium was refreshed every 24 to 48 hours and all procedures were performed under aseptic conditions following standard cell culture protocols.

Quercetin (CAS number: 117-39-5; Lot ID: SLBM7336V) was purchased from Sigma-Aldrich Pty Ltd. Stock solutions were prepared by dissolving quercetin in dimethyl sulfoxide (DMSO) at a concentration of 10 mM. For experimental treatments, cells were exposed to quercetin at final concentrations of 40 µM and 80 µM, chosen based on their proven efficacy in inhibiting cell proliferation. To minimize potential cytotoxic effects, the final concentration of DMSO in all treatment conditions was kept below 1%.

2.3. Proliferation Analysis

The effect of quercetin on cell proliferation was assessed using the Alamar Blue assay, a method that quantifies metabolic activity by detecting the reduction of resazurin to resorufin in viable cells. MCF-7 cells were seeded at a density of 1×10^4 cells per well in 96-well plates and incubated for 24 hours. Following incubation, the culture medium was replaced with fresh medium containing either 40 µM or 80 µM quercetin. These concentrations were determined by our preliminary experiments. To maintain consistency, the medium was refreshed daily at the same time and the treatment continued for 48 hours. At the end of the treatment period, the culture medium was carefully removed and the fresh medium containing Alamar Blue solution (Invitrogen, USA) at a 1:10 ratio was added to each well. The plates were shielded from light

and incubated for 4 hours under standard culture conditions. Absorbance was then measured at 570 nm and 600 nm using a microplate reader (Thermo MultiSkanIt, USA) to determine cell viability based on the recorded absorbance values (Aktas & Ayan, 2021). To ensure the reliability of the results, all experiments were performed in triplicate.

2.4. Total RNA Extraction and qPCR

Total RNA was extracted from the cells using the miRNeasy Mini Kit (Qiagen, Germany), following the manufacturer's instructions. The RNA concentration was determined by using a NanoDrop spectrophotometer and RNA integrity was assessed by electrophoresis on a 1.2% agarose gel. After RNA isolation, complementary DNA (cDNA) synthesis was carried out using the High Capacity cDNA Reverse Transcription Kit (Applied Biosystems™) according to the manufacturer's protocol. The synthesized cDNA was either utilized immediately for real-time PCR or stored at -80°C for future experiments. Quantitative real-time PCR (qRT-PCR) was performed using the BlasTaq 2X qPCR MasterMix (ABM, Canada), following the guidelines provided by the manufacturer Gene expression levels were analyzed using the delta-delta Ct (ΔΔCt) method, with normalization performed against suitable reference genes (RNU6 for miRNAs, GAPDH for p53) to ensure accurate quantification.

2.5. Western Blot Analysis

Cell disruption was performed using a RIPA lysis buffer system (Santa Cruz Biotechnology, USA). The lysates were then centrifuged at 14,000 rpm to separate the supernatant and the protein concentration was measured using the Bradford assay. Protein samples (40 µg) were resolved by 10% sodium dodecyl sulfate-polyacrylamide gel electrophoresis (SDS-PAGE) and subsequently transferred onto polyvinylidene difluoride (PVDF) membranes. For immunoblotting, membranes were blocked with 1% bovine serum albumin (BSA) to prevent non-specific binding and incubated overnight at 4°C with primary antibodies targeting p53 (1:1000; Boster Bio, China). After thorough washing, the membranes were incubated for one hour with horseradish peroxidase (HRP)-conjugated secondary antibodies at a 1:5000 dilution ratio. Protein bands were visualized using enhanced chemiluminescence (ECL) reagents (Santa Cruz Biotechnology, USA) and detected using an imaging system (Bio-Rad ChemiDoc Imaging System, USA).

2.6. Bioinformatics and Statistical Analysis

FunRich (Functional Enrichment Analysis Tool) is a standalone software application specifically designed for functional enrichment and interaction network analyses of genes, miRNAs, and proteins. In this study, FunRich version 3.1.3 was employed to perform functional enrichment analyses, enabling the identification of biologically relevant pathways, molecular functions, and cellular components that were significantly enriched within the datasets (Gungormez, 2024). At least three petri dishes were used for an experiment and each experiment was repeated at least three times. The results were presented as mean ± standard deviation (x ± SD). Statistical analysis was conducted using SPSS software. Differences in gene expression levels between control and treated cells were evaluated through one-way analysis of variance (ANOVA), followed by Dunnett's post hoc test for multiple comparisons. A p-value<0.05 was deemed statistically significant unless otherwise adjusted for FDR in enrichment analyses.

3. Results and Discussion

3.1. Quercetin induces miR-15a and miR-34a expression

The expression levels of miR-15a and miR-34a were assessed in MCF-7 cells following treatment with 40 µM and 80 µM quercetin. Relative expression analysis using the ΔΔCt method demonstrated that miR-15a expression increased by 1.48-fold at 40 µM and 1.69-fold at 80 µM quercetin, both statistically significant ($p<0.05$) (Fig. 1A). Similarly, miR-34a expression levels increased by 1.23-fold and 1.39-fold at the respective quercetin concentrations (Fig. 1B). No statistically significant difference was observed between DMSO-treated cells (used as a solvent control) and untreated cells ($p>0.05$). However, the differences in expression levels between quercetin-treated cells and the control group were statistically significant ($p<0.05$).

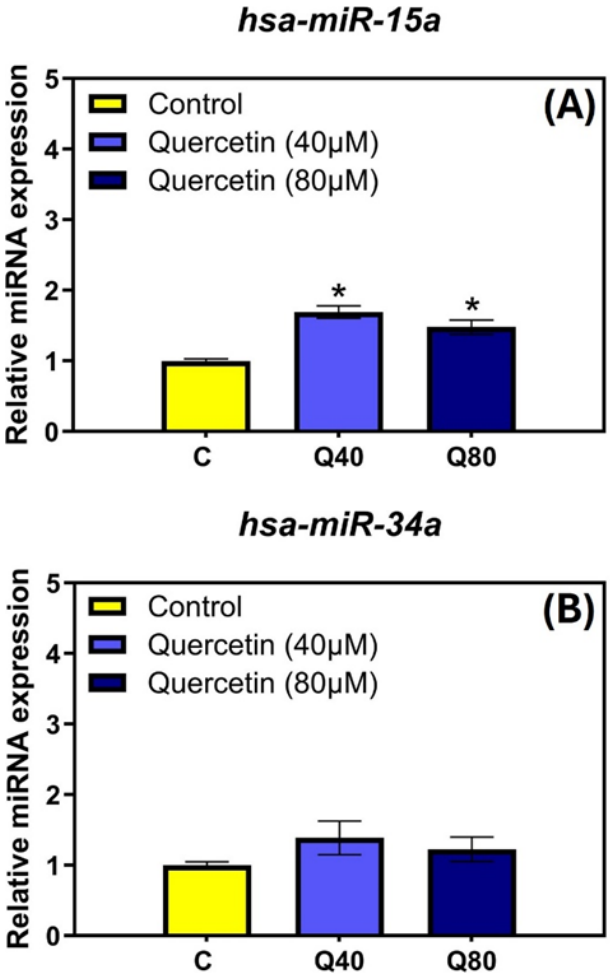

Figure 1. Relative epression level of (A) hsa-miR-34a and (B) hsa-miR-15a. * Statistically significant difference between control and quercetin treatment groups $p<0.05$.

miRNAs, particularly miR-34a, play critical roles in tumor suppression through mechanisms such as apoptosis induction and inhibition of the epithelial-mesenchymal transition (EMT) process via p53 pathways (Imani et al., 2016; Rodríguez-García et al., 2019; Gilbert & Liu, 2010). In breast cancer, metastasis remains the leading cause of

mortality and flavonoids such as quercetin have been identified as bioactive compounds capable of modulating these processes. Previous studies have reported that flavonoids can inhibit metastasis through miRNA activation, particularly miR-34a, which is a well-known tumor suppressor (Imani et al., 2018). Our results suggest that quercetin-mediated upregulation of miR-15a and miR-34a may contribute to tumor-suppressive pathways, aligning with findings that dietary phytochemicals can exert therapeutic effects by modulating miRNA expression.

3.2. Quercetin upregulates P53 expression at both mRNA and protein level

To further elucidate the anticancer effects of quercetin, we examined its impact on p53 expression. The results demonstrated that quercetin treatment significantly upregulated p53 expression in a dose-dependent manner. Specifically, p53 mRNA levels increased by 1.34-fold at 40 µM and 2.73-fold at 80 µM compared to the control ($p<0.05$). Western blot analysis also revealed a concentration-dependent increase in p53 protein levels. These results strongly suggest that quercetin enhances p53-mediated tumor suppression, corroborating previous findings that link flavonoids to p53 activation in cancer cells (Ezzati et al., 2020; Hashemzaei et al., 2017).

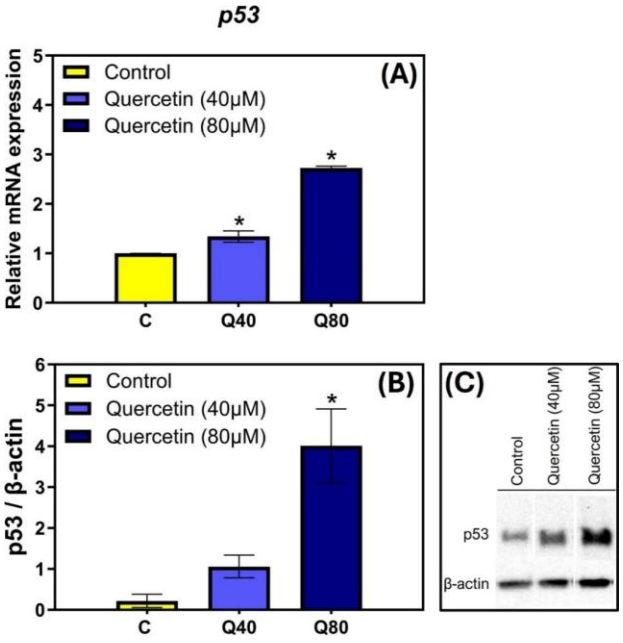

Figure 2. Relative (A) mRNA (B), (C) protein expression levels of p53 after quercetin treatment. *Statistically significant difference between control and quercetin treatment groups $p<0.05$.

The tumor suppressor p53 plays a critical role in regulating cell cycle arrest and apoptosis in response to DNA damage and oncogenic stress. Studies have shown that quercetin enhances p53-mediated tumor suppression mechanisms through multiple pathways, including transcriptional regulation of key apoptotic genes (Murakami et al., 2008). The observed upregulation of p53 protein expression in our study further corroborates quercetin's role in activating p53-dependent apoptotic mechanisms, which has been previously reported in multiple cancer models (Tang et al., 2021; Amit et al., 2020; Kim et al., 2014; Rauf et al., 2018). These results suggest that quercetin may be a promising natural compound for enhancing tumor suppression via p53 activation.

3.3. Bioinformatic analyses of miR-15a and miR-34a functions

The regulatory roles of miR-15a and miR-34a in tumor-suppressive pathways were assessed by bioinformatic analyses. Functional enrichment analysis performed using FunRich (version 3.1.3) demonstrated that miR-15a and miR-34a target genes were significantly enriched in the following molecular functions: transcription factor activity (6.5%), cell adhesion molecule activity (3.4%), and protein serine/threonine kinase activity (2.8%) ($p < 0.05$) (Fig. 3A). These findings suggest that miR-15a and miR-34a play essential roles in gene regulation and signal transduction, potentially through the p53 signaling pathway. Cellular component analysis indicated that these target genes are predominantly localized in the cytoplasm (46.6%), plasma membrane (29%), cytosol (11.1%), endosome (3.8%), and microtubule-associated complex (0.9%) ($p < 0.05$) (Fig. 3B). These results provide valuable information on the spatial distribution of miRNA-regulated proteins, emphasizing their functional relevance in various cellular compartments.

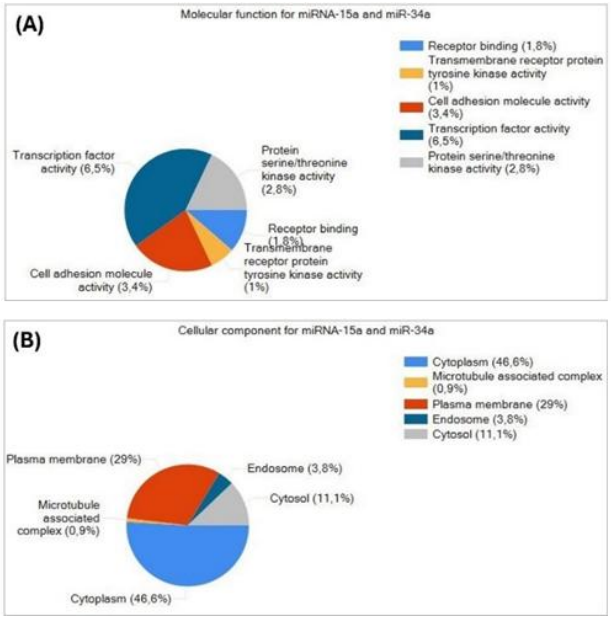

Figure 3. Functional Enrichment Analysis of miR-15a and miR-34a

The regulation of miRNA expression is crucial in breast cancer progression. miR-34a is known to function as a key tumor suppressor by targeting genes involved in cell proliferation, apoptosis, and EMT (Raver-Shapira et al., 2007; Misso et al., 2014). Additionally, miR-15a has been implicated in multiple cancer types, including breast, lung, and colon cancers (Hermeking, 2010; Pang et al., 2010). Given that quercetin significantly upregulated both miRNAs, our findings suggest that quercetin may exert its anticancer effects by modulating these key regulatory molecules.

3.4. Implications of quercetin-mediated miRNA regulation

Recent studies suggest that quercetin modulates multiple signaling pathways, including NF-κB, STAT3, and PI3K/AKT, all of which contribute to cancer progression (Hämäläinen et al., 2007; Kim et al., 2014; Rauf et al., 2018; Tang et al., 2021). Additionally, its regulatory effects on

miRNAs have gained attention due to their critical roles in post-transcriptional gene silencing (Mansoori et al., 2020). In this study, we demonstrated that quercetin enhances the expression of miR-34a and miR-15a, further supporting the hypothesis that dietary flavonoids can exert anticancer effects via miRNA-mediated gene regulation (Chen et al., 2022).

The observed interaction between miR-34a, miR-15a, and p53 in this study aligns with prior research indicating that p53 activation leads to the upregulation of these tumor suppressor miRNAs, facilitating apoptosis and inhibiting tumor growth (Misso et al., 2014; Raver-Shapira et al., 2007). Moreover, the potential of miR-34a as a non-invasive biomarker for breast cancer has been previously reported, highlighting its diagnostic and therapeutic value (Li et al., 2019). Given these findings, the modulation of miRNA expression by quercetin may provide new therapeutic avenues for breast cancer treatment.

Therapeutic strategies targeting miR-15a and miR-34a have been proposed as promising approaches for cancer treatment. Restoring or supplementing the expression of miR-15a has been shown to inhibit tumor growth and enhance chemotherapy sensitivity (Calin et al., 2008). Similarly, strategies that restore p53 function, such as MDM2 inhibitors, have demonstrated efficacy in various cancer models (Vousden & Lane, 2007). Given the observed increase in miR-15a, miR-34a, and p53 expression following quercetin treatment, our findings suggest that quercetin may serve as a potential adjunctive therapeutic agent for breast cancer treatment.

4. Conclusion

This study demonstrates the significant anticancer potential of quercetin through its regulatory effects on tumor suppressor miRNAs (miR-15a and miR-34a) and the p53 signaling pathway in MCF-7 breast cancer cells. Quercetin treatment resulted in a dose-dependent upregulation of miR-15a, miR-34a, and p53 at both the mRNA and protein levels, suggesting its ability to activate tumor suppressive mechanisms. Additionally, bioinformatic analyses revealed that these miRNAs are involved in critical cellular functions, including transcription factor activity and cell adhesion, emphasizing their role in cancer progression and metastasis inhibition.

Our findings align with previous reports on the therapeutic potential of quercetin as a natural compound that modulates key molecular pathways in cancer biology. Quercetin may promote apoptosis or inhibit cell proliferation and metastasis by activating p53 through increasing the expression of miR-15a and miR-34a. This multifaceted action highlights quercetin as a promising candidate for adjunctive cancer therapy, offering a natural and potentially less toxic alternative to conventional treatments.

Given the promising outcomes of this study, further in vivo investigations and clinical trials are warranted to validate the efficacy of quercetin and fully elucidate its therapeutic potential in breast cancer treatment. Additionally, exploring quercetin's role in combination therapies may provide new avenues for enhancing the effectiveness of existing cancer treatments.

Acknowledgment: This project was supported by Siirt University BAP project number "2022-SİÜTIP-050"

Ethics committee approval: Ethics committee approval is not required for this study.

Conflict of interest: The authors declare that there is no conflict of interest.

Author Contributions: Conception – CG.; Design – C.G., H.A.; Supervision – C.G., H.A., Z.C., B.E.; Fund – C.G., H.A.; Materials – C.G., H.A., Z.C., B.E.; Data Collection and Processing – C.G., H.A., Z.C., B.E.; Analysis Interpretation – C.G., H.A.; Literature Review – C.G., H.A.; Writing – C.G., H.A.; Critical Review – C.G., H.A.

References

Adinew, G. M., Taka, E., Mendonca, P., Messeha, S.S., & Soliman, K.F.A. (2021). The anticancer effects of flavonoids through miRNAs modulations in triple-negative breast cancer. *Nutrients*, 13(4), 1212. https://doi.org/10.3390/nu13041212

Agarwal, S., Hanna, J., Sherman, M.E., Figueroa, J., & Rimm, D.L. (2015). Quantitative assessment of miR34a as an independent prognostic marker in breast cancer. *British Journal of Cancer*, 112(1), 61–68. https://doi.org/10.1038/bjc.2014.573

Aktas, H.G., & Ayan, H. (2021). Oleuropein: A Potential Inhibitor for Prostate Cancer Cell Motility by Blocking Voltage-Gated Sodium Channels. *Nutrition and Cancer*, 73(9), 1758–1767. https://doi.org/10.1080/01635581.2020.1807575

Amit, M., Takahashi, H., Dragomir, M.P., Lindemann, A., Gleber-Netto, F.O., Pickering, C.R., ..., & Myers, J.N. (2020). Loss of p53 drives neuron reprogramming in head and neck cancer. *Nature*, 578(7795), 449–454. https://doi.org/10.1038/s41586-020-1996-3

Bandi, N., Zbinden, S., Gugger, M., Arnold, M., Kocher, V., Hasan, L., ..., & Vassella, E. (2009). miR-15a and miR-16 are implicated in cell cycle regulation in a Rb-dependent manner and are frequently deleted or down-regulated in non–small cell lung cancer. Cancer Research, 69(13), 5553-5559. https://doi.org/10.1158/0008-5472.CAN-08-4277

Calin, G. A., Cimmino, A., Fabbri, M., Ferracin, M., Wojcik, S.E., Shimizu, M., ..., & Croce, C. M. (2008). MiR-15a and miR-16-1 cluster functions in human leukemia. *Proceedings of the National Academy of Sciences*, 105(13), 5166-5171. https://doi.org/10.1073/pnas.0800121105

Chang, T.C., Wentzel, E.A., Kent, O.A., Ramachandran, K., Mullendore, M., Lee, K.H., ... & Mendell, J.T. (2007). Transactivation of miR-34a by p53 broadly influences gene expression and promotes apoptosis. *Molecular Cell*, 26(5), 745-752.. https://doi.org/10.1016/j.molcel.2007.05.010

Chen, X., Li., H., Zhang, B., Deng, Z., & Zhang, X. (2022). The role of quercetin in cancer prevention and therapy: A comprehensive review. *Phytotherapy Research*, 36(1), 1–15. https://doi.org/10.1002/ptr.7286

Erbes, T., Hirschfeld, M., Rücker, G., Jaeger, M., Boas, J., Iborra, S., ..., & Stickeler, E. (2015). Feasibility of urinary microRNA detection in breast cancer patients and its potential as an innovative non-invasive biomarker. *BMC Cancer*, 15, 193.

Ezzati, M., Yousefi, B., Velaei, K., & Safa, A. (2020). A review on anti-cancer properties of quercetin in breast cancer. *Life Sciences*, 248, 117463. https://doi.org/10.1016/j.lfs.2020.117463

Ferdin, J., Kunej, T., & Calin, G.A. (2010). Non-coding RNAs: Identification of cancer-associated microRNAs by gene profiling. *Technology in Cancer Research & Treatment*, 9, 123–138. https://doi.org/10.1177/153303461000900202

Gilbert, E.R., & Liu, D. (2010). Flavonoids influence epigenetic-modifying enzyme activity: Structure-function relationships and the therapeutic potential for cancer. *Current Medicinal Chemistry*, 17(17), 1756–1768.

Gungormez, C., & Acar, D. (2019). Identification of miR-145-1, miR-21-2 And miR-92-1 Expression and Target Genes in Colon Cancer Stage IIIA Patients. *Turkish Journal of Biochemistry*. Supplement, 44, 26-28.

Gungormez, C. (2024). Identification of hub genes and key pathways targeted by miRNAs in pancreatic ductal adenocarcinoma: MAPK3/8/9 and TGFBR1/2. *Human Gene*, 39, 201267.

Hämäläinen, M., Nieminen, R., Vuorela, P., Heinonen, M., & Moilanen, E. (2007). Anti-inflammatory effects of flavonoids: Genistein, kaempferol, quercetin, and daidzein inhibit STAT-1 and NF-kappaB activations, whereas flavone, isorhamnetin, naringenin, and pelargonidin inhibit only NF-kappaB activation along with their inhibitory effect on iNOS

expression and NO production in activated macrophages. *Mediators of Inflammation*, 2007, 45673. https://doi.org/10.1155/2007/45673

Hashemzaei, M., Delarami Far, A., Yari, A., Heravi, R.E., Tabrizian, K., Taghdisi, S.M., ..., & Rezaee, R. (2017). Anticancer and apoptosis-inducing effects of quercetin in vitro and in vivo. *Oncology Reports*, 38(2), 819–828. https://doi.org/10.3892/or.2017.5766

Hermeking, H. (2010). The miR-34 family in cancer and apoptosis. *Cell Death & Differentiation*, 17(2), 193–199.

Imani, S., Wei, C., Cheng, J., Khan, M.A., Fu, S., Yang, L., ..., & Fu, J. (2016). MicroRNA-34a targets epithelial to mesenchymal transition-inducing transcription factors (EMT-TFs) and inhibits breast cancer cell migration and invasion. *Oncotarget*, 7(8), 1–12. https://doi.org/10.18632/oncotarget.15214

Imani, S., Wu, R.C., & Fu, J. (2018). MicroRNA-34 family in breast cancer: From research to therapeutic potential. *Journal of Cancer*, 9(20), 3765–3775. https://doi.org/10.7150/jca.24187

Iqbal, J., Abbasi, B.A., Khalil, A.T., Ali, B., Mahmood, T., Kanwal, S., ..., & Ali, W. (2018). Dietary isoflavones, the modulator of breast carcinogenesis: Current landscape and future perspectives. *Asian Pacific Journal of Tropical Medicine*, 11(3), 186-193.

Kang, L., Mao, J., Tao, Y., Song, B., Ma, W., Lu, Y., ..., & Li, L. (2015). Retracted: Micro RNA-34a suppresses the breast cancer stem cell-like characteristics by downregulating Notch1 pathway. *Cancer Science*, 106(6), 700-708. https://doi.org/10.1111/cas.12656

Kawaguchi, T., Yan, L., Qi, Q., Peng, X., Gabriel, E.M., Young, J., ... & Takabe, K. (2017). Overexpression of suppressive microRNAs, miR-30a and miR-200c are associated with improved survival of breast cancer patients. *Scientific Reports*, 7(1), 15945. https://doi.org/10.1038/s41598-017-16112-y

Kim, G.T., Lee, S.H., Kim, J.I., & Kim, Y.M. (2014). Quercetin regulates the sestrin 2-AMPK-p38 MAPK signaling pathway and induces apoptosis by increasing the generation of intracellular ROS in a p53-independent manner. *International Journal of Molecular Medicine*, 33(4), 863-869.

Kopustinskiene, D.M., Jakstas, V., Savickas, A., & Bernatoniene, J. (2020). Flavonoids as anticancer agents. *Nutrients*, 12(2), 457.

Li, X.J., Ren, Z.J., Tang, J.H., & Yu, Q. (2019). MiR-34a: A potential therapeutic target in human cancer. *Cell Death & Disease*, 10(3), 193. https://doi.org/10.1038/s41419-019-1446-z

Li, Y., Yao, J., Han, C., Yang, J., Chaudhry, M.T., Wang, S., ..., & Yin, Y. (2020). Quercetin, inflammation and immunity. *Nutrients*, 12(2), 457. https://doi.org/10.3390/nu12020457

Mansoori, B., Mohammadi, A., Davudian, S., Shirjang, S., & Baradaran, B. (2020). The different mechanisms of cancer drug resistance: A brief review. *Advanced Pharmaceutical Bulletin*, 10(1), 1–8.

Misso, G., Di Martino, M.T., De Rosa, G., Farooqi, A.A., Lombardi, A., Campani, V., ..., & Caraglia, M. (2014). miR-34: A new weapon against cancer? *Molecular Therapy - Nucleic Acids*, 3, e194. https://doi.org/10.1038/mtna.2014.47

Muller, P.A., Vousden, K.H., & Norman, J.C. (2011). p53 and its mutants in tumor cell migration and invasion. *The Journal of cell biology*, 192(2), 209–218. https://doi.org/10.1083/jcb.201009059

Murakami, A., Ashida, H., & Terao, J. (2008). Multitargeted cancer prevention by quercetin. *Cancer Letters*, 269(2), 315–325. https://doi.org/10.1016/j.canlet.2008.03.046

O'Brien, J., Hayder, H., Zayed, Y., & Peng, C. (2018). Overview of MicroRNA Biogenesis, Mechanisms of Actions, and Circulation. *Frontiers in Endocrinology*, 9, 402.

Pang, R.T., Leung, C.O., Ye, T.M., Liu, W., Chiu, P.C., Lam, K.K., ..., & Yeung, W.S. (2010). MicroRNA-34a suppresses invasion through downregulation of Notch1 and Jagged1 in cervical carcinoma and choriocarcinoma cells. *Carcinogenesis*, 31(6), 1037–1044.

Rauf, A., Imran, M., Khan, I.A., Ur-Rehman, M., Gilani, S.A., Mehmood, Z., & Mubarak, M.S. (2018). Anticancer potential of quercetin: A comprehensive review. *Phytotherapy Research*, 32(11), 2109–2130. https://doi.org/10.1002/ptr.6155

Raver-Shapira, N., Marciano, E., Meiri, E., Spector, Y., Rosenfeld, N., Moskovits, N., ..., & Oren, M. (2007). Transcriptional activation of miR-34a contributes to p53-mediated apoptosis. *Molecular Cell*, 26(5), 731–743. https://doi.org/10.1016/j.molcel.2007.05.017

Rhman, M.A., Devnarain, N., Khan, R., & Owira, P.M.O. (2022). Synergism potentiates oxidative antiproliferative effects of naringenin and quercetin in MCF-7 breast cancer cells. *Nutrients*, 14(16), 3437.

Rodríguez-García, C., Sánchez-Quesada, C., & Gaforio, J. (2019). Dietary Flavonoids as Cancer Chemopreventive Agents: An Updated Review of Human Studies. *Antioxidants (Basel, Switzerland)*, 8(5), 137. https://doi.org/10.3390/antiox8050137

Siegel, R.L., Miller, K.D., & Jemal, A. (2020). Cancer statistics, 2020. CA: *A Cancer Journal for Clinicians*, 70(1), 7–30. https://doi.org/10.3322/caac.21590

Tang, J., Ahmad, A., & Sarkar, F.H. (2012). The role of microRNAs in breast cancer migration, invasion and metastasis. *International Journal of Molecular Sciences*, 13(10), 13414–13437. https://doi.org/10.3390/ijms131013414

Tang, S.M., Deng, X.T., Zhou, J., Li, Q.P., Ge, X.X., & Miao, L. (2021). Pharmacological basis and new insights of quercetin action in respect to its anti-cancer effects. *Biomedicine & Pharmacotherapy*, 133, 111017. https://doi.org/10.1016/j.biopha.2020.111017

Tao, S.F., He, H.F., & Chen, Q. (2015). Quercetin inhibits proliferation and invasion acts by up-regulating miR-146a in human breast cancer cells. *Molecular and Cellular Biochemistry*, 402(1–2), 93–100.

Vousden, K.H., & Lane, D.P. (2007). p53 in health and disease. *Nature Reviews Molecular Cell Biology*, 8(4), 275–283. https://doi.org/10.1038/nrm2147

Wang, W., Sun, C., Mao, L., Ma, P., Liu, F., Yang, J., & Gao, Y. (2021). The biological activities, chemical stability, metabolism and delivery systems of quercetin: A review. *Trends in Food Science & Technology*, 109, 1–15. https://doi.org/10.1016/j.tifs.2021.01.042

Zhang, L., Liao, Y., & Tang, L. (2019). MicroRNA-34 family: A potential tumor suppressor and therapeutic candidate in cancer. *Journal of Experimental & Clinical Cancer Research*, 38(1), 53. https://doi.org/10.1186/s13046-019-1059-5

Zhang, J.T., Chen, J., Ruan, H.C., Li, F. X., Pang, S., Xu, Y. J., ..., & Wu, X.H. (2021). Microribonucleic Acid-15a-5p alters Adriamycin resistance in breast cancer cells by targeting cell division cycle-associated protein 4. *Cancer Management and Research*, 13, 8425–8434.

Commagene Journal of Biology

Çoraman, (2025) *Comm. J. Biol.* 9(1), 86-92.
DOI: 10.31594/commagene.1680176

e-ISSN 2602-456X

Research Article/Araştırma Makalesi

Seasonal Acoustic Monitoring of Bat Activity from the Northern Marmara Coast, Türkiye: Insights into Autumn Migration and Conservation Implications

Emrah ÇORAMAN

İstanbul Technical University Eurasia Institute of Earth Sciences, Ecology and Evolution Department, İstanbul, TÜRKİYE
ORCID ID: Emrah ÇORAMAN: https://orcid.org/0000-0001-8188-8651

Received: 20.04.2025 **Accepted:** 06.05.2025 **Published online:** 26.05.2025 **Issue published:** 30.06.2025

Abstract: Migratory bats face increasing risks from habitat fragmentation, artificial light, and the expansion of wind energy infrastructure, yet their migration patterns remain poorly documented in many regions, including Türkiye. This study presents the results of seasonal acoustic monitoring conducted at a coastal site on the northern shore of the Sea of Marmara, a potential migratory corridor between Europe and Asia. Using a passive ultrasonic detector, bat activity across 18 nights in summer, autumn, and winter 2020 was recorded and analyzed for species-specific activity levels through count-per-minute values. A total of 18.937 bat passes were detected, representing at least six species, including *Myotis* sp., *Eptesicus serotinus*, *Pipistrellus pipistrellus*, *P. nathusii*, *Nyctalus noctula*, and *Plecotus* sp. *P. pipistrellus* was the most consistently active species year-round, while *P. nathusii* exhibited a pronounced activity peak during September and October, consistent with autumn migratory behavior documented in other parts of Europe. While acoustic misclassification with *P. kuhlii* cannot be entirely excluded, the seasonally restricted spike and carcass records from regional wind farms strengthen the identification of *P. nathusii* as a migratory species in the area. *N. noctula* and *E. serotinus* were also detected almost exclusively during autumn, likely indicating their migratory movements through the region. These findings underscore the importance of structured, seasonal monitoring to detect migratory activity and support conservation planning. Given the proximity of the site to the proposed offshore wind developments, the results highlight the need for broader spatial monitoring and improved integration of bat migration into environmental impact assessments in Türkiye.

Keywords: Bioacoustics, passive monitoring, ecological assessment

Kuzey Marmara Kıyısında Mevsimsel Yarasa Aktivitesinin Akustik İzlenmesi: Sonbahar Göçü ve Koruma İçin Çıkarımlar

Öz: Birçok göçmen yarasa türü; habitat parçalanması, yapay aydınlatma ve rüzgâr enerjisi altyapısının hızla genişlemesi gibi artan tehditlerle karşı karşıyadır. Ancak bu türlerin göç yolları hakkındaki bilgiler, Türkiye dahil birçok bölgede sınırlıdır. Bu çalışma, Avrupa ile Asya arasında olası bir göç koridoru oluşturan Marmara Denizi'nin kuzey kıyısında yer alan bir sahil noktasında yürütülen mevsimsel akustik izleme sonuçlarını sunmaktadır. Ultrasonik bir kayıt cihazı kullanılarak, 2020 yılının yaz, sonbahar ve kış mevsimlerine ait 18 gecede yarasa aktivitesi kaydedilmiş ve yarasa türlerinin aktivite düzeyleri, dakikadaki geçiş sayısı üzerinden analiz edilmiştir. *Myotis* sp., *Eptesicus serotinus*, *Pipistrellus pipistrellus*, *P. nathusii*, *Nyctalus noctula* ve *Plecotus* sp. türlerini temsil eden, toplam 18.937 yarasa geçişi kaydedilmiştir. *P. pipistrellus* yıl boyunca en düzenli şekilde kaydedilen tür olarak belirlenmiştir. Buna karşılık, *P. nathusii* Eylül ve Ekim aylarında belirgin bir aktivite artışı göstermiştir; bu durum Avrupa'nın diğer bölgelerinde belgelenen sonbahar göç davranışıyla tutarlıdır. Bu türün, *P. kuhlii*'den akustik olarak ayrılması tamamen mümkün olmasa da bu mevsimsel artış ve Tekirdağ'daki rüzgâr enerji santrallerinde bulunan ölü bireyler, *P. nathusii*'nin bölgede göçmen bir tür olduğunu desteklemektedir. Benzer şekilde, *N. noctula* ve *E. serotinus* kayıtlarının neredeyse tamamı sonbaharda tespit edilmiş olup, bu türlerin bölge üzerinden göç hareketlerine işaret etmektedir. Elde edilen bulgular, göçmen türlerin aktivitesini saptamak ve koruma stratejileri geliştirmek için mevsimsel akustik izlemelerin önemini vurgulamaktadır. Çalışma alanının yapılması planlanan deniz-üstü rüzgâr enerjisi projelerine yakınlığı göz önüne alındığında, daha geniş alanlarda izleme yapılması ve yarasa göçünün çevresel etki değerlendirmelerine daha etkin şekilde entegre edilmesi gerektiği ortaya konulmaktadır.

Anahtar kelimeler: Biyoakustik, pasif izleme, ekolojik değerlendirme

1. Introduction

Bats provide essential ecosystem services such as pest control, pollination, and seed dispersal. In the face of growing anthropogenic threats—including habitat loss, land-use change, and infrastructure development—understanding their spatial and temporal activity patterns is critical for informing effective conservation strategies. Migratory species, in particular, face heightened risks due to habitat fragmentation, light pollution, and the rapid expansion of wind energy infrastructure (Voigt et al., 2022). Despite increasing recognition of these pressures, key aspects of bat migration ecology—including routes, timing, and species-specific vulnerability—remain poorly understood in many regions, including Türkiye.

Acoustic monitoring has emerged as a powerful, non-invasive tool for studying bat ecology, enabling the detection of species presence, temporal activity patterns, and migratory behavior. While these techniques are

Corresponding author: coraman@itu.edu.tr

increasingly employed in Türkiye, their use has largely been restricted to documenting range extensions and compiling regional species inventories. Broader applications addressing conservation-relevant questions—such as seasonal dynamics, habitat use, or migration—remain limited. Nonetheless, recent passive acoustic surveys have extended known ranges for several species—for instance, *Barbastella barbastellus* (Karataş et al., 2020) and *Vespertilio murinus* (Karataş et al., 2022)—while deepening our understanding of regional bat diversity and activity in areas such as Köyceğiz–Dalyan (Ürker & Yorulmaz, 2020), Konya (Baş & Arslan, 2021), Antalya (Coşkun & Sert, 2023), Bolu (Gözütok, 2023), and Gökçeada (Şahin, 2024). These studies demonstrate the effectiveness of acoustic methods in filling critical data gaps, particularly for difficult-to-capture species.

Despite these advances, important aspects of seasonal and migratory bat activity remain insufficiently understood, particularly in ecologically strategic yet understudied regions. This study aims to document seasonal patterns of bat activity at the northern coast of the Sea of Marmara, with particular attention to identifying signals of migratory behavior during the autumn. Acoustic monitoring was conducted at a coastal site in Tekirdağ, Türkiye across three seasons—summer, autumn, and winter—using a passive ultrasonic detector to quantify temporal changes in species-specific activity levels.

The region represents a potential corridor for bats moving between Europe and Asia, yet it remains poorly studied. This study provides a baseline dataset that contributes to addressing this knowledge gap. Its relevance is heightened by the increasing expansion of wind energy infrastructure, both onshore and in proposed offshore zones within the Marmara Sea. Although bats are included in the environmental impact assessments in Türkiye, seasonal migration and high-risk periods are often not assessed in sufficient depth. Migratory bats, in particular, may be at increased risk from wind turbine collisions during periods of peak movement. By identifying temporal activity patterns and the species utilizing the site, this study offers foundational data for future research on bat movement ecology and supports the improved integration of bat conservation into spatial planning and impact assessment processes.

2. Material and Method

To assess seasonal variation in bat activity and to identify patterns potentially associated with autumn migration, acoustic monitoring was conducted at a coastal site along the northern coast of the Sea of Marmara. The study area is located in Tekirdağ, Türkiye (41.001°N, 27.672°E), within a region of high conservation interest due to its ecological position between Europe and Asia and its proximity to expanding wind energy infrastructure, both onshore and offshore (Fig. 1).

The site is situated within a semi-rural landscape that includes intensively cultivated agricultural fields, low-density residential settlements, and a narrow coastal strip. To the south lies the Sea of Marmara shoreline, separated from inland areas by a major highway running parallel to the coast. North of the highway, the landscape transitions into expansive farmlands, interspersed with small patches of natural vegetation and vegetated corridors usually associated with streams.

Figure 1. Geographic context and detailed location of the acoustic sampling point on the northern shore of the Sea of Marmara. (a) Regional overview of southeastern Europe and northwestern Anatolia with the study area outlined in white; (b) zoomed-in view of the Marmara Sea showing the extent of the detailed map in (c); (c) high-resolution satellite image of the sampling site with the passive ultrasonic detector marked by a white circle. North arrow and 1 km scale bar apply to panel (c) only.

The detector was positioned within a residential garden exposed to moderate levels of artificial lighting from nearby homes and streetlights, which may have influenced local bat activity. The site is located approximately 30 kilometers north of Marmara Island, near a potential migratory pathway between Europe and Asia. In addition, several proposed offshore wind energy development zones are situated in the central and southern parts of the Marmara Sea, within the broader region where migratory bats may traverse coastal and marine environments.

Acoustic surveys were conducted during three seasons—summer, autumn, and winter— in 2020 to capture temporal variation in bat activity. Monitoring occurred on 18 nights between June 30 and November 24. Four nights were sampled during the summer period (until late August), 11 nights during the autumn (September 1 to October 31), and two nights during winter (after November 1). Survey effort was intensified in the autumn to characterize potential peaks in migratory activity. Sampling was restricted to nights without rainfall to ensure favorable conditions for bat detection.

Data collection was carried out using an Elekon Batlogger M detector equipped with an omnidirectional FG Black microphone. The system operated with a crest-triggered recording algorithm and a sampling rate of 312,500 Hz. Recordings were automatically timestamped and ambient temperature was logged. The microphone was mounted approximately 2.5 meters above ground level to minimize ground-level interference and maximize call detection range.

All recordings were processed using BatExplorer v2.1.4. Species identification was performed manually, following classification protocols outlined by Barataud (2015) and supported by call parameters from Dietz & Kiefer (2014). Special attention was given to species with overlapping call characteristics, particularly *Pipistrellus nathusii* and *P. kuhlii*, as well as *Nyctalus noctula* and *N. leisleri*. When confident classification was not possible,

calls were conservatively assigned to species acoustic groups. Social calls were identified based on distinct structural and frequency characteristics (Barataud, 2015), though these were excluded from quantitative analyses.

To quantify activity, the total recording time was calculated for each survey night. Species-specific count-per-minute (CPM) values were derived by dividing the number of detected bat passes by the corresponding nightly recording duration in minutes. CPM values were used to standardize activity levels across survey nights and seasons and to support interspecies comparisons.

Finally, to explore potential patterns and associations between bat activity and environmental conditions, meteorological data were examined alongside species-specific bat activity. Meteorological data were obtained from NASA's Prediction of Worldwide Energy Resources (POWER) project, which incorporates outputs from the Clouds and the Earth's Radiant Energy System (CERES) and the Modern-Era Retrospective analysis for Research and Applications, Version 2 (MERRA-2) datasets (http://power.larc.nasa.gov/data-access-viewer/). For each survey night, average values of air temperature at 2 meters, wind speed and wind direction at 10 meters, and total precipitation were extracted to characterize meteorological conditions during monitoring.

3. Results

A total of 18.937 bat passes were recorded across summer, autumn, and winter surveys, revealing marked seasonal variations in abundance and activity intensity (Table 1). *Myotis* sp., *Eptesicus serotinus*, *P. pipistrellus*, *P. nathusii*, *N. noctula*, the *N. noctula/N. leisleri* acoustic group, and *Plecotus* sp. were detected. Count-per-minute (CPM), used as a proxy for relative activity, highlighted species-specific patterns, particularly for *P. pipistrellus* and *P. nathusii*, offering insights into their seasonal behaviors. A proportion of *P. nathusii* detections may include *P. kuhlii* due to acoustic overlap (especially in periods of increased activity) and some of the call sequences of *N. noctula* and *N. leisleri* were not distinguished individually as they cannot always be reliably separated using the methods applied.

Table 1. Seasonal and nightly bat-pass counts recorded at the sampling site. Rows are grouped by season (Summer = 4 nights; Autumn = 11 nights; Winter = 2 nights) with individual survey dates listed beneath each seasonal heading. Columns show total passes for each species or species group: *Myotis* sp. (Myo sp.), *E. serotinus* (Eser), *P. pipistrellus* (Ppip), *P. nathusii* (Pnat), *N. noctula* (Nnoc), the *N. noctula*/*N. leisleri* group (Nnoc/Nlei), and *Plecotus* sp. (Ple sp.), plus the overall total passes per date or season. The bottom row presents grand totals across all survey nights.

	Myo sp.	Eser	Ppip	Pnat	Nnoc	Nnoc/Nlei	Ple sp.	Total
Summer	13		2.783	68				2.864
30 Jun			65	1				66
02 Jul			121	2				123
21 Jul	1		1.144	11				1.156
14 Aug	12		1.453	54				1.519
Autumn	38	3	13.128	1.745	2	46	5	14.967
07 Sep	19	1	1.331	323		12		1.686
14 Sep	9	1	2.463	253	1	7		2.734
20 Sep			806	106				912
21 Sep			2.381	186		2		2.569
27 Sep	7		1.623	258	1	7		1.896
02 Oct	1		919	288		6	1	1.215
07 Oct			408	66		3	1	478
11 Oct	2	1	885	114		1		1.003
17 Oct			819	41		5		865
18 Oct			741	22		3	1	767
29 Oct			752	88			2	842
Winter			1.088	15		1	2	1.106
14 Nov			949	13		1	2	965
24 Nov			139	2				141
Total	51	3	16.999	1.828	2	47	7	1.8937

During the summer period (until late August), a total of 2.864 bat passes were recorded (Table 1). *P. pipistrellus* was the overwhelmingly dominant species, contributing 2.783 passes (97.17%), with CPM values ranging from 0.79 on July 2 to 2.54 on August 14. *P. nathusii* was present at much lower levels, with 68 passes (2.37%) and CPM values between 0.01 and 0.09, indicating limited summer activity. The highest summer detection occurred on August 14 when 1.519 total passes were recorded—1.453 of which were *P. pipistrellus* (CPM 2.54), suggesting a localized activity peak.

In the autumn (September 1 to October 31), activity levels peaked sharply, with 14.967 total bat passes, marking it as the most active and diverse period. *P. pipistrellus* remained

the dominant species with 13.128 passes (87.71%) and CPM values ranging from 1.03 (October 7) to 3.58 (September 21), indicating sustained and intense activity (Figs. 2-3). *P. nathusii* showed a notable seasonal increase, rising to 1.745 passes (11.66%) with CPMs reaching up to 0.53 on September 7—a nearly sixfold increase compared to summer. The autumn peak occurred on September 14 with 2,734 total passes, largely driven by *P. pipistrellus* (2.463 passes, CPM 3.74) and *P. nathusii* (253 passes, CPM 0.38). This strong autumn presence of *P. nathusii* is consistent with migratory activity documented in temperate European bat populations.

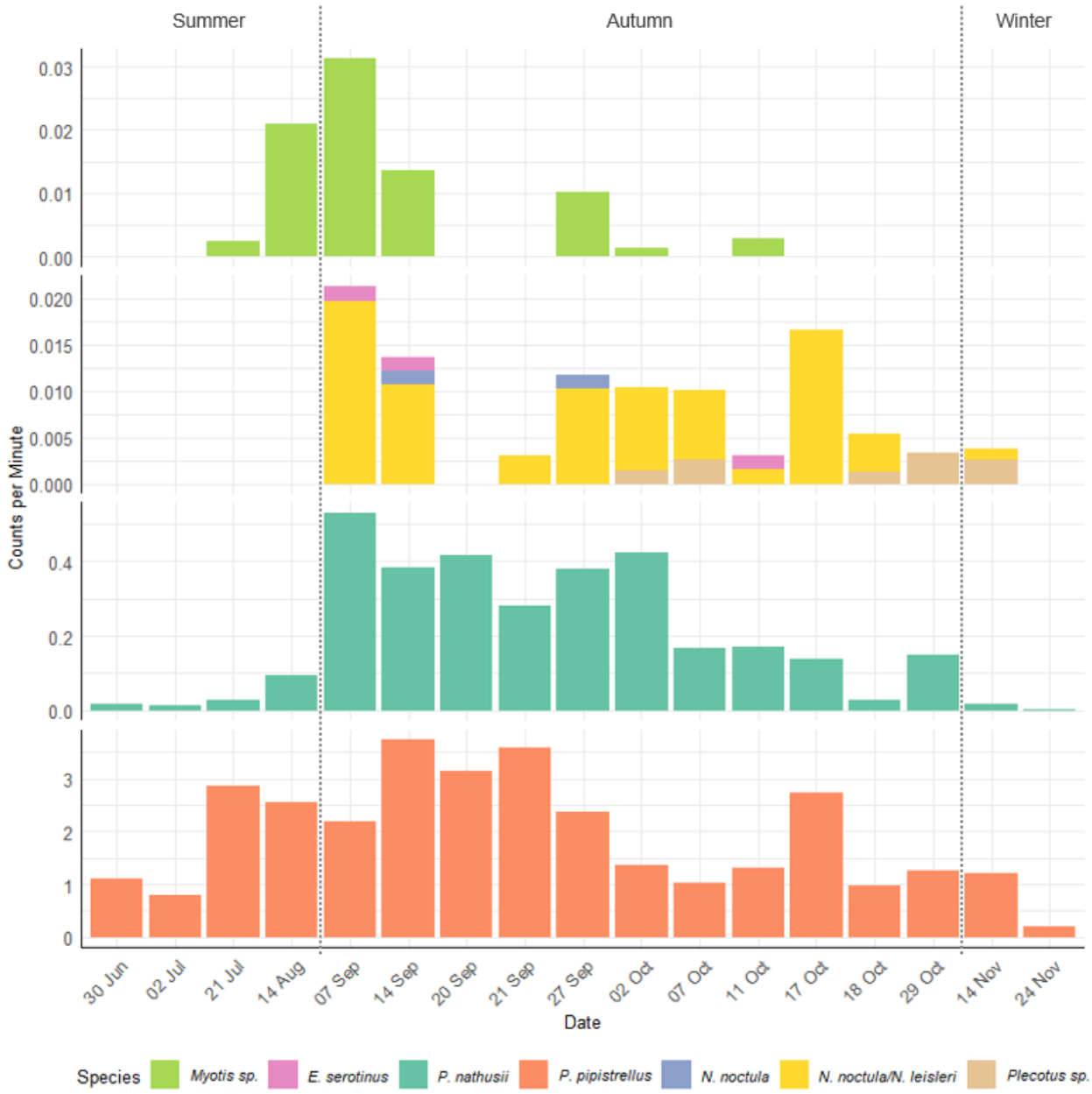

Figure 2. Nightly bat activity (counts per minute, CPM) for *Pipistrellus nathusii* (green) and P. pipistrellus (orange) at the Tekirdağ coastal sampling site. Each bar represents the CPM recorded on a survey night between 30 June and 24 November. Top labels denote the three monitoring periods (Summer, Autumn, Winter).

The autumn migration of *P. nathusii* in September and October showed some correlation with weather parameters with activity peaking in September and continuing into October (Fig. 4). In September, higher activity coincided with warmer temperatures (18.8°C–21.2°C) and variable wind speeds at 10 m (1.08 m/s–6.68 m/s) from usually north-eastern directions (~40°). In October, activity declined, aligning with cooler temperatures and shifting winds.

After November 1, in the winter period, activity declined significantly, with only 1.106 bat passes recorded. *P. pipistrellus* continued to dominate, contributing 1.088 passes (98.37%) with CPM values of 1.20 (November 14) and 0.20 (November 24), reflecting a persistent but reduced winter presence. In contrast, *P. nathusii* activity dropped markedly, with only 15 passes (1.36%; CPM 0.02), further supporting a pattern of seasonal movement out of the area.

Taken together, these findings highlight *P. pipistrellus* as the most abundant and consistently active species year-round with a total of 16.999 passes (89.76%) and CPM values ranging from 0.20 to 3.58. *P. nathusii*, by contrast,

accounted for 1,828 passes (9.65%) with a pronounced activity spike in autumn relative to summer and winter (Fig. 3). This pattern suggests a seasonal migratory influx of *P. nathusii* during early autumn, although the precise magnitude may be affected by acoustic misclassification with *P. kuhlii*. Overall, these results underscore strong seasonal dynamics in species-specific bat activity, particularly highlighting the dominance of *P. pipistrellus* and the transient autumn presence of *P. nathusii*.

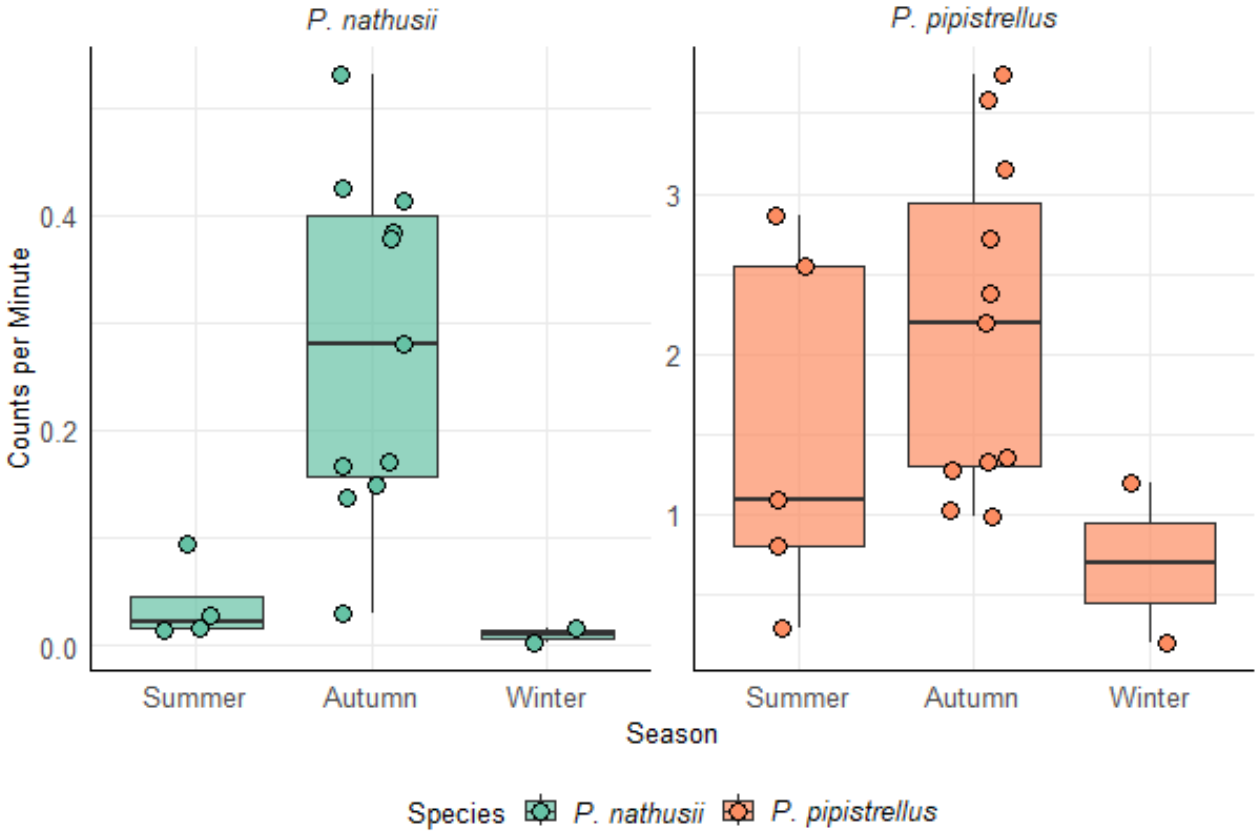

Figure 3. Seasonal variation in nightly bat activity (counts per minute, CPM) for *Pipistrellus nathusii* (left, green) and *P. pipistrellus* (right, orange) at the Tekirdağ coastal sampling site. Boxplots show the median, interquartile range, and 1.5 × IQR whiskers for each season (Summer: 4 nights; Autumn: 11 nights; Winter: 2 nights) with individual nightly CPM values overlaid as points.

4. Discussion

The acoustic monitoring conducted at a locality at the northern coast of the Sea of Marmara revealed clear seasonal variation in bat activity patterns. *P. pipistrellus* was the most consistently registered species across all seasons, indicating a resident population. In contrast, a temporally restricted surge in detections during autumn, peaking primarily in September, consistent with patterns reported in other parts of Europe. Similarly, *N. noctula*/*N. leisleri* and *E. serotinus* were detected almost exclusively during autumn, likely indicating their migratory movements through the region. These patterns support the interpretation of the site as a transit area for autumn migration. A sharp decline in detections during winter, when only two nights were sampled, aligns with the expected low bat activity in this season, limiting the need for extensive winter monitoring.

P. nathusii is known to undertake long-distance seasonal movements across Europe with documented migrations reaching up to 2.224 km between northeastern breeding areas and southwestern wintering grounds (Alcalde et al., 2021). These migrations predominantly occur in autumn, from mid-August through late October, with peak activity often observed in early September (Lagerveld et al., 2021). Studies have shown that *P. nathusii* tends to aggregate along coastlines, such as the Baltic Sea region, where activity levels decline sharply further inland (Ijäs et al., 2017). This coastal preference is likely shaped by the availability of navigational cues and foraging opportunities along shoreline habitats. The pattern observed in this study aligns closely with these continental-scale migration behaviors, suggesting that the Marmara Coast may form a part of a migratory route linking Europe and Asia.

While acoustic identification of *P. nathusii* is complicated by its similarity to *P. kuhlii*, which emits overlapping echolocation calls, several lines of evidence strengthen migratory interpretation. *P. kuhlii* is considered as a sedentary species and would be expected to occur consistently throughout the summer and autumn periods. The pronounced and seasonally restricted spike in detections suggests that the majority of calls recorded in autumn likely correspond to *P. nathusii*, not *P. kuhlii*. This interpretation is further supported by findings from Şaşmaz (2023) who reported that the second most frequently identified bat carcasses at several wind farms in Tekirdağ belonged to *P. nathusii*, while *P. kuhlii* was not reported. Nonetheless, the potential for misclassification cannot be entirely ruled out and some portion of the activity may reflect *P. kuhlii*.

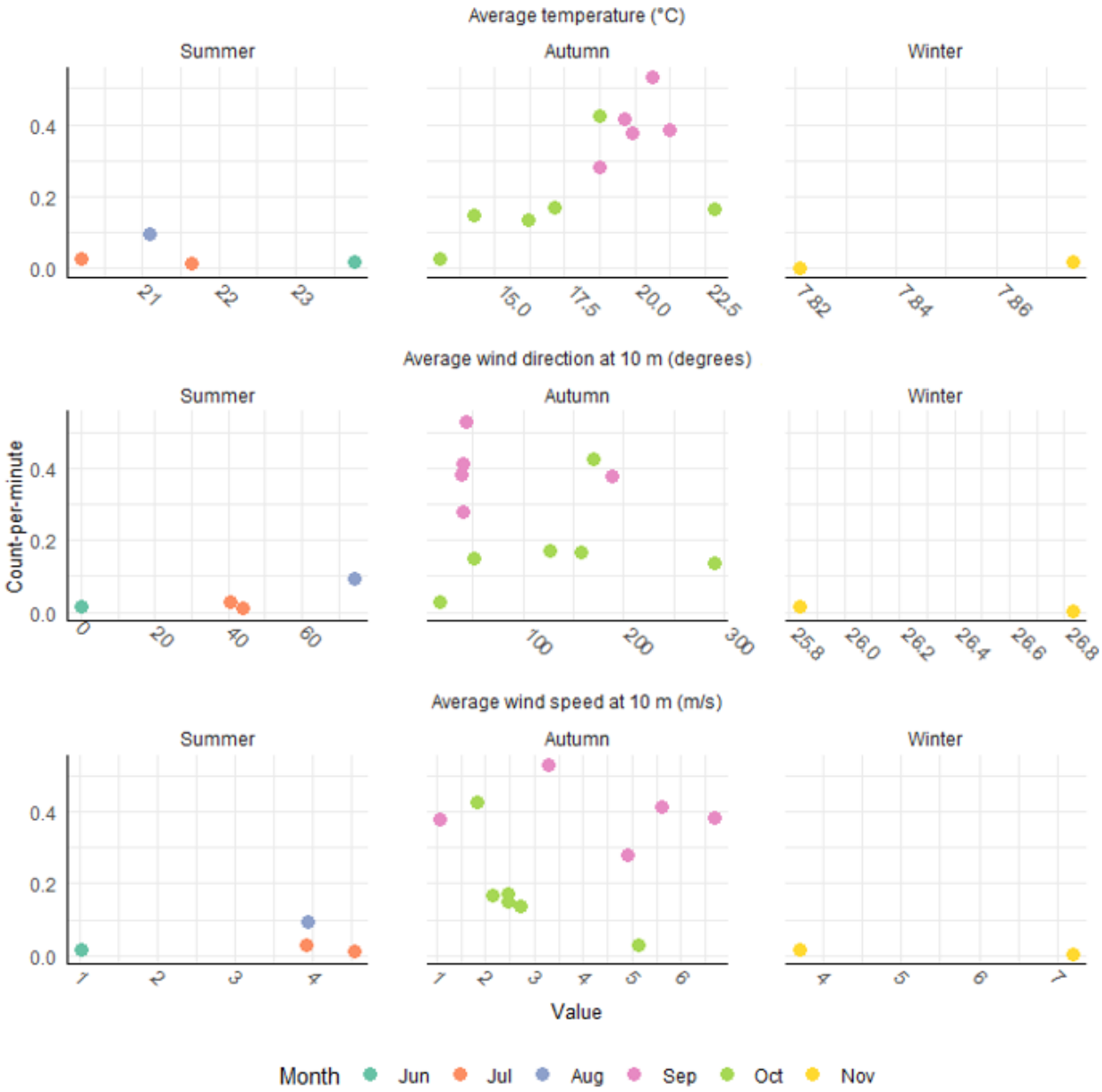

Figure 4. Relationship between nightly *Pipistrellus nathusii* activity (counts per minute, CPM; y-axis) and key weather variables at the Tekirdağ sampling site. Columns denote the three survey seasons—Summer, Autumn, and Winter—and rows show: (top) average nightly temperature (°C), (middle) mean wind direction at 10 m (degrees), and (bottom) average wind speed at 10 m (m/s). Each point represents one survey night and is colored by month (green = June, orange = July, blue = August, pink = September, light green = October, yellow = November).

The site's proximity to both existing and proposed wind energy developments, particularly offshore zones within the Marmara Sea, raises important conservation concerns. Migratory bats are especially vulnerable to turbine collisions during long-distance nocturnal flights along coastal and marine corridors. *P. nathusii*, in particular, is one of the most frequently detected species over offshore wind farms in the North Sea and is considered highly susceptible to turbine-related mortality (Kruszynski et al., 2022). Other migratory species, such as *N. noctula* and *N. leisleri*, also face high collision risks with annual turbine-related mortality estimates exceeding 200,000 individuals in Germany alone (Voigt et al., 2022). While only a small number of *Nyctalus* detections were recorded in this study, this may reflect habitat preference as these species are typically associated with more forested environments such as those found further north in the Thrace region. In parallel, this habitat mosaic—linking forested inland areas with coastal migratory routes—may also make the broader region suitable for *P. nathusii* during its autumn passage. These observations highlight the need for expanded, multi-site acoustic surveys that include inland and offshore components to more fully capture spatial patterns of migratory bat activity and inform risk assessments under wind energy development scenarios.

This study provides a baseline for understanding seasonal bat activity along the northern coast of the Sea of Marmara, offering preliminary evidence of migratory use by *P. nathusii*. Although limited to a single site and constrained by acoustic identification challenges, the results help fill a critical gap in the literature for the Eastern Mediterranean region. Future research should build on these findings by expanding monitoring to additional sites along potential flyways, incorporating spring migration periods and applying complementary methods such as

GPS telemetry or genetic analysis to improve species-level resolution. Such efforts are essential for the development of bat-inclusive conservation strategies in the context of expanding wind energy infrastructure across Türkiye's coastal landscapes.

Acknowledgment: This study was supported by the Scientific Research Projects Department of Istanbul Technical University to E.Ç. (Project Number: TGA-2021-42795).

Ethics committee approval: Ethics committee approval is not required for this study.

Conflict of interest: The author declares that there is no conflict of interest.

References

Alcalde, J.T., Jiménez, M., Brila, I., Vintulis, V., Voigt, C.C., & Pētersons, G. (2021). Transcontinental 2200 km migration of a Nathusius' pipistrelle (*Pipistrellus nathusii*) across Europe. *Mammalia*, 85(2), 161-163. https://doi.org/10.1515/mammalia-2020-0069

Barataud, M. (2015). Acoustic ecology of European bats. Species identification and studies of their habitats and foraging behaviour. Muséum National d'Histoire Naturelle, Paris; Biotope, Mèze, 352 pp.

Baş, M., & Arslan, A. (2021). Acoustical investigation of bats in Selçuklu District of Konya Province. *Kahramanmaraş Sütçü İmam Üniversitesi Tarım ve Doğa Dergisi*, 24(1), 186-195. https://doi.org/10.18016/ksutarimdoga.vi.722155

Coşkun, Ö., & Sert, H. (2023). Antalyadaki yarasa türlerinin akustik olarak araştırılması. *Kahramanmaraş Sütçü İmam Üniversitesi Tarım ve Doğa Dergisi* 26(6), 1405-1420. https://doi.org/10.18016/ksutarimdoga.vi.1163614

Dietz, C., & Kiefer, A. (2014). Die Fledermäuse Europas: Kennen, bestimmen, schützen. Franckh-Kosmos Verlags GmbH, 400 pp.

Gözütok, S. (2023). A new distribution record and some bioecological features of *Plecotus auritus* (Linnaeus, 1758) from Northwest Türkiye (Chiroptera: Vespertilionidae). *Commagene Journal of Biology*, 7(1), 38-43. https://doi.org/10.31594/commagene.1239398

Ijäs, A., Kahilainen, A., Vasko, V.V., & Lilley, T.M. (2017). Evidence of the migratory bat, *Pipistrellus nathusii*, aggregating to the coastlines in the Northern Baltic Sea. *Acta Chiropterologica*, 19(1), 127-139. https://doi.org/10.3161/15081109ACC2017.19.1.010

Karataş, A., Bulut, Ş., Sefali, A., Toprak, F., Şahin, M.K., & Özkurt, Ş.Ö. (2022). Contributions on the southern distribution of *Vespertilio murinus* Linnaeus, 1758 (Chiroptera: Vespertilionidae) from Türkiye. *Turkish Journal of Zoology*, 46(5), 434-443. https://doi.org/10.55730/1300-0179.3097

Karataş, A., Bulut, Ş., Karataş, A., Toprak, F., & Özkurt, Ş.Ö. (2020). Contribution to the natural history of *Barbastella barbastellus* in Turkey (Chiroptera: Vespertilionidae). *Lynx, series nova*, 51(1). https://doi.org/10.37520/lynx.2020.005

Kruszynski, C., Bailey, L.D., Bach, L., Bach, P., Fritze, M., Lindecke, O., ..., & Voigt, C.C. (2022). High vulnerability of juvenile Nathusius' pipistrelle bats (*Pipistrellus nathusii*) at wind turbines. *Ecological Applications*, 32(2), e2513. https://doi.org/10.1002/eap.2513

Lagerveld, S., Jonge Poerink, B., & Geelhoed, S.C. (2021). Offshore occurrence of a migratory bat, *Pipistrellus nathusii*, depends on seasonality and weather conditions. *Animals*, 11(12), 3442. https://doi.org/10.3390/ani11123442

Şahin, M.B. (2024). Gökçeada'nın (Çanakkale) yarasa varlığı ve aktivite örüntüsü. Retriewed from: https://tez.yok.gov.tr/UlusalTezMerkezi/giris.jsp

Şaşmaz, Y. (2023). Rüzgâr enerjisi santrallerinin yarasalar üzerine etkileri. Retrieved from: https://tez.yok.gov.tr/UlusalTezMerkezi/giris.jsp

Ürker, O., & Yorulmaz, T. (2020). Köyceğiz-Dalyan Özel Çevre Koruma Bölgesi'ndeki Anadolu sığla ormanlarında yarasa (Chiroptera) aktivitesinin belirlenmesi. *Ormancılık Araştırma Dergisi*, 7(1), 88-103. https://doi.org/10.17568/ogmoad.651223

Voigt, C.C., Kaiser, K., Look, S., Scharnweber, K. & Scholz, C. (2022) Wind turbines without curtailment produce large numbers of bat fatalities throughout their lifetime: A call against ignorance and neglect. *Global Ecology and Conservation*, 37, e02149. https://doi.org/10.1016/j.gecco.2022.e02149

Commagene Journal of Biology

Fırat & Fırat, (2025) *Comm. J. Biol.* 9(1), 93-98.
DOI: 10.31594/commagene.1651481

e-ISSN 2602-456X

Research Article/Araştırma Makalesi

A Toxicological Research in Atatürk Dam Lake: Toxicity and Stress Responses in Fish Blood

Özge FIRAT[1]*, Özgür FIRAT[2]

[1]*Adıyaman University, Kahta Vocational School, Veterinary Department, Adıyaman, TÜRKİYE*
[2]*Adiyaman University, Science and Letters Faculty, Biology Department, Adıyaman, TÜRKİYE*
ORCID ID: Özge FIRAT: https://orcid.org/0000-0001-9010-955X; Özgür FIRAT: https://orcid.org/0000-0002-9683-8945

Received: 04.03.2025 **Accepted:** 06.05.2025 **Published online:** 07.06.2025 **Issue published:** 30.06.2025

Abstract: Atatürk Dam Lake, where the study was conducted, the largest dam in Turkey, is located on the Euphrates River and it is an important freshwater resource with its diverse and nutritionally valuable aquatic products and some endemic organisms. *Cyprinus carpio* found in this dam is one of the most cultivated fish species in the world that has economic value and is consumed as a primary food source by the local people. This dam lake is unfortunately under the influence of many environmental pollutants. In the present study, parameters of hematological (leukocytes, erythrocytes, hemoglobin, hematocrit) and plasma biochemical [glucose, cholesterol, cortisol, total protein, alanine aminotransferase (ALT), aspartate aminotransferase (AST), lactate dehydrogenase (LDH), alkaline phosphatase (ALP), potassium, sodium, and chloride] of *C. carpio* that was caught from different regions (Samsat, Sitilce, and Bozova) in terms of pollution load of Atatürk Dam Lake in September in 2021 were investigated. Significant decreases were observed in erythrocyte, hemoglobin, hematocrit, total protein, and cholesterol levels in Bozova region compared to Samsat and Sitilce regions ($P<0.05$). However, significant increases were determined in plasma glucose, cortisol, ALT, AST, ALP, LDH, and potassium levels of fish in Sitilce and Bozova regions compared to Samsat region ($P<0.05$). Our study shows Atatürk Dam Lake is still under the influence of pollutants originating from agricultural and urban activities and the fishes in the dam lake are negatively affected by this pollution.

Keywords: Freshwater, *Cyprinus carpio*, pollution, hematological indices, plasma parameters.

Atatürk Baraj Gölü'nde Toksikolojik Bir Araştırma: Balık Kanındaki Toksisite ve Stres Yanıtları

Öz: Çalışmanın yürütüldüğü Atatürk Baraj Gölü Türkiye'deki en büyük baraj olup Fırat Nehri üzerinde yer almakta ve içerdiği çok çeşitli ve besin bakımından değerli su ürünleri ve bazı endemik canlıları ile önemli bir tatlı su kaynağıdır. Bu barajda bulunan *Cyprinus carpio* ekonomik değeri olan ve yöre halkı tarafından birinci dereceden besin kaynağı olarak tüketilen dünyada en fazla yetiştiriciliği yapılan balık türlerinden biridir. Atatürk Baraj Gölü ne yazık ki birçok çevresel kirleticilerin etkisi altındadır. Sunulan bu çalışmada, baraj gölünün kirlilik yükü bakımından farklı bölgelerinden (Samsat, Sitilce ve Bozova) 2021 yılının Eylül ayında yakalanan C. *carpio*'nun hematolojik (lökosit, eritrosit, hemoglobin, hematokrit) ve plazmanın biyokimyasal parametreleri [glukoz, kolesterol, kortizol, total protein, alanin aminotransferaz (ALT), aspartat aminotransferaz (AST), laktat dehidrojenaz (LDH), alkalen fosfataz (ALP), potasyum, sodyum ve klor] araştırılmıştır. Eritrosit, hemoglobin, hematokrit, total protein ve kolesterol düzeylerinde Samsat ve Sitilce bölgeleri ile karşılaştırıldığında Bozova bölgesinde anlamlı azalışların olduğu belirlenmiştir ($P<0,05$). Bununla birlikte Samsat bölgesine göre Sitilce ve Bozova bölgesi balıklarının plazma glukoz, kortizol, ALT, AST, ALP, LDH ve potasyum düzeylerinde ise anlamlı artışlar belirlenmiştir ($P<0,05$). Çalışmamız Atatürk Baraj Gölü'nün hala tarımsal ve kentsel aktivitelerden kaynaklı kirleticilerin etkisi altında olduğunu ve baraj balıklarının bu kirlilikten olumsuz etkilendiğini göstermektedir.

Anahtar kelimeler: Tatlısu, *Cyprinus carpio*, kirlilik, hematolojik indeksler, plazma parametreleri.

1. Giriş

Günümüzde hem tatlı su hem de tuzlu su ekosistemleri çevresel kirleticilerin etkisi altındadır (Abdallah et al., 2024) çünkü bu ortamlar hemen tüm kirleticilerin son uğrak alanlarıdır. İçme suyu, tarımsal alanların sulanması ve elektrik enerjisi temini için nehirler üzerine kurulan barajlar da ağır metaller, pestisitler gibi çok çeşitli kirleticilerden etkilenmektedir (Fırat & Kılınç, 2022). Fırat Nehri üzerine kurulan ve temel amacı sulama ve elektrik üretimi olan Türkiye'nin en büyük baraj gölü olarak bilinen Atatürk Baraj Gölü Adıyaman, Urfa ve Diyarbakır illeri arasında yer almakta olup her geçen gün baraj çevresinde artan kentsel, tarımsal ve endüstriyel aktivitelerden kaynaklı kirleticilerin doğrudan ya da dolaylı yollardan hedefi halindedir. Bu baraj gölü keza endemik ve ekonomik önemi yüksek olan birçok balık türünü de barındırmaktadır. Baraj gölünde olası bir kirlilik durumunda bu barajda tespit edilen 8 familyaya ait 25 balık türünün (Bayhan, 2021) ve bu türlerden birçoğunu besin olarak tüketen yöre halkının sağlığını olumsuz olarak etkileyebileceği düşünülmektedir. Bu nedenle bu su kütlesinin ekosistemi, geleceği ve sağlığı için bu barajda yapılacak toksikolojik araştırmalar önem kazanmaktadır.

Su ortamlarında yaygın olarak bulunan balıklar kimyasal kirleticiler de dahil olmak üzere çevresel değişikliklere duyarlılıkları nedeniyle biyoindikatör türler olarak ifade edilmekte ve balıkların birçok kan parametreleri, su ortamlarındaki kirleticilerin olası risklerinin hassas belirteçleri olarak kullanılmaktadır (Dewali et al., 2024). Balıklardaki fizyolojik ve

Corresponding author: ozfirat@adiyaman.edu.tr

biyokimyasal belirteçleri ölçmek sucul organizmaların kirleticilere verdiği tepkiyi değerlendirmek ve kirleticilerin organizmanın sağlığı üzerindeki olası olumsuz etkileri hakkında bilgi edinmek için önemlidir (Pramanik & Biswas, 2024). Balıklar ortamlarında bulunan kirleticilerin neden olduğu strese tepkiler verebilmekte ve iç dengesini tekrar sağlamak için çeşitli savunma yanıtları oluşturabilmektedir (Karadag et al., 2014; Fırat et al., 2022a). Araştırmacılar, balıklardaki birçok biyolojik yanıtları örneğin hematolojik (eritrosit, lökosit, hemoglobin, hematokrit) ya da biyokimyasal (plazma metabolitleri, enzimleri ve elektrolitleri gibi) parametreleri inceleyerek kirleticilerin sonuçlarını değerlendirebilir ve kirleticilerin sucul ekosistemler üzerine olumsuz etkileri ile ilgili öngörüde bulunabilirler. Su organizmalarındaki bu sözü edilen indeksler, bu canlıların sağlıklarını değerlendirmek için oldukça yararlıdır (El-Gaar et al., 2022).

Atatürk Baraj Gölü'ndeki kirlilik durumu ve bu kirliliğe neden olan kirletici türleri ile ilgili son zamanlarda yapılan çalışmalarda barajın birçok bölgesinin antropojenik aktivitelerden olumsuz etkilendiği rapor edilmiştir. Bu araştırmalarda baraj gölünün faklı bölgelerinde su, sediment ve omurgalı/omurgasız su canlılarının dokularındaki kirletici düzeyleri araştırılmış ve ağırlıklı olarak barajın Sitilce bölgesinde ağır metal kirliliği, Bozova bölgesinde ise pestisit kirliliği belirlenmiştir (Firat, 2016; Uçkun, 2017; Uçkun et al., 2017). Bu çalışmalarda Firat (2016) Samsat bölgesi ile karşılaştırıldığında Sitilce bölgesindeki *C. carpio*'nun solungaç, karaciğer ve kas dokularında anlamlı kadmiyum, kurşun, krom, bakır, çinko ve demir birikimi; Uçkun (2017) Bozova bölgesinde yine Samsat'a oranla sediment ve sazan karaciğerinde anlamlı organoklorlu pestisit (Dieldrin, p,p'- DDE; p-p'-DDD; o,p'- DDD; o,p'-DDT ve p,p'-DDT) kalıntıları; Uçkun et al. (2017) Sitilce bölgesi su, sediment ve *Unio mancus* türü tatlı su midyelerinde Samsat'a göre genel olarak daha yüksek ağır metal düzeyleri belirlemiş ve bu üç çalışmadaki araştırmacılar tarafından Sitilce ve Bozova bölgeleri kentsel, endüstriyel ve tarımsal aktivitelerden etkilenen kirli bölgeler, Samsat bölgesi ise göreceli temiz bölge olarak tanımlanmıştır. Sunulan bu çalışmada Atatürk Baraj Gölü'nün kirlilik yükü bakımından farklı bölgelerinden (Samsat, Sitilce ve Bozova) yakalanan *C. carpio*'da hematolojik (eritrosit, lökosit, hemoglobin, hematokrit) ve plazma biyokimyasal (glukoz, kolesterol, kortizol, total protein, ALT, AST, ALP, LDH, sodyum, potasyum ve klor) parametrelerdeki değişimler dikkate alınarak (i) Atatürk Baraj Gölü kirlilik durumu; (ii) bu kirlilik yükünün balık sağlığı açısından risk oluşturup oluşturmadığı ve (iii) 2016/2017 yıllarında faaliyete başlayan Adıyaman şehir/endüstriyel atıksu arıtma tesislerinin baraj gölünün kirlilik yükünü azaltıp azaltmadığının belirlenmesi amaçlanmaktadır. Bu çalışma bahsedilen atık su arıtma tesislerinden sonra bu baraj gölünde yapılan ilk toksikolojik araştırma olma özelliğindedir.

2. Materyal and Metot

Araştırmamızda *C. carpio* üzerinde yapılacak tüm prosedürler Adıyaman Üniversitesi Hayvan Deneyleri Yerel Etik Kurulu kararına uygun olarak yapılmıştır (Protokol No: 2020/067). Aynı zamanda Atatürk Barajı'nda yürütülen bu çalışmayla ilgili olarak Tarım ve Orman Bakanlığı Doğa Koruma ve Milli Parklar Genel Müdürlüğü'nden de araştırma izni temin edilmiştir (Sayı No: E-21264211-288.04-1734404, Tarih: 16.06.2021).

Atatürk Barajı'nda kirlilik durumları dikkate alınarak üç farklı bölge seçilmiştir (Şekil 1). Bu çalışma alanları önceki çalışmalar dikkate alınarak belirlenmiştir (Fırat & Alıcı, 2012; Karadag et al., 2014; Uçkun, 2017). Çalışmamızda göreceli olarak temiz bölge olarak dikkate alınan Samsat (Adıyaman) ile kentsel ve endüstriyel kirleticilerin etkisindeki Sitilce (Adıyaman) ve tarımsal kirleticilerin etkisindeki Bozova (Urfa) bölgelerinden balık örnekleri 2021 yılının Eylül ayında alınmıştır.

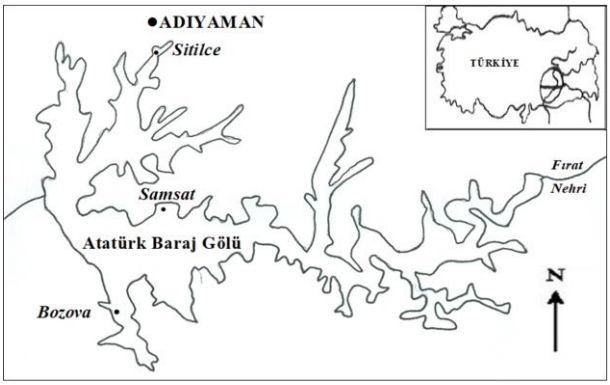

Şekil 1. Atatürk Baraj Gölü'nde balıkların yakalandığı Samsat, Sitilce ve Bozova bölgeleri

Figure 1. Samsat, Sitilce and Bozova regions where fish were caught from Atatürk Dam Lake

Çalışılan bölgelerdeki baraj suyunun sıcaklık, pH ve çözünmüş oksijen düzeyleri taşınabilir ölçüm cihazı ile ölçülmüş ve Tablo 1'de verilmiştir. Balık örneklerinin alınmasında Samsat ve Sitilce bölgesi aynı gün, Bozova bölgesi ise takip eden gün çalışılmıştır. Bir bölgedeki işlemler bitmeden diğer bölgeye gidilmemiştir. Balıkçılar tarafından bu üç bölgenin her birinden ağ atılarak 10'ar adet *C. carpio* yakalanmış ve çalışmamız toplamda 30 adet balıkla yürütülmüştür. Araştırmamızda kullanılan toplam balık sayısı (N=30) G*Power programı (Versiyon 3.1.9.7; Heinrich-Heine-Universität Düsseldorf, Düsseldorf, Germany) kullanılarak güç analizi ile belirlenmiştir (Faul et al., 2007; Faul et al., 2009). Samsat, Sitilce ve Bozova bölgelerinde yakalanan balıklara ait bazı biyolojik özellikler (yaş, total boy ve vücut ağırlığı) Tablo 2'de verilmiştir. Samsat bölgesinde yakalanan sazanlar barajdan alındıktan hemen sonra anestezik madde (3 amino benzoik asit etil ester, MS222, 75 mg/L) uygulanarak bayıltılmıştır ve kuyruk bölgesinden (kaudal pedinkül) kesilerek dorsal aortadan kanları alınmıştır (Karadag et al., 2014). Kan örnekleri tam kanda incelenecek parametrelerin analizi için içinde çökelmeyi önleyici antikoagülant madde (EDTA) bulunan tüplere alınmıştır. EDTA'lı tüplere alınan kan örnekleri zaman kaybetmeksizin soğuk zincirle analiz işlemlerinin yapılacağı araştırma laboratuvarına götürülmüştür. Samsat bölgesi için yapılan bu işlemlerin aynısı Sitilce ve Bozova bölgeleri için de yapılmıştır.

Kan örneklerinden bir kısmı hematolojik bir kısmı da plazma parametrelerinin analizi için kullanılmıştır. Kandaki eritrosit, lökosit, hemoglobin ve hematokrit düzeyleri Abbott (CD-RUBY) marka hemogram cihazında

(Abbott Laboratories, Diagnostic Division, Abbott Park, Illinois, ABD) belirlenmiştir. Biyokimyasal parametrelerin analizi için ise kanlar 10 dakika 3.000 rpm'de santrifüj edilerek plazma örnekleri elde edilmiştir. Plazma glukoz, kolesterol, total protein, ALT, AST, ALP, LDH, sodyum, potasyum ve klor analizleri Abbott (C16000); kortizol düzeyleri ise Beckman coulter DXI800 marka cihazlarda yapılmıştır. Analiz edilen tüm plazma biyokimyasal parametreleri için kullanılan yöntemler önceki çalışmalarımızda verilmiş olup detaylar için bu çalışmalara bakılabilir (Fırat & Alıcı, 2012; Fırat et al., 2022a). Analiz sonucunda elde edilen veriler için istatistiksel analizler One Way Anova ve Duncan testleri uygulanarak yapılmıştır ve sonuçlar P<0,05 düzeyinde ise anlamlı kabul edilmiştir.

Tablo 1. Atatürk Baraj Gölü örnekleme alanı sularının bazı fiziko-kimyasal parametreleri

Table 1. Some physico-chemical parameters of the waters of the Atatürk Dam Lake sampling area.

Örnekleme Alanı	Sıcaklık (°C)	Çözünmüş Oksijen (mg/L)	pH
Samsat Bölgesi	27,4	7,81	8,14
Sitilce Bölgesi	27,6	5,49	8,23
Bozova Bölgesi	28,1	7,18	8,09

Tablo 2. Atatürk Baraj Gölü'nde yakalanan *C. carpio*'nun bazı biyolojik özellikleri

Table 2. Some biological characteristics of *C. carpio* caught from Atatürk Dam Lake

Örnekleme Alanı	Balık Sayısı (n)	Yaş* (Yıl)	Total Boy** (cm)	Ağırlık** (g)
Samsat Bölgesi	10	4-6	39,53±2,41	1012±152
Sitilce Bölgesi	10	5-7	38,12±2,86	1035±117
Bozova Bölgesi	10	4-7	40,22±2,11	1029±109

*: Yaş tayini puldan yapılmıştır.

**: Aritmetik ortalama±standart sapma

3. Bulgular

Atatürk Barajı'nın Samsat, Sitilce ve Bozova bölgesinde yakalanan *C. carpio*'nun hematolojik parametreleri Tablo 3'te verilmiştir. Barajın üç bölgesindeki eritrosit sayısı 0,95-1,33x10^6/mm^3, lökosit sayısı 15,8-17,4x10^3/mm^3, hemoglobin düzeyi 6,05-7,86 mg/dL, hematokrit düzeyi %23,05-31,29 arasında değişim göstermiştir. Çalışılan bölgeler dikkate alındığında lökosit sayılarında anlamlı değişim olmadığı (P>0,05) ancak eritrosit, hemoglobin ve hematokrit düzeylerinde Samsat ve Sitilce bölgeleri ile karşılaştırıldığında Bozova bölgesinde anlamlı düşüşlerin olduğu belirlenmiştir (P<0,05).

Atatürk Barajı'nın farklı bölgelerinde yakalanan sazanların plazma enzim aktiviteleri Tablo 4'te verilmiştir. Barajın Samsat, Sitilce ve Bozova bölgesindeki ALT enzim aktivitesi 33,48-77,12 U/L; AST aktivitesi 152-249 U/L; ALP aktivitesi 12,7-50,8 U/L ve LDH aktivitesi 692-1326 U/L arasında değişim göstermiştir. Çalışılan bölgeler dikkate alındığında analiz edilen tüm enzim aktivitelerinde anlamlı değişimlerin olduğu tespit edilmiştir (P<0,05). Samsat bölgesiyle karşılaştırıldığında ALT, AST, ALP ve LDH enzim aktivitelerinde Sitilce ve Bozova bölgelerinde önemli artışların olduğu belirlenmiştir (P<0,05). Bu artışların Sitilce ve Bozova bölgelerinde sırasıyla yaklaşık olarak ALT için %41 ve %130; AST için %30 ve %64; ALP için %84 ve %300; LDH için %43 ve %92 düzeylerinde olduğu hesaplanmıştır.

Tablo 3. Atatürk Baraj Gölü'nün farklı bölgelerinde yakalanan *C. carpio*'nun hematolojik parametreleri

Table 3. Hematological parameters of *C. carpio* caught from different regions of Atatürk Dam Lake

Parametre	Samsat	Sitilce	Bozova
Eritrosit Sayısı (x10^6/mm^3)	1,33±0,03**a**	1,29±0,02**a**	0,95±0,04**b**
Lökosit Sayısı (x10^3/mm^3)	17,4±0,66**a**	16,9±0,81**a**	15,8±0,78**a**
Hemoglobin (g/dL)	7,86±0,21**a**	7,69±0,28**a**	6,05±0,21**b**
Hematokrit (%)	31,29±0,19**a**	31,15±0,20**a**	23,05±0,19**b**

Veriler aritmetik ortalama ± standart hata şeklinde verilmiştir. "a ve b" harfleri çalışma bölgeleri arasındaki ayırımı göstermek için kullanılmış olup farklı harfler P<0,05 düzeyinde istatistik ayrım olduğunu ifade etmektedir.

Tablo 4. Atatürk Baraj Gölü'nün farklı bölgelerinde yakalanan *C. carpio*'nun plazmasındaki enzim aktiviteleri (U/L)

Table 4. Enzyme activities (U/L) in the plasma of *C. carpio* caught from different regions of Atatürk Dam Lake

Enzim	Samsat	Sitilce	Bozova
ALT	33,48±2,61**a**	47,21±3,59**b**	77,12±5,19**c**
AST	152±9,8**a**	197±12**b**	249±16**c**
ALP	12,7±0,89**a**	23,4±0,71**b**	50,8±1,20**c**
LDH	692±32**a**	987±23**b**	1326±34**c**

Veriler aritmetik ortalama ± standart hata şeklinde verilmiştir. "a, b ve c" harfleri çalışma bölgeleri arasındaki ayırımı göstermek için kullanılmış olup farklı harfler P<0,05 düzeyinde istatistik ayrım olduğunu ifade etmektedir.

Atatürk Barajı'nda belirlenen çalışma bölgelerinde yakalanan sazanların plazma metabolit ve iyon düzeyleri Tablo 5'te verilmiştir. Barajın üç bölgesindeki glukoz düzeyi 72,69-163 mg/dL, kortizol düzeyi 8,83-18,24 ng/dL, kolesterol düzeyi 162-220 mg/dL ve total protein düzeyi 2,41-3,12 g/dL arasında değişim göstermiştir. İyon düzeylerinde ise bu değişimler sodyum için 120-131,9 mmol/L, klor için 90-101 mmol/L ve potasyum için ise 3,22-5,62 mmol/L arasında olmuştur. Plazma sodyum ve klor düzeylerinin üç bölge arasında önemli bir değişim göstermediği (P>0,05) bununla birlikte Samsat bölgesine göre Sitilce ve Bozova bölgesi balıklarının plazma glukoz, kortizol ve potasyum düzeylerinde anlamlı artışların olduğu belirlenmiştir (P<0,05). Bozova balıklarının plazma kolesterol ve total protein düzeyleri Samsat ve Sitilce bölgelerine göre anlamlı bir azalış göstermiştir (P<0,05).

4. Tartışma ve Sonuç

Hematolojik parametrelerin incelenmesi, balıkların sağlık durumlarının izlenmesi için önemli olup bu amaçla yapılan analizler büyük çoğunlukla eritrosit ve lökosit sayımlarının incelenmesini, hematokrit değerlerini ve hemoglobin seviyelerini içermektedir (Maftuch et al., 2020). Hematolojik parametreler kolaylıkla ölçülebilmekte ve kirleticilerin suda yaşayan canlılar üzerine toksik etkilerinin değerlendirilmesinde oldukça yararlıdır (Fırat & Tutuş, 2020). Lökosit, eritrosit, hemoglobin ve hematokrit; bağışıklık sisteminin ve kanın oksijen taşıma kapasitesinin fonksiyonel durumunun

değerlendirilmesinde ve sucul ortamlardaki toksik kirliliğin etkilerinin belirlenmesinde sıklıkla kullanılmaktadır (Fırat et al., 2022b). Çalışmada Bozova bölgesindeki balıklarda eritrosit, hemoglobin ve hematokrit düzeylerindeki azalmaların *C. carpio*'da anemik durumlara neden olduğu düşünülmektedir. Çevresel kirleticilerin balıklarda en belirgin toksik etkilerinden biri olan anemik durum, bu toksik maddelerin kan dokusu üzerindeki olumsuz etkilerinin bir belirteci olup, kanın oksijen taşıma kapasitesinin azalmasına, hücrelerde oksijen yetersizliğine ve canlı organizmaların zarar görmesine neden olmaktadır (Harabawy & Ibrahim, 2014). Araştırma sonuçlarımızla benzer olarak Fırat et al. (2022b) ve Fırat ve Tutuş (2020) ağır metallerin, metal nanopartiküllerin ve pestisitlerin Nil tilapiası *Oreochromis niloticus*'ta eritrosit sayısı, hemoglobin ile hematokrit düzeylerinde önemli azalışlara neden olduğunu ve bu azalışların kirleticilerin eritrosit sentezi, hemosentez, ozmoregülasyon ve kan hücrelerini oluşturan dokularda meydana getirdiği hasarlarla ilişkili olabileceğini belirtmişlerdir.

Tablo 5. Atatürk Baraj Gölü'nün farklı bölgelerinde yakalanan *C. carpio*'nun plazmasındaki metabolit ve iyon düzeyleri

Table 5. Metabolite and ion levels in the plasma of *C. carpio* caught from different regions of Atatürk Dam Lake

Parametre	Samsat	Sitilce	Bozova
Glukoz (mg/dL)	72,69±3,12**a**	121±4,32**b**	163±6,38**c**
Kortizol (ng/dL)	8,83±0,42**a**	12,09±0,83**b**	18,24±1,09**c**
Kolesterol (mg/dL)	220±12**a**	213±7**a**	162±9**b**
Total protein (g/dL)	3,12±0,09**a**	2,98±0,07**a**	2,41±0,04**b**
Sodyum (mmol/L)	131,9±2,5**a**	128±4,2**a**	120±5,1**a**
Klor (mmol/L)	101±3,09**a**	99±4,16**a**	90±3,8**a**
Potasyum (mmol/L)	3,22±0,18**a**	4,23±0,32**b**	5,62±0,28**c**

Veriler aritmetik ortalama ± standart hata şeklinde verilmiştir. "a, b ve c" harfleri çalışma bölgeleri arasındaki ayırımı göstermek için kullanılmış olup farklı harfler P<0,05 düzeyinde istatistik ayrım olduğunu ifade etmektedir.

Plazma enzim (ALT, AST, ALP ve LDH) aktiviteleri sıklıkla çevresel toksikantların balıkların karaciğer dokusu üzerindeki zararlı etkilerinin hassas belirteçleri olarak ölçülmektedir (Canli et al., 2018; Fırat et al., 2022a). Bu enzimler karaciğer kökenli olup hücre içi enzimlerdir. Karaciğer dokusu hasar görmediği sürece bu enzimlerin kan plazmasındaki düzeyleri düşüktür. Çalışmamızda Sitilce ve Bozova bölgesi balıklarının artan plazma enzim aktivitelerinin karaciğer hasarına bağlı olarak oluştuğu düşünülmektedir. Fırat et al. (2022a) çeşitli toksikantların etkisinde balıkların plazmasında ALT, AST, ALP ve LDH enzim aktivitelerinin hepatosit hücre zarlarının toksik maddeler varlığında hasar görmesi nedeniyle bu enzimlerin hücreler arası sıvıya ve ardından da kana geçerek arttığını vurgulamışlardır. Başka çalışmalarda da bu çalışmayla benzer olarak balıkların plazmasındaki enzim aktivitelerinde toksikantların etkisinde önemli artışların olduğu rapor edilmiştir (Fırat & Alıcı, 2012; Abdel-Latif et al., 2021). Bavia et al. (2024) insektisitler, herbisitler, fungusitler, ağır metaller ve mikroplastikler gibi çevresel kirleticilere maruz kalmanın balıkların ALT ve AST gibi serum enzim aktivitelerinde artışlara neden olduğunu bu parametrelerin kirletici toksisitesinin biyobelirteçleri olarak önemli olduğunu belirtmişlerdir.

Plazma glukoz ve kortizol düzeyleri balıklarda çevresel stresin hassas belirteçleri olarak ifade edilmekte ve kortizolün strese yanıt olarak homeostazın korunması için glukoz gibi enerji kaynaklarının düzeyinin ayarlanmasında rol oynadığı belirtilmektedir (Fırat et al., 2022a; Seo et al., 2023). Bu stres hormonu hem glukoneogenez hem de glikojenoliz yoluyla balıklarda glukoz üretimini arttırarak stres altındaki organizmanın gereksinim duyduğu enerjiyi sağlaması bakımından oldukça önemlidir (Lemos et al., 2023). Sitilce ve Bozova bölgelerindeki balıklarda plazma kortizol ve glukoz düzeyleri, büyük bir olasılıkla kirletici stresi altındaki balıkların artan enerji ihtiyacını karşılamak amacıyla artmış olabilir. Plazma proteinleri karaciğer kökenlidir. Kolesterol steroid hormonlarının öncüsü olmakla birlikte hücre zarlarının yapısında yer alan önemli bir metabolittir. Toksikantlar protein ve kolesterol sentezlerini etkileyebilmektedir. Çalışmamızda Bozova bölgesindeki balıklarda plazma total protein ve kolesterol düzeylerindeki azalmaların bu moleküllerin sentez mekanizmalarının hasar görmesinin bir sonucu olabilir. Bu sonuçlar insan aktivitesinden kaynaklı kirleticilerin etkisindeki Hebbal ve Chowkalli göllerinden (Hindistan) yakalanan *Labeo rohita* türü balıkların serumunda, referans bölgedeki balıklarla karşılaştırıldığında total protein ve kolesterol seviyelerinde düşüş olduğunu bildiren Zutshi et al. (2010)'un bulgularıyla uyumludur. Plazma iyonları çevresel stres faktörlerine karşı çok hassastır ve kirleticilere tepki olarak düzeylerinde genellikle değişim meydana geldiğinden araştırmamızda Sitilce ve Bozova örneklerindeki artan potasyum düzeylerinin benzer bir yanıt sonucu oluştuğu öngörülmektedir.

Araştırma sonuçlarımızla uyumlu olarak Atatürk Baraj Gölü'ndeki kirliliği değerlendirmek için *C. carpio*'daki çeşitli serum biyokimyasal belirteçlerin araştırıldığı ve barajın Samsat ve Sitilce bölgelerinde 2011 yılında yakalanan balıklarda da benzer sonuçlar bulunmuştur (Fırat & Alıcı, 2012). Araştırıcılar Samsat bölgesi ile karşılaştırıldığında Sitilce bölgesinden örneklenen balıklarda benzer şekilde ALT, AST, ALP ve LDH aktiviteleri ile kortizol, glukoz ve potasyum düzeylerinin daha yüksek; total protein ve kolesterol düzeylerinin ise daha düşük olduğunu belirlemişler ve Sitilce bölgesinin Adıyaman şehrinden gelen ve herhangi bir arıtmaya uğramayan evsel ve endüstriyel kirleticilerden etkilendiğini vurgulamışlardır. Atatürk Baraj Gölü ne yazık ki uzun yıllar boyunca herhangi bir atık su arıtma tesisine sahip olmayan Adıyaman şehrinden gelen atık sulardan ciddi boyutlarda etkilenmiştir. 2016 yılına kadar şehrin kanalizasyon suları arıtılmaksızın Sitilce bölgesinden doğrudan baraj gölüne ve ayrıca sanayi atıkları da 2017 yılına kadar gene arıtılmaksızın Eğriçay aracılığıyla Sitilce'ye çok yakın bir mevkiden baraja boşalmaktaydı (Fırat & Kılınç, 2022). Bu nedenle bu çalışma bahsedilen yıllarda yapılan evsel ve endüstriyel atık su arıtma tesislerinden sonra bu bölgede yapılan ilk toksikolojik araştırma olma özelliğindedir. Çalışmamız, daha önceki çalışma (Fırat & Alıcı, 2012) sonuçları ile karşılaştırıldığında analiz edilen tüm parametrelerdeki değişimlerin atık su arıtma tesislerinden sonra azalma eğiliminde ama Samsat bölgesi ile karşılaştırıldığında hala yüksek olduğunu göstermektedir. Sitilce bölgesindeki balıklarda hala istenmeyen hematoksik ve biyokimyasal hasarların gözlenmesi bu atık su arıtma tesislerinin

etkinliği ve kapasitelerinin dikkatle değerlendirilmesini ve gerekli tedbirlerin (kapasite artırımı, daha etkin arıtma yöntemleri gibi) zaman kaybetmeksizin alınması gerektiğini göstermektedir. Barajın Bozova bölgesi ise gene uzun yıllar esas olarak tarımsal aktivitelerden kaynaklı kirleticilerden etkilenmiştir. Atatürk Baraj Gölü'nde yapılan bir araştırmada Bozova bölgesinde yakalanan *C. carpio*'da organoklorlu pestisit (Dieldrin, p,p'- DDE; p-p'-DDD; o,p'- DDD; o,p'-DDT ve p,p'-DDT) kalıntıları tespit edilmiştir (Uçkun, 2017) ve bu bölgede örneklenen sazanların karaciğerinde biyokimyasal toksisite ve oksidatif hasar belirlenmiştir. Çalışmamızda da Samsat'a oranla Bozova bölgesinde yakalanan *C. carpio*'nun fizyolojik ve biyokimyasal parametrelerindeki azalış ve artışların daha yüksek olması bu bölgedeki tarımsal aktivite kaynaklı kirleticilerin olumsuz etkilerinin bir sonucu olabilir.

Tatlı su kaynakları okyanuslar ve denizlere oranla dünyada oldukça az bulunan kaynaklar olup bu kaynakların korunması hem su ortamında yaşayan bitkisel ve hayvansal organizmalar hem de insanların geleceği açısından oldukça elzemdir. Bununla birlikte mevcut tatlı suların ne yazık ki insan aktivitelerinden kaynaklı kirleticiler tarafından devamlı olarak kirletildiği de bir gerçektir. Sunulan araştırmada Atatürk Barajı'ndaki kirliliği değerlendirmek için *C. carpio*'daki birçok fizyolojik ve biyokimyasal parametrelerdeki değişimler incelenmiş ve sonuçlar ne yazık ki bu su kütlesinin evsel/endüstriyel (özellikle Sitilce bölgesi için) ve tarımsal (özellikle Bozova bölgesi için) aktivitelerden olumsuz etkilendiğini göstermektedir. Sitilce bölgesinin Adıyaman evsel/endüstriyel atık su arıtma tesisine rağmen hala etkileniyor olması kaygı vericidir. Bu nedenle baraj gölündeki kirletici yükünün azaltılması için Sitilce ve Bozova bölgelerinde daha etkili önlemlerin alınması bu barajın canlı içeriği, bu canlıların ve özellikle de baraj balıklarını besin olarak tüketen yöre halkının sağlığı için önemli olacağı değerlendirilmektedir.

Teşekkür: Sunulan çalışma KMYOMAP/2021-0001 nolu Adıyaman Üniversitesi (ADYÜ) Bilimsel Araştırma Projesi ile yürütülmüş olup ADYÜ Bilimsel Araştırma Projeleri Koordinasyon Biriminin yöneticilerine ve çalışanlarına teşekkür ederiz.

Etik kurul onayı: Bu çalışma, hayvan deneylerinin etik standartlarına uygun olarak yapılmıştır. Çalışma için yasal araştırma etik kurul onay izinleri Adıyaman Üniversitesi Deney Hayvanları Etik Kurulu'ndan alınmıştır (Tarih: 24/12/2020, Karar No:4, Protokol No: 2020/067).

Çıkar çatışması: Yazarlar, çıkar çatışması olmadığını beyan etmiştir.

Yazar Katkıları: Conception – ÖE.F.; Design – ÖR.F.; Supervision – ÖE.F.; Fund – ÖE.F.; Materials – ÖR.F.; Data Collection and Processing – ÖE.F.; Analysis Interpretation – ÖE.F., ÖR.F.; Literature Review – ÖE.F.; Writing – ÖE.F., ÖR.F.; Critical Review – ÖE.F., ÖR.F.

Kaynaklar

Abdel-Latif, H.M.R., Dawood, M.A.O., Mahmoud, S.F., Shukry, M., Noreldin, A.E., Ghetas, H.A., & Khallaf, M.A. (2021). Copper oxide nanoparticles alter serum biochemical indices, induce histopathological alterations, and modulate transcription of cytokines, HSP70, and oxidative stress genes in *Oreochromis niloticus*. *Animals*, 11(3), 652. https://doi.org/10.3390/ani11030652

Abdallah, S.M., Muhammed, R.E., Mohamed, R.E., Daous, H.E., Saleh, D.M., Ghorab, M.A., Chen, S., & Sayyad, G.S.E. (2024). Assessment of biochemical biomarkers and environmental stress indicators in some freshwater fish. *Environmental Geochemistry and Health*, 46, 464. https://doi.org/10.1007/s10653-024-02226-6

Bavia, L., Silva, A.P., Carneiro, M.C., Kmecick, M., Pozzan, R., Esquivel-Muelbert, J., Isaac, L., & Prodocimo, M.M. (2024). Health status biomarkers and hemato-biochemical indices in Nile tilapia. *Comparative Immunology Reports*, 7, 200168. https://doi.org/10.1016/j.cirep.2024.200168

Bayhan, Y.K. (2021). The fish fauna of the Atatürk Dam Lake (Adıyaman/Turkey). *Natural and Engineering Sciences*, 6, 237-255 https://doi.org/10.28978/nesciences.1036854

Canli, E.G., Dogan, A., & Canli, M. (2018). Serum biomarker levels alter following nanoparticle (Al_2O_3, CuO, TiO_2) exposures in freshwater fish (*Oreochromis niloticus*). *Environmental Toxicology and Pharmacology*, 62, 181-187. https://doi.org/10.1016/j.etap.2018.07.009

Dewali, S., Sharma, N.P., Rawat, G., Melkani, D.C., Miglani, R., Pathak, V.M., Kathayat, N., Panda, A.K., & Bisht, S.S. (2024). Chapter 5-Fish blood serum as a biomarker of water pollution. In: Mishra, R., Madhav, S., Dhaka, R.K., & Garg, P (Eds) Biomarkers in environmental and human health biomonitoring. Academic Press, San Diego, 81-107. https://doi.org/10.1016/B978-0-443-13860-7.00014-8

El-Gaar, D.M., Abdelaziz, G.S., Abbas, M.M.M., Anees, F.R., Genina, M.E., Ghannam, H.E., & Talab, A.S. (2022). Biochemical alterations of Nile tilapia fish in El-Manzala Lake as an indicator of pollution impacts. *Egyptian Journal of Aquatic Biology and Fisheries*, 26(3), 711–723. https://doi.org/10.21608/ejabf.2022.246093

Faul, F., Erdfelder, E., Lang, A.-G., & Buchner, A. (2007). G*Power 3: A flexible statistical power analysis program for the social, behavioral, and biomedical sciences. *Behavior Research Methods*, 39, 175-191. https://doi.org/10.3758/BF03193146

Faul, F., Erdfelder, E., Buchner, A., & Lang, A.-G. (2009). Statistical power analyses using G*Power 3.1: Tests for correlation and regression analyses. *Behavior Research Methods*, 41, 1149-1160. https://doi.org/10.3758/BRM.41.4.1149

Fırat. O., & Alıcı, M.F. (2012). Assessment of pollution in Ataturk Dam Lake (Adıyaman, Turkey) using several biochemical parameters in common carp, *Cyprinus carpio*. *Bulletin of Environmental Contamination and Toxicology*, 89, 474-478. https://doi.org/10.1007/s00128-012-0728-2

Fırat, Ö., Erol, R., & Fırat, Ö. (2022a). Effects of individual and co-exposure of copper oxide nanoparticles and copper sulphate on Nile tilapia *Oreochromis niloticus*: Nanoparticles enhance pesticide biochemical toxicity. *Acta Chimica Slovenica*, 69, 81-90. https://doi.org/10.17344/acsi.2021.6995

Fırat, Ö., Erol, R., & Fırat, Ö. (2022b). An investigation on freshwater fish *Oreochromis niloticus* (Linnaeus, 1758): Assessing hemotoxic effects of different copper compounds used as nanomaterial or pesticide. *Bulletin of Environmental Contamination and Toxicology*, 108, 549-554. https://doi.org/10.1007/s00128-021-03320-6

Fırat, Ö., & Kılınç, Ü. (2022). Assessment of lead, cadmium, chrome, iron, zinc and copper levels in tissues of *Cyprinus carpio* from Atatürk Dam Lake (Adıyaman). *Commagene Journal of Biology*, 6(1), 20-25. https://doi.org/10.31594/commagene.1079557

Fırat, Ö., & Tutus, R. (2020). Comparative acute toxicity assessment of organophosphate and avermectin insecticides on a freshwater fish *Oreochromis niloticus*. *Bulletin of Environmental Contamination and Toxicology*, 105, 582-587. https://doi.org/10.1007/s00128-020-02990-y

Firat, O. (2016). Evaluation of metal concentrations in fish species from Ataturk Dam Lake (Adiyaman, Turkey) in relation to human health. *Fresenius Environmental Bulletin*, 25, 3629-3634.

Harabawy, A.S.A., & Ibrahim, A.T.A. (2014). Sublethal toxicity of carbofuran pesticide on the African catfish *Clarias gariepinus* (Burchell, 1822): Hematological, biochemical and cytogenetic response. *Ecotoxicology and Environmental Safety*, 103, 61–67. https://doi.org/10.1016/j.ecoenv.2013.09.022

Karadag, H., Fırat, Ö., & Fırat, Ö. (2014). Use of oxidative stress biomarkers in *Cyprinus carpio* L. for the evaluation of water pollution in Ataturk Dam Lake (Adiyaman, Turkey). *Bulletin of Environmental Contamination and Toxicology*, 92, 289-293. https://doi.org/10.1007/s00128-013-1187-0

Lemos, L.S., Angarica, L.M., Hauser-Davis, R.A., & Quinete, N. (2023). Cortisol as a stress indicator in fish: Sampling methods, analytical techniques, and organic pollutant exposure assessments. *International Journal of Environmental Research and Public Health*, 20, 6237. https://doi.org/10.3390/ijerph20136237

Maftuch, E.S., Asmara, S.D., Haromain, A.F., Nurcholis, A., & Wijanarko, E. (2020). Hematological analysis of common carp (*Cyprinus carpio*)

using hematology analyzer tools and manual at fish seed center, Pasuruan, East Java. *Earth and Environmental Science*, 493, 12011. https://doi.org/10.1088/1755-1315/493/1/012011

Pramanik, S., & Biswas, J.K. (2024). Histopathological fingerprints and biochemical changes as multi-stress biomarkers in fish confronting concurrent pollution and parasitization. *iScience*, 27, 111432. https://doi.org/10.1016/j.isci.2024.111432

Seo, Y.S., Lee, H.B., Jeong, J.H., Mun, S.J., & Lim, H.K. (2023). Change in plasma cortisol and glucose levels of *Oncorhynchus keta* according to water temperature. *Fisheries and Aquatic Sciences*, 26(2), 117-132. https://doi.org/10.47853/FAS.2023.e10

Uçkun, A.A. (2017). Ecotoxicological evaluation of pesticide pollution in Ataturk Dam Lake (Euphrates River), Turkey. *Turkish Journal of Fisheries and Aquatic Sciences*, 17(2), 313-321. https://doi.org/10.4194/1303-2712-v17-2-10

Uçkun, A.A., Yologlu, E., & Uçkun, M. (2017). Seasonal monitoring of metals in water, sediment and mussel (*Unio mancus*) from Atatürk Dam Lake (Euphrates River). *Van Veterinary Journal*, 28(2), 75-83.

Zutshi, B., Raghu Prasad, S.G., & Nagaraja, R. (2010). Alteration in hematology of *Labeo rohita* under stress of pollution from Lakes of Bangalore, Karnataka, India. *Environmental Monitoring Assessm*ent, 168, 11–19. https://doi.org/10.1007/s10661-009-1087-2

Commagene Journal of Biology

Karadeniz Saygılı & Kendirci, (2025) *Comm. J. Biol.* 9(1), 99-102.
DOI: 10.31594/commagene.1685992

e-ISSN 2602-456X

Research Article/Araştırma Makalesi

Investigation of in *vitro* Cytotoxic Activity of Arbutin on Human Ovarian Cancer Cell Line

Suna KARADENIZ SAYGILI*[1], Remziye KENDIRCI[2]

[1]*Kutahya Health Sciences University, Faculty of Medicine, Department of Histology and Embriyology, Kutahya, TÜRKIYE*
[2]*Akdeniz University, Faculty of Medicine, Department of Histology and Embriyology, Antalya, TÜRKIYE*
ORCID ID: Suna KARADENIZ SAYGILI: https://orcid.org/0000-0003-1704-3720; Remziye KENDIRCI: https://orcid.org/0000-0002-6839-8823

Received: 28.04.2025 **Accepted:** 28.05.2025 **Published online:** 10.06.2025 **Issue published:** 30.06.2025

Abstract: Arbutin is one of the chemical compounds commonly found in cosmetics. Arbutin's potential effects on ovarian cancer were investigated in this study using the human serous cystadenoma cancer cell line (SKOV3). Cytotoxicity levels and IC50 values of arbutin were determined using the 3-(4,5-dimethyl-2-thiazolyl)-2,5-diphenyl-2H-tetrazolium bromide (MTT) method. Depending on the increase in the applied doses, arbutin was found to have toxic activity on cancer cells. As a result of the immunocytochemical analysis performed on the cells applied with the IC50 value, it was found that arbutin at the IC50 dose increased Caspase 3 immunoreactivity in SKOV3 cells compared to the control group. Considering that arbutin increased apoptotic Caspase 3 activation in SKOV3 cells at the IC50 dose, elucidation of the molecular mechanisms behind these effects of arbutin may contribute to the development of a new perspective in treatment.

Keywords: Arbutin, Ovarian cancer, SKOV3, cytotoxicity, caspase-3.

Arbutinin İnsan Yumurtalık Kanseri Hücre Hattında *in vitro* Sitotoksik Aktivitesinin Araştırılması

Öz: Arbutin kozmetik ürünlerde sıklıkla kullanılan aktif bileşiklerden biridir. Bu çalışmada arbutinin yumurtalık kanseri üzerindeki olası etkileri insan seröz kistadenoma kanser hücre hattında (SKOV3) belirlenmiştir. Arbutin sitotoksisite düzeyleri ve IC50 değerleri 3-(4,5-dimetil-2-tiyazolil)-2,5-difenil-2H-tetrazolium bromür (MTT) yöntemi kullanılarak belirlenmiştir. Uygulanan doz artışına bağlı olarak arbutinin hücreler üzerinde toksik aktiviteye sahip olduğu görülmüştür. IC50 değeri uygulanan hücrelerde yapılan immünositokimyasal analiz sonucunda arbutinin IC50 dozunda SKOV3 hücrelerinde kontrol grubuna göre Kaspaz 3 immünreaktivitesini artırdığı bulunmuştur. Arbutinin IC50 dozunda SKOV3 hücrelerinde apoptotik Kaspaz 3 aktivasyonunu artırdığı göz önüne alındığında, arbutinin bu etkilerinin ardındaki moleküler mekanizmaların aydınlatılması, tedavide yeni bir bakış açısı geliştirilmesine katkı sağlayabilir.

Anahtar kelimeler: Arbutin, Ovaryum kanseri, SKOV3, sitotoksisite, kaspaz-3.

1. Introduction

Around the world, ovarian cancer (OC) is still among the most common causes of cancer-related mortality for women. The American Cancer Society estimates that by 2024, some 19.680 newly identified cases of OC will be diagnosed and the disease would be linked to 12.740 fatalities. Geographically, the incidence varies; higher-income countries tend to have greater rates (Siegel et al., 2024). Ovarian cancer is typically detected at a late stage and is frequently mistaken for other illnesses due to its nonspecific symptoms that include abdominal bloating, pelvic pain, early satiety, and frequent urination (Gajjar et al., 2012). In current treatment, cytoreductive surgery is applied following chemotherapy. Although it varies according to the stage, platinum derivatives such as cisplatin and carboplatin used together with taxanes are used as chemotherapy agents (Chen et al., 2013). There is still no fully effective treatment for ovarian cancer as the majority of the late grade cases relapse due to drug resistance (Kim et al., 2017).

Conventional chemotherapy treatments have numerous adverse reactions or toxic side effects such as gastrointestinal discomfort, polyneuropathy, musculoskeletal pain, prolonged fatigue, and cognitive impairment (Berliere et al., 2021). In contrast, phytochemicals that can be isolated from many sources are becoming a popular and promising therapeutic option for clinical applications with their low toxicity, minimal side effects, and easy absorption properties (Naeem et al., 2022).

The hydroquinone glycoside arbutin (1, C12H16O7) was initially identified when it was extracted from the leaves of Arbutus unedo L. (family: Ericaceae). Alpha and beta arbutin are the two isomers of arbutin that differ based on how hydroquinone binds to the anomeric carbon atom in the glucose complex. About more than fifty plant families have been found to contain arbutin since it was first discovered. Since this glycoside can prevent melanin synthesis by blocking tyrosinase, it has long been utilized as a skin-whitening (depigmentation) ingredient in a variety of commercially available topical cosmetic products. Arbutin, which has been used for skin whitening for years, has been shown to have various therapeutically important biological potentials such as antioxidant, antimicrobial, anti-inflammatory (Xu et al., 2022; Shen et al., 2017), and anticancer (Nahar et al., 2022). According to studies, this substance is cytotoxic to a variety of human cancer cell lines, including those from the bladder, brain, breast, cervix, and skin (Hazman et al., 2021; Li et al., 2011; Su et al., 2020; Surapaneni & Arulselvan, 2021; Yang et al., 2021).

Corresponding author: suna.saygili@ksbu.edu.tr

This study aimed to examine the cytotoxic effects of Arbutin on the SKOV3 ovarian cancer cell line and to assess its potential as a therapeutic agent for ovarian cancer.

2. Materials and Methods

2.1. Cell Culture

The Human ovarian serous adenocarcinoma cell line SKOV3 was used to assess cytotoxic activity. SKOV3 cells were cultivated in RPMI 1640 media enriched with 10% fetal bovine serum (FBS), 2 mM/L glutamine, 100 U/mL penicillin, and streptomycin. The cells were kept at 37°C in an atmosphere of humidity providing 5% CO_2. Cell lines were purchased from ATCC (American Tissue Culture Company), a company that provides validated cell lines, and experiments were performed when the cells reached 70%–80% confluency.

2.2. MTT Assay and Calculation of IC_{50} Arbutin

An enhanced colorimetric MTT test (Mosmann, 1983) was used to assess the cytotoxicity of arbutin (A4256, Sigma Aldrich, USA) based on cell viability. The spectrophotometer (Thermo Multiskan Spectrum, Bremen, Germany) was used to measure optical density (OD) three times at 490 nm. The cells were initially seeded at a density of $1x10^4$ cells/mL in 96-well plates and they were subsequently incubated for 24 hours. A stock solution of arbutin was made at a concentration of 5 mM in phosphate-buffered saline (PBS) (Lim et al., 2009). Following the treatment with arbutin at different doses (1-200 mM), the cells were cultured for a further 48 hours at 37°C. All experiments were performed in six replicates. Following incubation with arbutin, the percentage of viable cells in each culture was calculated to assess cell viability. According to the following formula, the viability (%) was determined:

%Viable cells = 100 x [(absorbance of the treated cells) - (absorbance of blank)] / [(absorbance of control) - (absorbance of blank)].

Using a four-parameter logistic model, the data was fitted to a sigmoidal curve to determine the half-maximal inhibition of growth (IC50) values. The average of three independent observations was used to illustrate the findings. Using Prism 10 software (GraphPad10, San Diego, CA, USA), the IC50 values were calculated and given with a 95% confidence interval. Relative to the untreated controls, the IC50 was computed by subtracting the absorbance values from the blank wells from the treated and control cell wells.

2.3. Immunofluorescence Staining

Immunofluorescence staining was performed to determine the effectiveness of arbutin application on the apoptosis. 10 mm round coverslips were placed in 24-well plates and SKOV3 cells were seeded on them. Arbutin application was performed at an IC50 dose. Following the treatment for 48 hours, cells were fixed with 4% paraformaldehyde and rinsed with PBS. Then, they were kept in a blocking solution for 1 hour. After blocking, they were incubated with anti-caspase 3 primary antibody (PA5-77887, Thermo Scientific; USA) for overnight. After secondary antibody Alexa Fluor Plus 488 (A32790, Thermo Scientific, USA) application, nuclei were stained with 4',6-diamidino-2-phenylindole (DAPI) (P36962, Thermo Scientific, USA). Cells were examined under a fluorescent microscope (Zeiss Axio Observer, Germany).

2.4. Statistical Analysis

Normality tests were performed using the Shapiro-Wilk test. Parametric data were analyzed using One way-ANOVA followed by Tukey post hoc test, while non-parametric data were analyzed using Kruskal-Wallis test followed by post hoc Dunn's test. GraphPad Prism software version 9 was used for all statistical analyses and statistical significance was determined as P-value<0.05.

3. Results

The cytotoxic effects of arbutin were measured against the SKOV3 cell line after 48 h incubation. The arbutin exhibited a statistically significant ($p<0.05$) and concentration-dependent inhibitory effect on the viability of the SKOV3 cell line. Arbutin exhibited inhibition rates of 11.23% at a concentration of 5 mM, 14.5% at 10 mM, 18.7% at 25 mM, 19.8% at 50 mM, 56.4% at 75 mM, 81.6% at 100 mM, and 93.4% at 200 mM on the SKOV3 cell line. Paclitaxel (positive cytotoxic control agent) demonstrated inhibition rates of 20.9% at 1 µM, 42.3% at 2 µM, 56.2% at 4 µM, 69.5% at 6 µM, 75.4% at 8 µM, 91.8% at 10 µM, and 99.3% at 20 µM on the SKOV3 cell line.

The cytotoxic effect of arbutin on SKOV3 cells was dose-dependent. The half-maximal inhibitory concentration (IC_{50}) value was calculated as 68.94 mM using non-linear regression analysis. Each data point in the dose-response curve represents mean±standard deviation (SD) from three independent experiments (n=3). The regression model showed good fit with an R^2 value of 0.97 and the 95% confidence interval for the IC_{50} was calculated (Fig. 1). As a positive control, paclitaxel also showed a dose-dependent cytotoxic effect on SKOV3 cells. The IC_{50} value of paclitaxel was calculated as 2.85 µM using non-linear regression analysis. The data represents mean±SD from three independent experiments (n=3). The regression model showed good fit with an R^2 value of 0.98 and the 95% confidence interval for the IC_{50} was determined. (Fig. 2).

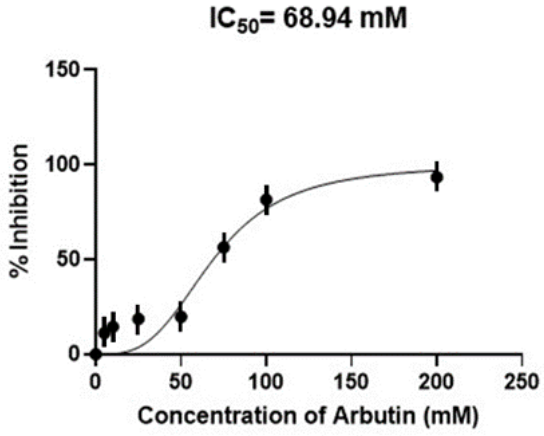

Figure 1. Dose-response curve showing the inhibitory effect of arbutin on SKOV3 cells after 48 h of treatment. The IC_{50} value was determined as 68.94 mM using non-linear regression analysis. Data are presented as mean±SD from three independent experiments (n = 3). The curve fitting showed a good correlation (R^2 = 0.97). Error bars represent the standard deviation.

To investigate the possible mechanism of arbutin-induced apoptosis, we performed immunofluorescence staining to examine the expression of caspase-3 at the cellular level. Quantitative analysis of fluorescence intensity showed that the arbutin-treated group had significantly higher caspase-3 expression than the control group ($p<0.05$, Fig. 3). All data are presented as mean±standard deviation. Statistical significance was accepted at $p<0.05$.

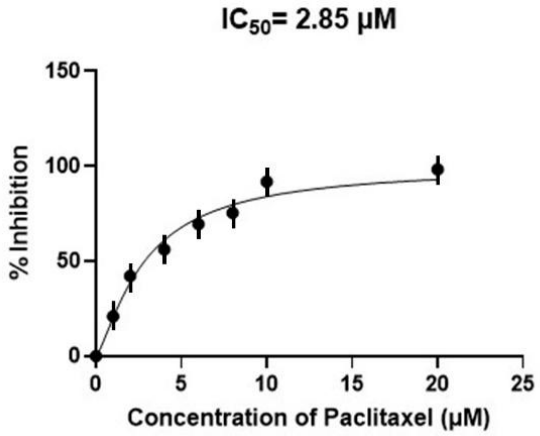

Figure 2. Dose-response curve showing the inhibitory effect of paclitaxel on SKOV3 cells after 48 h of treatment. The IC_{50} value was calculated as 2.85 µM using non-linear regression analysis. Data are presented as mean±SD of three independent experiments (n = 3). The regression model showed a good fit ($R^2 = 0.98$). Error bars indicate the standard deviation.

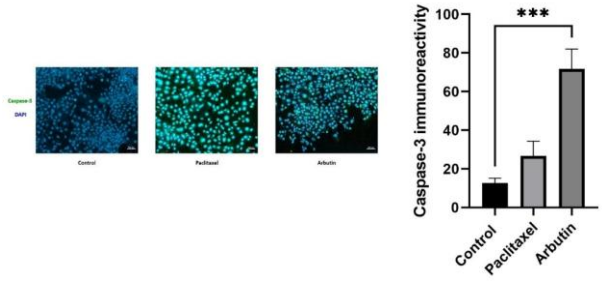

Figure 3. Immunofluorescence microscope images taken after arbutin and paclitaxel application on SKOV3 cells. Nuclei within the cell are shown with DAPI (blue fluorescence) and caspase-3 (green fluorescence), which is a marker of apoptosis. Quantitative analysis of fluorescence intensity revealed that the arbutin-treated group exhibited significantly higher caspase-3 expression compared to the control group ($p<0.05$). Data are presented as mean±SD.

4. Discussion and Conclusion

Ovarian cancer is among the most common female cancers and is one of the leading causes of cancer-related deaths among women. In most cases, survival rates are quite low because the cancer is detected in advanced stages. Unfortunately, despite current standard treatments, finding the most appropriate treatment option for both initial and relapsed cases have not yet been fully realized. In recent years, researchers have been conducting intensive scientific studies to identify compounds that can be beneficial for humans and have anticancer activity from natural sources (Chan et al., 2008). Numerous natural compounds have been found to have cytotoxic effect, particularly in SKOV3 ovarian cancer cells, as well as to alter the cell cycle and induce apoptosis (Hu et al., 2020; Liu et al., 2018; Qiao et al., 2025).

Arbutin is a bioactive hydrophilic polyphenol and it has been utilized in phytotherapy and phytocosmetics as a medicinal plant. Also, it comes from a variety of natural and artificial sources such as different plant species, enzyme reactions, and microorganism metabolic engineering. (Saeedi et al., 2021).

In our study, we observed that arbutin application in ovarian cancer can show toxic activity in the cell in a way that correlates with increasing doses and we calculated the IC50 value. Arbutin has been tested by many researchers on different cancer cells and has been shown to have cytotoxic activity. According to a study by Li et al.(2011) on a human bladder cancer cell line, arbutin inhibits cell proliferation in a way that depends on time and concentration. In a study investigating the possible effects of arbutin on breast cancer by Hazman et al. (2021), it was shown that both forms of arbutin had cytotoxic activity on human breast adenocarcinoma (MCF-7) cells at different concentrations. In addition, Hazman et al.'s study used MTT analysis data to compute lethal doses of α-arbutin, β-arbutin, and cisplatin in HepG2 cells. The lethal dose of β-arbutin in HepG2 cells was determined to be 61.270 mM (Hazman et al., 2022). In addition to the anticancer effects of arbutin, there are scientific studies showing its cytoprotective effects on normal cells (Pečivová et al., 2014; Khadir et al., 2015). In this respect, it is considered a safe treatment agent. The IC50 values and cytotoxic effects of pharmacological agents may vary depending on the cell line used and the application method (Cortés et al., 2001). In the light of these results, it was evaluated as an indication that the IC50 value may vary depending on the cell type and application conditions.

Caspases are catalytic activators that play a role in the initiation of apoptosis in cells. Caspase-3, a member of this family, is activated by both intracellular and extracellular apoptotic signals (Yadav et al., 2021). The goal of our study was to examine at the effects of arbutin on caspase 3 in SKOV3 ovarian cancer cells and as a result, we found that arbutin caused an increase in caspase 3 activity level in the treated cells. In one study, the genes for the apoptotic proteins Bax and Caspase 3 were expressed more in rat C6 glioma cells treated with varying concentrations of arbutin (30 and 40 µM) (Yang et al., 2021). In addition, as a result of gene expression analysis and immunocytochemical analysis performed with RT-PCR device, it was shown that the application of β-arbutin at LD50 dose increased caspase 3 activity in MCF-7 cells (Hazman et al., 2021). In light of our findings, considering that the IC50 dose increased apoptotic caspase 3 activation in SKOV3 cells, determining the mechanism behind these effects of arbutin may contribute to the development of a new perspective in treatment.

In conclusion, it is our opinion that this molecule in particular will provide insight into ovarian cancer research because, to the best of our knowledge, our work is the first to examine the impact of arbutin on ovarian cancer cells in the literature. A naturally occurring phytochemical called arbutin decreased the viability of ovarian cancer cells and activated caspase 3 to cause apoptosis. Consequently, we think that arbutin may be a promising ovarian cancer treatment. Arbutin's effects on different types of cancer cells as well as its impacts at the gene and protein levels

should be investigated for clinical research. Given the results, in vivo experimental animal investigations should be carried out in addition to in vitro studies.

This study has some limitations. Caspase-3 immunocytochemical staining provided supportive evidence for the apoptotic effects of arbutin in SKOV3 cells. However, for more detailed confirmation of caspase-3 activation at gene and protein levels, it would be useful to apply more quantitative techniques such as Western blot or qPCR in future studies. However, the immunocytochemical approach used in our study is widely accepted in the literature to evaluate apoptosis in similar cell culture models and was found to be sufficient to meet the objectives of our study. Future studies using more comprehensive molecular techniques will contribute to support these findings and reveal the apoptotic pathways associated with arbutin in more detail.

Ethics committee approval: Ethics committee approval is not required for this study.

Conflict of interest: The authors declare that there is no conflict of interest.

Author Contributions: Conception – S.K.S.; Design – S.K.S.; Supervision – S.K.S.; Fund – S.K.S.; Materials - S.K.S.; Data Collection and Processing – S.K.S., R.K.; Analysis Interpretation – R.K.; Literature Review – S.K.S., R.K.; Writing – S.K.S., R.K.; Critical Review – S.K.S., R.K.

Referances

Berliere, M., Piette, N., Bernard, M., Lacroix, C., Gerday, A., Samartzi, V., Coyette, M., Roelants, F., …, & Duhoux, F.O.P. (2021). Hypnosis Sedation Reduces the Duration of Different Side Effects of Cancer Treatments in Breast Cancer Patients Receiving Neoadjuvant Chemotherapy. *Cancers*, 13(16), 4147. https://doi.org/10.3390/cancers13164147

Chan, J.K., Teoh, D., Hu, J. M., Shin, J.Y., Osann, K., & Kapp, D.S. (2008). Do clear cell ovarian carcinomas have poorer prognosis compared to other epithelial cell types? A study of 1411 clear cell ovarian cancers. *Gynecologic oncology*, 109(3), 370–376. https://doi.org/10.1016/j.ygyno.2008.02.006

Chen, X., Wu, Y., Dong, H., Zhang, C.Y., & Zhang, Y. (2013). Platinum-based agents for individualized cancer treatment. *Current molecular medicine*, 13(10), 1603–1612. https://doi.org/10.2174/15665240136661311111125515

Cortés, A., Cascante, M., Cárdenas, M.L., & Cornish-Bowden, A. (2001). Relationships between inhibition constants, inhibitor concentrations for 50% inhibition and types of inhibition: new ways of analysing data. *The Biochemical journal*, 357(Pt 1), 263–268. https://doi.org/10.1042/0264-6021:3570263

Gajjar, K., Ogden, G., Mujahid, M.I., & Razvi, K. (2012). Symptoms and risk factors of ovarian cancer: a survey in primary care. *ISRN obstetrics and gynecology*, 2012, 754197. https://doi.org/10.5402/2012/754197

Hazman, Ö., Sarıova, A., Bozkurt, M.F., & Ciğerci, İ.H. (2021). The anticarcinogen activity of β-arbutin on MCF-7 cells: Stimulation of apoptosis through estrogen receptor-α signal pathway, inflammation and genotoxicity. *Molecular and cellular biochemistry*, 476(1), 349–360. https://doi.org/10.1007/s11010-020-03911-7

Hazman, Ö., Evin, H., Bozkurt, M.F., & Ciğerci, İ.H. (2022). Two faces of arbutin in hepatocellular carcinoma (HepG2) cells: Anticarcinogenic effect in high concentration and protective effect against cisplatin toxicity through its antioxidant and anti-inflammatory activity in low concentration. *Biologia*, 77(1), 225-239. https://doi.org/10.1007/s11756-021-00921-8

Hu, H., Zhu, S., Tong, Y., Huang, G., Tan, B., & Yang, L. (2020). Antitumor activity of triptolide in SKOV3 cells and SKOV3/DDP in vivo and in vitro. *Anti-cancer drugs*, 31(5), 483–491. https://doi.org/10.1097/CAD.0000000000000894

Khadir, F., Pouramir, M., Joorsaraee, S.G., Feizi, F., Sorkhi, H., & Yousefi, F. (2015). The effect of arbutin on lipid peroxidation and antioxidant capacity in the serum of cyclosporine-treated rats. *Caspian journal of internal medicine*, 6(4), 196–200.

Kim, J.Y., Cho, C.H., & Song, H.S. (2017). Targeted therapy of ovarian cancer including immune check point inhibitor. *The Korean journal of internal medicine*, 32(5), 798–804. https://doi.org/10.3904/kjim.2017.008

Li, H., Jeong, Y.M., Kim, S.Y., Kim, M.K., & Kim, D.S. (2011). Arbutin inhibits TCCSUP human bladder cancer cell proliferation via up-regulation of p21. *Die Pharmazie*, 66(4), 306–309. https://doi.org/10.1691/ph.2011.0785

Lim, Y.J., Lee, E.H., Kang, T.H., Ha, S.K., Oh, M.S., Kim, S.M., Yoon, T.J., Kang, C., Park, J.H., & Kim, S.Y. (2009). Inhibitory effects of arbutin on melanin biosynthesis of alpha-melanocyte stimulating hormone-induced hyperpigmentation in cultured brownish guinea pig skin tissues. *Archives of pharmacal research*, 32(3), 367–373. https://doi.org/10.1007/s12272-009-1309-8

Liu, J., Liu, X., Ma, W., Kou, W., Li, C., & Zhao, J. (2018). Anticancer activity of cucurbitacin-A in ovarian cancer cell line SKOV3 involves cell cycle arrest, apoptosis and inhibition of mTOR/PI3K/Akt signaling pathway. *Journal of B.U.ON.: official journal of the Balkan Union of Oncology*, 23(1), 124–128.

Mosmann T. (1983). Rapid colorimetric assay for cellular growth and survival: application to proliferation and cytotoxicity assays. *Journal of immunological methods*, 65(1-2), 55–63. https://doi.org/10.1016/0022-1759(83)90303-4

Naeem, A., Hu, P., Yang, M., Zhang, J., Liu, Y., Zhu, W., & Zheng, Q. (2022). Natural Products as Anticancer Agents: Current Status and Future Perspectives. *Molecules* (Basel, Switzerland), 27(23), 8367. https://doi.org/10.3390/molecules27238367

Nahar, L., Al-Groshi, A., Kumar, A., & Sarker, S.D. (2022). Arbutin: Occurrence in Plants, and Its Potential as an Anticancer Agent. *Molecules* (Basel, Switzerland), 27(24), 8786. https://doi.org/10.3390/molecules27248786

Pečivová, J., Nosál, R., Sviteková, K., & Mačičková, T. (2014). Arbutin and decrease of potentially toxic substances generated in human blood neutrophils. *Interdisciplinary toxicology*, 7(4), 195–200. https://doi.org/10.2478/intox-2014-0028

Qiao, L.J., Li, C.Z., Ji, A., & Feng, Q. (2025). Four meroterpenoids from the leaves of Psidium guajava L. and their cytotoxicity activities. *Natural product research*, 1–9. https://doi.org/10.1080/14786419.2025.2469323

Saeedi, M., Khezri, K., Seyed Zakaryaei, A., & Mohammadamini, H. (2021). A comprehensive review of the therapeutic potential of α-arbutin. *Phytotherapy research: PTR*, 35(8), 4136–4154. https://doi.org/10.1002/ptr.7076

Shen, X., Wang, J., Wang, J., Chen, Z., Yuan, Q., & Yan, Y. (2017). High-level De novo biosynthesis of arbutin in engineered Escherichia coli. *Metabolic engineering*, 42, 52–58. https://doi.org/10.1016/j.ymben.2017.06.001

Siegel, R.L., Miller, K.D., Wagle, N.S., & Jemal, A. (2023). Cancer statistics, 2023. *CA: a cancer journal for clinicians*, 73(1), 17–48. https://doi.org/10.3322/caac.21763

Su, Y., Sun, X., Wu, R., Zhang, X., & Tu, Y. (2020). Molecular spectroscopic behaviors of beta-arbutin in anti-skin cancer. *Spectroscopy Letters*, 53(3), 172–183. https://doi.org/10.1080/00387010.2020.1715441

Surapaneni, K. M., & Arulselvan, P. (2021). Arbutin exerts anticancer activity against rat C6 glioma cells by inducing apoptosis and inhibiting the inflammatory markers and P13/Akt/mTOR cascade. Journal of biochemical and molecular toxicology, 35(9), e22857. https://doi.org/10.1002/jbt.22857

Xu, K.X., Xue, M.G., Li, Z., Ye, B.C., & Zhang, B. (2022). Recent Progress on Feasible Strategies for Arbutin Production. *Frontiers in bioengineering and biotechnology*, 10, 914280. https://doi.org/10.3389/fbioe.2022.914280

Yadav, P., Yadav, R., Jain, S., & Vaidya, A. (2021). Caspase-3: A primary target for natural and synthetic compounds for cancer therapy. *Chemical biology & drug design*, 98(1), 144–165. https://doi.org/10.1111/cbdd.13860

Yang, Z., Shi, H., Chinnathambi, A., Salmen, S.H., Alharbi, S.A., Veeraraghavan, V.P., Surapaneni, K.M., & Arulselvan, P. (2021). Arbutin exerts anticancer activity against rat C6 glioma cells by inducing apoptosis and inhibiting the inflammatory markers and P13/Akt/mTOR cascade. *Journal of biochemical and molecular toxicology*, 35(9), e22857. https://doi.org/10.1002/jbt.22857

Commagene Journal of Biology

Gumushan Aktas, (2025) *Comm. J. Biol.* 9(1), 103-111.
DOI: 10.31594/commagene.1667137

e-ISSN 2602-456X

Research Article/Araştırma Makalesi

Chemotherapeutic Drug Delivery from 3D-Printed Biodegradable Polymer for Breast Cancer Treatment

Hatice GUMUSHAN AKTAS

Harran University, Faculty of Arts and Science, Biology Department, Şanlıurfa, TÜRKIYE
ORCID ID: Hatice GUMUSHAN AKTAS: https://orcid.org/0000-0002-6650-184X

Received: 27.03.2025 **Accepted:** 31.05.2025 **Published online:** 10.06.2025 **Issue published:** 30.06.2025

Abstract: The controlled delivery of chemotherapeutic agents is critical for enhancing therapeutic efficiency and minimizing side effects in cancer treatment. This study investigates the drug release, thermal stability, and mechanical performance of polylactic acid (PLA) resin doped with boric acid (H_3BO_3) and 5-fluorouracil (5-FU), fabricated through digital light processing (DLP) 3D printing technology. Samples with various concentrations of 5-FU (0-30 wt.%) and 1 wt.% boric acid were prepared and characterized structurally, mechanically, thermally, and biologically. Incorporation of 1% H_3BO_3 improved compressive strength significantly by approximately 13%, reaching 55.04 MPa compared to 48.86 MPa in pure PLA, and enhanced elongation at break from 5.75% to 7.24%. Thermally, boric acid slightly increased the glass transition temperature from 58°C to 61°C and melting temperature from 179°C to 184°C, indicating improved polymer stability. Swelling behavior peaked around day 9 with up to 50% water uptake for some formulations. Moreover, drug release profiles exhibited sustained release over 15 days, reaching a maximum release amount of 4.24% on day 9 at low drug loadings. Cytotoxicity tests against MCF-7 breast cancer cells demonstrated significant reductions in viability, notably achieving 33.39% after 15 days at the highest 5-FU concentration (30%). These findings suggest that boric acid and 5-FU-doped PLA composites produced via 3D printing offer promising mechanical and controlled-release drug delivery characteristics suitable for developing advanced biomedical applications, particularly in targeted cancer therapy.

Keywords: Controlled drug release, cancer, 5-fluorouracil, boric acid, polylactic acid (PLA).

Meme Kanseri Tedavisi için 3D Baskılı Biyobozunur Polimerden Kemoterapötik İlaç Salınımı

Öz: Kemoterapötik ajanların kontrollü dağıtımı, kanser tedavisinde terapötik etkinliği artırmak ve yan etkileri en aza indirmek için kritik öneme sahiptir. Bu çalışma, dijital ışık işleme (DLP) 3D baskı teknolojisiyle üretilen borik asit (H_3BO_3) ve 5-florourasil (5-FU) ile katkılanmış polilaktik asit (PLA) reçinesinin ilaç salımını, termal kararlılığını ve mekanik performansını araştırmaktadır. Çeşitli 5-FU (%0-%30 ağırlıkça) ve %1 ağırlıkça borik asit konsantrasyonlarına sahip numuneler hazırlandı ve yapısal, mekanik, termal ve biyolojik olarak karakterize edildi. %1 H_3BO_3 eklenmesi, basınç dayanımını yaklaşık %13 oranında önemli ölçüde iyileştirerek saf PLA'daki 48,86 MPa'ya kıyasla 55,04 MPa'ya ulaştı ve kopma anındaki uzamayı %5,75'ten %7,24'e çıkardı. Termal olarak, borik asit cam geçiş sıcaklığını 58°C'den 61°C'ye ve erime sıcaklığını 179°C'den 184°C'ye hafifçe artırarak polimer kararlılığında iyileşme gösterdi. Şişme davranışı, bazı formülasyonlar için %50'ye kadar su alımıyla 9. gün civarında zirveye ulaştı. Aynı zamanda, ilaç salım profilleri 15 gün boyunca sürekli salım sergiledi ve düşük ilaç yüklemelerinde 9. günde %4,24'lük maksimum salım miktarına ulaştı. MCF-7 meme kanseri hücrelerine karşı sitotoksisite testleri önemli canlılık azalmaları gösterdi, özellikle en yüksek 5-FU konsantrasyonunda (%30) 15 gün sonra %33,39 canlılığa ulaşıldı. Bu bulgular, 3B baskı yoluyla üretilen borik asit ve 5-FU katkılı PLA kompozitlerinin, özellikle hedefli kanser tedavisinde ileri biyomedikal uygulamalar geliştirmek için uygun, umut verici mekanik ve kontrollü salımlı ilaç verme özellikleri sunduğunu göstermektedir.

Anahtar kelimeler: Kontrollü ilaç salınımı, kanser, 5-florourasil, borik asit, polilaktik asit (PLA).

1. Introduction

Cancer continues to pose a significant global health challenge, remaining one of the leading causes of morbidity and mortality worldwide. This underscores the urgent need for continuous advancements in cancer treatments aimed at improving patient outcomes (Wu et al., 2024). A highly effective cancer treatment strategy involves accurately targeting therapeutic agents to tumor sites to maximize drug efficacy while minimizing systemic toxicity. Controlled drug delivery systems have emerged as essential tools in achieving this objective, significantly enhancing the safety and effectiveness of cancer therapies (Chavoshi et al., 2019). These systems ensure therapeutic drugs reach their intended targets, thereby reducing adverse effects commonly associated with systemic drug administration.

Among the materials used extensively for controlled drug delivery, polylactic acid (PLA) stands out due to its excellent biodegradability, biocompatibility, and versatile mechanical properties. PLA's suitability for biomedical applications, particularly drug delivery systems, is well-established in the scientific literature, which documents its favorable degradation kinetics and tissue compatibility (Balla et al., 2021; Pirkani et al., 2024). Leveraging these advantageous characteristics, researchers continue to develop advanced polymer-based systems designed to enhance therapeutic efficacy while minimizing associated side effects.

Recent advances in additive manufacturing technologies, particularly digital light processing (DLP)

Corresponding author: haticeaktas@harran.edu.tr

3D printing, have opened new avenues for fabricating customized polymer scaffolds with intricate geometries and precise internal architectures (Yuan et al., 2024; Wang et al., 2023). This technology facilitates the direct integration of bioactive agents within polymer scaffolds, enabling controlled and targeted drug delivery directly to tumor sites. One prominent chemotherapeutic agent extensively utilized in these systems is 5-fluorouracil (5-FU), known for its effective anticancer properties against cancers such as breast and colorectal cancer (Jubeen et al., 2022; Hu et al., 2023). Studies demonstrate that embedding 5-FU within PLA scaffolds significantly enhances localized therapeutic effects and reduces systemic chemotherapy-associated side effects, highlighting the critical role of localized drug delivery approaches (Yun et al., 2017; Carotenuto et al., 2023).

Additionally, recent research has explored the benefits of incorporating additives such as boric acid (H_3BO_3) into polymer matrices. Boric acid has been shown to enhance key polymer properties, including thermal stability, mechanical strength, and controlled degradation behavior, which are essential for biomedical applications (Avci et al., 2024). These improvements directly impact drug release profiles and scaffold performance, potentially leading to better therapeutic outcomes and enhanced patient safety.

This study aims to investigate the effects of incorporating 1% boric acid and various concentrations of 5-FU into PLA scaffolds fabricated through DLP 3D printing. The innovative approach presented systematically evaluates how these additives influence the scaffolds' structural, thermal, mechanical, swelling, degradation, drug release, and cytotoxic properties. Understanding these interactions is crucial for advancing targeted drug delivery technologies, improving therapeutic effectiveness, and offering substantial clinical advantages in cancer treatment (Croitoru et al., 2021). Through such approaches, this research aims to facilitate the development of efficient drug delivery scaffolds capable of providing effective localized treatment while significantly reducing systemic chemotherapy-related adverse effects.

2. Material and Methods

2.1. Sample Preparation

In this study, polylactic acid (PLA) resin (PH100 eResin-PLA Pro, eSUN, China) was used as the primary material, while boric acid (H_3BO_3, 99% purity, Sigma-Aldrich, St. Louis, MO, USA, Cat. No: B0394) and 5-fluorouracil (5-FU, $C_4H_3FN_2O_2$, Sigma-Aldrich, St. Louis, MO, USA, Cat. No: F6627) served as additives. Specifically, 5-FU was incorporated into the PLA resin as a chemotherapeutic agent to enable controlled drug release with the exact compositions detailed in Table 1. The H_3BO_3 powder and 5-FU drug, weighed according to the compositions specified in Table 1, were gradually added into the UV-curable PLA resin. Eight different sample formulations were prepared for this purpose: B0F0 contained pure PLA without any additives; B0F10, B0F20, and B0F30 included 10, 20, and 30 wt.% 5-FU respectively without boric acid; B1F0 contained 1 wt.% H_3BO_3 alone; and B1F10, B1F20, and B1F30 included both 1 wt.% H_3BO_3 and 10, 20, and 30 wt.% 5-FU, respectively. The resulting mixture was homogenized using a magnetic stirrer at 500 rpm for 30 minutes at room temperature. Subsequently, this prepared resin mixture was employed to fabricate samples using a digital light processing (DLP) 3D printer (Elegoo, China) intended for characterization, mechanical testing, cytotoxicity evaluation, and drug release analyses. After the 3D printing process was completed, residual resin on the sample surfaces was removed by immersion in an ethanol-filled ultrasonic bath for 30 seconds. Following this cleaning procedure, the printed parts were fully cured and hardened by exposure to UV light in a curing device for 1 minute (Aktas et al., 2024).

Table 1. Compositions and densities of prepared samples.

Sample code	Polylactic acid (PLA), wt.%	Boric acid (H_3BO_3), wt.%	5-Fluorouracil (5-FU), wt.%	Density (g/cm³)
B0F0	100	0	0	1.153
B0F10	90	0	10	1.171
B0F20	80	0	20	1.098
B0F30	70	0	30	1.175
B1F0	99	1	0	1.162
B1F10	89	1	10	1.189
B1F20	79	1	20	1.064
B1F30	69	1	30	1.104

2.2. Structural, Thermal, and Mechanical Characterization

M_t denotes the drug mass measured at time t (mg), while M_0 represents the initially loaded drug mass (mg). Structural analysis of the samples was performed using a Bruker Hyperion 3000 Fourier Transform Infrared Spectroscopy (FTIR) system, covering a wavenumber range of 400–4000 cm^{-1} (Aktas et al., 2019). The thermal properties of the produced samples were investigated via differential thermal analysis (DTA/TG). Approximately 10 mg of powdered pure PLA and H_3BO_3-doped PLA were placed in a platinum crucible and heated to 600°C at a rate of 10°C/min under a nitrogen atmosphere (Rasul et al., 2025). The tensile and compressive strengths of the produced samples were measured using a computer-controlled universal testing machine equipped with a 10 kN load cell. The tensile and compressive strength values were obtained by averaging the results from five individual samples (Demircan et al., 2020; Alkabbanie et al., 2024).

2.3. Physical Characterization: Density, Swelling, and Degradation

The densities of the samples fabricated by 3D printing were measured using the Archimedes method as described previously (Aktas et al., 2024).

Swelling tests were conducted by immersing the samples in phosphate-buffered saline (PBS) (pH: 7.4) for durations of 1, 5, 9, and 15 days and the swelling rates were determined according to Eq. 1 (Mamidi et al., 2019).

$$Swelling\ Rate\ (\%) = 100 \times (W_w - W_d)/W_d \quad (1)$$

Where W_d represents dry weight, W_w is measured at the end of the specified periods.

Biodegradation tests were performed by placing

samples in PBS for 1, 5, 9, and 15 days, after which their masses were recorded, and biodegradation amounts were calculated as weight loss (%) using Eq. 2 (Chu et al., 2018).

$$Weight\ Loss\ (\%) = 100 \times (W_0 - W_t)/W_0 \quad (2)$$

W_0 is the sample's initial weight (mg) and W_t is the weight measured after drying the samples at various time intervals (mg).

2.4. Drug Release Study

The concentration of 5-fluorouracil (5-FU) released from the samples was determined using UV spectrophotometry at a wavelength of 266 nm (MultiSkan, Thermo Scientific, USA). A stock solution of 5-FU was initially prepared in phosphate-buffered saline (PBS) at a concentration of 1 mg/mL. From this stock, a series of standard solutions were prepared at concentrations of 2, 4, 6, 8, 10, 12 and 14 µg/mL to generate a calibration curve (Samy et al., 2022). For the release study, the samples were immersed in equal volumes of PBS and incubated at predetermined time intervals (1, 5, 9, and 15 days). At each time point, the absorbance of the PBS solutions was recorded at 266 nm and the corresponding 5-FU concentrations were determined using the calibration curve. The percentage of drug release was then calculated using Equation (3) as described by Mamidi et al. (2019).

$$Released\ drug\ amount\ (\%) = 100 \times (M_t/M_0) \quad (3)$$

M_t represents the amount of drug released (mg/mL), while M_0 denotes the initial amount of drug loaded (mg/mL).

2.5. Cytotoxicity Analysis

Cytotoxicity analyses were conducted on MCF-7 breast cancer cells. Initially, the samples were incubated in a complete cell culture medium (DMEM/F12 supplemented with 10% FBS and 1% Penicillin/Streptomycin, Gibco, Thermo Fisher Scientific Inc., Waltham, MA USA, Cat. Numbers: 11320033, A5670201, 15140122) at 37°C for 1, 5, 9, and 15 days. After the incubation period, the collected media were applied to the cells and cell viability was assessed using the MTT assay (Sigma-Aldrich, St. Louis, MO, USA, Cat. No: M5655) following the method described previously (Gumushan Aktas & Altun, 2016; Gumushan Aktas & Akgun, 2018). 5-FU (25µM) was used as positive control. The concentration was chosen according to the literature (Azimi et al., 2022) and our preliminary studies. Absorbance measurements, reflecting the density of viable cells, were taken at 570 and 690 nm. Cell viability (%) was calculated based on the absorbance values. All experiments were performed in triplicate to ensure reproducibility. Differences between groups were statistically evaluated with One-Way ANOVA and Student's *t*-test using the GraphPad Prism 10 software.

3. Results and Discussion

3.1. Structural, Thermal, and Mechanical Characterization

The FT-IR spectrums of $H3BO_3$ and 5FU-doped PLA are shown in Figure 1. The bands observed between 3800-3600 cm^{-1} are due to OH groups. The main component PLA in this study shows characteristic stretching frequencies for C=O, $-CH_3$ asymmetric, $-CH_3$ symmetric, and C–O at 1719, 2994, 2900, and 1062 cm^{-1} respectively (Chieng et al., 2014). The characteristic bands at 1615 cm^{-1} and 1515 cm^{-1} are associated with amide I due to the asymmetric coupling of C=O stretching vibration of the peptide bond and amide II (N–H bending/C–N Stretching) (Rani et al., 2018). The band seen at 1444 cm^{-1} is due to C=C vibration. The C—O—C bond has been seen at around 1021 cm^{-1}. The peak at around 1367 cm^{-1} refers to the vibration of the pyrimidine compound confirming 5-fluorouracil. Further, the peak at around 1235, 1515, and 2353 cm^{-1} belong to C—F stretching or C—N stretching and N—H in plane bending, CH3–N and N—H stretch in 5FU (Mngadi et al., 2021; Olukman et al., 2012). The vibration, which is the presence of Amide IV, has been seen at 675 cm^{-1} and assigned to N–C=O in plane bending (Rani et al., 2018).

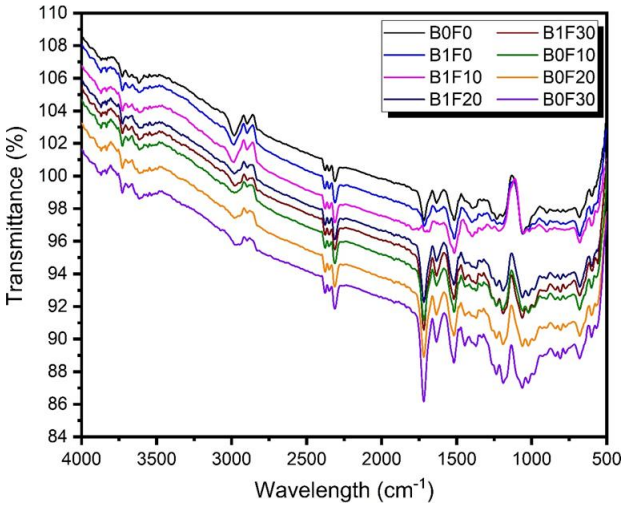

Figure 1. The FT-IR Spectra of PLA samples.

The results obtained from DTA/TG analyses (Fig. 2) demonstrate that incorporating 1% H_3BO_3 into PLA slightly influences the polymer's thermal properties. Specifically, the glass transition temperature (T_g) increased from 58°C to 61°C, indicating improved thermal stability and reduced chain mobility within the polymer structure due to the presence of boric acid. This finding aligns well with previous studies that reported similar enhancements in T_g upon the addition of fillers or additives that restrict polymer chain mobility (Nofar et al., 2019; Rasal et al., 2010). Moreover, the melting temperature (T_m) also rose from 179°C to 184°C with the addition of H_3BO_3, confirming enhanced crystalline stability in the polymer matrix. This observation is consistent with the existing literature where boron-based additives were shown to enhance crystallinity and overall thermal performance in biodegradable polymers (Avci et al., 2024). Such improved crystallinity is beneficial for drug delivery applications as it can facilitate more controlled and sustained drug release by decreasing polymer erosion rates under physiological conditions (Middleton & Tipton, 2000).

The tensile and compressive strength properties of 3D-printed pure PLA (B0F0) and PLA samples containing 1 wt% H_3BO_3 additive (B1F0) were performed to assess the effect of H_3BO_3 incorporation on mechanical performance. The results, presented in Table 2 and Figure 3, clearly demonstrate how the addition of H_3BO_3 influences the tensile and compressive behavior of PLA. The tensile strength of the pure PLA sample (B0F0) was measured as 24.45 MPa, while the H_3BO_3-added PLA sample (B1F0) exhibited a slightly improved tensile strength of 25.30

MPa. This increase in tensile strength can be attributed to the dispersion of H_3BO_3 particles within the PLA matrix that likely enhances interfacial bonding and stress transfer. Studies in the literature have shown that adding ceramic or inorganic fillers can enhance the mechanical properties of polymer matrices by reinforcing the polymer structure and restricting molecular mobility (Kangallı et al., 2022).

Table 2. Tensile and compressive strength data of PLA samples with and without H_3BO_3 additive.

Sample code	Tensile strength (MPa)	% Elongation at break	Elastic modulus (GPa)	Compressive strength (MPa)
B0F0	24.45 ± 1.07	5.75 ± 0.55	0.71 ± 0.068	48.86 ± 0.85
B1F0	25.30 ± 1.85	7.24 ± 2.47	0.69 ± 0.047	55.04 ± 5.68

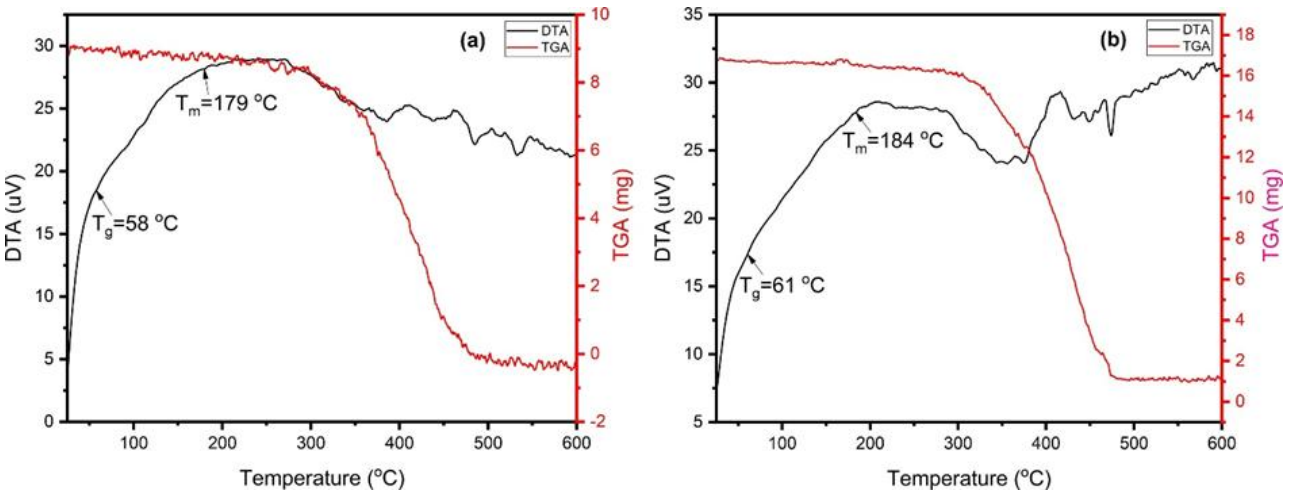

Figure 2. DTA/TG analyses of samples; (a) PLA, (b) 1 wt% H_3BO_3-doped PLA

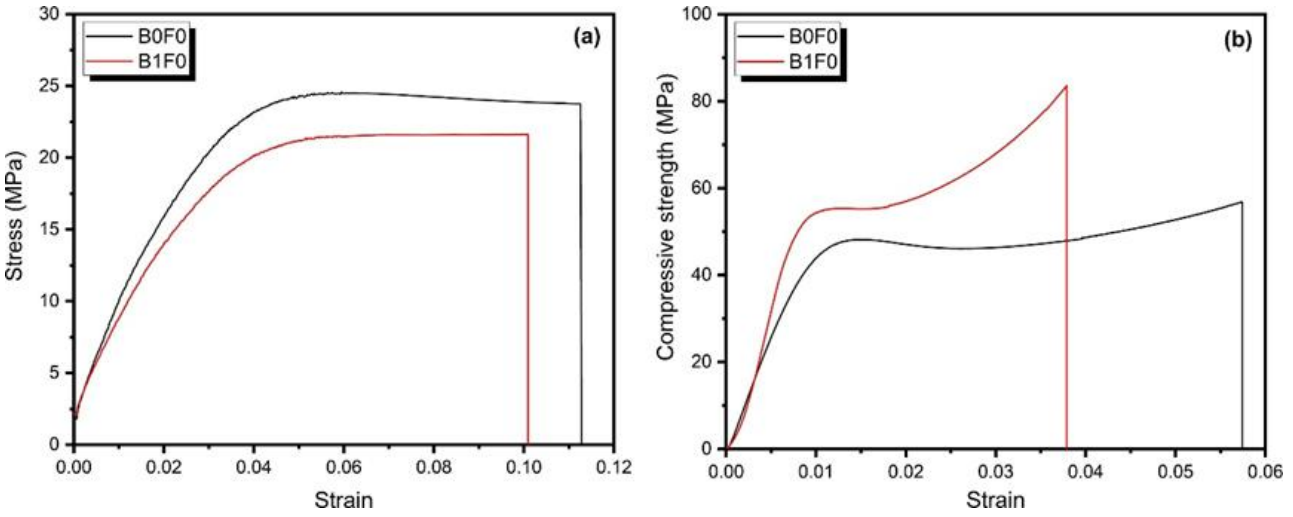

Figure 3. Mechanical properties of the samples: (a) Tensile strength, (b) Compressive strength.

The elongation at break significantly increased from 5.75% in pure PLA to 7.24% in the H_3BO_3-added sample. This improvement suggests that the presence of H_3BO_3 contributes to a more flexible polymer network possibly due to the plasticizing effect or the formation of a composite structure that allows more deformation before fracture. Similar findings have been reported by Avci et al. (2024) who observed increased elongation in PLA composites reinforced with boron-containing compounds. However, the elastic modulus of the PLA sample slightly decreased from 0.71 GPa in pure PLA to 0.69 GPa in the H_3BO_3-added PLA. This reduction indicates that the incorporation of H_3BO_3 might reduce the stiffness of the composite possibly due to the formation of softer interphases within the polymer matrix. Regarding compressive strength, the pure PLA sample demonstrated a value of 48.86 MPa, while the H_3BO_3-added sample showed a notable improvement to 55.04 MPa. This increase of approximately 13% indicates that the presence of H_3BO_3 enhances the material's resistance to compressive forces potentially due to the filler-induced densification and improved load distribution.

In conclusion, the incorporation of H_3BO_3 into PLA via 3D printing demonstrates a positive impact on compressive strength and elongation at break while maintaining tensile strength at an acceptable level.

3.2. Swelling and Degradation

Figure 4 provides quantitative swelling data, revealing notable differences among samples over time. Initial observations (day 1) indicated that PLA samples without additives (B0F0) exhibit relatively low swelling ratios,

around 12.98%, whereas the addition of 5-FU alone (B0F10, B0F20, and B0F30) significantly enhances water absorption capabilities (up to 35.00%). Remarkably, PLA samples containing only 1% H_3BO_3 without 5-FU (B1F0) showed elevated swelling ratios (29.20%), inherent hydrophilic properties of boric acid. The swelling ratios varied dynamically over time, peaking around day 9 for several formulations, such as B0F10 and B0F20, with values reaching up to 50.00% and 39.24%, respectively. This temporal fluctuation is characteristic of polymeric drug delivery systems and is influenced by the continuous interplay between water uptake and the structural integrity of the polymer matrix (Dash & Konkimalla, 2012). Interestingly, samples combining both H_3BO_3 and varying amounts of 5-FU (B1F10, B1F20, B1F30) exhibited inconsistent swelling behaviors over time, suggesting complex interactions between the polymer, drug, and additive. For instance, sample B1F20 demonstrated an unusually low initial swelling ratio (7.60% on day 1), slightly increasing to 15.93% by day 15. Such variations may result from competition between drug-polymer interactions and H_3BO_3-induced structural alterations affecting water diffusion pathways (Byun et al., 2008).

Figure 5 illustrates the degradation behavior of PLA samples incorporating various concentrations of 5-FU, with or without boric acid. On day 1, the most pronounced degradation (27.69%) was observed in PLA samples containing 10% 5-FU but no boric acid (B0F10), implying that the absence of boric acid may facilitate more extensive water infiltration and initial hydrolytic activity. In contrast, the 1% H_3BO_3 (e.g., B1F0, at 6.70%) might stabilize the polymer against early-phase degradation (Tawiah et al., 2018; Byun et al., 2008). Over the 15-day study period, the progression of degradation might be influenced by multiple factors, including water penetration, polymer hydrolysis, and concurrent drug release. By day 15, samples with 5-FU content, such as B0F10 (28.46%) and B0F30 (18.22%), show markedly greater breakdown, reinforcing the notion that drug loading can enhance the hydrophilicity and susceptibility to hydrolysis of polymer (Singh, & Lillard, 2009; Liechty et al., 2010). Meanwhile, formulations that combine 1% H_3BO_3 and increased levels of 5-FU (e.g., B1F20 and B1F30) have exhibited unique degradation patterns, pointing to potential synergistic or antagonistic interactions between the additive and the drug.

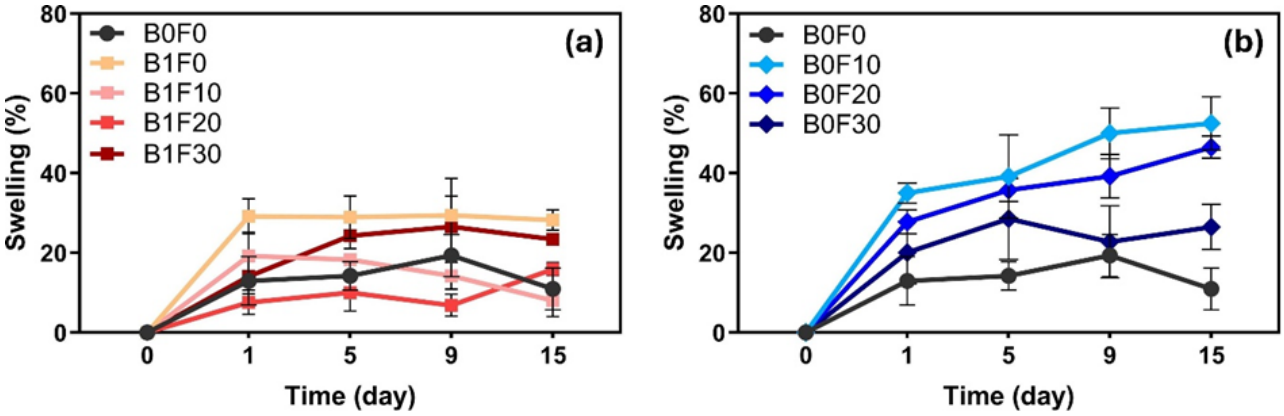

Figure 4. Time-dependent swelling ratios of the samples: (a) PLA samples containing 1% H_3BO_3 and varying concentrations of 5-FU (10, 20, 30 wt%), (b) PLA samples containing varying concentrations of 5-FU (10, 20, 30 wt%).

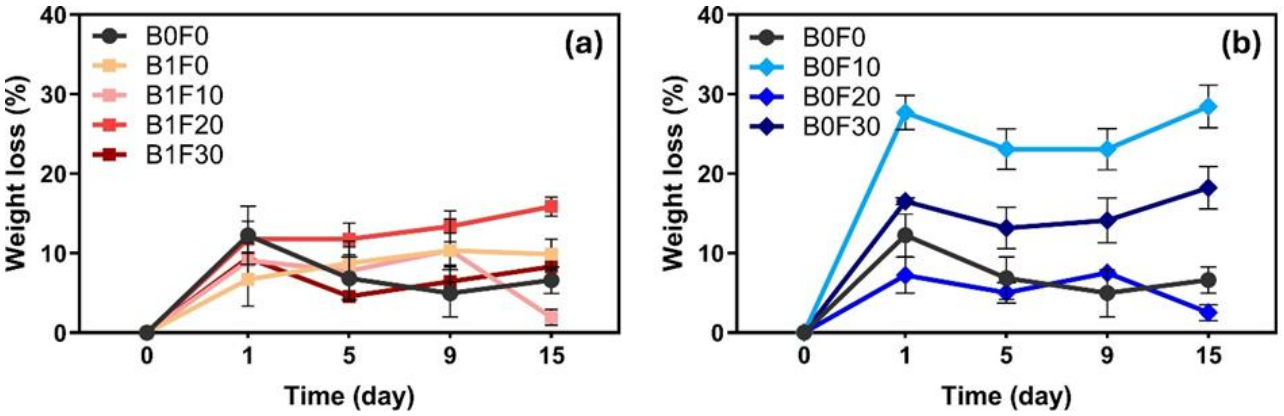

Figure 5. Degradation profiles over time of PLA samples loaded (a) with (b) without 1% H_3BO_3, and varying amounts of 5-FU.

3.3. Drug Release Profile

The drug release profiles reveal that the rate of 5-FU release from the samples is significantly influenced by both the concentration of 5-FU and the presence of H_3BO_3 (Fig. 6). PLA samples containing 1% H_3BO_3 (B1F10, B1F20, B1F30) consistently showed higher drug release rates compared to their counterparts without H_3BO_3 (Fig. 6a-c). This increment likely may result from reducing polymer matrix rigidity induced by boric acid. On the first day, sample B1F20 exhibited the highest initial drug release percentage (2.32%). Interestingly, increasing the concentration of 5-FU to 30% (samples B1F30 and B0F30) did not enhance the initial drug release. This suggests a possible saturation effect or altered polymer-drug interactions at higher concentrations as supported by previous findings on PLA-based systems (Proikakis et al., 2006; Lasprilla et al., 2012). Between days 5 and 9, drug

release steadily increased for all formulations (Fig. 6d-e) with samples containing H_3BO_3 consistently showing slightly higher release percentages than their counterparts lacking boric acid (Fig. 6a-c). For instance, after 9 days, sample B1F10 demonstrated the highest release amount (4.24%) compared to 3.30% observed for sample B0F10 without H_3BO_3. Such findings align with the literature indicating that incorporating additives such as boric acid can modify polymer matrix interactions, potentially enhancing drug diffusion by altering polymer hydrophilicity or network structure (Makadia & Siegel, 2011; Gagliardi et al., 2021). Among the samples without H_3BO_3 (B0F10, B0F20, B0F30), the B0F10 sample showed the highest release amount (3.30%) after 9 days, while the B0F30 sample exhibited a significantly lower release of 2.33% at the same time point (Fig. 6e). This pattern is consistent with other polymeric drug delivery systems where the encapsulated drug diffuses gradually through the polymer matrix over time (Lee & Yeo, 2015). Such behavior aligns with previous reports indicating that higher drug loading can reduce initial release rates due to denser packing or agglomeration of drug particles within the polymer matrix which limits the diffusion of the drug (Herdiana et al., 2022; Vlachopoulos et al., 2022).

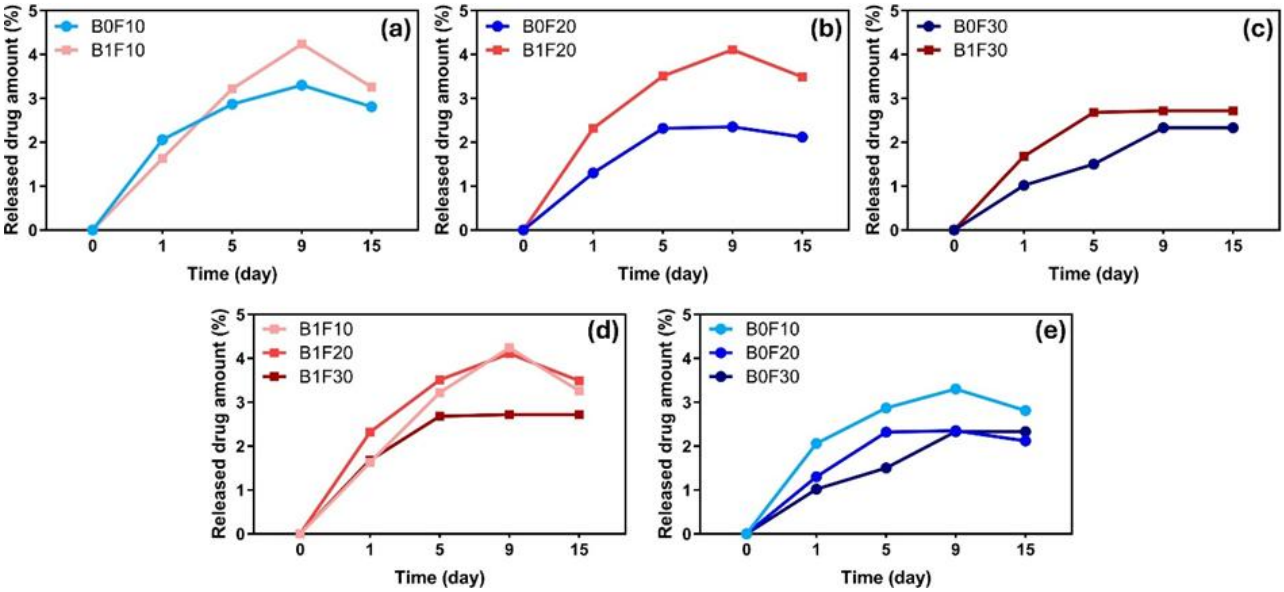

Figure 6. Drug release profiles over time for PLA samples doped with 5-FU.

3.4. Cytotoxic Activity

In this part of the study, the cytotoxic effects and drug release performance of polylactic acid (PLA) scaffolds containing different concentrations of 5-fluorouracil (5-FU) and boric acid (H_3BO_3) were evaluated using MCF-7 breast cancer cells. Cell viability was assessed at four time points (days 1, 5, 9, and 15) using the MTT assay and the results are presented in Figure 7.

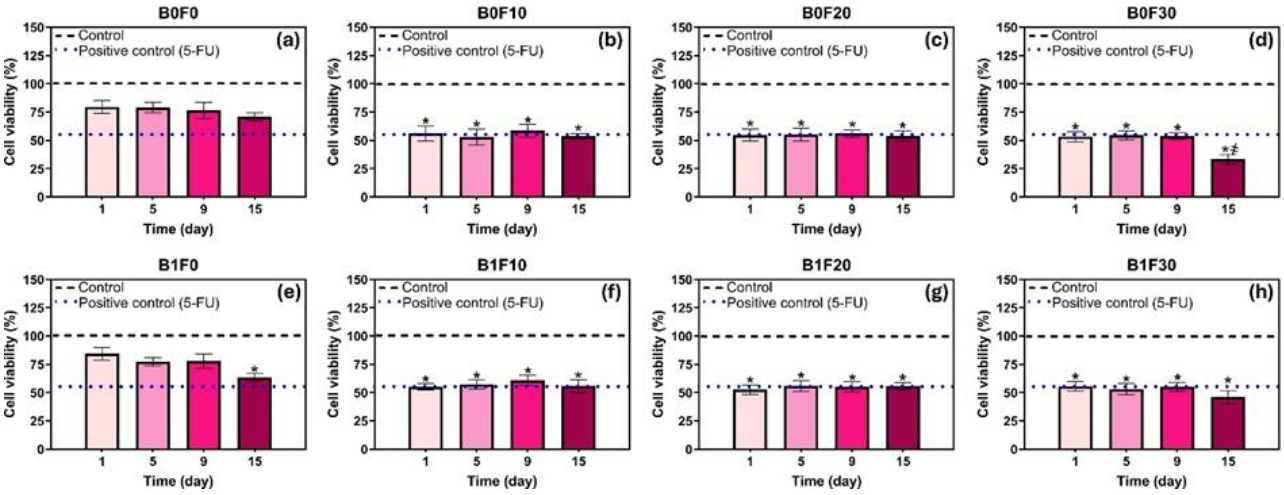

Fig. 7. Cell viability (%) measured on MCF-7 breast cancer cells exposed to samples (a) undoped PLA, (b)-(d) different ratios (10%, 20%, 30%) of 5-FU; (e)-(h) H_3BO_3 (1%) and different ratios (10%, 20%, 30%) of 5-FU for different periods of time (1, 5, 9, 15 days).

*: Statistically significant difference between test and control groups ($p<0.05$).

≠: Statistically significant difference between test and positive control (5-FU) groups ($p<0.05$)

Undoped PLA (B0F0) exhibited consistently high cell viability across all time points, maintaining 79.60% viability on day 1 and 70.96% on day 15 (Fig. 7a, Fig. 8a), confirming its excellent biocompatibility. This observation is consistent with previous findings that PLA is well-tolerated in vivo and degrades gradually into non-toxic by-products. For instance, Majola et al. (1991) observed that PLA scaffolds implanted in rat femurs were

biocompatible and slowly absorbed over 1 to 48 weeks. Similarly, Robert et al. (1993) demonstrated that PLA membranes implanted subcutaneously in rats maintained biodegradability and compatibility. Middleton and Tipton (2000) further emphasized that PLA's slow hydrolysis kinetics and inert degradation products make it an ideal matrix for drug delivery systems.

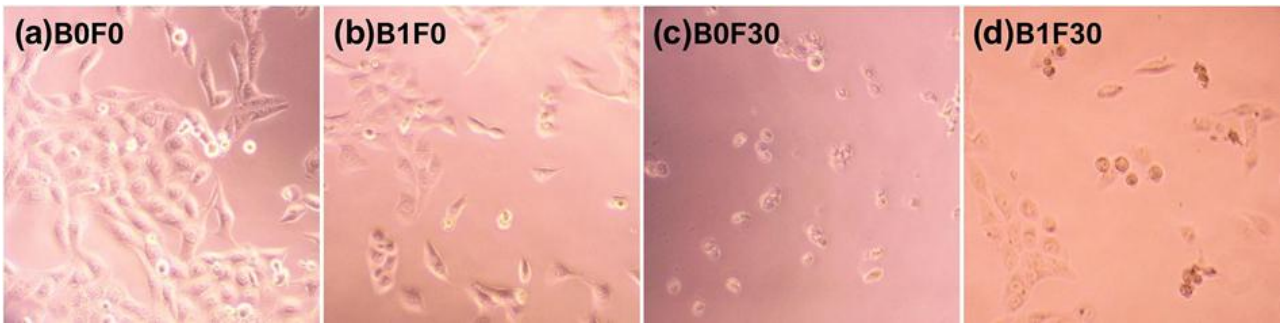

Fig. 8. Cell morphology after treatment with PLA samples doped with different amounts of boric acid and 5-FU by day 15. (Olympus CKX41 invert microscope, Magnification: 20×)

In the present study, upon incorporation of 5-FU, a significant ($p<0.05$) and concentration-dependent decrease in cell viability was observed. In all samples doped with 5FU addition (with or without boric acid), cell viability decreased significantly ($p<0.05$) compared to the control group at all time intervals (1, 5, 9, and 15 days). For instance, the B0F30 sample (30 wt% 5-FU, no boric acid) showed a reduction in cell viability from 53.47% on day 1 to 33.39% on day 15 (Fig 7d, Fig 8c). This progressive cytotoxicity is attributed to the sustained release of 5-FU from the PLA matrix. The release behavior of PLA is known to be influenced by its molecular weight and hydrophilicity. Makadia and Siegel (2011) reported that low molecular weight PLA releases drugs more rapidly, while modifications to the polymer composition can tailor its hydrophilic character and control the release rate. In a related study, Ocal et al. (2014) demonstrated that 5-FU-loaded low molecular weight PLA microspheres significantly suppressed Caco-2 cell viability by approximately 50%. Similarly, Karavelidis and Bikiaris (2012) observed 50% viability in HepG2 and 20% in HeLa cells using paclitaxel-loaded PLA systems.

The addition of 1 wt% H_3BO_3 notably influenced cytotoxicity profiles. Interestingly, the B1F30 sample (containing both boric acid and 30 wt% 5-FU) exhibited higher viability (46.12% at day 15) compared to B0F30 (33.39%) (Fig. 7h vs. Fig. 7d, Fig. 8d vs. Fig. 8c). This suggests that boric acid may modulate drug release behavior, leading to a more controlled and gradual release of 5-FU. Previous studies report that boron-containing additives can form secondary interactions with polymer chains, thus influencing polymer network density or hydrophilicity, altering degradation kinetics, and drug diffusion pathways (Ailincai et al., 2020). For instance, Aliasgharlou et al. (2020) demonstrated that incorporating boric acid into ethyl cellulose and polyvinyl alcohol films altered their degradation and drug release profiles. Vedelago et al. (2021) also showed that boric acid crosslinking in polymer networks significantly impacted mechanical performance and enabled the design of controlled release systems.

Moreover, boric acid itself displayed anticancer activity. The B1F0 sample (1% H_3BO_3 only) showed a noticeable reduction in cell viability after 15 days compared to undoped PLA (B0F0), indicating its bioactive potential (Fig. 7e, Fig. 8b). Prior studies have shown that boric acid can induce oxidative stress, cause cell cycle arrest, and promote apoptosis in various cancer cell lines, including those derived from breast, liver, and prostate tumors (Khaliq et al., 2018; Scorei & Popa, 2010).

Samples containing lower concentrations of 5-FU (10% and 20%) along with H_3BO_3 (B1F10 and B1F20) exhibited moderate and stable cytotoxic responses (~55–60% viability), indicating a balanced profile of sustained drug release and material biocompatibility (Fig. 7f, Fig. 7g). Such steady responses are beneficial for long-term therapeutic applications where continuous drug delivery at sub-cytotoxic levels is desired to inhibit tumor progression without inducing acute toxicity (Musumeci et al., 2006; Kumar et al., 2017).

Overall, the combined use of H_3BO_3 and 5-FU in DLP 3D-printed PLA scaffolds demonstrates a synergistic potential for localized cancer therapy. Boric acid not only enhances structural and thermal scaffold properties but also contributes to the modulation of drug release and may exhibit independent anticancer activity. These multifunctional properties position the scaffold system as a promising platform for sustained, site-specific chemotherapeutic delivery.

4. Conclusions

In this study, PLA-based scaffolds incorporating 5-fluorouracil (5-FU) and boric acid (H_3BO_3) were successfully fabricated via digital light processing (DLP) 3D printing to achieve controlled drug release for cancer treatment. Comprehensive characterization revealed that introducing 1% H_3BO_3 moderately affected drug release kinetics, slightly lowering early-stage release rates and influencing overall drug efficacy. Meanwhile, the addition of 1% H_3BO_3 markedly enhanced PLA's thermal properties, elevating the glass transition temperature (Tg) from 58 °C to 61 °C and the melting temperature (Tm) from 179 °C to 184 °C. Mechanical testing indicated an increase in tensile strength from 24.45 MPa (pure PLA) to 25.30 MPa alongside a significant rise in elongation at break from 5.75% to 7.24%, suggesting improved flexibility. Compressive strength also increased from 48.86 MPa to 55.04 MPa with 1% H_3BO_3. Swelling analyses showed that scaffolds containing 10% 5-FU without boric acid reached a maximum swelling ratio of about 50.00% by day 9, while degradation tests revealed the highest mass

loss (28.46%) at day 15 in these same formulations. In contrast, boric acid-containing samples (B1F10, B1F20, B1F30) exhibited higher or more controlled 5-FU release compared to samples without boric acid. For instance, by day 9, B1F10 released 4.24% of 5-FU versus 3.30% in B0F10. At higher drug loads (30% 5-FU), the initial release was somewhat lower yet more sustained, possibly due to denser drug packing within the polymer matrix. In terms of cytotoxicity, undoped PLA (B0F0) displayed good biocompatibility (>70% cell viability at day 15). However, the introduction of 5-FU significantly reduced cell viability, particularly in the 30% 5-FU sample (B0F30), which dropped from about 53.47% on day 1 to 33.39% by day 15. Combining 1% boric acid with 5-FU (B1F30) resulted in 46.12% cell viability at day 15, indicating boric acid's modulatory effect on 5-FU cytotoxicity. Additionally, the B1F0 sample (1% boric acid without 5-FU) also lowered viability relative to undoped PLA due to probable anticancer or antiproliferative properties of boric acid itself.

In conclusion, the findings demonstrate that DLP 3D-printed PLA scaffolds co-loaded with H_3BO_3 and 5-FU possess desirable structural, mechanical, and biological properties for localized chemotherapeutic delivery platforms. The synergistic integration of PLA, boric acid, and 5-fluorouracil offers a promising strategy for enhancing the therapeutic efficacy and safety of cancer treatments through localized and sustained drug release. Further in vivo investigations are warranted to validate the clinical applicability of this system.

Ethics committee approval: Ethics committee approval is not required for this study.

Conflict of interest: The author declares that there is no conflict of interest.

References

Ailincai, D., Gavril, G., & Marin, L. (2020). Polyvinyl alcohol boric acid – A promising tool for the development of sustained release drug delivery systems. *Materials Science and Engineering: C*, 107, 110316. https://doi.org/10.1016/j.msec.2019.110316

Aktas, B., Yalcin, S., Dogru, K., Uzunoglu, Z., & Yilmaz, D. (2019). Structural and radiation shielding properties of chromium oxide doped borosilicate glass. *Radiation Physics and Chemistry*, 156, 144-149. https://doi.org/10.1016/j.radphyschem.2018.11.012

Aktas, B., Das, R., Acikgoz, A., Demircan, G., Yalcin, S., Aktas, H.G., & Balak, M.V. (2024). DLP 3D printing of TiO2-doped Al2O3 bioceramics: Manufacturing, mechanical properties, and biological evaluation. *Materials Today Communications*, 38, 107872. https://doi.org/10.1016/j.mtcomm.2023.107872

Aliasgharlou, N., Sana, F.A., Khoshbakht, S., Zolfaghari, P., & Charkhian, H. (2020). Fabrication and characterization of boric acid-crosslinked ethyl cellulose and polyvinyl alcohol films as potential drug release systems for topical drug delivery. *Turkish Journal of Chemistry*, 44(6), 1723-1732. https://doi.org/10.3906/kim-2008-23

Alkabbanie, R., Aktas, B., Demircan, G., & Yalcin, S. (2024). Short carbon fiber-reinforced PLA composites: influence of 3D-printing parameters on the mechanical and structural properties. *Iranian Polymer Journal*, 33(8), 1065-1074. https://doi.org/10.1007/s13726-024-01315-8

Avci, A., Akdogan Eker, A., Bodur, M.S., & Küçükyildirim, B.O. (2024). The effects of various boron compounds on the thermal, microstructural and mechanical properties of PLA biocomposites. *Thermochimica Acta*, 731, 179656. https://doi.org/10.1016/j.tca.2023.179656

Azimi, S., Esmaeil Lashgarian, H., Ghorbanzadeh, V., Moradipour, A., Pirzeh, L., & Dariushnejad, H. (2022). 5-FU and the dietary flavonoid carvacrol: a synergistic combination that induces apoptosis in MCF-7 breast cancer cells. *Medical Oncology*, 39(12), 253. https://doi.org/10.1007/s12032-022-01863-0

Balla, E., Daniilidis, V., Karlioti, G., Kalamas, T., Stefanidou, M., Bikiaris, N. D., Vlachopoulos, A., Koumentakou, I., & Bikiaris, D.N. (2021). Poly(lactic Acid): A Versatile Biobased Polymer for the Future with Multifunctional Properties—From Monomer Synthesis, Polymerization Techniques and Molecular Weight Increase to PLA Applications. *Polymers*, 13(11), 1822. https://doi.org/10.3390/polym13111822

Byun, H., Hong, B., Nam, S.Y., Jung, S.Y., Rhim, J.W., Lee, S.B., & Moon, G.Y. (2008). Swelling behavior and drug release of poly (vinyl alcohol) hydrogel cross-linked with poly (acrylic acid). *Macromolecular Research*, 16, 189-193. https://doi.org/10.1007/BF03218851.

Carotenuto, P., Pecoraro, A., Brignola, C., Barbato, A., Franco, B., Longobardi, G., ... & Russo, A. (2023). Combining β-Carotene with 5-FU via Polymeric Nanoparticles as a Novel Therapeutic Strategy to Overcome uL3-Mediated Chemoresistance in p53-Deleted Colorectal Cancer Cells. *Molecular Pharmaceutics*, 20(5), 2326-2340.

Chavoshi, S., Rabiee, M., Rafizadeh, M., Rabiee, N., Shamsabadi, A. S., Bagherzadeh, M., ... & Tayebi, L. (2019). Mathematical modeling of drug release from biodegradable polymeric microneedles. *Bio-Design and Manufacturing*, 2, 96-107. https://doi.org/10.1007/s42242-019-00041-y

Chieng, B.W., Azowa, I.N., Yunus, W.M.Z.W., & Hussein, M.Z. (2014). Effects of graphene nanopletelets on poly (lactic acid)/poly (ethylene glycol) polymer nanocomposites. *Advanced materials research*, 1024, 136-139.

Chu, L., Jiang, G., Hu, X-L., James, T.D., He, X-P., Yaping Li, Y., & Tang, T. (2018). Biodegradable macroporous scaffold with nano-crystal surface microstructure for highly effective osteogenesis and vascularization. *Journal of Materials Chemistry B*, 6, 1658-1667. https://doi.org/10.1039/C7TB03353B

Croitoru, A., Karaçelebi, Y., Saatcioglu, E., Altan, E., Ulag, S., Aydoğan, H., … & Ficai, A. (2021). Electrically triggered drug delivery from novel electrospun poly(lactic acid)/graphene oxide/quercetin fibrous scaffolds for wound dressing applications. *Pharmaceutics*, 13(7), 957. https://doi.org/10.3390/pharmaceutics13070957

Dash, T.K., & Konkimalla, V.B. (2012). Polymeric modification and its implication in drug delivery: Poly-ε-caprolactone (PCL) as a model polymer. *Molecular Pharmaceutics*, 9(9), 2365-2379.

Demircan, G., Kisa, M., Özen, M., Açikgöz, A., Aktaş, B., & Ali Kurt, M. (2020). A bio-based epoxy resin from rosin powder with improved mechanical performance. *Emerging Materials Research*, 9(4), 1076-1081. https://doi.org/10.1680/jemmr.20.00001

Gagliardi, A., Giuliano, E., Venkateswararao, E., Fresta, M., Bulotta, S., Awasthi, V., & Cosco, D. (2021). Biodegradable Polymeric Nanoparticles for Drug Delivery to Solid Tumors. *Frontiers in Pharmacology*, 12, 601626. https://doi.org/10.3389/fphar.2021.601626

Gumushan Aktas, H., & Akgun, T. (2018). Naringenin inhibits prostate cancer metastasis by blocking voltage-gated sodium channels. *Biomedicine & Pharmacotherapy*, 106, 770-775. https://doi.org/10.1016/j.biopha.2018.07.008

Gumushan-Aktas, H., & Altun, S. (2016). Effects of *Hedera helix* L. extracts on rat prostate cancer cell proliferation and motility. *Oncology Letters*, 12, 2985-2991. https://doi.org/10.3892/ol.2016.4941

Herdiana, Y., Wathoni, N., Shamsuddin, S., & Muchtaridi, M. (2021). Drug release study of the chitosan-based nanoparticles. *Heliyon*, 8(1), e08674. https://doi.org/10.1016/j.heliyon.2021.e08674

Hu, J., Li, A., Guo, Y., Ma, T., & Feng, S. (2023). The relationship between tumor metabolism and 5-fluorouracil resistance. *Biochemical Pharmacology*, 218, 115902. https://doi.org/10.1016/j.bcp.2023.115902

Jubeen, F., Ijaz, S., Jabeen, I., Aftab, U., Mehdi, W., Altaf, A., Alissa, S.A., Al-Ghulikah, H.A., Ezzine, S., Bejaoui, I., & Iqbal, M. (2022). Anticancer potential of novel 5-Fluorouracil co-crystals against MCF7 breast and SW480 colon cancer cell lines along with docking studies. *Arabian Journal of Chemistry*, 15(12), 104299. https://doi.org/10.1016/j.arabjc.2022.104299

Kangallı, E., & Bayraktar, E. (2022). Preparation and characterization of poly(lactic acid)/boron oxide nanocomposites: Thermal, mechanical, crystallization, and flammability properties. *Journal of Applied Polymer Science*, 139(28), e52521. https://doi.org/10.1002/app.52521

Karavelidis, V., & Bikiaris, D. (2012). New biocompatible aliphatic polyesters as thermosensitive drug nanocarriers. Application in Targeting Release Pharmaceutical Systems for Local Cancer Treatment. *Journal of Nanomedicine Nanotechnology*, 3(134), 2. https://doi.org/10.4172/2157-7439.1000134

Khaliq, H., Juming, Z. & Ke-Mei, P. (2018). The Physiological Role of Boron on Health. *Biological Trace Element Research*, 186, 31–51. https://doi.org/10.1007/s12011-018-1284-3

Kumar, S., Singh, S., Senapati, S., Singh, A.P., Ray, B., & Maiti, P. (2017). Controlled drug release through regulated biodegradation of

poly(lactic acid) using inorganic salts. *International Journal of Biological Macromolecules*, 104, 487-497. https://doi.org/10.1016/j.ijbiomac.2017.06.033

Lasprilla, A.J., Martinez, G.A., Lunelli, B.H., Jardini, AL., & Filho, R. M. (2011). Poly-lactic acid synthesis for application in biomedical devices — A review. *Biotechnology Advances*, 30(1), 321-328. https://doi.org/10.1016/j.biotechadv.2011.06.019

Lee, J.H., & Yeo, Y. (2015). Controlled drug release from pharmaceutical nanocarriers. *Chemical Engineering Science*, 125, 75-84. https://doi.org/10.1016/j.ces.2014.08.046

Liechty, W. B., Kryscio, D. R., Slaughter, B. V., & Peppas, N. A. (2010). Polymers for drug delivery systems. *Annual review of chemical and biomolecular engineering*, 1(1), 149-173. https://doi.org/10.1146/annurev-chembioeng-073009-100847

Majola, A., Vainionpää, S., Vihtonen, K., Mero, M., Vasenius, J., Törmälä, P., & Rokkanen, P. (1991). Absorption, biocompatibility, and fixation properties of polylactic acid in bone tissue: an experimental study in rats. *Clinical Orthopaedics and Related Research* (1976-2007), 268, 260-269.

Makadia, H.K., & Siegel, S.J. (2011). Poly Lactic-co-Glycolic Acid (PLGA) as Biodegradable Controlled Drug Delivery Carrier. *Polymers*, 3(3), 1377-1397. https://doi.org/10.3390/polym3031377

Mamidi, N., Gonzalez-Ortiz, A., Lopez Romo, I., Barrera, E.V. (2019). Development of Functionalized Carbon Nano-Onions Reinforced Zein Protein Hydrogel Interfaces for Controlled Drug Release. *Pharmaceutics*, 11(12), 621. https://doi.org/10.3390/pharmaceutics11120621

Middleton, J.C., & Tipton, A.J. (2000). Synthetic biodegradable polymers as orthopedic devices. *Biomaterials*, 21(23), 2335–2346. https://doi.org/10.1016/S0142-9612(00)00101-0

Mngadi, S., Singh, M., & Mokhosi, S. (2021). PVA coating of ferrite nanoparticles triggers pH-responsive release of 5-fluorouracil in cancer cells. *Journal of Polymer Engineering*, 41(7), 597-606.

Musumeci, T., Ventura, C., Giannone, I., Ruozi, B., Montenegro, L., Pignatello, R., & Puglisi, G. (2006). PLA/PLGA nanoparticles for sustained release of docetaxel. *International Journal of Pharmaceutics*, 325(1-2), 172-179. https://doi.org/10.1016/j.ijpharm.2006.06.023

Nofar, M., & Park, C.B. (2014). Poly(lactic acid) foaming. *Progress in Polymer Science*, 39(10), 1721–1741.

Olukman, M., Şanlı, O., & Solak, E.K. (2012). Release of anticancer drug 5-Fluorouracil from different ionically crosslinked alginate beads. *Journal of Biomaterials and Nanobiotechnology*, 3(4), 469-479.

Öcal, H., Arıca-Yegin, B., Vural, I., Goracinova, K., & Çalış, S. (2014). 5-Fluorouracil-loaded PLA/PLGA PEG–PPG–PEG polymeric nanoparticles: formulation, in vitro characterization and cell culture studies. *Drug Development and Industrial Pharmacy*, 40(4), 560-567. https://doi.org/10.3109/03639045.2013.775581

Pirkani, Z., Kamalinejad, F., Zare, Y., Abdollahi Boraei, S.B. (2024). Advancing Breast Cancer Treatment: The Role of PLA-based Scaffolds in Tumor Microenvironment and Drug Delivery. *Multidisciplinary Cancer Investigation*, 8(1), 1-14. https://doi.org/10.61186/mci.8.1.2

Proikakis, C., Tarantili, P., & Andreopoulos, A. (2006). The role of polymer/drug interactions on the sustained release from poly(dl-lactic acid) tablets. *European Polymer Journal*, 42(12), 3269-3276. https://doi.org/10.1016/j.eurpolymj.2006.08.023

Rani, K.V., Chandwani, N., Kikani, P., Nema, S.K., Sarma, A.K., & Sarma, B. (2018). Optimization and surface modification of silk fabric using DBD air plasma for improving wicking properties. *The Journal of the Textile Institute*, 109(3), 368-375.

Rasal, R.M., Janorkar, A.V., & Hirt, D.E. (2010). Poly(lactic acid) modifications. *Progress in Polymer Science*, 35(3), 338–356.

Rasul, S.Y., Aktas, B., Yilmaz, D., Pathman, A.F., Yalcin, S., & Acikgoz, A. (2025). Impact of HfO2 on the structural, thermal, gamma, and neutron shielding properties of boro-tellurite glasses. *Inorganic Chemistry Communications*, 113993. https://doi.org/10.1016/j.inoche.2025.113993

Robert, P., Mauduit, J., Frank, R.M., & Vert, M. (1993). Biocompatibility and resorbability of a polylactic acid membrane for periodontal guided tissue regeneration. *Biomaterials*, 14(5), 353–358. https://doi:10.1016/0142-9612(93)90054-6

Samy, M., Abdallah, H.M., Awad, H.M., & Ayoub, M.M. (2022). In vitro release and cytotoxicity activity of 5-fluorouracil entrapped polycaprolactone nanoparticles. *Polymer Bulletin*, 1-27. https://doi.org/10.1007/s00289-021-03804-9

Scorei, R.I., & Popa, R., Jr (2010). Boron-containing compounds as preventive and chemotherapeutic agents for cancer. *Anti-cancer agents in medicinal chemistry*, 10(4), 346–351. https://doi.org/10.2174/187152010791162289

Singh, R., & Lillard, J.W. (2009). Nanoparticle-based targeted drug delivery. *Experimental and Molecular Pathology*, 86(3), 215-223. https://doi.org/10.1016/j.yexmp.2008.12.004

Tawiah, B., Yu, B., Cheung, W.Y., Chan, S.Y., Yang, W., & Fei, B. (2018). Synthesis and application of synergistic azo-boron-BPA / polydopamine as efficient flame retardant for poly(lactic acid). *Polymer Degradation and Stability*, 152, 64-74. https://doi.org/10.1016/j.polymdegradstab.2018.03.018

Vedelago, J., Mattea, F., Triviño, S., Montesinos, M.D.M., Keil, W., Valente, M., & Romero, M. (2021). Smart material based on boron crosslinked polymers with potential applications in cancer radiation therapy. *Scientific reports*, 11(1), 12269. https://doi.org/10.1038/s41598-021-91413-x

Vlachopoulos, A., Karlioti, G., Balla, E., Daniilidis, V., Kalamas, T., Stefanidou, M., … & Bikiaris, D.N. (2022). Poly(Lactic Acid)-Based Microparticles for Drug Delivery Applications: An Overview of Recent Advances. *Pharmaceutics*, 14(2), 359. https://doi.org/10.3390/pharmaceutics14020359

Wang, X., Liu, J., Zhang, Y., Kristiansen, P.M., Islam, A., Gilchrist, M., & Zhang, N. (2023). Advances in precision microfabrication through digital light processing: system development, material and applications. *Virtual and Physical Prototyping*, 18(1). https://doi.org/10.1080/17452759.2023.2248101

Wu, Z., Xia, F. & Lin, R. (2024). Global burden of cancer and associated risk factors in 204 countries and territories, 1980–2021: a systematic analysis for the GBD 2021. *Journal of Hematology and Oncology*, 17, 119. https://doi.org/10.1186/s13045-024-01640-8

Yuan, X., Zhu, W., Yang, Z., He, N., Chen, F., Han, X., & Zhou, K. (2024). Recent Advances in 3D Printing of Smart Scaffolds for Bone Tissue Engineering and Regeneration. *Advanced Materials*, 36(34), 2403641. https://doi.org/10.1002/adma.202403641

Yun, Q., Wang, S.S., Xu, S., Yang, J.P., Fan, J., Yang, L.L., Chen, Y., Fu, S.Z., & Wu, J.B. (2017). Use of 5-Fluorouracil Loaded Micelles and Cisplatin in Thermosensitive Chitosan Hydrogel as an Efficient Therapy against Colorectal Peritoneal Carcinomatosis. *Macromolecular Bioscience*, 17(4), 1600262. https://doi.org/10.1002/mabi.201600262

Commagene Journal of Biology

Kahya & Mahmood, (2025) *Comm. J. Biol.* 9(1), 112–122.
DOI: 10.31594/commagene.1641548

e-ISSN 2602-456X

Review / Derleme

The Relationship between Stress and Immune Function: A Review Article

Hasan Faisal Hussein KAHYA[1]*, Mohammed Taha MAHMOOD[2]

[1]*Department of Biology, College of Education for Pure Sciences, University of Mosul, Mosul, IRAQ*
[2]*Department of Basic Sciences, College of Nursing, University of Mosul, Mosul, IRAQ*
ORCID ID: Hasan Faisal Hussein KAHYA: https://orcid.org/0000-0002-2699-5291, Mohammed Taha MAHMOOD: https://orcid.org/0000-0002-6651-4421

Received: 17.02.2025 **Accepted:** 25.04.2025 **Published online:** 04.05.2025 **Issue published:** 30.06.2025

Abstract: The intricate nexus between stress levels and immune system efficacy has drawn considerable scientific interest, given its profound implications for human health and quality of life. Persistent or chronic stress can precipitate deleterious outcomes on the immune system, inducing immune system imbalance, heightened vulnerability to infections, and elevated probability of contracting a diverse range of diseases. This analytical review presents an exhaustive exploration of the complex interaction between stress conditions and immune responses. It delves into the effects of stress stimuli on the activity of immune cells, the production of cytokines, inflammation levels, and the equilibrium of pro-inflammatory and anti-inflammatory processes. Furthermore, this paper examines various stress management methodologies such as mindfulness-based stress reduction, meditation practices, physical exercise, and social support networks that can potentially ameliorate immune system performance and mitigate the harmful consequences of chronic stress. Comprehending the interconnectivity between stress and immune responses is indispensable for fostering optimal health and quality of life. Subsequent research endeavors should concentrate on demystifying the underlying mechanisms of stress-induced immune imbalances and individual variances in stress reactions to devise bespoke strategies for stress regulation and immune system fortification.

Keywords: Stress and immune functionality, Immune suppression, chronic stress, stress-induced immune.

Stres ile Bağışıklık Fonksiyonu Arasındaki İlişki: Bir Derleme Makalesi

Öz: Stres düzeyleri ile bağışıklık sistemi etkinliği arasındaki karmaşık ilişki, insan sağlığı ve yaşam kalitesi üzerindeki derin etkileri nedeniyle önemli bilimsel ilgi görmüştür. Sürekli veya kronik stres, bağışıklık sistemi üzerinde olumsuz sonuçlar doğurarak bağışıklık dengesizliğine, enfeksiyonlara karşı artan hassasiyete ve çok çeşitli hastalıklara yakalanma olasılığının yükselmesine yol açabilir. Bu analitik derleme, stres koşulları ile bağışıklık tepkileri arasındaki karmaşık etkileşimi kapsamlı bir şekilde incelemektedir. Metin, stres uyaranlarının bağışıklık hücrelerinin aktiviteleri, sitokin üretimi, iltihap düzeyleri ve proinflamatuar (iltihap artırıcı) ile antiinflamatuar (iltihap önleyici) süreçlerin dengesi üzerindeki etkilerini ele almaktadır. Ayrıca bu çalışma, bağışıklık sistemi performansını iyileştirebilecek ve kronik stresin zararlı etkilerini hafifletebilecek farkındalığa dayalı stres azaltma, meditasyon uygulamaları, fiziksel egzersiz ve sosyal destek ağları gibi çeşitli stres yönetimi yöntemlerini de incelemektedir. Stres ile bağışıklık tepkileri arasındaki karşılıklı bağlantıyı anlamak, sağlığın ve yaşam kalitesinin en iyi düzeye çıkarılması için vazgeçilmezdir. Gelecekteki araştırmalar, strese bağlı bağışıklık dengesizliklerinin altında yatan mekanizmaların ve bireysel stres tepkilerindeki farklılıkların anlaşılmasına odaklanarak stresin düzenlenmesi ve bağışıklık sisteminin güçlendirilmesi için kişiye özel stratejiler geliştirmeyi amaçlamalıdır.

Anahtar kelimeler: Stres ve bağışıklık işlevselliği, bağışıklık baskılanması, kronik stres, strese bağlı bağışıklık.

Introduction

Stress and immune functionality represent two interrelated facets of human physiological processes, which have undergone rigorous scientific scrutiny in contemporary years. The connection between these two phenomena, stress, and immune functionality, has attracted substantial scholarly interest due to the profound implications it holds for human health and quality of life. In this analytical review, we intend to present an exhaustive evaluation of the prevailing comprehension of the complex interaction between stress stimuli and immune responses (Dhabhar, 2014; Morey et al., 2015).

Stress constitutes a natural physiological reaction to situations perceived as complex or menacing. Many environmental, psychological, and physiological stressors can instigate it. The onset of stress initiates a multifaceted series of physiological and psychological reactions, collectively called the stress response. This reaction encompasses stimulating the hypothalamic-pituitary-adrenal (HPA) axis and the secretion of stress-related hormones, such as cortisol (Tsigos et al., 2020; Chu et al., 2020).

The immune system bears the crucial responsibility of safeguarding the body against harmful pathogens and upholding general health. It encompasses a coordinated network of cells, tissues, and organs collaborating to detect and eradicate foreign intruders. The immune system is instrumental in shielding the body from infections, diseases, and other health conditions (Nicholson, 2016).

Numerous studies have indicated that stress can exert a profound influence on immune function. Acute stressors have been observed to temporarily augment

Corresponding author: dr.hasankahya@uomosul.edu.iq

certain facets of immune functionality, such as mobilizing immune cells toward sites of infection or injury. However, persistent or long-term stress can precipitate immune dysregulation and suppression, enhancing individuals' vulnerability to infections and diseases (Dhabhar, 2014; Morey et al., 2015).

The mechanisms that underpin the effects of stress on immune functionality are intricate and multilayered. A primary pathway involves the secretion of stress hormones, specifically cortisol, which can modulate immune cell activity and functionality. Cortisol has been demonstrated to possess both immunostimulatory and immunosuppressive impacts, contingent on the timing and duration of stress exposure (Dhabhar, 2009).

Alongside hormonal influences, stress can also impact immune functionality via alterations in inflammatory processes. Chronic stress has been correlated with elevated production of pro-inflammatory cytokines, potentially contributing to chronic low-grade inflammation within the body. This persistent inflammation is postulated to play a part in the development of various diseases, encompassing cardiovascular disease, metabolic conditions, autoimmune disorders, and mental health conditions (Liu et al., 2017; Seiler et al., 2020).

Comprehending the connection between stress and immune functionality holds significant implications for both medical and psychological domains. It underscores the necessity for interventions and strategies aimed at minimizing the adverse effects of stress on immune functionality and general health. Stress management techniques, such as mindfulness-based stress reduction, meditation, physical exercise, and social support systems, have demonstrated the potential to enhance immune functionality and mitigate the deleterious effects of chronic stress (Antoni & Dhabhar, 2019).

This review article delves into the complex relationship between stress and immune functionality. It examines the impact of stress on immune cell activity, the mechanisms underlying stress-induced immune suppression, the interplay between stress and inflammation, and the repercussions of chronic stress on immune functionality and disease susceptibility. Moreover, it discusses stress management techniques that can be implemented to enhance immune functionality and overall well-being. Through illuminating this significant topic, we aim to contribute towards a more comprehensive understanding of how stress impacts our immune system and how we can counteract its adverse effects for improved health outcomes.

1. Overview of Stress and Immune Function

Stress is an innate physiological reaction to situations perceived as challenging or threatening. Various elements, including environmental, psychological, and physiological stressors, can instigate it. These stressors can span day-to-day life occurrences, such as occupational stress or relational conflicts, to more severe traumatic experiences. Regardless of the origin, the body's response to stress encompasses physiological and psychological modifications to prepare the individual for a fight-or-flight reaction (Schneiderman et al., 2005).

1.1. Hypothalamic-pituitary-adrenal (HPA) axis

One important physiological system that plays a key part in the body's reaction to stress is the hypothalamic-pituitary-adrenal (HPA) axis. The pituitary, adrenal glands, and hypothalamus are all included in this complex network. Corticotropin-releasing hormone (CRH), released by the brain in response to stress, instructs the pituitary gland to release adrenocorticotropic hormone (ACTH). ACTH then stimulates the adrenal glands to produce stress hormones, mainly cortisol (Fig. 1) (Sheng et al., 2021; Smith & Vale, 2006).

Known as the "stress hormone," cortisol is an essential mediator of the effects of stress on immunological function. It modifies the activity and reactivity of many immunological cells and tissues throughout the body. Specific components of immunological function have been reported to be enhanced by cortisol in acute stress circumstances. Most notably, it can speed up and improve the immune response by facilitating the migration and mobilization of immune cells to infection or damage sites (Thau et al., 2019).

However, long-term or persistent stress can cause immune system dysregulation and suppression. Prolonged exposure to elevated levels of cortisol can impede the functionality of immune cells, thereby compromising the body's ability to mount an effective immune response. Chronic stress has been associated with reduced proliferation of immune cells, diminished production of antibodies, and alterations in cytokine profiles (Segerstrom & Miller, 2004).

1.2. Other hormonal stimulants for stress mediation

The impacts of stress on immune functionality are not exclusively mediated by cortisol. Other stress-related factors, such as catecholamines (e.g., adrenaline and noradrenaline), other glucocorticoids, neuropeptides, and neurotransmitters, also play significant roles in modulating immune cell activity. These factors can act directly on immune cells or indirectly through interactions with other components of the immune system, such as cytokines or immune cell receptors (Arora & Bhattacharjee, 2008; Liu et al., 2017; Liu et al., 2022).

Besides hormonal influences, stress can also impact immune functionality by altering inflammatory processes. Chronic stress has been correlated with elevated production of pro-inflammatory cytokines like interleukin-6 (IL-6) and tumor necrosis factor-α (TNF-α). These cytokines play crucial roles in initiating and regulating inflammatory responses. While acute inflammation is necessary for combating infections and fostering tissue repair, chronic low-grade inflammation can be detrimental to health (Tian et al., 2014).

Stress-induced inflammation can disrupt the delicate equilibrium between pro-inflammatory and anti-inflammatory processes in the body, leading to chronic inflammation contributing to disease pathogenesis (Furman et al., 2019; Liu et al., 2017).

The interaction between stress and immune functionality is bidirectional – not only does stress influence immune functionality but immune functionality can also modulate the body's response to stress. The

immune system contains specialized cells called microglia, responsible for detecting and responding to pathogens or foreign substances in the brain. These cells also play a role in regulating neuroinflammation and neuroprotection (Holzer et al., 2017; Schramm & Waisman, 2022).

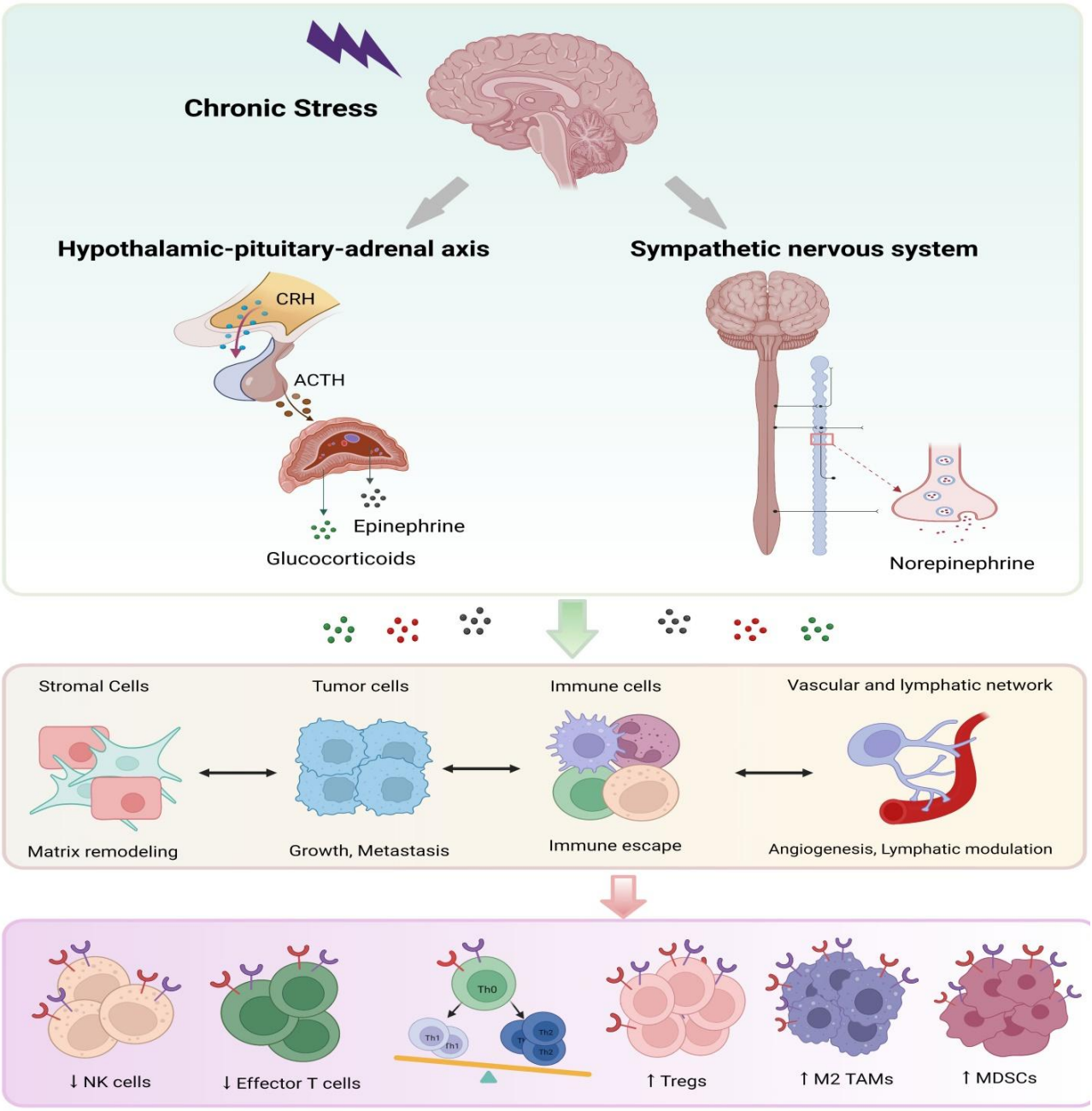

Figure 1. Overview of chronic stress impacts on immune response. Stress can trigger hypothalamus activation and sympathetic nerve system. This effect leads to hyper secretion of catecholamines and glucocoticoids (Liu et al., 2022).

Emerging evidence suggests that chronic stress can activate microglia, leading to an increased production of pro-inflammatory cytokines in the brain. This neuroinflammatory response has been associated with the development of mood disorders such as depression and anxiety. Conversely, dysregulation of immune functionality due to chronic stress can impair neuroprotective mechanisms and contribute to neurodegenerative conditions (Wang et al., 2022).

Understanding the relationship between stress and immune functionality holds significant implications for both medical and psychological fields. It underscores the necessity for interventions aimed at minimizing the adverse effects of stress on immune functionality and general health. Stress management techniques, such as mindfulness-based stress reduction, meditation, physical exercise, and social support systems, have demonstrated the potential to enhance immune functionality and mitigate the deleterious effects of chronic stress (Antoni & Dhabhar, 2019).

2. The Impact of Stress on the Immune System

One of the fundamental mechanisms by which stress impacts the immune system involves alterations in the distribution and functionality of immune cells. During acute stress situations, cortisol can enhance specific aspects of immune functionality, such as facilitating the mobilization and migration of immune cells towards sites of infection or injury. This response proves advantageous

in the short term, facilitating prompt immune responses and aiding in tissue repair (Dhabhar, 2009; Seiler et al., 2020).

Nonetheless, chronic stress can give rise to the dysregulation and suppression of immune cell functionality. Prolonged exposure to heightened cortisol levels can impede the production and activity of key immune cells, encompassing lymphocytes (such as T cells and B cells), natural killer (NK) cells, and macrophages. These cellular components play indispensable roles in the recognition and elimination of pathogens or aberrant cells within the body (Zhang et al., 2020).

Research findings suggest that chronic stress is associated with a decrease in both the quantity and functionality of lymphocytes. Since lymphocytes are in charge of producing antibodies and coordinating immune responses directed against certain antigens, they are essential to adaptive immunity. The presence of chronic stress is linked to reduced proliferation of lymphocytes and impaired production of antibodies, resulting in a compromised ability of the body to mount an effective immune response (Arruga et al., 2020).

Moreover, research indicated that enduring stress hampers the efficacy of natural killer (NK) cells. NK cells constitute a fundamental component of the innate immune system and assume a pivotal role in identifying and eradicating cancerous and virus-infected cells. In the presence of chronic stress, NK cell activity is curtailed, culminating in decreased cytotoxicity and compromised surveillance against neoplasms. Consequently, this heightened vulnerability to viral infections and compromised tumor defense mechanisms can contribute to the advancement and progression of specific cancer types (Fig. 1) (Liu et al., 2022; Mishra et al., 2014; Raulet & Guerra, 2009).

Macrophages, being a critical constituent of the immune system, are susceptible to the influence of chronic stress. These specialized cells perform the crucial task of engulfing and eliminating pathogens or cellular debris through a process called phagocytosis. Chronic stress has been empirically shown to compromise the functionality of macrophages, thereby diminishing their efficacy in clearing invading pathogens and maintaining tissue homeostasis effectively (Bajgar & Krejčová, 2023; Hirayama et al., 2017).

In addition to modulating immune cell functionality, chronic stress possesses the capacity to disturb the production and signaling of cytokines, which are pivotal chemical messengers involved in immune responses. Cytokines can be categorized into two overarching groups: pro-inflammatory and anti-inflammatory cytokines. Pro-inflammatory cytokines, including interleukin-6 (IL-6) and tumor necrosis factor-α (TNF-α), play a significant role in promoting inflammation and initiating immune responses. Conversely, anti-inflammatory cytokines such as interleukin-10 (IL-10) and transforming growth factor-beta (TGF-beta) serve to attenuate inflammation and foster tissue repair (Al-Karawi et al., 2023; Kany et al., 2019; Li et al. , 2017; Zhang & An, 2007).

Chronic stress has been linked to an imbalance in the production of cytokines, tipping the scale towards an excess of pro-inflammatory cytokines relative to anti-inflammatory cytokines. This shift towards a pro-inflammatory state is implicated in the development of chronic low-grade inflammation, a condition believed to contribute to the pathogenesis of diverse diseases, encompassing cardiovascular disease, autoimmune disorders, and mental health conditions (Golovatscka et al., 2012; Tian et al., 2014).

Moreover, it has been empirically substantiated that stress hormones, particularly cortisol, significantly influence cytokine signaling pathways. The inherent capacity of cortisol to both modulate the expression and activity of cytokine receptors on immune cells has been observed to directly affect their receptivity to cytokine signals. Consequently, this alteration potentially induces changes in cytokine synthesis, fostering a climate conducive to the imbalance of immune reactions (Aquino-Acevedo et al., 2022).

The ramifications of stress on the immunological system are far-reaching, transcending the confines of cellular and molecular constituents to impinge on a multitude of physiological mechanisms. Persistent stress, as an example, has been linked to the impairment of intestinal barrier wholeness, culminating in increased permeability. This occurrence, often denoted as 'intestinal hyperpermeability', facilitates the migration of bacteria along with other harmful entities into the circulatory system, thereby inciting immune reactions and instigating systemic inflammation (Doney et al., 2022; Segerstrom & Miller, 2004).

Furthermore, protracted stress has the potential to upset the intricate balance of the gut microbiota, a multifaceted microbial consortium that plays an instrumental role in immunological regulation and comprehensive wellbeing. Disturbances in the composition of the gut microbiota, precipitated by stress, have been associated with alterations in immune cell demographics and an escalated susceptibility to infections and inflammatory states (Madison & Kiecolt-Glaser, 2019).

2.1. Mechanisms of stress-induced immune suppression

Cortisol, serving as the chief agent in stress-induced immunosuppression, is a stress hormone produced by the adrenal glands. This hormone is integral in orchestrating numerous aspects of immune cell activity. The manifestation of elevated cortisol levels may precipitate a decrease in the proliferation and operation of immune cells, which include lymphocytes, natural killer (NK) cells, and macrophages (Morey et al., 2015).

Cortisol imparts its effect on immune cells via engagement with specialized glucocorticoid receptors (GRs) situated on the cellular surface. Following binding, cortisol establishes complexes with GRs that subsequently relocate to the nucleus where they regulate the expression of genes integral to immune cell function. Such a process results in substantial modifications to the operation of immune cells (Meijer et al., 2019).

Cortisol inhibits immune cell activity through several mechanisms, one of which involves obstructing the development and maturation of lymphocytes. These particular cells are crucial in adaptive immunity due to their role in producing antibodies and organizing immune

responses targeted at distinct antigens. Persistent stress has been connected to reduced lymphocyte proliferation, deficient antibody synthesis, and irregular activation of T-cells. Such impacts could potentially undermine the capacity of the immune system to generate a proficient immune response (Arora & Bhattacharjee, 2008).

Furthermore, natural killer (NK) cells, a vital part of the innate immune system that plays a crucial role in identifying and removing cancerous cells and virus-infected cells, are also suppressed by cortisol. Chronic stress has been demonstrated to diminish NK cell activity, resulting in reduced cytotoxicity and impaired surveillance against tumor development (Mavoungou et al., 2005).

Moreover, cortisol has the capacity to influence the functionality of macrophages, cellular components responsible for the phagocytosis and clearance of pathogens as well as cellular debris. Chronic stress has been empirically shown to impair the function of macrophages, consequently diminishing their capability to effectively eliminate invading pathogens and sustain tissue homeostasis (Diaz-Jimenez et al., 2021).

Besides cortisol, there are additional stress-related factors that contribute to immune suppression. Catecholamines, including adrenaline and noradrenaline, are released in response to stress and possess the ability to modulate immune cell activity. These neurotransmitters can exert their influence either directly on immune cells or indirectly through interactions with other constituents of the immune system (Liu et al., 2017).

Catecholamines possess the ability to hinder the production and functionality of immune cells, such as lymphocytes and NK cells, through their binding to adrenergic receptors located on the cell surface. This interaction elicits modifications in intracellular signaling pathways, resulting in alterations in immune cell activity. Moreover, catecholamines can influence the production and signaling of cytokines, thereby further contributing to immune suppression induced by stress (Flierl et al., 2008).

An additional method through which stress precipitates immunosuppression is by destabilizing the equilibrium between pro-inflammatory and anti-inflammatory mechanisms within the organism. Persistent stress has been correlated with an augmented synthesis of pro-inflammatory cytokines, notably interleukin-6 (IL-6) and tumor necrosis factor-α (TNF-α). The presence of these cytokines fosters inflammation and augments immune system activity (Hassamal, 2023).

Enduring exposure to the elevated concentrations of pro-inflammatory cytokines can detrimentally impact the functionality of immune cells and, ultimately, comprehensive health. This scenario may instigate a state of persistent, low-grade inflammation, a condition postulated to play a contributory role in the genesis of a myriad of ailments, encompassing cardiovascular disease, autoimmune disorders, and psychiatric health conditions (Zhang & An, 2007).

Furthermore, perpetual inflammation has the capacity to further inhibit immune cell functionality via negative feedback systems. This process can stimulate an enhanced production of anti-inflammatory cytokines, including interleukin-10 (IL-10) and transforming growth factor-β (TGF-β, which subsequently attenuate immune responses. Although this anti-inflammatory response serves as a pivotal regulatory mechanism, chronic exposure to excessive levels of anti-inflammatory cytokines potentially contributes to the immune dysregulation and a weakened defense against infections (Iyer & Cheng, 2012).

Finally, the suppression of the immune system induced by stress involves a multifaceted interaction of numerous mechanisms. Cortisol, catecholamines, and pro-inflammatory cytokines serve as key agents in modulating the activity and function of immune cells. These elements hinder lymphocyte proliferation, compromise NK cell cytotoxicity, and disrupt macrophage functionality. Moreover, enduring stress can disturb the equilibrium between pro-inflammatory and anti-inflammatory mechanisms within the body, culminating in persistent, low-grade inflammation and immune dysregulation. Comprehending these mechanisms is indispensable for the creation of strategies that alleviate stress-induced immune suppression and foster optimal immune functionality (Liu et al., 2022).

3. Stress and Inflammation: The Interplay

Inflammation embodies a natural immunological response, designed to shield the body from deleterious stimuli, encompassing pathogens or tissue damage. Nonetheless, an enduring or excessive occurrence of inflammation can potentially jeopardize health and is strongly correlated with the manifestation of diverse diseases. It has been established that stress wields an impact on the inflammatory process where a complex reciprocal relationship exists between these two factors. In this segment, we aim to probe deeper into the nuanced association between stress and inflammation as well as the fundamental mechanisms orchestrating their interaction (Bennett et al., 2018; Chen et al., 2018).

Persistent or extended stress has been correlated with elevated levels of inflammation within the organism. Stress has the capacity to stimulate the hypothalamic-pituitary-adrenal (HPA) axis, subsequently inciting the secretion of stress hormones, particularly cortisol. These stress hormones possess the ability to modulate the activity of immune cells and cytokine production, thus inducing modifications in inflammatory processes (Herman et al., 2016; Stephens & Wand, 2012).

Furthermore, stress hormones, specifically cortisol, can exert a direct influence on immune cells and their synthesis of pro-inflammatory cytokines. Cortisol attaches to glucocorticoid receptors located on immune cells, thereby affecting gene expression and instigating alterations in cytokine production. Remarkably, cortisol has been observed to enhance the production of certain pro-inflammatory cytokines while simultaneously inhibiting the synthesis of anti-inflammatory cytokines, thereby fostering inflammation (Fig. 2) (Shimba et al., 2021).

Beyond promoting the synthesis of pro-inflammatory cytokines, stress can additionally modify the sensitivity of immune cells to these signaling molecules. It is demonstrated that chronic stress can

enhance the expression of cytokine receptors on immune cells, making them more receptive to pro-inflammatory signals. This amplified sensitivity can further intensify the inflammatory response, thereby contributing to chronic inflammation (Tian et al., 2014).

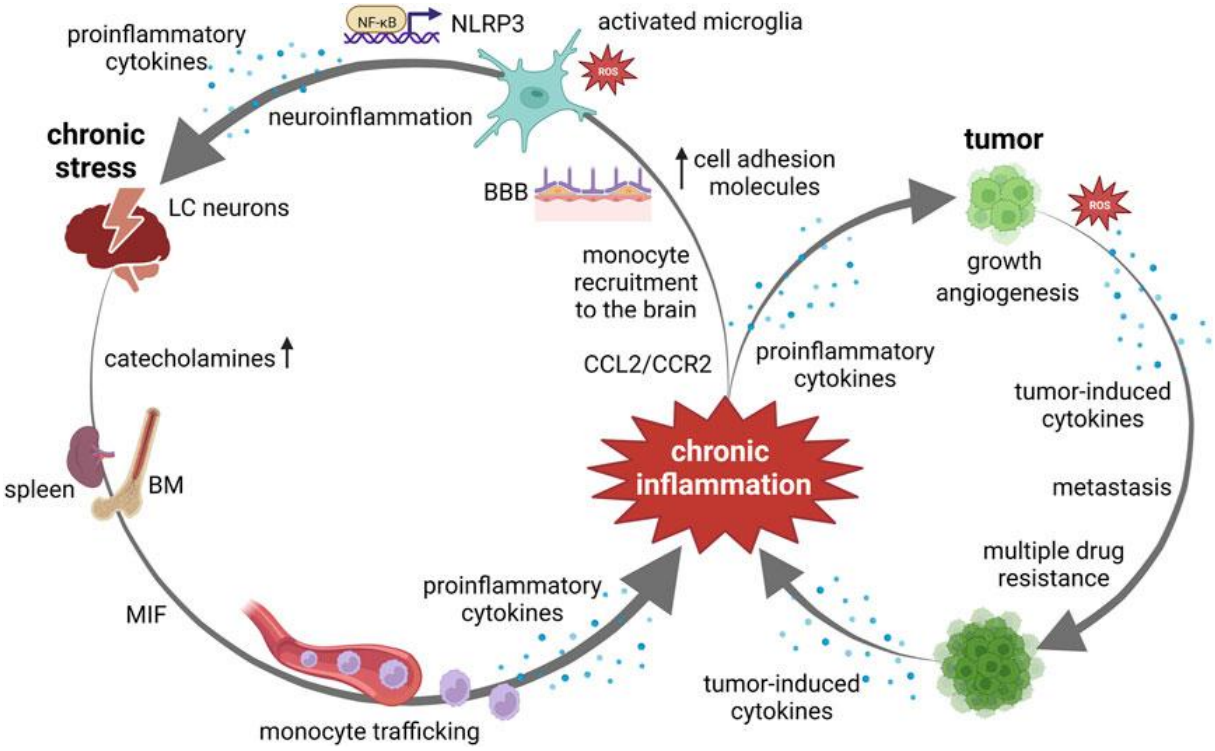

Figure 2. Chronic inflammation as a result of chronic stress. During chronic stress, catecholamine release, induces the recruitment of monocytes from bone marrow and spleen to the brain. Monocyte trafficking is induced *via* up-regulated macrophage migration inhibitory factor (MIF) and C–C ligand 2—(CCL2)/C–C chemokine receptor 2 (CCR2) pathway (Vignjević Petrinović et al., 2023).

While an anti-inflammatory response is integral in averting excessive inflammation, continuous exposure to elevated concentrations of anti-inflammatory cytokines can yield undesirable outcomes. This may result in immune suppression and a weakened defense against infections. The imbalance between pro-inflammatory and anti-inflammatory processes, triggered by chronic stress, can lead to immune dysfunction and heightened susceptibility to diseases (Bennett et al., 2018).

The interaction between stress and inflammation surpasses the realm of immune cells and cytokines. Stress can also impact other constituents of the inflammatory response, including endothelial cells, which encompass the lining of blood vessels. Stress has the capacity to incite the activation and dysfunction of these cells, culminating in enhanced vascular permeability and the attraction of immune cells to inflammation sites (Theofilis et al., 2021; Zhang, 2008).

Moreover, inflammation induced by stress can influence other physiological systems beyond the scope of the immune system. For example, chronic low-grade inflammation is linked with modifications in neurotransmitter functionality, including diminished serotonin levels, a neurotransmitter involved in mood regulation. This may provide insights into the connection between inflammation instigated by stress and mental health disorders such as depression and anxiety (Liu et al., 2017; Miller & Raison, 2016).

4. Chronic Stress and Immune Dysfunction

A pivotal mechanism in which chronic stress affects the immune system is by destabilizing the equilibrium between pro-inflammatory and anti-inflammatory processes. The association of chronic stress with an augmented production of pro-inflammatory cytokines, namely interleukin-6 (IL-6) and tumor necrosis factor-α (TNF-α), has been established. These cytokines instigate inflammation and stimulate immune activation (Hassamal, 2023; Liu et al., 2017).

Extended exposure to the elevated concentrations of pro-inflammatory cytokines can detrimentally affect the functionality of immune cells. This can precipitate immune cell exhaustion and debilitate their capacity to effectively respond to pathogens or abnormal cells. Consequently, this may yield compromised immune surveillance and heightened susceptibility to infections (Fajgenbaum & June, 2020).

Furthermore, chronic stress has the potential to disrupt the balance and functionality of regulatory immune cells such as regulatory T cells (Tregs). Tregs play a pivotal role in preserving immune homeostasis by inhibiting excessive immune responses. Chronic stress is demonstrated to diminish Treg numbers and compromise their suppressive function, resulting in dysregulated immune responses and heightened inflammation (Kondělková et al., 2010; Rocamora-Reverte et al., 2020).

An additional facet of the immune dysfunction induced by chronic stress is connected to the influence exerted on the gut-brain axis. Chronic stress has the potential to impair the integrity of the gut barrier, resulting in augmented permeability. This condition facilitates the leakage of bacteria and other injurious substances into the

bloodstream, instigating immune responses and systemic inflammation. Dysbiosis, defined as an imbalance in the composition of gut microbiota, is also correlated with chronic stress and can further contribute to immune dysfunction (Doney et al., 2022; Tang et al., 2020).

The repercussions of immune dysfunction instigated by chronic stress surpass the realm of heightened susceptibility to infections. It has been correlated with an elevated risk of manifesting chronic inflammatory diseases, autoimmune disorders, allergies, and mental health conditions such as depression and anxiety. The dysregulation of the immune system, brought about by chronic stress, can also impede wound healing and prolong recovery from injuries or surgical procedures (Marshall, 2011; Salleh, 2008).

Comprehending the intricate association between chronic stress and immune dysfunction is imperative for the formulation of strategies aimed at alleviating the adverse impacts of chronic stress on health. Stress management techniques, encompassing mindfulness-based stress reduction, meditation, physical exercise, and social support, have demonstrated potential in enhancing immune functionality and diminishing the harmful effects of chronic stress on the immune system.

5. Stress, Immune Function, and Disease Susceptibility

One repercussion of immune suppression induced by stress is heightened susceptibility to infections. Chronic stress has been demonstrated to debilitate the immune response against viral, bacterial, and fungal pathogens. This can trigger an elevated risk of manifesting respiratory infections, such as the common cold or influenza, in addition to other types of infections across the body (Marshall, 2011; Kahya & Mahmood, 2022).

Furthermore, chronic stress has the potential to influence the immune system's capacity to regulate and eradicate cancer cells. Immune dysfunction induced by stress can compromise the surveillance and cytotoxicity of immune cells, notably natural killer (NK) cells and cytotoxic T cells, which serve pivotal roles in identifying and eliminating abnormal cells. This can contribute to a heightened risk of cancer development and progression (Seiler et al., 2020; Zhang et al., 2020).

Additionally, chronic stress has been associated with an increased susceptibility to autoimmune disorders. Such disorders arise when the immune system erroneously targets healthy cells and tissues. The dysregulation of immune responses, induced by stress, can disrupt the balance between self-tolerance and autoimmunity, potentially instigating or intensifying autoimmune conditions (Stojanovich & Marisavljevich, 2008).

Beyond infectious diseases and autoimmune disorders, chronic stress has been linked with an elevated risk of chronic inflammatory diseases. Chronic low-grade inflammation, frequently observed in individuals undergoing chronic stress, is implicated in the pathogenesis of conditions such as cardiovascular disease, diabetes, rheumatoid arthritis, and inflammatory bowel disease (Liu et al., 2017).

Inflammation induced by stress can contribute to the development and progression of these diseases by fostering endothelial dysfunction, plaque formation in arteries, insulin resistance, joint inflammation, and gastrointestinal inflammation. Over time, chronic inflammation can lead to tissue damage and organ dysfunction (Liu et al., 2017; Theofilis et al., 2021).

Mental health conditions represent another domain where stress can impinge on immune function and disease susceptibility. Chronic stress has been linked to an elevated risk of manifesting mood disorders such as depression and anxiety. These conditions are associated with alterations in immune function, including dysregulated cytokine production and heightened inflammation (Salleh, 2008; Schneiderman et al., 2005).

The reciprocal relationship between stress and mental health is multifaceted. Stress can contribute to the manifestation of mental health disorders via its impact on neurotransmitter systems, neural circuits involved in mood regulation, and structural changes within the brain. Conversely, mental health disorders themselves can exert influence on immune function and heighten susceptibility to certain diseases (Mariotti, 2015).

5.1. Stress with cancer

Stress can exert a substantial influence on individuals diagnosed with cancer, encompassing both physical and emotional aspects. The following are some pivotal points elucidating the association between stress and cancer:

5.1.1. Psychological impact

The diagnosis of cancer can precipitate considerable psychological distress, encompassing feelings of fear, anxiety, depression, and uncertainty. The emotional weight imposed by cancer can result in heightened stress levels, influencing an individual's comprehensive well-being and quality of life (Wang & Feng, 2022).

5.1.2. Physiological response

Stress elicits the secretion of stress hormones, such as cortisol, which can exert detrimental effects on the body. Prolonged or chronic stress has the potential to disrupt immune system functioning, impede the process of wound healing, and contribute to inflammation. These factors collectively may exert a negative influence on the advancement and management of cancer (Segerstrom & Miller, 2004).

5.1.3. Treatment-related stress

Cancer treatments, including chemotherapy, radiation therapy, and surgery, can induce physical discomfort and give rise to side effects that contribute to stress. Additionally, the apprehension regarding treatment outcomes, potential side effects, and the unpredictable nature of the future can further augment the overall stress endured by individuals undergoing cancer treatment (Chandwani et al., 2012; Seol et al., 2021).

5.1.4. Coping mechanisms

Individuals facing cancer diagnosis necessitate the cultivation of efficacious coping mechanisms to effectively manage stress. This process may entail seeking support from loved ones, participating in support groups, employing relaxation techniques such as meditation or deep breathing exercises, adhering to a healthy lifestyle

encompassing regular exercise and a balanced diet as well as seeking professional assistance from therapists or counselors.

5.1.5. Impact on treatment outcomes

While stress itself does not directly induce the onset of cancer, chronic stress and its physiological ramifications may impede the body's ability to respond optimally to cancer treatment. Some research studies postulate that elevated levels of stress may be linked to less favorable treatment outcomes and an increased likelihood of cancer recurrence. However, further investigation is required to comprehensively comprehend the intricate relationship between stress and the progression of cancer (Moreno-Smith et al., 2010).

6. Stress Management Techniques to Improve Immune Function

Efficient management of stress is of paramount importance for preserving optimal immune function and overall well-being. Chronic or prolonged stress has the potential to impair the immune system, rendering individuals more vulnerable to infections and diseases. In the forthcoming section, we delve into an array of stress management techniques that can aid in enhancing immune function.

6.1. Mindfulness-based stress reduction (MBSR)

MBSR is a technique that encompasses the practice of mindfulness meditation and the integration of mindfulness into one's daily life. This approach emphasizes the cultivation of non-judgmental awareness of the present moment. Scientific investigations have demonstrated that MBSR holds the potential to diminish stress, ameliorate mood, and augment immune function (Keng et al., 2011).

6.2. Meditation and deep breathing

Consistent engagement in meditation and deep breathing exercises can facilitate relaxation and alleviate stress. Deep breathing techniques, including diaphragmatic or box breathing, serve to activate the body's relaxation response, thereby counteracting the physiological repercussions of stress (Ma et al., 2017).

6.3. Regular exercise

Physical activity has been extensively demonstrated to yield myriad advantages for both mental and physical well-being, encompassing stress reduction, and amelioration of immune function. Consistent participation in exercise, regardless of whether it entails aerobic activities, strength training, or yoga, has the potential to diminish stress levels and bolster immune cell activity (da Silveira et al., 2021).

6.4. Adequate sleep

Attaining adequate and high-quality sleep is imperative for the preservation of a robust immune system. Chronic inadequacy of sleep or suboptimal sleep quality has the potential to heighten stress levels and compromise the functionality of immune cells. Establishing a consistent sleep routine and cultivating an environment conducive to sleep can play a contributory role in fostering improved sleep patterns and enhanced immune function (Besedovsky et al., 2019).

6.5. Healthy diet

A well-balanced diet incorporating ample quantities of fruits, vegetables, whole grains, lean proteins, and healthy fats furnishes the essential nutrients indispensable for optimal immune function. Chronic stress may engender unhealthy eating habits; hence, prioritizing the consumption of nutrient-dense foods can serve as a means to bolster immune health (Cena & Calder, 2020).

6.6. Social support

Sustaining robust social connections and actively seeking support from friends, family, or support groups can facilitate the amelioration of stress. Engaging in open dialogue with others regarding concerns or engaging in social activities can furnish emotional support, diminish feelings of isolation, and augment comprehensive well-being (Ozbay et al., 2007).

6.7. Time management and prioritization

The sensation of being encumbered with manifold tasks and obligations can act as a potential contributor to stress. The development of proficient time management competencies, in conjunction with the capacity to identify and rank tasks, can function as potent strategies for alleviating stress levels and nurturing a perception of control over one's quotidian existence.

6.8. Relaxation techniques

Engagement in relaxation practices, including progressive muscle relaxation, guided imagery, or aromatherapy, can promote a state of relaxation and decrease stress levels. These methodologies play a crucial role in triggering the body's relaxation response, consequently dampening the physiological impacts of stress (Toussaint et al., 2021).

6.9. Hobbies and leisure activities

Involvement in endeavors that induce pleasure and relaxation can aid in the mitigation of stress and the augmentation of overall well-being. Undertaking hobbies, such as painting, horticulture, playing a musical instrument, or engaging in sports, can cultivate a sense of gratification and serve as a beneficial conduit for stress management.

6.10. Cognitive-behavioral therapy (CBT)

Cognitive-Behavioral Therapy (CBT) is a therapeutic approach primarily focused on recognizing and altering adverse cognitive patterns and behaviors that augment stress levels. This approach facilitates the development of adaptive coping strategies and fosters resilience in navigating stressors (Nakao et al., 2021).

It is noteworthy to acknowledge that individuals exhibit varying responses to stress management techniques, necessitating an exploratory approach to identify the most effective strategies for each person. The amalgamation of multiple techniques or seeking guidance from healthcare professionals or therapists can yield advantageous outcomes. By integrating these stress management techniques into daily routines, individuals have the potential to diminish stress levels, ameliorate immune function, and elevate comprehensive well-being. Emphasizing self-care and adopting proactive measures to

manage stress constitute fundamental elements in upholding a robust immune system.

7. Conclusion and Future Directions

In summary, the connection between stress and immune function is intricate and multifaceted. Chronic or prolonged stress has the potential to impair the immune system, resulting in immune dysfunction, heightened vulnerability to infections, and an elevated risk of developing diverse diseases. Stress can exert an influence on immune cell activity, cytokine production, and inflammation as well as the delicate equilibrium between pro-inflammatory and anti-inflammatory processes.

Comprehending the intricate dynamic between stress and immune function holds paramount significance in fostering comprehensive health and well-being. Through the implementation of efficacious stress management techniques, individuals have the capacity to ameliorate the adverse impacts of stress on immune function. Approaches such as mindfulness-based stress reduction, meditation, regular exercise, sufficient sleep, a nutritious diet, social support, relaxation techniques, effective time management, engaging in hobbies, and cognitive-behavioral therapy all represent valuable strategies for stress management and enhancement of immune function.

Future research directions in this domain encompass delving further into the underlying mechanisms through which stress impacts immune function and susceptibility to disease. Gaining a comprehensive comprehension of the specific molecular pathways and signaling cascades implicated in stress-induced immune dysregulation holds promise in identifying potential targets for therapeutic intervention.

Moreover, it is imperative to investigate the enduring consequences of chronic stress on immune function and disease outcomes. Longitudinal studies offer valuable insights into the long-term impact of chronic stress on immune health and its role in the development of chronic diseases.

Additionally, elucidating the significance of individual differences in stress responses and resilience to stress-related immune dysfunction represents an area of interest. Certain individuals may exhibit greater resilience to the deleterious effects of stress on immune function due to genetic or psychosocial factors. Identifying these factors can aid in devising personalized approaches for stress management and immune support.

In summary, effective stress management plays a pivotal role in maintaining optimal immune function and reducing the risk of diseases associated with immune dysfunction. By implementing stress management techniques and adopting a healthy lifestyle, individuals can provide support to their immune system and foster comprehensive well-being. Continued research endeavors in this field will further enhance our understanding of the intricate relationship between stress and immune function, paving the way for innovative interventions and personalized approaches to enhance immune health.

Ackowledgement: This study is supported by the Department of Biology, College of Education for Pure Science, University of Mosul. A great thankful Central Laboratories/ Nenawa Health Office including doctors and nurses who were supportive to accomplish this study.

Ethics committee approval: Ethics committee approval is not required for this study.

Conflict of interest: The authors declare that there is no conflict of interest.

Author Contributions: Conception – H.F.H.K.; Design – H.F.H.K.; Supervision – M.T.M.; Fund – M.T.M.; Materials – H.F.H.K.; Data Collection and Processing – H.F.H.K.; Analysis Interpretation – M.T.M.; Literature Review – H.F.H.K.; Writing – H.F.H.K.; Critical Review – M.T.M.

References

Al-Karawi, A.S., Atoom, A.M., Al-Adwan, S.M., & Adwan, S.W. (2023). Assessment of selected biochemical and immunological parameters after treatment by Cosmetic Procedures. *Journal of Population Therapeutics and Clinical Pharmacology,* 30(2), 201-213.

Antoni, M.H., & Dhabhar, F.S. (2019). The impact of psychosocial stress and stress management on immune responses in patients with cancer. *Cancer,* 125(9), 1417-1431. https://doi.org/10.1002/cncr.31943

Aquino-Acevedo, A.N., Knochenhauer, H., Castillo-Ocampo, Y., Ortiz-León, M., Rivera-López, Y.A., Morales-López, C., ..., & Armaiz-Pena, G. N. (2022). Stress hormones are associated with inflammatory cytokines and attenuation of T-cell function in the ascites from patients with high grade serous ovarian cancer. *Brain, Behavior, & Immunity-Health,* 26, 100558. https://doi.org/10.1016/j.bbih.2022.100558

Arora, S., & Bhattacharjee, J. (2008). Modulation of immune responses in stress by Yoga. *International Journal of Yoga,* 1(2), 45-55. https://doi.org/10.4103/0973-6131.43541

Arruga, F., Gyau, B.B., Iannello, A., Vitale, N., Vaisitti, T., & Deaglio, S. (2020). Immune Response Dysfunction in Chronic Lymphocytic Leukemia: Dissecting Molecular Mechanisms and Microenvironmental Conditions. *International Journal of Molecular Sciences,* 21(5). https://doi.org/10.3390/ijms21051825

Bajgar, A., & Krejčová, G. (2023). On the origin of the functional versatility of macrophages. *Frontiers in Physiology,* 14, 1128984. https://doi.org/10.3389/fphys.2023.1128984

Bennett, J.M., Reeves, G., Billman, G. E., & Sturmberg, J.P. (2018). Inflammation-Nature's Way to Efficiently Respond to All Types of Challenges: Implications for Understanding and Managing "the Epidemic" of Chronic Diseases. *Frontiers in Medicine,* 5, 316. https://doi.org/10.3389/fmed.2018.00316

Besedovsky, L., Lange, T., & Haack, M. (2019). The Sleep-Immune Crosstalk in Health and Disease. *Physiological Reviews,* 99(3), 1325-1380. https://doi.org/10.1152/physrev.00010.2018

Cena, H., & Calder, P.C. (2020). Defining a Healthy Diet: Evidence for The Role of Contemporary Dietary Patterns in Health and Disease. *Nutrients,* 12(2). https://doi.org/10.3390/nu12020334

Chandwani, K.D., Ryan, J.L., Peppone, L.J., Janelsins, M.M., Sprod, L.K., Devine, K., ..., & Mustian, K.M. (2012). Cancer-related stress and complementary and alternative medicine: a review. *vidence-Based Complementary and Alternative Medicine,* 2012, 979213. https://doi.org/10.1155/2012/979213

Chen, L., Deng, H., Cui, H., Fang, J., Zuo, Z., Deng, J., ..., & Zhao, L. (2018). Inflammatory responses and inflammation-associated diseases in organs. *Oncotarget,* 9(6), 7204.

Chu, B., Marwaha, K., Sanvictores, T., & Ayers, D. (2021). Physiology, stress reaction. In *StatPearls [Internet]*: StatPearls Publishing.

da Silveira, M.P., da Silva Fagundes, K.K., Bizuti, M.R., Starck, É., Rossi, R. C., & de Resende, E.S.D.T. (2021). Physical exercise as a tool to help the immune system against COVID-19: an integrative review of the current literature. *Clinical and Experimental Medicine,* 21(1), 15-28. https://doi.org/10.1007/s10238-020-00650-3

Dhabhar, F.S. (2009). Enhancing versus suppressive effects of stress on immune function: implications for immunoprotection and immunopathology. *Neuroimmunomodulation,* 16(5), 300-317. https://doi.org/10.1159/000216188

Dhabhar, F.S. (2014). Effects of stress on immune function: the good, the bad, and the beautiful. *Immunologic Research,* 58(2-3), 193-210. https://doi.org/10.1007/s12026-014-8517-0

Diaz-Jimenez, D., Kolb, J.P., & Cidlowski, J.A. (2021). Glucocorticoids as Regulators of Macrophage-Mediated Tissue Homeostasis. *Frontiers in Immunology,* 12, 669891. https://doi.org/10.3389/fimmu.2021.669891

Doney, E., Cadoret, A., Dion-Albert, L., Lebel, M., & Menard, C. (2022). Inflammation-driven brain and gut barrier dysfunction in stress and mood disorders. *European Journal of Neuroscience,* 55(9-10), 2851-2894. https://doi.org/10.1111/ejn.15239

Fajgenbaum, D.C., & June, C.H. (2020). Cytokine Storm. *New England Journal of Medicine,* 383(23), 2255-2273. https://doi.org/10.1056/NEJMra2026131

Flierl, M.A., Rittirsch, D., Huber-Lang, M., Sarma, J.V., & Ward, P.A. (2008). Catecholamines-crafty weapons in the inflammatory arsenal of immune/inflammatory cells or opening pandora's box? *Molecular Medicine, 14*(3-4), 195-204. https://doi.org/10.2119/2007-00105.Flierl

Furman, D., Campisi, J., Verdin, E., Carrera-Bastos, P., Targ, S., Franceschi, C., ... & Slavich, G.M. (2019). Chronic inflammation in the etiology of disease across the life span. *Nature Medicine,* 25(12), 1822-1832. https://doi.org/10.1038/s41591-019-0675-0

Golovatscka, V., Ennes, H., Mayer, E.A., & Bradesi, S. (2012). Chronic stress-induced changes in pro-inflammatory cytokines and spinal glia markers in the rat: a time course study. *Neuroimmunomodulation,* 19(6), 367-376. https://doi.org/10.1159/000342092

Hassamal, S. (2023). Chronic stress, neuroinflammation, and depression: an overview of pathophysiological mechanisms and emerging anti-inflammatories. *Frontiers in Psychiatry,* 14, 1130989. https://doi.org/10.3389/fpsyt.2023.1130989

Herman, J.P., McKlveen, J.M., Ghosal, S., Kopp, B., Wulsin, A., Makinson, R., ..., & Myers, B. (2016). Regulation of the Hypothalamic-Pituitary-Adrenocortical Stress Response. *Comprehensive Physiology,* 6(2), 603-621. https://doi.org/10.1002/cphy.c150015

Hirayama, D., Iida, T., & Nakase, H. (2017). The Phagocytic Function of Macrophage-Enforcing Innate Immunity and Tissue Homeostasis. *International Journal of Molecular Sciences,* 19(1). https://doi.org/10.3390/ijms19010092

Holzer, P., Farzi, A., Hassan, A. M., Zenz, G., Jačan, A., & Reichmann, F. (2017). Visceral inflammation and immune activation stress the brain. *Frontiers in Immunology*, 8, 1613. https://doi.org/10.3389/fimmu.2017.01613

Iyer, S.S., & Cheng, G. (2012). Role of interleukin 10 transcriptional regulation in inflammation and autoimmune disease. *Critical Reviews™ in Immunology,* 32(1), 23-63. https://doi.org/10.1615/critrevimmunol.v32.i1.30

Kahya, H.F.H., & Mahmood, M.T. (2022). Detection of IgG and IgM Levels in Patients with COVID-19 in Mosul Province, Iraq. *Journal of Pure and Applied Microbiology,* 16(1), 167-173. https://doi.org/10.22207/JPAM.16.1.05

Kany, S., Vollrath, J.T., & Relja, B. (2019). Cytokines in Inflammatory Disease. *International* journal *of* molecular sciences, 20(23). https://doi.org/10.3390/ijms20236008

Keng, S.L., Smoski, M.J., & Robins, C.J. (2011). Effects of mindfulness on psychological health: a review of empirical studies. *Clinical Psychology Review,* 31(6), 1041-1056. https://doi.org/10.1016/j.cpr.2011.04.006

Kondělková, K., Vokurková, D., Krejsek, J., Borská, L., Fiala, Z., & Ctirad, A. (2010). Regulatory T cells (TREG) and their roles in immune system with respect to immunopathological disorders. *Acta Medica (Hradec Kralove),* 53(2), 73-77. https://doi.org/10.14712/18059694.2016.63

Li, Q.Y., Xu, H.Y., & Yang, H.J. (2017). Effect of proinflammatory factors TNF-α, IL-1β, IL-6 on neuropathic pain. *Zhongguo Zhong Yao Za Zhi,* 42(19), 3709-3712. https://doi.org/10.19540/j.cnki.cjcmm.20170907.004

Liu, Y., Tian, S., Ning, B., Huang, T., Li, Y., & Wei, Y. (2022). Stress and cancer: The mechanisms of immune dysregulation and management. *Frontiers in Immunology,* 13, 1032294. https://doi.org/10.3389/fimmu.2022.1032294

Liu, Y.Z., Wang, Y.X., & Jiang, C.L. (2017). Inflammation: The Common Pathway of Stress-Related Diseases. *Frontiers in Human Neuroscience,* 11, 316. https://doi.org/10.3389/fnhum.2017.00316

Ma, X., Yue, Z.Q., Gong, Z.Q., Zhang, H., Duan, N.Y., Shi, Y.T., …, & Li, Y. F. (2017). The Effect of Diaphragmatic Breathing on Attention, Negative Affect and Stress in Healthy Adults. *Frontiers in Psychology,* 8, 874. https://doi.org/10.3389/fpsyg.2017.00874

Madison, A., & Kiecolt-Glaser, J.K. (2019). Stress, depression, diet, and the gut microbiota: human-bacteria interactions at the core of psychoneuroimmunology and nutrition. *Current Opinion in Behavioral Sciences,* 28, 105-110. https://doi.org/10.1016/j.cobeha.2019.01.011

Mariotti, A. (2015). The effects of chronic stress on health: new insights into the molecular mechanisms of brain-body communication. *Future Science OA,* 1(3), Fso23. https://doi.org/10.4155/fso.15.21

Marshall, G.D., Jr. (2011). The adverse effects of psychological stress on immunoregulatory balance: applications to human inflammatory diseases. *Immunology and Allergy Clinics,* 31(1), 133-140. https://doi.org/10.1016/j.iac.2010.09.013

Mavoungou, E., Bouyou-Akotet, M.K., & Kremsner, P.G. (2005). Effects of prolactin and cortisol on natural killer (NK) cell surface expression and function of human natural cytotoxicity receptors (NKp46, NKp44 and NKp30). *Clinical & Experimental Immunology,* 139(2), 287-296. https://doi.org/10.1111/j.1365-2249.2004.02686.x

Meijer, O.C., Buurstede, J.C., & Schaaf, M.J.M. (2019). Corticosteroid Receptors in the Brain: Transcriptional Mechanisms for Specificity and Context-Dependent Effects. *Cellular and Molecular Neurobiology, 39*(4), 539-549. https://doi.org/10.1007/s10571-018-0625-2

Miller, A.H., & Raison, C.L. (2016). The role of inflammation in depression: from evolutionary imperative to modern treatment target. *Nature Reviews Immunology,* 16(1), 22-34. https://doi.org/10.1038/nri.2015.5

Mishra, R., Welsh, R., & Szomolanyi-Tsuda, E. (2014). NK cells and virus-related cancers. *Critical Reviews™ in Oncogenesis*, 19(1-2). https://doi.org/10.1615/critrevoncog.2014010866

Moreno-Smith, M., Lutgendorf, S.K., & Sood, A.K. (2010). Impact of stress on cancer metastasis. *Future Oncology,* 6(12), 1863-1881. https://doi.org/10.2217/fon.10.142

Morey, J.N., Boggero, I.A., Scott, A.B., & Segerstrom, S.C. (2015). Current Directions in Stress and Human Immune Function. *Current Opinion in Psychology,* 5, 13-17. https://doi.org/10.1016/j.copsyc.2015.03.007

Nakao, M., Shirotsuki, K., & Sugaya, N. (2021). Cognitive-behavioral therapy for management of mental health and stress-related disorders: Recent advances in techniques and technologies. *BioPsychoSocial Medicine,* 15(1), 16. https://doi.org/10.1186/s13030-021-00219-w

Nicholson, L.B. (2016). The immune system. *Essays in Biochemistry,* 60(3), 275-301.

Ozbay, F., Johnson, D.C., Dimoulas, E., Morgan, C.A., Charney, D., & Southwick, S. (2007). Social support and resilience to stress: from neurobiology to clinical practice. *Psychiatry (Edgmont),* 4(5), 35-40.

Raulet, D.H., & Guerra, N. (2009). Oncogenic stress sensed by the immune system: role of natural killer cell receptors. *Nature Reviews Immunology,* 9(8), 568-580. https://doi.org/10.1038/nri2604

Rocamora-Reverte, L., Melzer, F.L., Würzner, R., & Weinberger, B. (2020). The Complex Role of Regulatory T Cells in Immunity and Aging. *Frontiers in Immunology,* 11, 616949. https://doi.org/10.3389/fimmu.2020.616949

Salleh, M.R. (2008). Life event, stress and illness. *The Malaysian Journal of Medical Sciences,* 15(4), 9-18.

Schneiderman, N., Ironson, G., & Siegel, S.D. (2005). Stress and health: psychological, behavioral, and biological determinants. *Annual Review of Clinical Psychology,* 1, 607-628. https://doi.org/10.1146/annurev.clinpsy.1.102803.144141

Schramm, E., & Waisman, A. (2022). Microglia as Central Protagonists in the Chronic Stress Response. *Neurol Neuroimmunol Neuroinflamm,* 9(6). https://doi.org/10.1212/nxi.0000000000200023

Segerstrom, S.C., & Miller, G.E. (2004). Psychological stress and the human immune system: a meta-analytic study of 30 years of inquiry. *Psychological Bulletin,* 130(4), 601-630. https://doi.org/10.1037/0033-2909.130.4.601

Seiler, A., Fagundes, C.P., & Christian, L.M. (2020). The Impact of Everyday Stressors on the Immune System and Health. In A. Choukèr (Ed.), *Stress Challenges and Immunity in Space: From Mechanisms to Monitoring and Preventive Strategies* (pp. 71-92). Cham: Springer International Publishing.

Seol, K.H., Bong, S.H., Kang, D.H., & Kim, J.W. (2021). Factors Associated with the Quality of Life of Patients with Cancer Undergoing Radiotherapy. *Psychiatry Investigation,* 18(1), 80-87. https://doi.org/10.30773/pi.2020.0286

Sheng, J.A., Bales, N.J., Myers, S.A., Bautista, A.I., Roueinfar, M., Hale, T.M., & Handa, R.J. (2021). The Hypothalamic-Pituitary-Adrenal Axis: Development, Programming Actions of Hormones, and Maternal-Fetal Interactions. *Frontiers in Behavioral Neuroscience, 14.* https://doi.org/10.3389/fnbeh.2020.601939

Shimba, A., Ejima, A., & Ikuta, K. (2021). Pleiotropic Effects of Glucocorticoids on the Immune System in Circadian Rhythm and Stress. *Frontiers in Immunology,* 12, 706951. https://doi.org/10.3389/fimmu.2021.706951

Smith, S.M., & Vale, W.W. (2006). The role of the hypothalamic-pituitary-adrenal axis in neuroendocrine responses to stress. *Dialogues in Clinical Neuroscience,* 8(4), 383-395. https://doi.org/10.31887/DCNS.2006.8.4/ssmith

Stephens, M.A., & Wand, G. (2012). Stress and the HPA axis: role of glucocorticoids in alcohol dependence. *Alcohol Research: Current Reviews,* 34(4), 468-483.

Stojanovich, L., & Marisavljevich, D. (2008). Stress as a trigger of autoimmune disease. *Autoimmun Reviews,* 7(3), 209-213. https://doi.org/10.1016/j.autrev.2007.11.007

Tang, W., Zhu, H., Feng, Y., Guo, R., & Wan, D. (2020). The Impact of Gut Microbiota Disorders on the Blood-Brain Barrier. *Infection and Drug Resistance,* 13, 3351-3363. https://doi.org/10.2147/idr.S254403

Thau, L., Gandhi, J., & Sharma, S. (2019). Physiology, Cortisol. National Library of Medicine.

Theofilis, P., Sagris, M., Oikonomou, E., Antonopoulos, A. S., Siasos, G., Tsioufis, C., & Tousoulis, D. (2021). Inflammatory Mechanisms Contributing to Endothelial Dysfunction. *Biomedicines,* 9(7). https://doi.org/10.3390/biomedicines9070781

Tian, R., Hou, G., Li, D., & Yuan, T. F. (2014). A possible change process of inflammatory cytokines in the prolonged chronic stress and its ultimate implications for health. *Scientific World Journal,* 2014, 780616. https://doi.org/10.1155/2014/780616

Toussaint, L., Nguyen, Q.A., Roettger, C., Dixon, K., Offenbächer, M., Kohls, N., …, & Sirois, F. (2021). Effectiveness of Progressive Muscle Relaxation, Deep Breathing, and Guided Imagery in Promoting Psychological and Physiological States of Relaxation. *Evidence-Based Complementary and Alternative Medicine,* 2021, 5924040. https://doi.org/10.1155/2021/5924040

Tsigos, C., Kyrou, I., Kassi, E., & Chrousos, G. P. (2020). Stress: endocrine physiology and pathophysiology. *Endotext [Internet].*

Vignjević Petrinović, S., Milošević, M.S., Marković, D., & Momčilović, S. (2023). Interplay between stress and cancer—A focus on inflammation. *Frontiers in Physiology,* 14, 1119095. https://doi.org/10.3389/fphys.2023.1119095

Wang, H., He, Y., Sun, Z., Ren, S., Liu, M., Wang, G., & Yang, J. (2022). Microglia in depression: an overview of microglia in the pathogenesis and treatment of depression. *Journal of Neuroinflammation,* 19(1), 132. https://doi.org/10.1186/s12974-022-02492-0

Wang, Y., & Feng, W. (2022). Cancer-related psychosocial challenges. *General Psychiatry,* 35(5), e100871. https://doi.org/10.1136/gpsych-2022-100871

Zhang, C. (2008). The role of inflammatory cytokines in endothelial dysfunction. *Basic Research in Cardiology,* 103(5), 398-406. https://doi.org/10.1007/s00395-008-0733-0

Zhang, J.M., & An, J. (2007). Cytokines, inflammation, and pain. *International Anesthesiology Clinics,* 45(2), 27-37. https://doi.org/10.1097/AIA.0b013e318034194e

Zhang, L., Pan, J., Chen, W., Jiang, J., & Huang, J. (2020). Chronic stress-induced immune dysregulation in cancer: implications for initiation, progression, metastasis, and treatment. *American Journal of Cancer Research,* 10(5), 1294-1307.